THE REGULATION OF DYNAMIN I INTERACTIONS IN SYNAPTIC VESICLE ENDOCYTOSIS

KAREN JANET SMILLIE

BSc (Hons)

THESIS SUBMITTED FOR THE DEGREE

OF DOCTOR OF PHILOSOPHY

SEPTEMBER 2005

THE UNIVERSITY OF EDINBURGH

TABLE OF CONTENTS

LIST OF FIGURES

LIST OF TABLES

ACKNOWLEDGEMENTS

I would firstly like to thank my Mum and Dad for their support, encouragement and faith in me through out. Without them I would not be where I am today. A huge thank you also to my sister for being there when I needed that extra boost.

A heartfelt thank you goes to my supervisor, Dr. Mike Cousin, for his patience, infectious enthusiasm and excellent guidance from the start, not to mention the speed with which drafts were turned around!

I would like to acknowledge the financial support from The University of Edinburgh (Medical Faculty Research Scholarship), The Cunningham Trust and the Wellcome Trust, for without them, the work in this thesis would not have been possible. I would also like to thank Dr. Peter Flatman for the generous use of his fluorimeter.

Lastly, thank you to all members of the MBG, past and present: there was always a friendly face and someone from whom to seek advice. A special thank you to fellow MAC lab members for keeping my experiments on the straight and narrow and for putting things on the shelves that I couldn't reach! Thanks also to friends from my various walks of life for restoring my sanity over a meal, a drink or weekends away. Special thanks are due to Gerald for proof reading this thesis, and Mairéad for keeping things in perspective, or failing that, providing the chocolate!!

DECLARATION

I, Karen Janet Smillie, candidate for a PhD in Biomedical Sciences, declare that this thesis has been composed solely by myself, and that the work herein described is my own, except where indicated, and that this work has not been submitted for any other degree or professional qualification.

Karen J. Smillie

BSc (Hons)

ABSTRACT

Synaptic vesicle endocytosis is essential for the maintenance of synaptic transmission. The process involves a cascade of protein-protein interactions involving many proteins, the majority of which are essential. This pathway was investigated by perturbation of protein-protein interactions using the penetratin vector system. This thesis shows that penetratin tagging of peptides is a powerful tool to allow translocation of peptides across the lipid bilayer of isolated nerve terminals where the effect on synaptic vesicle turnover was monitored using styryl dyes. Depending on the target sequence the peptides were able to specifically inhibit either synaptic vesicle exocytosis or endocytosis.

Dynamin I is a 96kDa GTPase and is one of eight proteins known to undergo coordinated dephosphorylation upon nerve terminal stimulation and subsequent rephosphorylation. They are collectively referred to as the dephosphins and are all dephosphorylated by calcineurin and at least three are rephosphorylated by cyclin-dependent kinase 5. Phosphomimetic peptides were used to investigate the specific role of dynamin I phosphorylation in synaptic vesicle endocytosis. The peptide mimicking dephosphorylated dynamin I was nearly four times more effective at inhibiting synaptic vesicle endocytosis than the peptide mimicking phosphorylated dynamin I, indicating that there is an essential role for these phosphorylation sites in endocytosis. Experiments to probe the function of the phosphoryation sites identified syndapin I as a stimulation dependent binding partner to this region of dynamin I. The interaction was further characterised by immunoprecipitation and GST-pulldown assays.

Dynamin I can also be regulated by Ca^{2+} either directly or indirectly through Ca^{2+}-dependent binding partners. Dynamin I has been shown to bind to the cytosolic C-terminus of the integral vesicle protein synaptophysin in a Ca^{2+}-dependent manner. This thesis shows that the over-expression of the C-terminus of synaptophysin-eGFP in cerebellar granule neurons inhibits synaptic vesicle recycling and that a peptide designed from this region of synaptophysin also inhibits synaptic vesicle recycling in isolated nerve terminals. GST-pulldowns with the C-terminus of synaptophysin extracted dynamin I, in the presence of Ca^{2+}, but also a more prominent band shown by western blot to be amphiphysin I. Amphiphysin I was confirmed to bind to the C-terminus of synaptophysin independently from dynamin I through the use of a peptide which disrupts binding of dynamin I and amphiphysin I and through an *in vitro* binding assay. This suggests that amphiphysin I, as well as dynamin I, may interact with synaptophysin in nerve terminals, linking synaptophysin to a potential role in synaptic vesicle endocytosis.

PUBLICATIONS ARISING FROM THIS THESIS

1. Anggono V, Smillie KJ, Graham ME, Valova VA, Cousin MA and Robinson PJ (2005) Syndapin I is the phosphorylation-regulated dynamin I partner in synaptic vesicle endocytosis. *Nat. Neurosci In Press*.

2. Smillie KJ and Cousin MA (2005) Dynamin I phosphorylation and the control of synaptic vesicle endocytosis. *Biochem. Soc. Symp.* **72,** 87-97.

3. Cousin MA, Malladi CS, Tan TC, Raymond CR, Smillie KJ, and Robinson PJ (2003) Synapsin I-associated phosphatidylinositol 3-kinase mediates synaptic vesicle delivery to the readily releasable pool. *J. Biol. Chem.* **278** (31), 29065-29071

4. Smillie KJ, Evans GJO and Cousin MA (2005) Developmental change in the calcium sensor for synaptic vesicle endocytosis in central nerve terminals. *J Neurochem* **94,** 452-458.

LIST OF ABREVIATIONS

Abreviation	Definition
µg	microgram
µl	microlitre
µM	micromolar
4-AP	4-aminopyridine
AAKI	Adapter associated kinase I
ANTH	AP180 N-terminal homology
ATP	Adenosine triphosphate
BAR	Bin/Amphiphysin/Rvs
C2	Calcium binding domain 2
Ca^{2+}	Calcium
CamKI	Ca^{2+}/calmodulin-dependent kinase I
Cdk5	Cyclin dependent kinase 5
DH	Disabled homology
DLL	Aspartate-leucine-leucine
DPF	Aspartate-proline-phenylalanine
DPW	Aspartate-proline-tryptophan
EBSS	Earle's balanced salt solution
EDTA	Ethylenediaminetetraacetic acid
eGFP	enhanced green fluorescent protein
EGTA	Ethyleneglycol-bis(2-aminoethyl-ether) tetraacetic
EH	Epsin homology

EM	Electron microscopy
ENTH	Epsin N-terminal homology
FRET	Fluorescence resonance energy transfer
GDH	Glutamate dehydrogenase
GED	GTPase effector domain
GPI	Glycosylphosphaitdylinositol
GSH	Gluthatione sepharose
GST	Glutathione S-transferase
GTP	Guanine triphosphate
HIV	Human immunodeficiency virus
HRP	Horseradish peroxidase
Hz	Hertz
IPTG	Isopropyl-thiogalactopyranoside
KCl	Potassium chloride
kDa	kilo daltons
LPAAT	Lysophosphatidic acid acyl transferase
MAPK	Microtubule associated protein kinase
MARCKS	Myristolated alanine-rich C-kinase substrate
MEM	Minimum essential media
mg	milligram
min	minute
ml	millilitre
mM	millimolar

NADP	Nicotinamide adenine dinucleotide phosphate
NADPH	Reduced NADP
NPF	Asparagine-proline-phenylalanine
NSF	N-ethylmaleimide-sensitive fusion protein
PH	Pleckstrin homology
PI3K	Phosphatidylinositol 3-kinase
PIP	Phosphatidylinositol
PIP_2	Phosphatidylinositol-(4,5)-bisphosphate
PIPKIγ	Phosphatidylinositol kinase Iγ
PKA	Protein kinase A
PKC	Protein kinase C
PP2A	Protein phosphatase 2A
PRD	Proline rich domain
RRP	Readily releasable pool
SBTI	Soluble trypsin inhibitor
SDS-PAGE	Sodium dodecyl sulphate-polyacrylamide gel electrophoresis
SH3	Src-homology 3
SNAP	Soluble NSF attachment proteins
SNARE	SNAP receptor proteins
Sr^{2+}	Strontium
SV	Synaptic vesicle
Syp C-term-GST	Synaptophysin C-terminus-GST

CHAPTER 1

INTRODUCTION

1.1 Constitutive exocytosis and endocytosis

Intracellular vesicle trafficking is essential for cell function. Secretion, or exocytosis, is essential for all cells to transport and release molecules destined for the cell surface as well as new membrane for cell growth or repair (Burgoyne and Morgan 2003). It involves the fusion of intracellular vesicles containing the proteins with the plasma membrane. Following exocytosis, excess membrane is then retrieved by endocytosis. In most cell types this occurs continuously and is referred to as constitutive exo/endocytosis.

Cells have a variety of different ways to retrieve membrane or absorb nutrients such as phagocytosis, pinocytosis, macropinocytosis and caveolar endocytosis (Conner and Schmid 2003). Cells can also absorb essential nutrients such as low density lipoprotein and iron by a form of constitutive endocytosis called receptor mediated endocytosis (Jarousse and Kelly 2001a) where plasma membrane invagination is triggered by the ligand binding to receptors on the cell surface. Receptor mediated endocytosis is also used by cells to modulate their response to extracellular signals. Some viruses and toxins can also exploit this pathway in order to be internalised and infect cells.

1.2 Synaptic vesicle recycling is essential for neurotransmission

Specialised cells (such as neurons, neuroendocrine cells, cells in the pancreas, stomach and intestine, mast cells and neutrophils) also undertake regulated exocytosis in order to secrete their cargos of neurotransmitters, hormones, peptides, enzymes or antibodies at precisely the right moment and in regulated quantities

(Burgoyne and Morgan 2003). Following regulated exocytosis the membrane is rapidly retrieved by compensatory endocytosis (Jarousse and Kelly 2001a). The molecular mechanisms of compensatory endocytosis are broadly similar to that of constitutive or receptor-mediated endocytosis although compensatory endocytosis is more adapted to ensure tighter spatial and temporal control.

Synaptic vesicle (SV) exocytosis and endocytosis are the processes by which neuronal cells secrete neurotransmitter (regulated exocytosis) and retrieve the plasma membrane to regenerate SVs (compensatory endocytosis). SV recycling is essential for efficient neuronal signalling and therefore functioning of the nervous system. Mutation or aberrant expression of proteins involved in SV recycling can lead to various neurological conditions such as epilepsy (Garcia et al. 2004), Alzheimer's disease (Cataldo et al. 1997; Yao 2004; Kelly et al. 2005; Carey et al. 2005), mania and depression (Saito et al. 2001; Stopkova et al. 2004), Spinocerebellar ataxia (Ralser et al. 2005) and Charcot-Marie-Tooth diease (McNiven 2005; Zuchner et al. 2005).

1.3 Synapse structure and function

The site of regulated exocytosis and endocytosis in a neuron is the nerve terminal which forms a junction called a synapse with a post-synaptic dendrite of another neuron (fig 1.1). When neurotransmitter release is required, an action potential travels down the axon depolarising the presynaptic cell membrane and causing an influx of extracellular calcium (Ca^{2+}). The Ca^{2+} influx triggers the SVs to undergo exocytosis and fuse with the presynaptic membrane, releasing the neurotransmitter

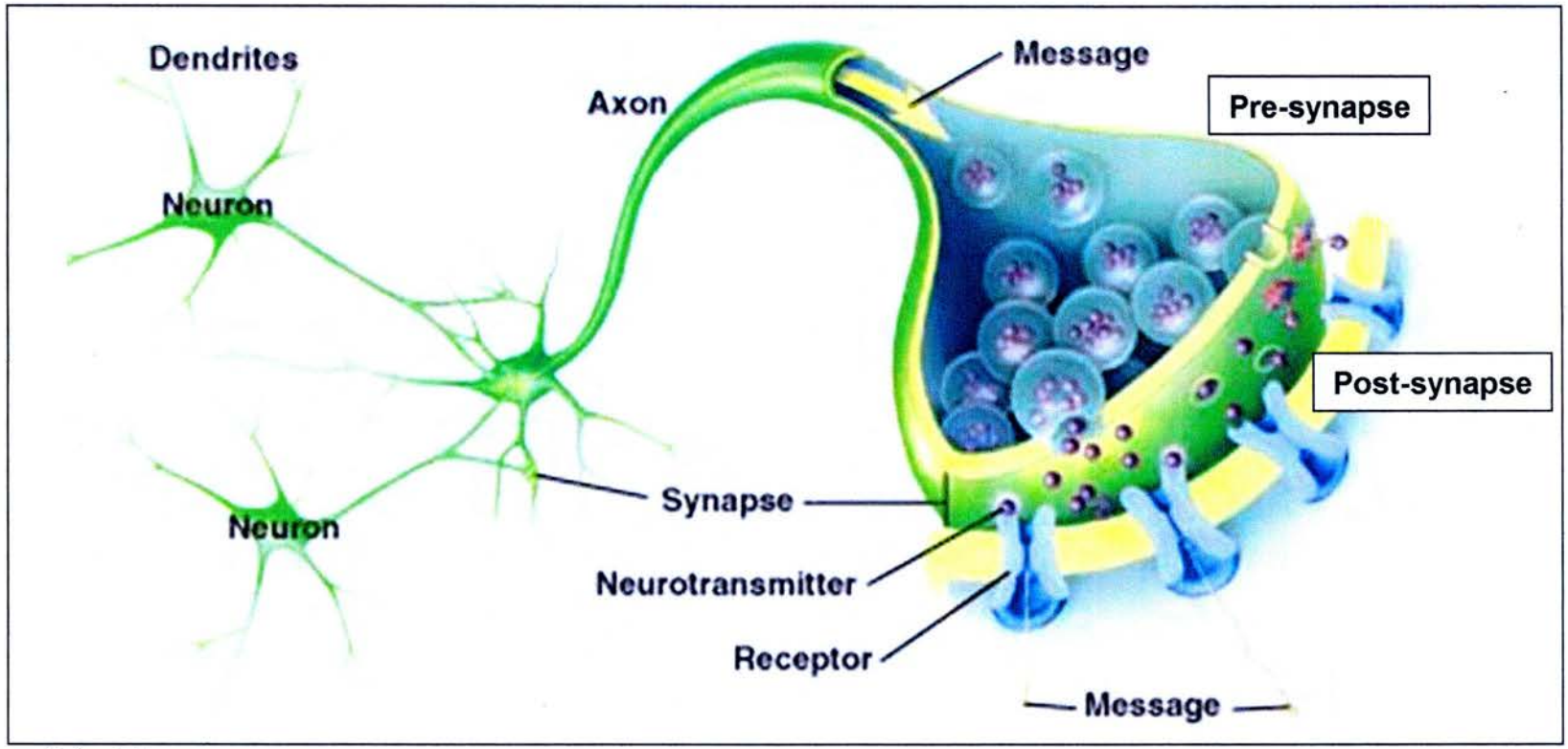

Figure 1.1 – The synapse

A representation of a neuronal synapse showing the neurons with multiple dendrites and an axon, through which an action potential is propagated. The blown up region shows the presynaptic neuron with neurotransmitter containing vesicles. Following depolarisation, these vesicles fuse with the plasma membrane and release the neurotransmitter into the synapse. The neurotransmitter can then cross to the post-synaptic cell and interact with receptors, thus continuing the signal. (Figure adapted from a website no longer available.)

into the synaptic cleft (fig 1.1). The neurotransmitters can diffuse across the synapse and interact with receptors on the post-synaptic cell membrane, thus propagating the signal.

There are several structural features that define the presynaptic nerve terminal (Murthy and De Camilli 2003). The electron micrograph of a lamprey reticulospinal synapse in figure 1.2 illustrates these. The first is the active zone which directly faces the synaptic cleft and post-synaptic cell and is the site of SV release. It is seen as an electron-dense area due to a protein scaffold (Murthy and De Camilli 2003), which seen at higher resolution is a disk-shaped structure made up of a hexagonal grid (Sudhof 2004). The active zone also has docked vesicles embedded in the grid which are immediately ready for release upon Ca^{2+} influx. The second characteristic is clustering of SVs behind the active zone (Murthy and De Camilli 2003). The underlying mechanism explaining SV retention within the cluster is not completely understood, but one possibility is that actin filaments around the outside of the cluster prevent their dispersion (Sankaranarayanan et al. 2003).

1.4 SV lifecycle

The number of SVs present in a nerve terminal depends on the type and function of the synapse, although a typical central nerve terminal has approximately 200 – 250 SVs (Schikorski and Stevens 2001). SVs have a diameter of approximately 40 – 60 nm (Sudhof 2004) and are able to undergo one to two thousand rounds of exocytosis and endocytosis without need for degradation or regeneration. This is important

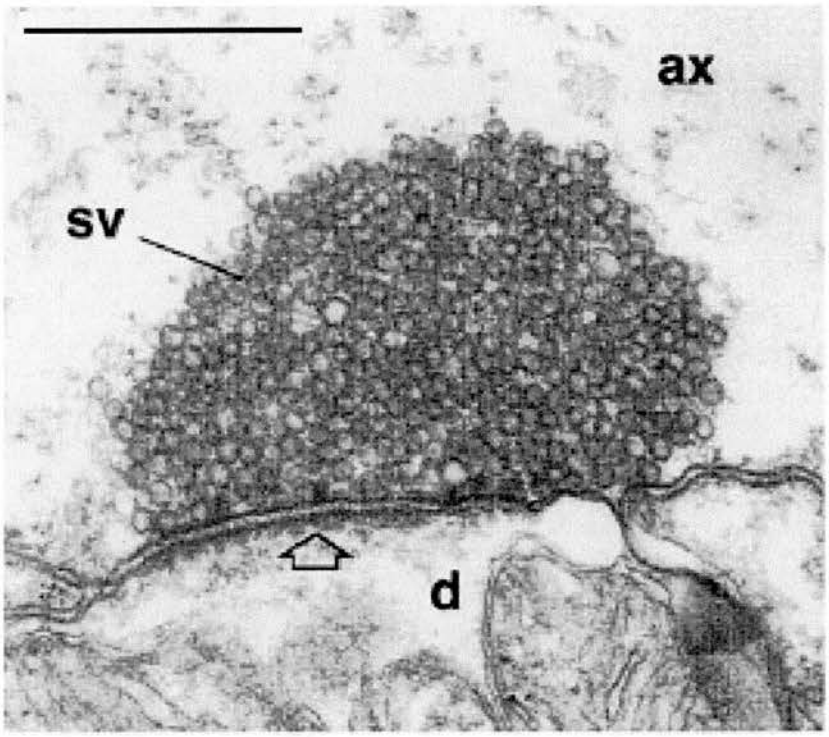

Figure 1.2 – The presynaptic terminal

An electron micrograph of a lamprey reticulospinal synapse showing the electron dense active zone surrounded by a cluster of synaptic vesicles (SV). The open arrow indicates the post-synaptic density opposite the active zone. The axon is labeled (ax) and the dendrite (d). The scale bar represents 0.5 μm. Image is taken from Gad *et al*, 2000.

since nerve terminals are located a large distance from the neuronal cell body and thus would be too far for *de novo* generation of SVs from the Golgi.

The SV cycle can be broken down into several stages (fig 1.3): 1) filling of the vesicle with neurotransmitter via a proton-motive force, 2) trafficking of the vesicles to the plasma membrane where the vesicles dock and are primed, 3) exocytosis of the SV contents in response to the Ca^{2+}-influx, 4) retrieval of the SV locally by a 'kiss and run' mechanism or 5) clathrin-mediated endocytosis. The retrieved SV can then be refilled with neurotransmitter and enter into the recycling SV pool once more.

Each SV contains a vacuolar proton pump which takes up about 10 % of the SV volume (Sudhof 2004). This pump creates an electrochemical gradient of protons (proton motive force) across the SV membrane. Neurotransmitter transporters, also present in the SV membrane, utilise the proton motive force to concentrate the neurotransmitter inside the lumen of the SV. Glutamate is the predominant neurotransmitter with over 90 % of the central synapses being glutamatergic (Nicholls 1993).

The exact mechanism of SV trafficking to the active zone has not been resolved to date, although actin has been implicated as having a role at this stage in some types of synapse (Murthy and De Camilli 2003; Burgoyne and Morgan 2003). Synapsin proteins have also been implicated as having a role in the delivery of synaptic SVs from the reserve pool (see section 1.5 for SV pools) to the readily releasable pool (Pieribone et al. 1995; Li et al. 1995b; Mozhayeva et al. 2002; Cousin et al. 2003).

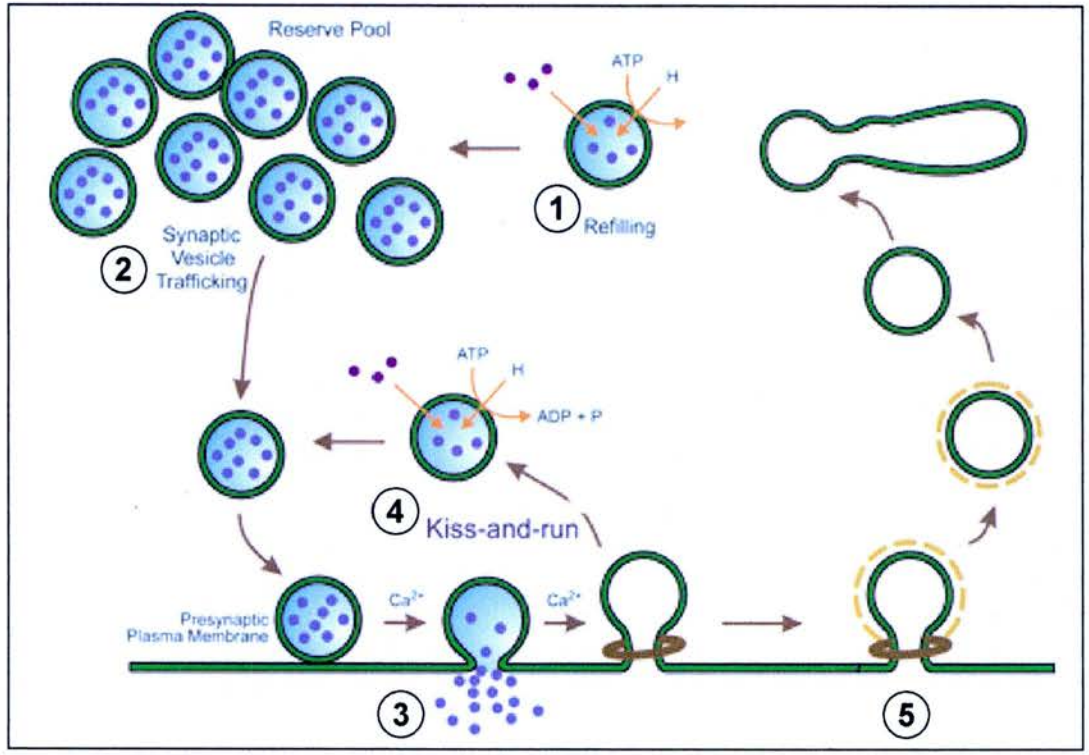

Figure 1.3 – The SV cycle

A schematic representing the SV cycle. **1)** The vesicles are filled with neurotransmitter via a proton motive force before **2)** trafficking to the plasma membrane where they are docked and primed ready for release. **3)** Following depolarisation, Ca^{2+} enters the nerve terminal evoking exocytosis – fusion of the SVs with the plasma membrane. The SV membrane is then retrieved locally by a 'kiss and run' mechanism **(4)** or via a clathrin-mediated endocytosis pathway **(5)**. Figure adapted from http://www.bms.ed.ac.uk/research/idg/mbg/index.htm

They are abundant peripheral SV proteins that contain a conserved protein kinase A (PKA) and Ca^{2+}/calmodulin-dependent protein kinase I (CamKI) phosphorylation site. Phosphorylation of this site abolishes binding of to SVs and thus promotes dissociation of the synapsins (Sudhof 2004), potentially liberating SVs from the reserve pool.

Synapsin associated phosphatidylinositol 3-kinase (PI3K) activity also has a role in the delivery of SVs to the readily releasable pool. The activity of PI3K is localised via an interaction between the p85 subunit of PI3K and synapsin I (Cousin et al. 2003). Inhibition of PI3K activity selectively inhibited the late phase of glutamate release corresponding to the reserve pool release (Cousin et al. 2003).

Once docked at the plasma membrane, the SVs are primed for exocytosis and following Ca^{2+} influx fuse with the plasma membrane and release the neurotransmitter into the synaptic cleft (Section 1.6). The SV membrane can then be retrieved by one of at least two different methods of endocytosis. These are 1) 'kiss and run' where the fusion pore closes and the SV pinches off and recycles locally at the active zone or 2) clathrin-mediated endocytosis which involves the complete fusion of the SV with the plasma membrane and retrieval via clathrin coated pits outside of the active zone. Once the SVs are formed the clathrin coat has to be removed before they can participate in another round of recycling (Section 1.7).

1.5 SV pools and their functions

SVs exist in functionally distinct pools. In central nerve terminals there are two main pools: the readily releasable pool (RRP) and the reserve pool. Together these make up the recycling pool of SVs. The SVs in the RRP are released first upon stimulation and are thought to be docked at the plasma membrane (Burgoyne and Morgan 2003; Sudhof 2004). During high frequency or prolonged stimulation the RRP may not be sufficient to maintain release and so SVs are recruited from the reserve pool (Sudhof 2000). There is a third pool of SVs termed the resting pool which under normal conditions is not required for release (Sudhof 2000).

It is tempting to speculate that the different mechanisms of SV retrieval represent filling of different vesicle pools – for example, the rapid 'kiss and run' retrieval would fill the RRP, explaining the observation that the rapidly retrieved vesicles are preferentially reused, and the slower clathrin-mediated or bulk endocytosis would fill the reserve and resting pools (Matthews 2004). There is some evidence to support this model from the *Drosophila* larval neuromuscular junction where stimulation at low frequency, evoking the 'kiss and run' mode, preferentially recycles SVs near the active zone. During high stimulation, the nerve terminal evokes other mechanisms to recycle the SVs to the centre of the bouton (Kuromi and Kidokoro 2005). At hippocampal synapses too, recently recycled SVs are preferentially located near the active zone (Schikorski and Stevens 2001).

However, Rizzoli and Betz (2004) found that after labelling the RRP SVs using photoconversion, the labelled vesicles were often located far from the active zone,

arguing against 'kiss and run' being the sole endocytic mechanism for recycling the RRP. The labelled SVs were also found randomly distributed through the unlabelled vesicles and not necessarily on the periphery of the vesicle cluster suggesting that proximity to the active zone is not the only marker of the RRP.

What does seem clear is that the SVs in the RRP are recycled with a rapid form of endocytosis and the SVs in the reserve pool are generally retrieved by a slower mode of endocytosis (Rizzoli et al. 2003). The SV pools appear to be functionally discrete but the molecular identity of the retrieval pathways remain to be determined.

1.6 Exocytosis: docking, priming and fusion

Exocytosis broadly involves the regulated fusion of the SV membrane with the plasma membrane allowing release of the neurotransmitter into the synaptic cleft. The minimum machinery required for membrane fusion are the SNAP receptor (SNARE) proteins since when reconstituted in lipid bilayers they mediate membrane fusion (Weber et al. 1998). In nerve terminals the SNAREs which mediate exocytosis are synaptobrevin 2/vesicle associated membrane protein 2 (VAMP2), syntaxin 1 and synaptosomal associated protein of 25 kDa (SNAP-25). Synaptobrevin 2 is enriched upon the SV membrane and syntaxin 1 and SNAP-25 are enriched on the plasma membrane (Rizo and Sudhof 2002; Murthy and De Camilli 2003; Burgoyne and Morgan 2003; Sudhof 2004).

SNARE proteins contain a homologous region termed the SNARE motif. This can be an R-SNARE if it contains an arginine or a Q-SNARE if it contains a glutamine

(Rizo and Sudhof 2002; Burgoyne and Morgan 2003; Sudhof 2004). The core SNARE complex consists of three Q-SNARE motifs and one R-SNARE motif (fig 1.4). In the case of SV exocytosis, synaptobrevin 2 contributes the R-SNARE motif, SNAP-25 contributes two Q-SNARE motifs and syntaxin 1 contributes the remaining Q-SNARE motif (Rizo and Sudhof 2002; Burgoyne and Morgan 2003; Sudhof 2004). The four helices wind around one another forming a very stable parallel helical bundle with the effect of pulling the SV and plasma membranes close together, enabling membrane fusion (Rizo and Sudhof 2002).

Although the SNARE proteins are necessary and sufficient for membrane fusion, the fusion reaction is slow compared to the seconds or sub-second time for *in vivo* membrane fusion (Weber et al. 1998), indicating that other proteins and / or lipids are required *in vivo*. There are several proteins involved in the regulation of SNARE complex assembly which act at different stages of the SV lifecycle: both before vesicle fusion, i.e. docking and priming, as well as during and after fusion.

Docking probably involves the reorganisation of the actin cytoskeleton at the active zone as well as the munc18 / syntaxin I complex and rab3 proteins and effectors. Syntaxin I exists in a closed or open conformation. The open conformation can be incorporated into the SNARE complex but the closed conformation cannot. Munc18 binds to the closed conformation, preventing syntaxin I entry into the core complex. Thus the role of munc18 may be to act as a chaperone and prevent premature complex formation (Burgoyne and Morgan 2003; Sudhof 2004).

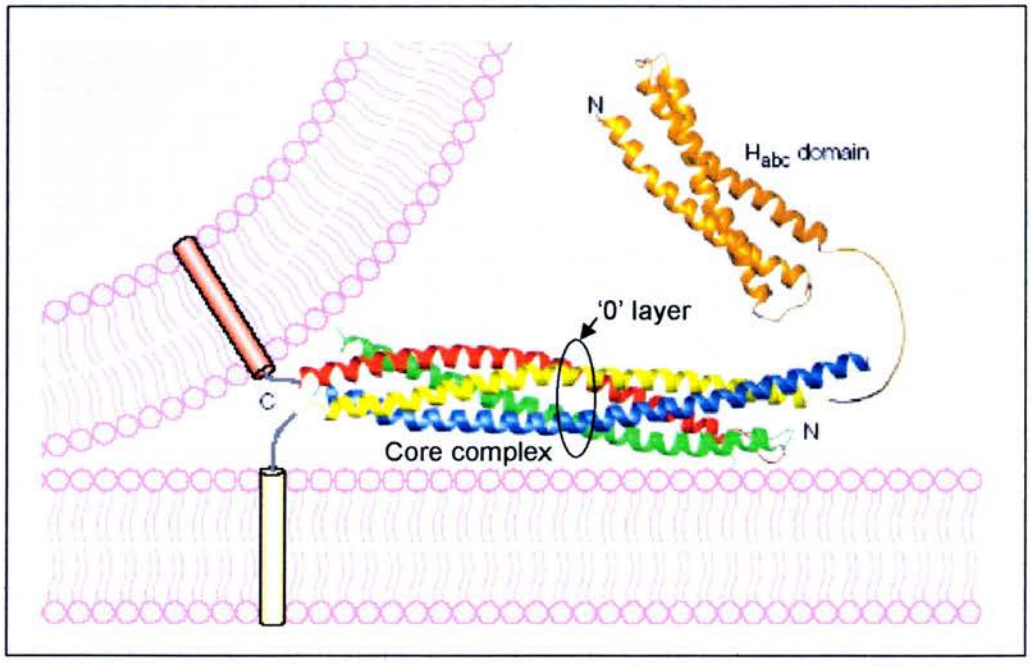

Figure 1.4 – The SNARE complex

Schematic illustrating the neuronal core SNARE complex. The helices forming the SNARE motif from each of the SNARE proteins are colour coded as follows: the SV SNARE protein, synaptobrevin (red) and the plasma membrane SNARE proteins syntaxin (yellow), SNAP-25 (blue and green). The regulatory H_{ABC} domain of syntaxin is displayed in orange and the C-terminal transmembrane domains of synaptobrevin and syntaxin are also shown (red and yellow cylinders, respectively). The conserved glutamine and arginine residues form a polar layer (the '0' layer) at the centre of the bundle. Figure adapted from Rizo and Sudhof, 2002.

Rab proteins are small GTPases which cycle on and off SVs in a stimulation-dependent manner, potentially determining how long SVs are competent for fusion and controlling recruitment to the RRP (Burgoyne and Morgan 2003). Rab effector proteins RIM1α/2α are active zone proteins therefore may contribute to the docking of vesicles via their interaction with rab3-GTP and munc13 (Sudhof 2000).
Priming is an ATP dependent process during which the core SNARE complex is formed and the SVs become competent for release. Munc13 and synaptophysin may mediate priming by the release of SNARE proteins, stimulating the formation of the core SNARE complex. Munc13 can release syntaxin I from munc18, thus freeing syntaxin I to enter the SNARE complex (Rizo and Sudhof 2002). Synaptophysin interacts with synaptobrevin 2 in a stimulation dependent manner (Pennuto et al. 2002; Reisinger et al. 2004), thus upon nerve terminal depolarisation releases synaptobrevin 2, allowing synaptobrevin 2 to interact with the other SNARE proteins and form the SNARE complex (Valtorta et al. 2004; Sudhof 2004). In agreement with a role in priming, munc13 knock out mice have no primed SVs (Varoqueaux et al. 2002).

Complexins are small proteins which are highly enriched in the brain. They form a helical structure which can bind and stabilise the core complex, representing a second late stage of priming with the formation of a 'tight' SNARE complex. The complexin knock out mouse showed that complexins are not required for exocytosis stimulated by hypertonic sucrose, but are required for normal Ca^{2+}-triggered release, supporting a role in priming (Rizo and Sudhof 2002).

Fusion of SVs is triggered by Ca^{2+}-influx. The most likely candidate protein involved at this stage is the integral SV protein, synaptotagmin (Burgoyne and Morgan 2003; Sudhof 2004). Synaptotagmin 1 has two cytoplasmic C2 (Ca^{2+} binding) domains: the C2A domain can bind three Ca^{2+} ions and the C2B domain two (Burgoyne and Morgan 2003; Sudhof 2004). The apparent Ca^{2+} affinity of the C2 domains is low since the coordination of the Ca^{2+} ions is incomplete. However, synaptotagmins can bind to phospholipid membranes in a Ca^{2+}-dependent manner, thus stabilising the Ca^{2+} ions and increasing the affinity (Sudhof 2004).

Binding of synaptotagmin I to the SNARE complex is greatly increased in the presence of Ca^{2+}. This interaction is not essential for exocytosis, however, since Sr^{2+} can substitute for Ca^{2+} in triggering exocytosis but cannot stimulate SNARE interaction (Burgoyne and Morgan 2003; Sudhof 2004). An alternative model was proposed where synaptotagmin I binds to the SNARE complex in the absence of Ca^{2+} and binds to the phospholipid membrane upon Ca^{2+} entry. Synaptotagmin I could insert hydrophobic residues into the membrane, destabilising the fusion intermediate and causing the fusion pore to open (Sudhof 2004). The exact mechanism is still unclear but synaptotagmin I is almost certainly the exocytosis Ca^{2+} sensor.

The SNARE complex is disassembled by the action of the ATPase N-ethylmaleimide-sensitive fusion (NSF) protein. NSF is targeted to the SNARE complex by the soluble NSF attachment proteins (SNAPs) (Rizo and Sudhof 2002; Burgoyne and Morgan 2003). One model of action suggests that a conformational

change in NSF upon ATP hydrolysis enables the SNAP protein to be used as a lever to untwist and disassemble the SNARE core complex (Rizo and Sudhof 2002; Burgoyne and Morgan 2003). Since this step is ATP dependent, it has also been proposed that SNARE complex disassembly may even have a role in SV priming prior to fusion (Burgoyne and Morgan 2003).

1.7 Endocytosis

Following exocytosis, SV endocytosis must occur in order to prevent the nerve terminal becoming depleted of SVs and to remove the extra membrane added to the plasma membrane. The debate concerning the mechanism of SV retrieval began three decades ago with conflicting results from two laboratories. Both groups were looking at the frog neuromuscular junction by electron microscopy. Heuser and Reese stimulated at 10 Hz for 1 min and saw clathrin coated pits which were located away from the active zone (fig 1.5A). They also saw intracellular cisternae, although not attached to the plasma membrane, and postulated that this was due to coalescence of endocytosed SVs (Heuser and Reese 1973; Wilkinson and Cole 2001; Royle and Lagnado 2003). Ceccarelli and colleagues stimulated at a frequency of 2 Hz for up to 4 hr and in contrast to Heuser and Reese, did not see a change in the ultrastructure of the nerve terminal (fig 1.5B). In their model the SVs were recycled at the active zone in a clathrin-independent fashion (Ceccarelli et al. 1973; Wilkinson and Cole 2001; Royle and Lagnado 2003).

These models are now thought to represent at least two different endocytosis pathways which can both occur in a nerve terminal. The models have been adapted

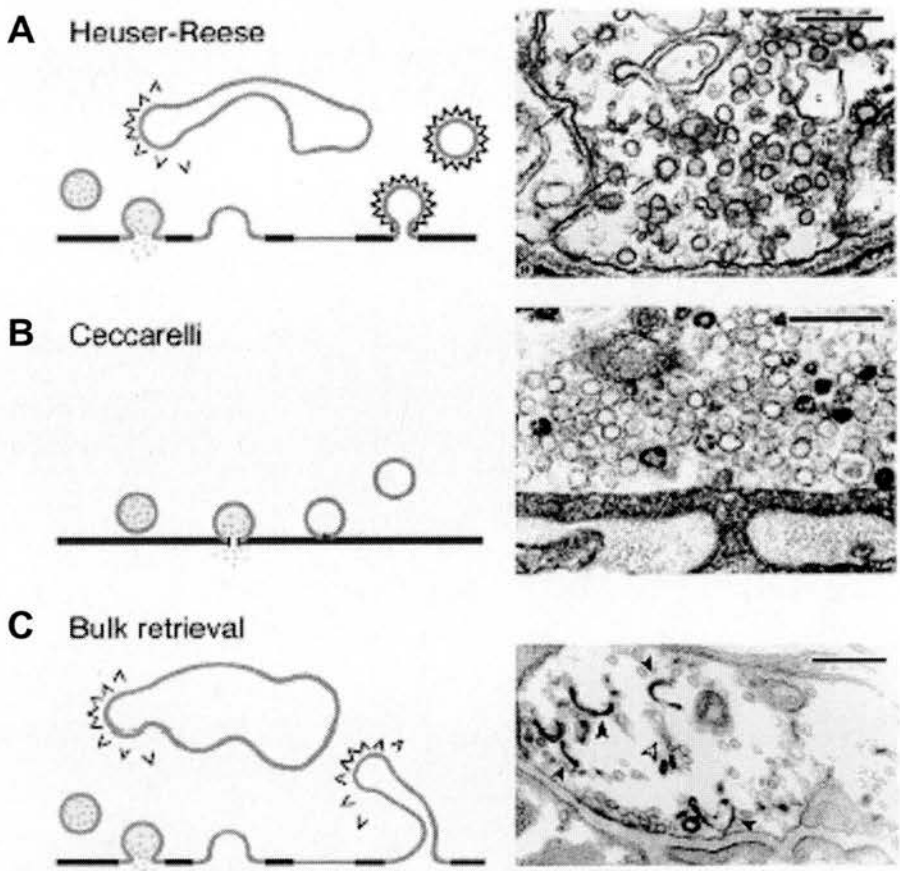

Figure 1.5 – Models of SV retrieval

In all cases the schematic on the left represents the model suggested from the electron micrographs of the neuromuscular junction following stimulation with the different paradigms, examples of which are on the right. The scale bars represent 250 nm. **A)** The Heuser-Reese model where the vesicles collapse fully into the membrane and are retrieved by clathrin-mediated endocytosis. **B)** The Ceccarelli model where the vesicles retrieve by 'kiss and run' through a transient fusion pore, explaining the lack of clathrin-coated intermediates. **C)** The bulk retrieval mode where large areas of plasma membrane are internalised, forming cisternae from which clathrin-coated vesicles can bud. Figure taken from Royle and Lagnado, 2003.

over the years but the profiles that Heuser and Reese saw are thought to reflect SVs which have fused fully with the plasma membrane and been retrieved by clathrin mediated budding and the fast retrieval witnessed by Ceccarelli *et al* is frequently referred to as 'kiss and run' endocytosis where SVs retrieve locally at the active zone without collapse into the membrane (fig 1.5, Royle and Lagnado 2003).

A third mechanism of endocytosis involving the formation of deep invaginations from the plasma membrane at sites away from the active zone was also derived from the Heuser and Reese model. The invaginations are thought to resemble the cisternae seen by Heuser and Reese although the accepted view is that they are formed by a clathrin-independent mechanism and not by coalescence of endocytosed SVs. SVs can then pinch off of the invaginations by clathrin mediated endocytosis. This pathway is referred to as bulk retrieval (fig 1.5, Royle and Lagnado 2003).

Proof that more than one type of SV recycling occurs at the synapse has come from several sources. Richards *et al* (2000) took advantage of two fluorescent dyes with different membrane affinities. Following stimulation in the presence of both dyes the nerve terminals were washed to remove excess dye. After photoconversion both dyes labelled structures near the active zone but only the dye with the greater affinity (FM1-43) for membranes labelled cisternae type structures. The lower affinity dye (FM2-10) had been washed out of these structures. Also, nerve terminals loaded by tetanic stimulation with both dyes had different destaining rates: very little FM1-43 was released, correlating with the dye being in the cisternae, but the majority of the FM2-10 was released, suggesting the FM2-10 labelled vesicles which were retrieved

quickly were competent for release once more (Richards et al. 2000). This suggests that the differentially labelled structures represented functionally distinct pathways which were both active simultaneously. De Lange *et al* (2003) also observed a shift from HRP-labelled SVs to HRP-labelled cisternae type structures with more intense stimulation protocols in the Calyx of Held. Gandhi and Stevens (2003) followed the fate of single SVs with the fluorescent SV marker protein, synaptophluorin. Three different time constants for endocytosis were detected also suggesting the presence of more than one mode of recycling at the synapse (Gandhi and Stevens 2003; Rizzoli and Betz 2003).

1.7.1 Endocytosis: Clathrin-mediated

Clathrin-mediated compensatory endocytosis at the synapse is broadly similar to receptor-mediated endocytosis and is the best characterised mode of endocytosis. Both processes involve the formation of a clathrin coated vesicle. Clathrin was first isolated from purified coated vesicles and was found to form structures with variable numbers of clathrin molecules arranged in pentagons and hexagons (Pearse 1976). Clathrin is composed of heavy (170 kDa) and light (35 kDa) chains which oligomerise to form a three-legged triskelion (fig 1.7). It is these oligomers which form the basic clathrin unit which in turn polymerises into a lattice of pentagons and hexagons surrounding the vesicle (Slepnev and De Camilli 2000). The oligomerisation is mediated by interactions between the C-terminus of the clathrin heavy chains. The light chains bind to the heavy chains via contacts on α-helices involving conserved tryptophan residues (Chen et al. 2002). They have a regulatory role to prevent spontaneous polymerisation, although this can be overcome by

clathrin adapter molecules. The light chains can also bind Ca^{2+}, via an EF-hand motif, and calmodulin. The binding of calmodulin in particular is thought to aid in the bending of the triskelia to form a curved lattice (Chen et al. 2002).

The N-terminal domain of the clathrin heavy chain forms a β-propeller which interacts with proteins containing a "clathrin box" which has the consensus LLpL(-) where p is an amino acid with a polar side-chain and (-) represents a negatively charged sidechain. Many adapter and scaffolding proteins such as AP2, AP180, epsin and amphiphysin contain a clathrin box and regulate vesicle formation via an interaction with clathrin (ter Haar et al. 2000).

The proteins involved in clathrin-mediated endocytosis at the synapse have homologues that are ubiquitously expressed and involved in receptor-mediated endocytosis. Analysis of both sets of proteins and their modes of action have provided valuable insights into the mechanism of clathrin-mediated endocytosis which can be applied to endocytosis in all cell types as well as at the synapse.

The major difference between compensatory endocytosis and receptor-mediated endocytosis is that the regulation at the synapse is very different and rigorously controlled. In the nerve terminal clathrin-mediated endocytosis is tightly coupled to exocytosis. Exocytosis, however, is not sufficient to stimulate endocytosis. Endocytosis is also Ca^{2+}-dependent (Cousin 2000).

Clathrin-mediated endocytosis involves the formation of a clathrin coated pit which invaginates to form a SV that is pinched off of the membrane. The clathrin coat is removed from the SV by uncoating before re-entry into the SV recycling pool. The pathway can be broken down into five main stages: activation, nucleation, invagination, fission and uncoating. These are illustrated in figure 1.6 and discussed below.

1.7.1.1 Clathrin-mediated endocytosis: Activation

Activation of clathrin-mediated SV endocytosis involves the Ca^{2+}/calmodulin dependent phosphatase calcineurin (Cousin 2000). Calcineurin is highly expressed in the nervous system (Rusnak and Mertz 2000) and is the only serine/threonine phosphatase under the control of Ca^{2+}/calmodulin (Klee et al. 1998). Calcineurin functions as a heterodimer of a catalytic subunit and a regulatory subunit (Bandyopadhyay et al. 2004; Hou et al. 2004). The catalytic subunit, as well as containing a catalytic domain, has a binding domain for the regulatory subunit, a calmodulin binding domain and an autoinhibitory domain. The regulatory subunit is the site of Ca^{2+}-binding which is mediated through an 'EF-hand' motif. The catalytic subunit is inactive without the regulatory subunit. The subunits form a salt bridge which stabilises the dimer allowing the binding of the regulatory subunit to activate the phosphatase activity of the catalytic subunit (Hou et al. 2004).

A role for the phosphatase activity of calcineurin in SV endocytosis has been shown using calcineurin inhibitors. Incubation of synaptosomes with either cyclosporin A

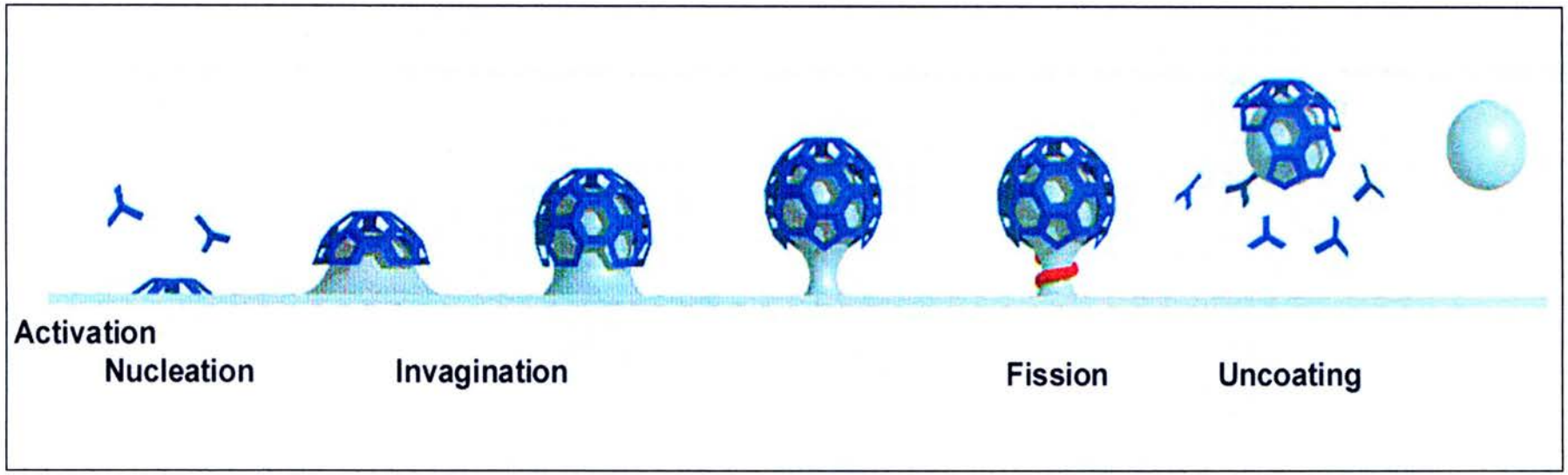

Figure 1.6 – The process of clathrin-mediated SV endocytosis

Illustration showing the five stages of clathrin-mediated SV endocytosis: 1) activation, 2) nucleation of the clathrin coated pit, 3) invagination of the clathrin coated pit to form a vesicle on a stalk, 4) fission of the vesicle and 5) uncoating of the vesicle. Figure adapted from Gad *et al*, 2000.

(Marks and McMahon 1998; Cousin et al. 2001) or FK506 (Marks and McMahon 1998) blocked SV endocytosis but had no detectable effect on exocytosis.

The targets of the calcineurin phosphatase activity are a group of proteins known as the dephosphins. They are grouped together because they are all essential for SV endocytosis and they are co-ordinately dephosphorylated by calcineurin following Ca^{2+} influx into the nerve terminal (Cousin and Robinson 2001). Eight dephosphins have been identified to date: dynamin I, amphiphysin I and II, epsin, eps15, AP180, synaptojanin and phosphatidylinositol kinase I γ (PIPKIγ) (Cousin and Robinson 2001; Wenk et al. 2001). They are all involved at different stages of the endocytosis pathway and will be discussed in more detail in the following sections, but the dephosphorylation of these proteins is essential to stimulate the interactions between the dephosphins and other proteins required for the formation of a clathrin coated SV (Cousin and Robinson 2001).

In different neuronal preparations however, the role of calcineurin is conflicting: in adult synaptosome preparations calcineurin is essential for SV endocytosis (Marks and McMahon 1998; Cousin et al. 2001; Smillie et al. 2005) but in primary neuronal cultures there is no reported requirement for calcineurin (Sankaranarayanan and Ryan 2001) and at the *Drosophila* neuromuscular junction calcineurin inhibits SV endocytosis (Kuromi et al. 1997; Kuromi and Kidokoro 1999). Chromaffin cells also show a disparity in the requirement for calcineurin: cells prepared from adult animals require calcineurin for endocytosis (Engisch and Nowycky 1996; Chan and Smith 2001) but in those prepared from immature animals endocytosis is inhibited by

calcineurin (Artalejo et al. 1996). Recent research into this disparity showed that a requirement for calcineurin activity in SV endocytosis developed with age, implying that in embryonic or neonatal tissue there was a different calcium sensor coupling Ca^{2+} influx to endocytosis or perhaps a different mode of SV endocytosis (Smillie et al. 2005).

Calcineurin is also negatively regulated by cain. Overexpression of cain inhibits transferrin uptake and is targeted to sites of SV activity via its proline-rich domain (PRD) which binds to the src-homology 3 (SH3) domain of amphiphysin I. Binding of cain to amphiphysin does not prevent binding of amphiphysin partners such as dynamin I suggesting that the mechanism of inhibition is by inhibiting calcineurin activity rather than preventing endocytic complex formation (Lai et al. 2000).

1.7.1.2 Clathrin-mediated endocytosis: Nucleation

Nucleation involves the determination of the site for SV endocytosis and the recruitment of the proteins involved in the formation of a clathrin-coated pit. The adapter protein AP2 is thought to be crucial for this stage. It is composed of four subunits: α, β2, μ2 and σ2 (fig 1.7) and is structurally similar to the AP1 complex required for vesicle budding from the Golgi. The α and β2 subunits are the largest (100 kDa) and form a brick-like structure with the C-termini of the two subunits protruding to form ears or appendage domains. The μ2 and σ2 subunits are smaller, 50 kDa and 19kDa respectively, and form part of the central core of the AP2 complex (Slepnev and De Camilli 2000). The β2 subunit binds clathrin at two sites: one on the ear domain and the other in the hinge region between the ear domain and

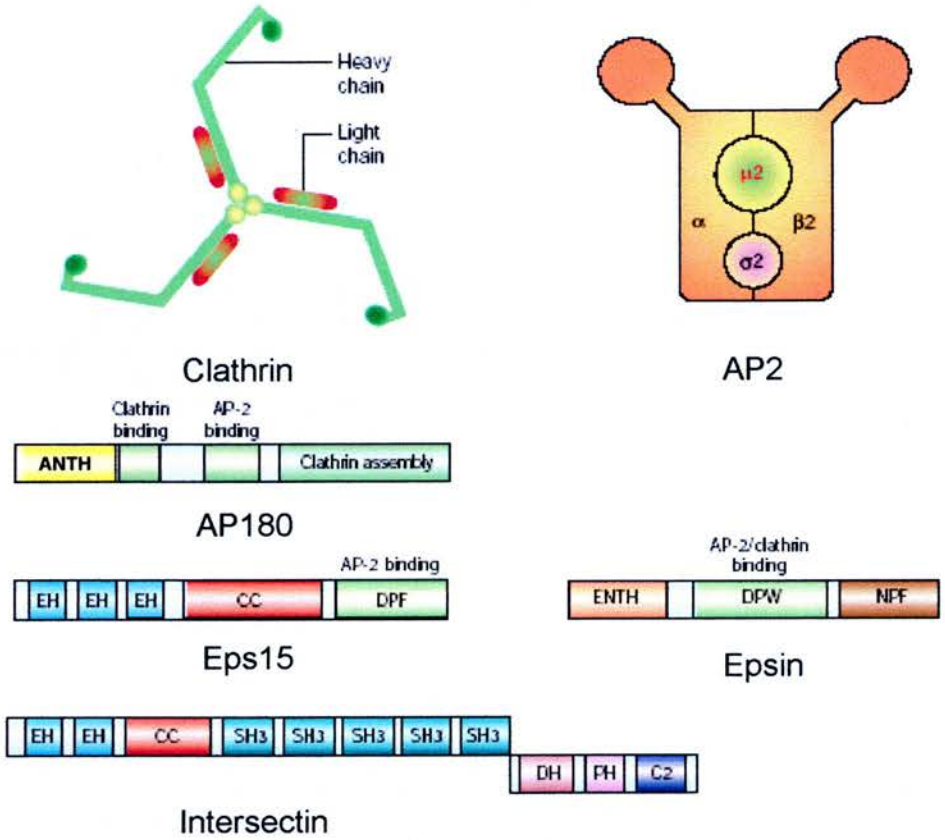

Figure 1.7 – Molecules involved in SV endocytosis (1)

Schematic representation of the modular domain and motif structure of the proteins involved in SV endocytosis. A clathrin triskelion consists of three heavy and three light chains. Adapter protein 2 (AP2) is a heteroligomer composed of four subunits: α, β2, μ2 and σ2. The other protein domains are abbreviated as follows: AP180 homology (ANTH) domain for sensing membrane curvature , Eps15 homology (EH) domain to interact with Asn-Pro-Phe (NPF) motifs, Epsin N-terminal homology (ENTH) domain for generating membrane curvature, Asn-Pro-Trp (DPW) or Asn-Pro-Phe (DPF) motifs to bind to AP2, Src-homolgy (SH3) domain to bind proline rich domains (PRD), Disabled homology (DH) domain to activate Cdc42, pleckstrin homology (PH) domain for mediating lipid binding and C2 domain to bind Ca^{2+}. Figure adapted from Slepnev and De Camilli, 2000.

the rest of the subunit. The ear domains of both α and β2 subunits bind to various other accessory proteins required for the formation of a clathrin-coated SV. The core region of the AP2 complex binds to phosphoinositides, particularly phosphatidylinositol-(4, 5)-bisphosphate (PIP_2), as well as endocytic motifs present on other proteins in the plasma membrane (Slepnev and De Camilli 2000). This complex, therefore, forms the centre of an adaptor complex which serves to recruit clathrin and the other adapter proteins to the plasma membrane.

Synaptotagmin has also been implicated in endocytosis. It is thought to form docking sites on the plasma membrane for AP2 to bind to and nucleate a clathrin coated pit. The C2B domain of synaptotagmin can bind to AP2 and could mediate this role (Jorgensen et al. 1995; Zhang et al. 1994; Li et al. 1995a; Haucke and De Camilli 1999), although subsequent research showed that synaptotagmin bound to AP2 via a site in the C-terminus and that the C2B domain had more of a regulatory role (Haucke et al. 2000; Jarousse and Kelly 2001b).

The μ2 subunit of AP2 can bind to internalisation motifs in various SV proteins, such as SV2, which are found in the plasma membrane following exocytosis and may also contribute to clathrin coat nucleation. The internalisation motifs can take two forms: a tyrosine based motif conforming to the consensus YXXϕ, where ϕ represents a bulky hydrophobic amino acid, and a dileucine motif often of the form DXXLL. The μ2 subunit can be phosphorylated on threonine 156 by adaptor-associated kinase I (AAKI). Phosphorylation of this residue increases the affinity of AP2 for internalisation motifs (Fingerhut et al. 2000; Ricotta et al. 2002; Smythe 2002;

Jackson et al. 2003; Flett et al. 2005), thus increasing the probability of clathrin coated pits following exocytosis. The binding of the μ2 subunit of AP2 to tyrosine based motifs in fact stimulates the recruitment of AP2 to synaptotagmin and so a role for both internalisation motifs and synaptotagmin may be important for nucleation (Haucke and De Camilli 1999).

The μ2 subunit can bind PIP_2 on the plasma membrane, stabilising the AP2 complex at the membrane (Rohde et al. 2002). However, recent research has shown that recognition of tyrosine and dileucine internalisation motifs depends on binding concurrently with PIP_2. Höning and colleagues (2005) showed that AP2 binding to the membrane was a two stage process: firstly PIP_2 was bound weakly at a site on the α subunit and then at a second site on the μ2 subunit simultaneously with binding of tyrosine internalisation motifs. Phosphorylation of the μ2 subunit facilitated the second stage by causing a conformational change, making the internalisation motif binding pocket more accessible. The binding of dileucine internalisation motifs was not enhanced by μ2 phosphorylation and their binding pocket is thought to be on the α subunit (Honing et al. 2005).

Cargo recruitment appears to have an important role in stabilising the formation of clathrin-coated pits in receptor-mediated endocytosis since the initiation of new coated pits is random and many pits disassemble without forming a vesicle if cargo molecules are not recruited (Ehrlich et al. 2004; Smythe 2004). A similar process may well connect coated pit stabilisation in SV endocytosis.

Clathrin itself has a regulatory role in receptor-mediated coated pit formation as well as a structural role. Clathrin can activate the μ2 kinase, and in doing so, promote cargo sequestration into clathrin coated pits (Jackson et al. 2003; Flett et al. 2005).

The dephosphin AP180 is essential for the correct formation of SVs. The N-terminus of AP180 contains an AP180 N-terminal homology (ANTH) domain which binds phosphoinositides and a 'clathrin box' motif to bind clathrin. AP180 binds also to both the ear domains of the α and β2 subunits of AP2. Via all of these motifs AP180 is localised to sites of endocytosis on the plasma membrane. The C-terminal domain of AP180 contains a clathrin assembly domain composed of several asparatate-leucine-leucine (DLL) motifs (Slepnev and De Camilli 2000). Progressive deletion of the DLL motifs reduced clathrin binding and clathrin assembly activity of AP180 (Morgan et al. 2000). AP180 is four times as effective as AP2 at assembling clathrin coats (Lindner and Ungewickell 1992; McMahon 1999) but both proteins together can assemble clathrin coats much more effectively than either alone (Hao et al. 1999).

Perhaps most interesting, is the proposed role for AP180 in SV size. Perturbation of AP180 function by injection of a peptide designed from the AP180 C-terminal domain inhibited synaptic transmission in the giant squid synapse. EM studies of peptide treated synapses showed that as well as decreased numbers of SVs and an increase in plasma membrane, the SVs present were not of a homogenous size (Morgan et al. 1999). AP180 null mutant homologues in *Drosophila* (Zhang et al.

1998) and *C. elegans* (Nonet et al. 1999) also showed an increase in SV size thus implicating an additional role for AP180 as well as clathrin assembly.

Two other dephosphins, epsin and eps15 have important roles in nucleation and the initiation of invagination of a clathrin coated pit. Epsin and Eps15 are found localised to the fringes of a forming clathrin coated pit and form a complex surrounding the adaptor complex (Cousin and Robinson 2001). Both proteins contain many binding motifs and domains (fig 1.7) allowing association with clathrin, AP2, PIP_2 and other endocytic proteins (Slepnev and De Camilli 2000).

Epsin consists of an epsin N-terminal homology (ENTH) domain and an unstructured C-terminus containing multiple peptide motifs mediating binding with other proteins. The ENTH domain is related to the ANTH domain but as well as PIP_2 binding activity, it is capable of causing mechanical stress on the membrane, deforming it (Legendre-Guillemin et al. 2004). The binding of PIP_2 to epsin induces the formation of an N-terminal α-helix which can insert between the lipid headgroups pushing them apart and facilitating membrane curvature. Clathrin polymerisation into a lattice could then stabilise this structure (Ford et al. 2002; Hurley and Wendland 2002; Schmidt 2002).

The unstructured C-terminus of epsin consists of eight copies of the Asp-Pro-Trp (DPW) motif for interaction with the α-ear of AP2, two clathrin binding motifs and three Asn-Pro-Phe (NPF) motifs for binding to eps15 and another endocytosis protein, intersectin (Legendre-Guillemin et al. 2004). Eps15 likewise consists of

many protein binding motifs: Asp-Pro-Phe (DPF) motifs for binding to the α-ear of AP2 and three eps15 homology (EH) domains which mediate binding to NPF motif containing proteins such as epsin and AP180 (Chen et al. 1999). Although eps15 does not have an intrinsic clathrin assembly activity it is able to stimulate the clathrin assembly activity of AP180 (Morgan et al. 2003). Eps15 also has a central coiled coil domain for homodimerisation and heterodimerisation with intersectin (Slepnev and De Camilli 2000).

These two proteins are very good examples of a continuing theme in endocytosis proteins: the multiplicity of protein binding domains within the same protein. This approach enables many weak interactions to build up into a strong avidity as well as the efficient recruitment of proteins to the sites of endocytosis (Praefcke et al. 2004).

Another common factor regarding the proteins involved in nucleation is the ability to bind to PIP_2. PIP_2 is concentrated at the plasma membrane (Lee et al. 2005) and since AP2, AP180, synaptotagmin and epsin can all bind PIP_2 these proteins can thus become anchored in the plasma membrane. The main PIP_2 synthesising enzyme at the synapse is PIPKIγ, (Wenk et al. 2001). PIPKIγ is also a dephosphin (Wenk et al. 2001) and therefore it is tempting to speculate that dephosphorylation upon nerve terminal stimulation could activate PIP_2 synthesis at sites of endocytosis. However, phosphorylation of PIPKIγ did not affect its catalytic activity (Lee et al. 2005) suggesting that this is not the case since phosphorylation would be predicted to decrease activity.

To summarise activation, clathrin lattices are polymerised via the action of the adapter complex consisting of AP2 and AP180. The adapter complex is targeted to sites of endocytosis possibly by synaptotagmin or cargo molecules with tyrosine or dileucine internalisation motifs but definitely through the binding of PIP_2 by most of the proteins involved in nucleation. The membrane is partly deformed by the insertion of the epsin N-terminal helix. The forming lattice along with the adapter complexes and eps15 can then stabilise the curving clathrin pit. AP180 also has a role in the regulation of the size of the lattice formed creating a homogenous population of SVs.

1.7.1.3 Clathrin-mediated endocytosis: Invagination

The next stage of endocytosis involves the invagination of the clathrin coated pit to form a deeply invaginated pit with a narrow neck. The proteins involved at this stage mainly have a scaffolding role and serve to recruit proteins for the final stages of SV formation.

Intersectin is a large multidomain protein containing two EH domains and five SH3 domains (fig 1.7). This allows intersectin to bind to the nucleation machinery (via epsin) and to late SV fission machinery (including dynamin I, synaptojanin and endophilin). The main splice variant of intersectin in neurons contains a C-terminal insert with a disabled homology (DH) domain which acts as a guanine nucleotide exchange factor for Cdc42, a pleckstrin homology (PH) domain to mediate lipid binding and a C2 domain (fig 1.7, Slepnev and De Camilli 2000; Broadie 2004). This C-terminal region allows coupling of the endocytosis machinery to the actin

cytoskeleton and intracellular signalling. Loss-of-function mutations of the *Drosophila* homolog of intersectin, Dap160, show defects in endocytosis as well as a marked decrease in the levels of dynamin I, synaptojanin and endophilin, suggesting that intersectin has a role in stabilising the endocytic complex (Broadie 2004; Koh et al. 2004; Marie et al. 2004).

The dephosphins amphiphysins I and II (fig 1.8) are thought to link the invaginated SV to the late endocytosis fission machinery. Amphiphysin I and II exist as a functional dimer – shown by the amphiphysin I knock out mouse. This mouse exhibited decreased SV recycling and impaired learning, although was viable. It did however, have a dramatic decrease in the levels of amphiphysin II, suggesting that the dimer is necessary for stability of the proteins (Di Paolo et al. 2002).

The most investigated amphiphysin interaction has been that with dynamin I. This interaction is essential for SV endocytosis and is mediated via the SH3 domain of amphiphysin and the PRD of dynamin I (Grabs et al. 1997; Slepnev and De Camilli 2000). Disruption of this interaction causes an inhibition of SV endocytosis at the stage of a deeply invaginated pit (Shupliakov et al. 1997; Wigge et al. 1997b; Simpson et al. 1999). The invaginated pits are reminiscent of the structures seen with dynamin I mutants although they lack an electron dense collar suggesting that the main role for amphiphysin is in the recruitment of dynamin I to the neck of an invaginating SV (Shupliakov et al. 1997).

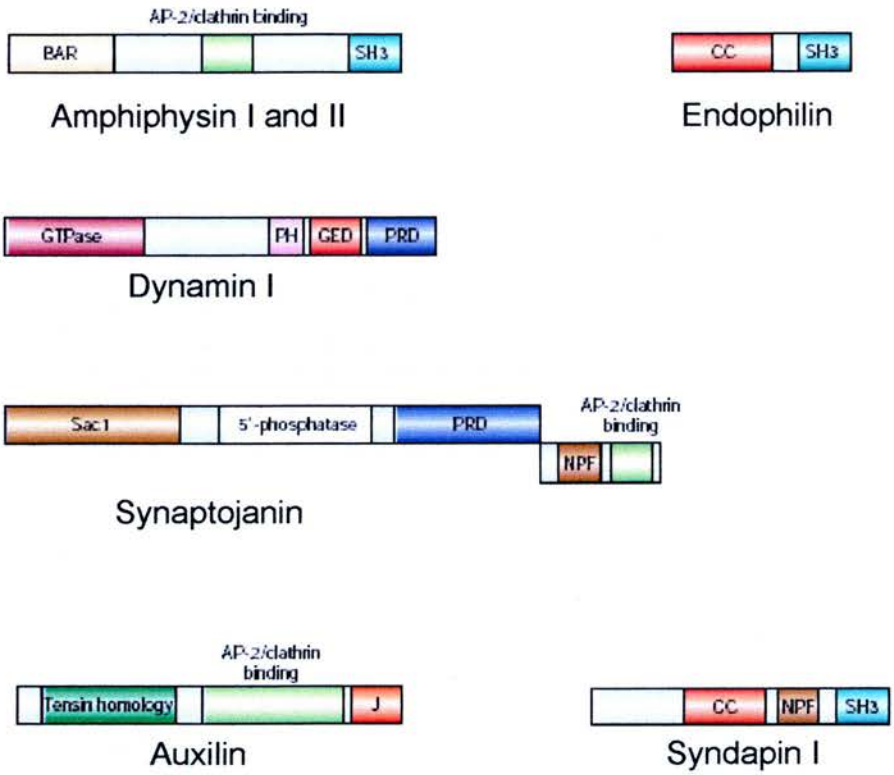

Figure 1.8 – Molecules involved in SV endocytosis (2)

Schematic representation of the modular domain and motif structure of the proteins involved in SV endocytosis. The protein domains are abbreviated as follows: Bin/Amphiphysin/Rvs (BAR) domain for lipid binding and dimerisation, Src-homology (SH3) domain to bind proline rich domains (PRD), coiled-coil (CC) domain, pleckstrin homology (PH) domain for mediating lipid binding, GTPase effector domain (GED), suppressor of actin (Sac) phosphatase domain, Asn-Pro-Phe (NPF) domain to bind Eps15 homology (EH) domains and DNAJ (J) homology domain. Figure adapted from Slepnev and De Camilli, 2000.

The dimerisation of amphiphysin I and II is mediated by the N-terminal domain (Wigge et al. 1997a) and thus the functional dimer unit has two SH3 domains available to bind the PRD of dynamin I. The ability of the dimer to bind multiple dynamin I molecules, *in vitro* at least, can also stimulate the GTPase activity of dynamin I (Wigge et al. 1997a). The SH3 domain of amphiphysin can also bind synaptojanin, the poly-phosphoinositol phosphatase required for uncoating, although with lower affinity than dynamin I (Slepnev and De Camilli 2000).

The amphiphysins can also bind to clathrin and to the α-ear of AP2 (McMahon et al. 1997; Slepnev and De Camilli 2000), targeting them to the forming SV allowing dynamin I recruitment. The crystal structure for the clathrin terminal domain bound to a peptide from amphiphysin I showed that there was another binding site separate to the 'clathrin box' motif termed a W box (consists of the sequence PWXXW). These multiple interactions allow amphiphysin to bind more tightly to clathrin than other proteins (Miele et al. 2004).

The N-terminus of amphiphysin I and II contains a Bin-Amphiphysin-Rvs (BAR) domain, which is a coiled-coil structure required for dimerisation and lipid binding (Zhang and Zelhof 2002). The crystal structure showed this domain to be like an elongated banana-shaped dimer forming a six helix bundle. The helices are amphipathic and the concave surface has several positively charged patches to mediate interaction with the membrane phospholipids (Peter et al. 2004). Amphiphysin has an N-BAR domain which means that the BAR domain has an unstructured region of amino acids at the N-terminus of the BAR domain. Upon

lipid binding these residues form an amphipathic helix and are responsible for the lipid tubulating activity of amphiphysin (Peter et al. 2004).

Amphiphysin can directly stimulate clathrin recruitment *in vitro*, and this recruitment is enhanced when dynamin I is bound to amphiphysin or the free SH3 domain is present, suggesting that amphiphysin binds back on itself so that the C-terminal SH3 domain binds to the central PRD domain. Binding of another PRD domain, for example dynamin, can open the structure allowing access to the clathrin and AP2 binding sites mediating recruitment of amphiphysin, and dynamin I, to the forming SV (Farsad et al. 2003). The ability of amphiphysin to stimulate dynamin I GTPase activity, and thus mediate fission, is dependent on the binding to the lipid bilayer (Takei et al. 1999; Yoshida et al. 2004) and since amphiphysin I and II BAR domain dimers are best suited to a highly curved membrane (Peter et al. 2004), the amphiphysins may preferentially bind to the neck of the SV locating dynamin I for fission (Lee and Schekman 2004). The ability of dynamin I to displace clathrin from amphiphysin would also create a free zone around the neck allowing dynamin I to polymerise into a ring (McMahon et al. 1997).

Another protein, endophilin I, also has a putative role in invagination. Endophilin I is similar in structure to the amphiphysins with an N-terminal BAR domain and C-terminal SH3 domain (fig 1.8, Peter et al. 2004). Endophilin I exists as a homodimer although there are other endophilin isoforms expressed in the brain (Ringstad et al. 2001). The N-terminus of endophilin I also has lysophosphatidic acid acyl transferase (LPAAT) activity suggesting that endophilin can catalyse the conversion

of the inverted-cone shaped lysophosphatidic acid into the cone shaped phosphatidic acid, promoting membrane curvature (Scales and Scheller 1999). However, the catalytic activity is low suggesting that this is not the major function of endophilin (Conner and Schmid 2003).

The SH3 domain of endophilin I binds both the PRD of synaptojanin and dynamin I although synaptojanin binds with higher affinity (Slepnev and De Camilli 2000). The injection of antibodies against endophilin into a lamprey synapse showed a block in endocytosis at the shallow coated pit stage implicating endophilin in the transition between shallow to deeply invaginated pit (Ringstad et al. 1999). Injection of the SH3 domain of endophilin, however, caused a block of endocytosis at the deeply invaginated pit stage, suggesting a role later in invagination and possibly in fission (Gad et al. 2000). Injection of a peptide blocking the SH3 domain of endophilin also caused the accumulation of free clathrin coated SV indicating that endophilin may also have a role in uncoating (Gad et al. 2000).

Genetic studies with loss-of-function mutants in *Drosophila* and *C. elegans* showed that a range of endocytic intermediates were observed and that the phenotype for the loss of synaptojanin (Verstreken et al. 2003) and the loss of endophilin (Schuske et al. 2003) were very similar and thus the two proteins must be part of the same pathway (Song and Zinsmaier 2003). Therefore, the main role of endophilin may be to localise and stabilise synaptojanin at the forming SV (Schuske et al. 2003). However, endophilin can tubulate liposomes via the N-BAR domain (Farsad et al. 2001; Huttner and Schmidt 2002), suggesting an active role in invagination.

Although synaptojanin binds with higher affinity to endophilin than dynamin I, endophilin may also have a role similar to amphiphysin in the targeting of dynamin I to the neck of the SV. The pleiotrophic effects of the disruption of endophilin function may be explained by the multiple roles of this protein.

To summarise invagination, a shallow clathrin coated pit is transformed into a deeply invaginated pit with a narrow neck via the action of BAR domain containing proteins such as amphiphysins I and II and endophilin I. Dynamin I is also recruited to the neck of SV allowing polymerisation for the fission reaction.

1.7.1.4 Clathrin-mediated endocytosis: Fission

The main protein involved in fission of the clathrin coated SV from the plasma membrane in nerve terminals is another dephosphin, the large GTPase dynamin I. Dynamin I was originally discovered as a microtubule binding protein (Shpetner and Vallee 1989), but identification of dynamin I as the homologue of the *Drosophila* protein *shibire* suggested a role in SV endocytosis (van der Bliek and Meyerowitz 1991). Temperature sensitive *shibire* alleles showed that at the restrictive temperature, SV endocytosis was inhibited at a late stage causing paralysis. An accumulation of deeply invaginated pits as well as large invaginations from the plasma membrane were seen and in some cases a ring of electron density around the neck of constricted pits was observed (Kosaka and Ikeda 1983). This electron dense collar was identified as dynamin I.

Dynamin I is one of three isoforms expressed in mammalian tissue. Dynamin I is neuronally expressed whereas dynamin II is ubiquitously expressed and thought to have a role in clathrin-mediated endocytosis in all cell types (Urrutia et al. 1997). A third isoform, dynamin III, is expressed in the testis as well as dendritic spines suggesting a role in post-synaptic recycling (Gray et al. 2003). All of the dynamins are differentially spliced leading to potentially twelve different isoforms expressed in the brain (Urrutia et al. 1997).

Dynamin I consists of four different regions (fig 1.8): an N-terminal GTPase domain, a PH domain for lipid binding, a GTPase effector domain (GED) and a C-terminal PRD (Urrutia et al. 1997; Slepnev and De Camilli 2000; Smillie and Cousin 2005). The PRD domain also contains the sites for dynamin I phosphorylation (Tan et al. 2003; Larsen et al. 2004; Smillie and Cousin 2005). Dynamin I exists as a tetramer (Muhlberg et al. 1997) and when diluted in low ionic strength buffers, assembles into rings and spirals (Hinshaw and Schmid 1995). Self-oligomerisation also stimulates the GTPase activity of dynamin I (Warnock et al. 1996).

The GTPase activity of dynamin I is essential for SV endocytosis. Many of the *shibire* alleles have mutations in or near the GTPase domain, leading to the characteristic block in endocytosis (Urrutia et al. 1997). Similar structures are also observed in nerve terminals treated with the non-hydrolysable GTP analogue GTPγS (Takei et al. 1995). Overexpression of GTPase deficient dynamin I mutants in mammalian cell lines also inhibit receptor-mediated endocytosis at the same constricted coated pit stage, indicating a more general role for dynamin function in

endocytosis (Damke et al. 1994). However, GTPase activity is not sufficient for SV endocytosis and the resulting conformational change induced by GTP hydrolysis is also essential (Marks et al. 2001).

The GTPase activity of dynamin I is regulated by several mechanisms including its phosphorylation status, interaction with membrane phospholipids, interactions with other proteins via the PRD domain and the internal GED domain activated upon oligomerisation (Liu and Robinson 1995). The exact function of the GTPase activity, however, remains to be elucidated.

There are several models of dynamin I action based on the *in vitro* properties of purified dynamin I and point mutations to tease apart the function of the different dynamin I domains. The first model proposes that dynamin I 'pops' the SV off of the plasma membrane. This is based on the finding that on GTP hydrolysis the pitch of the oligomerised dynamin on lipid nanotubules nearly doubles, thus providing the mechanical action to 'pop' off the SV (Stowell et al. 1999; Kelly 1999). The second model is similar to the 'poppase' model except that GTP hydrolysis is proposed to 'pinch' the SV neck. This model is again based on *in vitro* data with dynamin I assembled around liposomes. GTP hydrolysis caused lipid constriction and also facilitated vesiculation suggesting that the conformational change induced upon hydrolysis could provide force to squeeze off the SV (Sweitzer and Hinshaw 1998). Cyro-EM has been used to determine the structure of dynamin I which is in agreement with a large conformational change upon GTP hydrolysis driving membrane constriction (Zhang and Hinshaw 2001; Chen et al. 2004) as well as time

resolved cyro-EM showing that dynamin I can constrict lipid tubules (Danino et al. 2004). In support of this theory, dynamin I mutants which can bind GTP but not hydrolyse it and mutants which have a normal GTPase cycle but cannot transduce the conformation change, all inhibit transferrin uptake implying that both GTPase activity and a conformational change are required for endocytosis (Marks et al. 2001).

Amphiphysin I is thought to target dynamin I to the SV neck and in the presence of amphiphysin I the structure of the dynamin I helix is altered. Amphiphysin I and dynamin I can form ring structures together which neither alone can form in the absence of lipids. Amphiphysin also enhances the vesiculation activity of dynamin I upon addition of GTP (Takei et al. 1999), suggesting a further role for amphiphysin.

The third model suggests that dynamin I acts as a conventional GTPase and that the role of hydrolysis is to activate downstream effectors. Mutations in the GED domains which either inhibited self-assembly, or prevented self-assembly from enhancing GTP hydrolysis, stimulated endocytosis. If dynamin I was acting as a mechanochemical enzyme these mutations would have been expected to inhibit endocytosis. This model suggests that when dynamin I is in the GTP-bound form downstream effectors are recruited to the invaginated pit. As the neck narrows dynamin I self-assembly triggers GTP hydrolysis, dissociating from the downstream effectors and allowing fission. The impairment of self-assembly by the GED mutants prolonged the GTP-dynamin state and therefore could enhance SV formation (Sever et al. 1999; Kelly 1999; Sever et al. 2000; Song and Schmid 2003).

Most recently, studies with the *shibire* mutant showed that the phenotype could be rescued with mutations in the GED domain, illustrating that the GED does act as an internal GTPase activating protein (GAP) which negatively regulates GTPase activity, in line with other conventional GTPases (Narayanan et al. 2005).

Further research will be required to determine whether dynamin I is a mechanochemical enzyme providing force for fission or a regulatory enzyme providing the timing for fission. Comparison of dynamin I with other molecular motors and GTPases has yielded mixed results since dynamin I is a mixture of both (Song and Schmid 2003). Structurally, dynamin I contains the conserved GTPase domain and has as a similar rate of hydrolysis as other GTPases, but has a similar affinity for nucleotides as a motor enzyme. Dynamin I is also unique in that it has a rapid rate of GDP dissociation which neither motor or regulatory enzymes have (Song and Schmid 2003). Another factor not considered is the ability of dynamin I to a bind to wide range of SH3 domain containing proteins and the effects that these could have before or after fission, modifying any model of SV fission (Song and Schmid 2003).

1.7.1.5 Clathrin-mediated endocytosis: Uncoating

The final stage of SV endocytosis involves the uncoating of the clathrin-coated SV. The dephosphin synaptojanin I is a polyphosphoinositide phosphatase which can dephosphorylate PIP_2 to PIP. PIP_2 is a positive regulator of endocytosis and so degradation may facilitate uncoating. Synaptojanin I has two phosphatase domains (fig 1.8) which act at different points on the phosphoinositide ring (Slepnev and De

Camilli 2000). Synaptojanin I also has a C-terminal PRD which binds to the SH3 domain of endophilin. There is an alternative splice variant of synaptojanin I, synaptojanin II which has a C-terminal extension with an NPF motif and an AP2 binding site (Slepnev and De Camilli 2000). Synaptojanin II is ubiquitously expressed and may have a role early in receptor-mediated endocytosis which is distinct to that of synaptojanin I (Rusk et al. 2003).

Synaptojanin I knock out mice (Kim et al. 2002), *C. elegans* null mutants of the synaptojanin homologue (Harris et al. 2000) and injection of synaptojanin antibodies into the lamprey synapse (Gad et al. 2000) all display an increase in the number of clathrin coated pits as well as delays in synaptic transmission suggesting that synaptojanin I has a role in uncoating and trafficking of SVs back to the recycling pool.

Auxilin is also required for uncoating. Auxilin has an N-terminal tyrosine phosphatase-like domain but catalytic activity is not conserved. The functional domains are the AP2 and clathrin binding sites which target auxilin to a coated SV and the J domain which binds and activates the ATPase Hsc70, providing the energy for uncoating (fig 1.8, Slepnev and De Camilli 2000). The interaction between auxilin and Hsc70 is critical to uncoating since peptides which disrupt this interaction inhibit SV recycling and cause a build up of clathrin coated SVs (Morgan et al. 2001). Auxilin binds to the clathrin lattice at a region where several clathrin molecules come together, locating Hsc70 to destabilise the clathrin coat (Fotin et al. 2004). The candidate clathrin box motif in auxilin can also bind to the terminal

domain of the clathrin heavy chain displacing the adapter proteins, such as AP2. This is achieved with a slightly different clathrin box motif which has a higher affinity for clathrin. In this way auxilin could also aid clathrin coat disassembly (Smith et al. 2004).

1.7.1.6 Clathrin-mediated endocytosis: Role of the actin cytoskeleton

The actin cytoskeleton has been implicated in having roles at several stages during the endocytosis process including deformation of the membrane, force generation for the fission reaction, SV detachment from the plasma membrane and trafficking of the newly formed SVs to the recycling pools (Qualmann et al. 2000; Gundelfinger et al. 2003). The actin cytoskeleton could also have a more passive structural role in the organisation and anchoring of endocytic components (Qualmann et al. 2000; Gundelfinger et al. 2003). Application of actin depolymerising drugs has provided inconclusive results (Betz and Henkel 1994; Kuromi and Kidokoro 1998; Job and Lagnado 1998; Shupliakov et al. 2002; Sankaranarayanan et al. 2003). However, perturbation of actin by injection of several different toxins into the lamprey reticulospinal synapse caused inhibition of SV trafficking as well as increasing the proportion of unconstricted clathrin coated pits suggesting that actin does have a role at several stages in endocytosis (Shupliakov et al. 2002).

Several proteins implicated in endocytosis can interact with proteins involved in the regulation of actin polymerisation. The scaffolding protein intersectin, for example, has a C-terminal disabled domain which can interact with Cdc42 and thus activate actin polymerisation. Syndapin I is another candidate to link the endocytic

machinery to actin polymerisation. Syndapin I has a conserved N-terminal coiled coil domain, a central region containing NPF motifs to mediate binding with EH domain containing proteins and a C-terminal SH3 domain (fig1.8). The SH3 domain can bind to dynamin I and to N-WASP, a potent activator of the actin nucleating Arp2/3 complex (Slepnev and De Camilli 2000; Kessels and Qualmann 2004). The SH3 domain of syndapin I is able to inhibit endocytosis (Qualmann and Kelly 2000; Qualmann et al. 2000; Slepnev and De Camilli 2000; Kessels and Qualmann 2004), suggesting this region is required for endocytosis, perhaps through regulating localised actin polymerisation to sites of endocytosis (Qualmann et al. 2000; Kessels and Qualmann 2004).

1.7.1.7 Clathrin-mediated endocytosis: re-setting the system

The dephosphins exist in the nerve terminal in their phosphorylated form and therefore are rephosphorylated following SV endocytosis. The requirement of the rephosphorylation for SV endocytosis was investigated using protein kinase inhibitors (Cousin et al. 2001; Tan et al. 2003). The kinase inhibitors did not block the first round of exo/endocytosis but strongly inhibited endocytosis following a second stimulation (Cousin et al. 2001; Tan et al. 2003). This is logical since before the first stimulation the dephosphins will be in the phosphorylated state. This means that dephosphorylation is required before the kinase inhibitors can inhibit rephosphorylation, explaining why inhibition of SV endocytosis is not observed until after a second stimulation. These experiments showed that rephosphorylation was just as important as dephosphorylation for the maintenance of synaptic transmission.

However, where there is one phosphatase, calcineurin, which dephosphorylates all of the dephosphins, there is not an equivalent kinase. To date, cyclin dependent kinase 5 (Cdk5) has been identified as a dephosphin kinase but Cdk5 is so far only responsible for the rephosphorylation of dynamin I (Tan et al. 2003; Larsen et al. 2004), synaptojanin I (Lee et al. 2004) and PIPKIγ (Lee et al. 2004) *in vivo*, despite other dephosphins being Cdk5 substrates *in vitro* (Tomizawa et al. 2003). PKC inhibitors, which are also active against Cdk5, failed to inhibit the rephosphorylation of AP180 and amphiphysin (Cousin et al. 2001) and thus there is at least one more dephosphin kinase unidentified.

1.7.2 Endocytosis: Bulk retrieval

Bulk retrieval at the synapse may well be required when the synapse is stimulated hard or at high frequency and the normal modes of SV retrieval cannot keep up. Certainly with increasing strength of stimulation the speed of SV retrieval decreases, suggesting that SV endocytosis has a limited capacity and can be saturated (Sankaranarayanan and Ryan 2000). Bulk retrieval is characterised by large infoldings of the plasma membrane, or cisternae, which can remain attached by a tubulated neck to the plasma membrane or have detached from the membrane (Royle and Lagnado 2003). These structures have been observed in several systems suggesting that this is a common method of SV recycling (Takei et al. 1996; Gad et al. 1998; Teng et al. 1999; Teng and Wilkinson 2000; Richards et al. 2000; Paillart et al. 2003; Royle and Lagnado 2003).

The molecules involved in bulk retrieval have not been identified to date but the formation of the cisternae appears to be clathrin-independent since the structures are not clathrin coated (Richards et al. 2000; Royle and Lagnado 2003). There are several proteins in nerve terminals with the ability to tubulate liposomes in the absence of clathrin, such as epsin, amphiphysin and endophilin, and thus it has been proposed that these proteins may represent the minimum machinery that can operate when the synapse is depleted of clathrin-dependent factors (Royle and Lagnado 2003). SVs can then bud off of the cisternae when the machinery becomes available. Clathrin-coated buds have been observed on cisternae in lamprey and snake motor terminals (Shupliakov et al. 1997; Teng and Wilkinson 2000; Royle and Lagnado 2003). Dynamin I is also predicted to have a role in bulk retrieval too since the cisternae remain attached to the plasma membrane in *shibire* mutants at the restrictive temperature (Koenig and Ikeda 1996; Royle and Lagnado 2003).

1.7.3 Endocytosis: 'Kiss and run'

'Kiss and run' endocytosis is a more rapid mechanism of SV retrieval where the SVs do not completely fuse with the plasma membrane but following opening of the fusion pore, reseal and pinch off of the membrane. This is potentially the principal route of SV recycling during mild stimulation. At high frequency or during prolonged stimulation, the synapse can no longer keep up and thus evokes the slower, clathrin-mediated pathway. 'Kiss and run' has been documented in chromaffin cells through the use of parallel capacitance measurements and amperometry (Ales et al. 1999) but direct evidence of 'kiss and run' in nerve

terminals has been made more difficult to obtain due to the size of the SVs and the speed with which they recycle.

Indirect evidence of the existence of 'kiss and run' in nerve terminals has been obtained using fluorescent styryl dyes with different membrane departitioning times. During full fusion, there is enough time for the dye to fully departition from the membrane regardless of the affinity. However, during 'kiss and run', the pore is open only transiently and so dyes with longer departitioning times are unable to be released. This discrepancy was observed in hippocampal neurons and taken to be evidence for 'kiss and run' (Klingauf et al. 1998; Kjaerulff et al. 2002).

Comparison of the amount of dye and neurotransmitter released has also suggested the existence of 'kiss and run'. For example, in two different studies there was no effect on the amount of dye released compared to control, but an increase in neurotransmitter release when synaptosomes were stimulated with 4-aminopyridine (4-AP). The difference was proposed to be due to 'kiss and run' release since the pore is open long enough to discharge the neurotransmitter but not the dye (Cousin and Robinson 2000b; Baldwin et al. 2003).

Studies with mutant proteins involved in endocytosis have also suggested that 'kiss and run' is present at nerve terminals. The synaptic defect caused by *shibire* mutants at the restrictive temperature was present within 20ms which is too fast to be due entirely to SV depletion from arrested clathrin-mediated endocytosis, implicating dynamin in the control of 'kiss and run' (Kawasaki et al. 2000; Kjaerulff et al. 2002).

When endophilin function in *Drosophila* was ablated the larval neuromuscular junction had an expanded pre-synaptic membrane, was depleted of SVs and was unable to take up styryl dyes, indicating inhibition of endocytosis. However, mutant larvae were able to sustain 15 – 20% of neurotransmitter release at high stimulation suggesting that another pathway, 'kiss and run', was able to maintain neurotransmission (Verstreken et al. 2002; Kjaerulff et al. 2002). There is also some evidence that dynamin I and synaptophysin may be involved in a clathrin-independent method of SV recycling since disruption of this interaction caused an increase in the number of coated SVs suggesting that the clathrin-dependent mode of recycling had an increased load (Daly et al. 2000).

Recently, direct capacitance measurements at the Calyx of Held have enabled measurement of the mean fusion pore open time. The time measured was very short (56 ms) and found to increase with stronger stimulation, suggesting that the synapse did switch the mode of recycling with increasing stimulation (Sun et al. 2002; Kjaerulff et al. 2002). Capacitance measurements of single SVs at posterior pituitary neurons showed that capacitance increases, reflecting membrane fusion, were rapidly followed by capacitance decreases of the same amplitude, reflecting membrane retrieval or closure of the fusion pore (Klyachko and Jackson 2002; Kjaerulff et al. 2002).

The data gained from experiments in neuronal cells points to a major role for 'kiss and run' recycling at central synapses, although more research into the molecular mechanisms and regulation of the process is required for a better understanding.

1.7.4 Endocytosis: Clathrin-independent

There are also clathrin-independent mechanisms of endocytosis operating inside a cell, thought to have roles in cell-surface recycling and remodelling, regulation of plasma membrane lipid composition and regulation of signal transduction (Nichols and Lippincott-Schwartz 2001). These pathways are less well characterised than clathrin-dependent endocytosis but they generally do not involve coat complexes or budding of vesicles and instead use specialised regions of the plasma membrane (Nichols and Lippincott-Schwartz 2001).

Caveolar uptake predominates in endothelial cells and involves the formation of non-coated plasma membrane invaginations characterised by the presence of cholesterol binding proteins called caveolins. Caveolins and the cargo to be internalised localise to lipid rafts on the membrane (Nichols and Lippincott-Schwartz 2001). Lipid rafts are regions of the plasma membrane which are resistant to detergents and are enriched in cholesterol, glycosphingolipids, glycosylphosphatidylinositol (GPI)-anchored proteins and some membrane proteins. Interestingly, proteins endocytosed by a clathrin-dependent mechanism are generally excluded from these regions (Nichols and Lippincott-Schwartz 2001). There is also a role for dynamin in the budding of caveolae, and *in vitro* dynamin is able to cause vesiculation of the caveolae (Henley et al. 1998; Nichols and Lippincott-Schwartz 2001). Dynamin II binds directly to caveolin I and can inhibit cholera toxin uptake possibly implicating dynamin II in caveolar uptake (Yao et al. 2005).

Macropinocytosis is used by some cells to recycle membrane components and is the formation of large, irregular endocytic vesicles formed from lamellipodia generated at the ruffling edge of a motile cell. The components of a macropinosome are not thought to be different to the lamellipodia although they may well be enriched in some way from the plasma membrane. The recycling of the membrane probably involves the small GTPase ARF6 since mutants of ARF6 cause an increase in ruffling and the accumulation of macropinosomes (Nichols and Lippincott-Schwartz 2001). Bulk endocytosis has been proposed to be similar to macropinocytosis due to the actin and PI3K requirements (Holt et al. 2003; Richards et al. 2004).

In some cell types caveolin is not expressed and thus there are no caveoli but there is a further mode of constitutive clathrin-independent endocytosis which can be identified when clathrin-dependent endocytosis is arrested. This pathway is cholesterol sensitive and functions to transport plasma membrane lipids and lipid raft markers to the Golgi. The molecular mechanisms of this pathway are unknown but ARF6 is implicated (Nichols and Lippincott-Schwartz 2001).

Some proteins, such as the epidermal growth factor receptor (EGFR) can be internalised by both clathrin-dependent and clathrin-independent pathways. The switch between pathways appears to involve the ubiquitination of the receptor. The EGFR is internalised by a standard clathrin-dependent mechanism but when ubiquitinated, the EGFR is internalised completely through a lipid raft, clathrin-independent pathway (Sigismund et al. 2005). This pathway was dependent on

proteins with ubiquitin interacting motifs implicating several endocytosis proteins, such as epsin and eps15 in this clathrin independent pathway (Sigismund et al. 2005).

1.8 The regulation of SV endocytosis by Ca^{2+}

The processes of exocytosis and endocytosis are intimately linked to the Ca^{2+} influx following nerve terminal depolarisation. Both processes require Ca^{2+} and therefore many of the protein-lipid and protein-protein interactions involved in SV recycling are regulated by Ca^{2+}.

Ca^{2+} influx upon nerve terminal stimulation has long been accepted as being the trigger for SV exocytosis and the picture emerging now is that Ca^{2+} is also required for SV endocytosis (Cousin 2000). For a long time it was assumed that SV endocytosis was Ca^{2+}-independent and only required SV exocytosis to precede it. However, experiments using α-latrotoxin to stimulate mass exocytosis in the absence of Ca^{2+} showed that SV endocytosis only occurred after the addition of Ca^{2+} (Henkel and Betz 1995; Ramaswami et al. 1994). Endocytosis was also inhibited in the lamprey by removal of Ca^{2+} following exocytosis, with re-introduction of Ca^{2+} stimulating the process (Gad et al. 1998). Chelation of Ca^{2+} also inhibits SV endocytosis (Mansvelder and Kits 1998) and substitution of Ca^{2+} with other divalent cations such as Ba^{2+} (Marks and McMahon 1998; Cousin and Robinson 1998) or Sr^{2+} (Guatimosim et al. 1998) does not support SV endocytosis, underlying the importance of Ca^{2+} influx in the process (Cousin 2000).

Recent work studying Ca^{2+} influx at the *Drosophila* neuromuscular junction has suggested that the Ca^{2+} influx which stimulates exocytosis is not mediated by the same Ca^{2+}-channels that stimulate endocytosis. Kuromi and colleagues (2004) used different Ca^{2+}-channel blockers and found that treatment with a spider toxin, PLTXII, inhibited exocytosis whereas treatment with flunarizine and lanthanum preferentially inhibited endocytosis. The differential effects of the toxins suggested that there were different Ca^{2+} entry routes into the nerve terminal. Modelling this, the authors proposed that the Ca^{2+}-channels which could be blocked with PLTXII were found at the active zone, whereas the Ca^{2+}-channels which were inhibited with flunarizine or lanthanum and thus predominantly involved in endocytosis, were outside the active zone at sites of clathrin-mediated endocytosis (Kuromi et al. 2004).

Although both SV exocytosis and endocytosis are dependent on Ca^{2+}, the Ca^{2+} sensitivity of the two processes is very different. SV endocytosis can be stimulated with as little as 0.1 mM extracellular Ca^{2+} where as 1.3 mM Ca^{2+} is required to stimulate exocytosis effectively (Marks and McMahon 1998). This means that when exocytosis is activated, endocytosis will always be activated, suggesting why endocytosis may have appeared to be Ca^{2+}-independent (Cousin 2000). The other conclusion which can be drawn is that the Ca^{2+}-sensor for SV endocytosis has a higher affinity for Ca^{2+} than that for SV exocytosis (Cousin 2000).

Once SV endocytosis has been initiated by Ca^{2+}, the process can proceed in its absence (Cousin 2000). This has been shown in hippocampal neurons (Ryan et al.

1996) as well as in lamprey neurons (Gad et al. 1998) illustrating that once SV endocytosis has been triggered, it is predominantly Ca^{2+}-independent (Cousin 2000).

1.8.1 The Ca^{2+} sensor for SV endocytosis

Synaptotagmin is thought to be the Ca^{2+} sensor for SV exocytosis. It is unlikely to be the Ca^{2+} sensor for endocytosis since the Ca^{2+} affinity of the sensor is higher than that of synaptotagmin (Cousin 2000) and SV endocytosis specifically requires Ca^{2+}, whereas exocytosis can be stimulated with other divalent cations (Marks and McMahon 1998; Cousin and Robinson 1998; Cousin 2000).

A potential candidate for the Ca^{2+} sensor is calmodulin. Calmodulin has two EF-hand motifs for binding Ca^{2+} separated by a flexible helical linker region (Voet and Voet 1995). Ba^{2+} and Sr^{2+} cannot substitute for Ca^{2+} and activate calmodulin (Robinson and Dunkley 1983), giving calmodulin the correct selectivity to be the endocytosis Ca^{2+} sensor. Calmodulin has also been implicated in endocytosis in chromaffin cells as a result of anti-calmodulin reagents inhibiting endocytosis (Artalejo et al. 1996).

A downstream target of calmodulin is calcineurin (Cousin 2000; Bandyopadhyay et al. 2004) and since calcineurin is essential for SV endocytosis (Marks and McMahon 1998; Cousin et al. 2001), this suggests that calmodulin does have a role in activating the endocytosis machinery upon Ca^{2+} influx.

1.8.2 Regulation of dynamin I by Ca^{2+}

Once activated by calmodulin, calcineurin can dephosphorylate the dephosphins (Cousin 2000). Calcineurin has been shown to interact with dynamin I in a Ca^{2+}-dependent manner (Lai et al. 1999). When this interaction was disrupted with peptides in PC12 cells clathrin-mediated endocytosis was inhibited, revealing the physiological relevance of this interaction (Lai et al. 1999). Since the interaction is Ca^{2+}-dependent, this also adds an extra level of regulation to prevent the activation of the endocytosis machinery prematurely. This complex can also interact with amphiphysin although this interaction is mediated by dynamin I and is not Ca^{2+}-dependent (Lai et al. 1999).

In the presence of high concentrations of Ca^{2+}, dynamin I can form a complex with the integral SV protein, synaptophysin (Daly and Ziff 2002). Disruption of this interaction inhibits neurotransmitter release during high frequency stimulation, suggesting an inhibition of SV recycling (Daly et al. 2000). Electron microscopy of squid giant synapses injected with the GST-C-terminus of synaptophysin showed depletion of synaptic vesicles and an increase in the number of clathrin coated synaptic vesicles (Daly et al. 2000). The authors suggest that the dynamin I – synaptophysin interaction could be important for a clathrin independent form of recycling, explaining why the defect is only apparent at high frequency stimulation and that the increase in clathrin-coated synaptic vesicles is due to the clathrin pathway having to compensate (Daly et al. 2000). Further investigation will be required to determine if dynamin I does have a role in clathrin-independent endocytosis.

Dynamin I can also be regulated directly by Ca^{2+}. The PRD domain of dynamin I is the site of Ca^{2+} binding, since enzymatic digestion of the PRD eliminated Ca^{2+} binding (Liu et al. 1996). Interestingly, phosphorylated dynamin I bound more Ca^{2+} than non-phosphorylated dynamin I (Liu et al. 1996). Ca^{2+} binding also inhibited the GTPase activity of dynamin I, as well as the ability of dynamin I to vesiculate phospholipids (Cousin and Robinson 2000b). Therefore the *in vitro* binding of Ca^{2+} to dynamin I may be of physiological relevance since its essential enzymatic activity is regulated, and thus by extrapolation, the efficiency of SV endocytosis. An interesting paradox, however, is apparent since Ca^{2+} inhibits the GTPase and vesiculation activity of dynamin but also promotes endocytosis. Cousin and Robinson (2000a) addressed this with their Ca^{2+} shunting model of SV endocytosis. They proposed that high levels of Ca^{2+}, such as would be experienced at the active zone, would prevent endocytosis occurring in this area since 20 - 30μM is sufficient to inhibit the GTPase and vesiculation activity of dynamin I. This would allow exocytosis to continue unobstructed in this region. The internal Ca^{2+} concentration decreases exponentially from the active zone and thus outside of the active zone, dynamin I activity is not inhibited, allowing endocytosis to proceed (Cousin 2000; Cousin and Robinson 2000a).

1.8.3 Ca^{2+} regulates other proteins involved in SV endocytosis

Coupling of the endocytic machinery to the sites of endocytosis can also be regulated by Ca^{2+}. Voltage-gated Ca^{2+} channels would seem a logical choice to anchor the endocytic machinery to the sites at the plasma membrane for endocytosis since the Ca^{2+} signal enters neurons and stimulates exocytosis at these sites. Endophilin has

been isolated as a binding partner of voltage gated Ca^{2+} channels and this interaction is Ca^{2+}-dependent (Chen et al. 2003). A mutant of endophilin which constitutively binds to Ca^{2+}-channels inhibits SV endocytosis - presumably because it occupies the binding sites for endogenous endophilin preventing correct localisation and function. This suggests that there is a role for the localisation of the endocytic machinery directly to Ca^{2+}-channels.

The binding of Ca^{2+} to endophilin also regulates the interaction between endophilin and dynamin I. Both complexes dissociate at high Ca^{2+} concentrations when the Ca^{2+}-channels are open (Chen et al. 2003). A model has been proposed where at low Ca^{2+} concentrations, endophilin can interact with both Ca^{2+} channels and dynamin I. As the Ca^{2+} concentration increases upon depolarisation, endophilin binds Ca^{2+}, increasing the affinity of the C-terminal SH3 domain of endophilin for the central PRD, i.e. the endophilin molecule bends back on itself. This conformation prevents interaction with Ca^{2+}-channels and dynamin I, releasing endophilin and dynamin I for endocytosis (Chen et al. 2003). This model would place endophilin at the beginning of the endocytosis pathway, however, injection of a peptide consisting of the endophilin binding site on synaptojanin and injection of the SH3 domain of endophilin lead to inhibition of endocytosis at a late stage (Gad et al. 2000). Likewise, an endophilin null mutant in *Drosophila* revealed an accumulation of late endocytic vesicle profiles (Fabian-Fine et al. 2003). Furthermore, injection of anti-endophilin antibodies resulted in accumulation of shallow pits, suggesting a role for endophilin in the invagination process (Ringstad et al. 1999). Upon initial inspection the studies discussed above appear contradictory to the Chen model; however, it may

be that endophilin has distinct roles at several stages of the SV pathway and thus further work requires to be done to dissect out the roles of endophilin.

The Ca^{2+} binding protein calmodulin, essential for the activation of calcineurin upon nerve terminal depolarisation also participates in a Ca^{2+}-dependent interaction with growth associated protein (GAP) 43. GAP43 has a role in SV endocytosis and neuronal plasticity and binds calmodulin when the Ca^{2+} concentration inside the neuron is low. Following stimulation, the intracellular Ca^{2+} concentration is high, causing dissociation of calmodulin and GAP43 (Neve et al. 1998). This releases GAP43 to interact with proteins such as rabaptin-5, an effector of the GTPase Rab5 involved in membrane fusion (Neve et al. 1998). By the same logic calmodulin is also released from GAP43 upon depolarisation freeing it to mediate the activation of SV endocytosis. However, calmodulin is activated by relatively low levels of Ca^{2+} (K_D of 0.5 – 5 μM, (Chin and Means 2000)) and is very abundant in neurons (10 – 100 μM, (Xia and Storm 2005)) making the release from GAP43 unlikely to be a rate limiting step in the activation of SV endocytosis.

1.9 The regulation of SV endocytosis by phosphorylation

Phosphorylation is the most common covalent modification of proteins in cells (Liu 1997) and allows very dynamic and reversible regulation of protein-protein interactions. Ca^{2+} acts as a trigger for both SV exocytosis and endocytosis but the coordinated phosphorylation and dephosphorylation of proteins upon nerve terminal stimulation controls many interactions essential for efficient SV cycling.

1.9.1 Phosphorylation of endocytosis proteins on stimulation

The AP2 complex is phosphorylated on several subunits, although it is the phosphorylation of the μ2 subunit which is important for binding to phospholipids and internalisation motifs on cargo proteins. There is no direct evidence to date to prove that μ2 subunit phosphorylation is stimulated upon nerve terminal depolarisation but there is evidence to suggest that phosphorylation is required to elicit a conformational change to facilitate tighter binding of AP2 to the phospholipid membrane and to internalisation motifs (Honing et al. 2005). Without this, AP2 would not be able to efficiently nucleate clathrin coat polymerisation.

The μ2 subunit is phosphorylated on threonine 156 by adapter-associated kinase 1 (AAK1, Conner and Schmid 2002) and phosphorylation by AAK1 increases the affinity of μ2 for internalisation motifs (Ricotta et al. 2002). Mutation of threonine 156 to alanine substantially inhibited transferrin uptake illustrating the importance of this phosphorylation site for efficient endocytosis (Olusanya et al. 2001). AAK1 was originally identified as a binding partner for the α ear domain of AP2 but AAK1 also contains several endocytic interaction motifs including a DPF motif, a NPF motif and a DLL motif (Flett et al. 2005) to localise AAK1 to the sites of endocytosis. DLL motifs are recognised by the clathrin heavy chain and clathrin can activate the kinase activity of AAK1 (Jackson et al. 2003; Flett et al. 2005). However, mutation of the DLL motif failed to totally inhibit binding to clathrin and had little effect on the activation of AAK1 suggesting that clathrin binding to this motif is not the only regulator of this kinase (Flett et al. 2005). Further investigation into the regulation of the kinase is required to fully understand the mechanisms of activation, but

phosphorylation of the μ2 subunit does appear to have an important role in endocytosis.

1.9.2 Dephosphorylation upon stimulation: the dephosphins

Dephosphorylation, and in particular, that of the dephosphins is crucial for SV endocytosis. The dephosphins, amphiphysin I and II, AP180, epsin, eps15, dynamin I, synaptojanin (Cousin and Robinson 2001) and PIPKIγ (Wenk et al. 2001), are all co-ordinately dephosphorylated upon nerve terminal depolarisation by calcineurin and rephosphorylated following the termination of SV endocytosis by their respective kinases. Both the dephosphorylation and the rephosphorylation are required to maintain multiple rounds of neurotransmitter release (Cousin and Robinson 2001).

Phosphorylation of the dephosphins, and several other endocytosis proteins, prevents interactions required for the formation of clathrin-coated vesicles and thus dephosphorylation stimulates SV endocytosis (Cousin and Robinson 2001). These interactions are summarised in figure 1.9.

The α and β2 subunits of AP2 and the clathrin heavy and light chains are phosphoproteins *in vivo* (Wilde and Brodsky 1996). The phosphorylation sites of the α and β2 subunits are in the hinge regions of these subunits, which are the regions implicated in clathrin binding. *In vitro* clathrin-binding assays showed that the phosphorylated AP2 subunits could no longer bind clathrin (Wilde and Brodsky 1996), suggesting that AP2 α and β2 subunits have to be dephosphorylated for

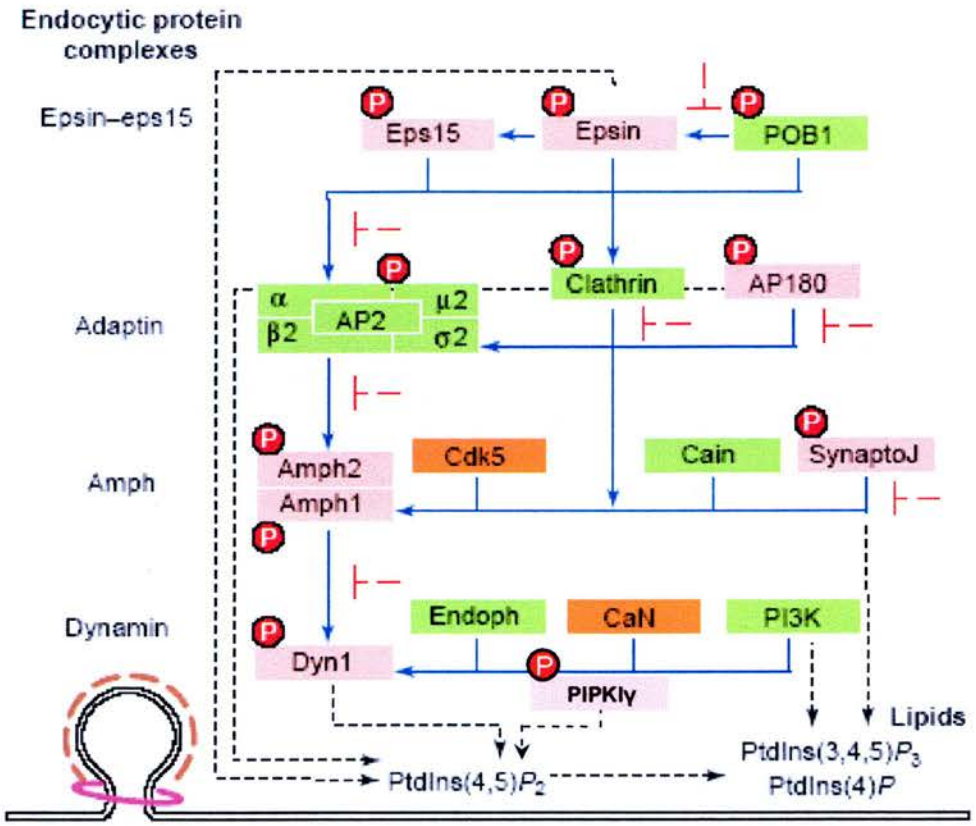

Figure 1.9 – Interactions controlled by phosphorylation in SV endocytosis

Phosphorylation inhibits many of the protein-protein interactions involved in SV endocytosis. The schematic shows only the interactions known to be regulated by phosphorylation. The dephosphins (pink) are epsin, eps15, AP180, amphiphysin (Amph) 1 and 2, synaptojanin (SynaptoJ), dynamin I (Dyn 1) and PIP kinase Iγ (PIPKIγ). The other endocytosis proteins (green) are partner of Ral-binding protein 1 (POB1), adapter protein 2 (AP2), clathrin, cain, endophilin (Endoph) and phosphatidylinositol-3-kinase (PI3K). Essential interactions are shown by blue lines and those inhibited by phosphorylation as shown by pink dashed lines. Interactions with membrane phospholipids are shown by black dashed lines. Adapted from Cousin and Robinson, 2001.

binding to occur. β2 subunit dephosphorylation has been shown to be mediated by PP2A and rephosphorylated by a staurosporine-sensitive kinase. Incubation of cells with a PP2A inhibitor, okadaic acid, also inhibited transferrin uptake, implying dephosphorylation was required for endocytosis (Lauritsen et al. 2000). Although a cycle of phosphorylation of the AP2 subunits exists no demonstration of stimulation-dependent dephosphorylation is apparent at this stage.

Phosphorylation of AP180 by casein kinase II inhibits its interaction with AP2 and impairs clathrin-coat assembly (Hao et al. 1999) and the interactions of epsin and eps15 with AP2 are stimulated by their dephosphorylation (Chen et al. 1999), further suggesting that dephosphorylation is crucial for complex formation.

The ability of amphiphysin to regulate the final stages of SV endocytosis are dependent on its phosphorylation state as well as the phosphorylation of several binding partners (Cousin and Robinson 2001), ensuring that the fission reaction does not proceed at the wrong time or place. Phosphorylation of amphiphysin inhibits the interaction with the α-ear domain of AP2 (Slepnev et al. 1998), preventing localisation of amphiphysin to sites of endocytosis. When brain lysate was incubated with ATP to promote phosphorylation, binding of dynamin I and synaptojanin I to the SH3 domain of amphiphysin was reduced (Slepnev et al. 1998), suggesting that phosphorylation potentially inhibits the targeting of the fission complex and the uncoating machinery. However, other studies have shown that dynamin I phosphorylated by Cdk5 does not affect binding of the SH3 domain of amphiphysin although does inhibit binding of the endophilin SH3 domain (Solomaha et al. 2005).

In vitro studies also showed that the binding of dynamin I to amphiphysin prevented the phosphorylation of dynamin I, suggesting that dissociation of the two proteins is required before rephosphorylation can take place (Tan et al. 2003). Interestingly, not all the amphiphysin interactions are regulated by phosphorylation since binding of the SH3 domain to clathrin and the α and β2 subunits of AP2 is independent of their phosphorylation state (Slepnev et al. 1998).

Synaptojanin I is phosphorylated on serine 1144 by Cdk5. This serine residue is adjacent to the endophilin binding site and mimicking phosphorylation by mutation to aspartic acid inhibited the interaction with endophilin (Lee et al. 2004). Endophilin stimulates the phosphatase activity of synaptojanin and so prevention of this interaction indirectly regulates the amount of PIP_2 available. Synaptojanin can also be phosphorylated by the ephrin receptor kinase and again, phosphorylation inhibits binding of endophilin (Irie et al. 2005). Ephrin signalling is thought to be important for AMPA receptor internalisation and expression of a kinase dead mutant of the ephrin receptor kinase inhibits internalisation (Irie et al. 2005). It is possible then that phosphorylation of synaptojanin on a tyrosine residue stimulates an early phase of endocytosis while dephosphorylation is important for a late phase involving the interaction with endophilin (Hopper and O'Connor 2005).

Dephosphorylation on nerve terminal stimulation may also have a role in the localisation of the proteins required for endocytosis to the sites of endocytosis on the plasma membrane (Cousin and Robinson 2001). The majority of the dephosphins as well as the α and β subunits of AP2 and clathrin are unbound cytosolic proteins

which are phosphorylated at rest (Slepnev et al. 1998; Cousin and Robinson 2001). They can then translocate to the plasma membrane upon depolarisation induced dephosphorylation. Phosphorylation reverses this and thus a cycle of phosphorylation may regulate the cycling of these proteins. By maintaining the proteins in the cytosol in a form which does not favour their interaction, futile and premature complex formation can be prevented (Cousin and Robinson 2001).

1.9.3 The regulation of dynamin I by phosphorylation

Dynamin I was the first dephosphin to be characterised and was found to undergo a rapid stimulation-dependent dephosphorylation (< 5s) followed by a much slower rephosphorylation (half-time of 40s) upon termination of stimulation (Robinson et al. 1994). The rephosphorylation time correlates well with the time for SV recycling (Robinson et al. 1994) supporting the role for rephosphorylation as well as dephosphorylation.

Calcineurin was identified as the dynamin I phosphatase since the calcineurin inhibitor, cyclosporin A, prevented the stimulation-dependent modulation of intrinsic GTPase activity (Liu et al. 1994b). Calcineurin was also able to dephosphorylate dynamin I *in vitro* and has a high affinity for dynamin I (Liu et al. 1994b). Cyclosporin A also prevented the dephosphorylation of dynamin I, synaptojanin and amphiphysins I and II *in vivo*, confirming that calcineurin was the physiological dynamin I phosphatase (Marks and McMahon 1998).

Several kinases phosphorylate dynamin I *in vitro*, including casein kinase II (Robinson et al. 1993), Cdc2 kinase (Hosoya et al. 1994), minibrain kinase (Chen-Hwang et al. 2002), mitogen-activated protein kinase (MAPK) Erk2 (Earnest et al. 1996) and PKC (Robinson et al. 1993; Powell et al. 2000). Dynamin I is an excellent PKC substrate and PKC inhibitors block dynamin I rephosphorylation *in vivo* (Cousin et al. 2001), initially suggesting that PKC was the *in vivo* kinase. However, PKC did not fully fit the profile of a dephosphin kinase, since it is maximally active during nerve terminal depolarisation when intracellular Ca^{2+} levels are high. The dephosphin kinase however, would be predicted to be maximally active following exo- and endocytosis and thus during nerve terminal repolarisation when the Ca^{2+} levels were low. Dynamin I also had a different phosphorylation profile to other PKC substrates, such as myristoylated alanine-rich C-kinase substrate (MARCKS) and GAP43, which were phosphorylated on stimulation, not dephosphorylated (Robinson et al. 1994).

This conflict was resolved with the identification of Cdk5 as the *in vivo* dynamin I kinase (Tan et al. 2003). Cdk5 inhibitors block the rephosphorylation of dynamin I in synaptosomes and expression of dominant negative Cdk5 in neuronal culture inhibits dynamin I rephosphorylation (Tan et al. 2003). The PKC inhibitors used in previous studies also potently inhibit Cdk5 activity (Tan et al. 2003), and therefore masked the identity of the kinase. Cdk5 is constitutively active in nerve terminals thus explaining the problem of the kinase requiring activation (Smillie and Cousin 2005) and the slow rephosphorylation profile since rephosphorylation would be

competing against calcineurin-mediated dephosphorylation as long as the Ca^{2+} signal was present.

The phosphorylation sites of *in vitro* phosphorylated dynamin I were determined by mass-spectrometry to be serines 774 and 778 in the PRD (Tan et al. 2003). These sites were also found to be the *in vivo* phosphorylation sites (Tan et al. 2003; Larsen et al. 2004) and are distinct from the *in vitro* PKC phosphorylation site, serine 795 (Powell et al. 2000). Threonine 780 has also been proposed to be a physiologically relevant Cdk5-dependent dynamin I phosphorylation site (Tomizawa et al. 2003). However, this was an *in vitro* study using Cdk5 phosphorylated dynamin I and thus may not reflect the *in vivo* phosphorylation sites. The interpretation of the mass spectrometry data is also subject to intense debate – analysis of the presented data showed that it is compatible with phosphorylation of serine 778 as well as threonine 780 (P.J. Robinson, personal communication). The inhibition of endocytosis seen following mutation of the threonine 780 (Tomizawa et al. 2003) could also be explained by stearic hinderance of serines 774 and 778 which are in very close proximity to threonine 780. A more recent paper using a new protocol allowing better purification of phosphopeptides prior to mass-spectrometry, has shown that there was no detectable phosphate on threonine 780 on endogenous dynamin I, confirming that serines 774 and 778 are the *in vivo* sites (Larsen et al. 2004). Interestingly, when the peptides were singly phosphorylated, it was serine 774 that was predominantly phosphorylated suggesting that this site may be more important than serine 778 in the phosphoregulation of dynamin I (Larsen et al. 2004).

In vitro studies looking at the effect of phosphorylation on the biological activity of dynamin I have shown that phosphorylation regulates its GTPase activity as well as interactions with other proteins and lipids. Studies conducted with PKC phosphorylated dynamin I showed a twelve fold increase in GTPase activity (Robinson et al. 1993), however, the protocol used stimulated self-assembly which also stimulates the GTPase activity, and further analysis with a different protocol showed that PKC did not in fact stimulate GTPase activity (Tan et al. 2003, supplementary data). Using this protocol, Cdk5 was able to stimulate the GTPase activity, albeit only three fold, but the data illustrates that phosphorylation may have a role in the regulation of GTPase activity.

Protein-protein and protein-lipid dynamin I interactions can also be regulated by dynamin I phosphorylation. However, since most of the studies have been conducted *in vitro*, the results have to be interpreted with some caution when being applied *in vivo*. Incubation of a brain lysate with ATP and phosphatase inhibitors to enhance the phosphorylated states of the endocytosis proteins showed that global phosphorylation reduced binding of dynamin I to amphiphysin (Slepnev et al. 1998). *In vitro* phosphorylation of purified dynamin I with minibrain kinase (Chen-Hwang et al. 2002) or Cdk5 (Tomizawa et al. 2003) also inhibited binding to amphiphysin but *in vitro* phosphorylation of the PRD of dynamin I with Cdk5 did not (Tan et al. 2003). Further studies *in vivo*, will be required to determine the effect of phosphorylation on dynamin I protein interactions with amphiphysin and other proteins.

Phosphorylated dynamin I is found exclusively in the cytosol of nerve terminals (Liu et al. 1994a) and the phosphorylation of dynamin I, *in vitro*, with either PKC (Powell et al. 2000) or Cdk5 (Tan et al. 2003) decreased binding to phospholipids. Mutations in the domain responsible for lipid binding (PH domain) also prevented association of dynamin I with the plasma membrane (Vallis et al. 1999). Taken together, dephosphorylation of dynamin I upon nerve terminal stimulation may facilitate translocation of dynamin I from the cytosol to the plasma membrane. Rephosphorylation could then decrease the affinity for phospholipids, aiding in the return of dynamin I to the cytosol ready for the next round of endocytosis (Smillie and Cousin 2005).

Dynamin I was first discovered as a phosphoprotein in 1991 (Robinson 1991) and in the intervening decade and a half, the biochemical properties of this GTPase have been characterised. Now that the *in vivo* phosphatase and kinase have been identified and the phosphorylation sites mapped, further research into the role of the phosphorylation of dynamin I in SV endocytosis can be addressed.

1.10 Conclusion

SV endocytosis is essential for the maintenance of efficient neurotransmission. Many of the proteins involved in SV endocytosis have been identified and research into their role and regulation in this process is continuing. Ca^{2+} influx following nerve terminal stimulation is established as being the trigger for SV exocytosis and also having a role in the activation of SV endocytosis. It is not surprising, therefore,

that many protein-protein interactions and the properties of some proteins, such as lipid binding affinity, are sensitive to changes in the intracellular Ca^{2+} concentration.

Nerve terminal depolarisation also triggers the dephosphorylation of the dephosphins, allowing the cascade of protein-protein interactions required for SV endocytosis to take place. The phosphorylation state can also determine the physiological properties of the proteins facilitating translocation to sites of endocytosis on the plasma membrane. Rephosphorylation of the dephosphins is also required to re-set the system, underpinning the importance of a cycle of phosphorylation.

Dynamin I is one of the most studied SV endocytosis proteins. It is essential for the fission stage of vesicle formation and when function is impaired can give rise to a dramatic phenotype where vesicles are trapped at the deeply invaginated pit stage. The GTPase activity of dynamin I is required for SV endocytosis and is controlled by several means including self-polymerisation, lipid binding, interactions with SH3 domain containing proteins and phosphorylation. Many of the protein-protein interactions involving dynamin I, as well as the biochemical properties, are controlled by Ca^{2+} or the phosphorylation status. Research into the regulation of dynamin I will not only elucidate the molecular mechanisms of action but will also increase the understanding of the process of SV endocytosis as a whole.

1.11 Aims of the thesis

The overall aim of this thesis is to investigate the molecular mechanisms of SV endocytosis, specifically the role of dynamin I. Thus I sought to determine how both Ca^{2+} and protein phosphorylation regulate the interactions of dynamin I with its endocytic partners and also to determine the role of these regulated interactions in SV endocytosis.

CHAPTER 2

MATERIALS AND METHODS

2.1 Materials

2.1.1Chemicals and Reagents

FM2-10 and FM4-64 were purchased from Molecular Probes (Oregon, USA). Glutamate dehydrogenase, glutamate, NADP, lysozyme, Protein G beads, 4-aminopyridine, and leupeptin were purchased from Sigma-Aldrich Ltd (Poole, UK). Percoll, gluathione-sepharose 4B beads and ProbeQuant G-50 columns were obtained from Amersham Biosciences UK Ltd (Buckinghamshire, UK). Cuvettes were obtained from Optiglass (Essex, UK). Sulpholink® beads, Slide-A-Lyzer® dialysis cassettes and Supersignal West Pico Chemoluminescent reagent were purchased from Pierce Biotechnology Inc. (Illinois, USA). Cyclosporin A was purchased from Calbiochem (Merck Biosciences Ltd, Nottingham, UK). Nitrocellulose membrane and acrylamide was bought from Bio-Rad (California, USA). Complete protease inhibitor tablets and EDTA-free complete protease inhibitor tablets were purchased from Roche (Mannheim, Germany). Sodium cacodylate, glutaraldehyde and osmium tetroxide were purchased from AGAR Scientific Ltd (Essex, UK). Maxi-prep kits, Nickel-NTA agarose and 5 ml disposable columns were bought from Qiagen Ltd. (West Sussex, UK). Bacto-tryptone was purchased from BD Biosciences (Oxford, UK). Yeast extract was purchased from ICN (Ohio, USA). Select agar and MEM media were purchased from Invitrogen (Paisley, UK). All other general laboratory reagents were obtained from Sigma-Aldrich (Poole, UK) or Fisher Scientific (Leicestershire, UK).

2.1.2 Strains of *E. Coli* used

For bacterial protein expression BL21 RIL cells were used and for DNA production, TOP10 cells were used (both from Invitrogen, Paisley, UK).

2.1.3 Constructs used

The SH3 domain of amphiphysin I (residues 545 – 695) and the PRD of dynamin I (residues 751 – 864) N-terminally tagged with GST were gifted by P. De Camilli (Yale University Medical School, Connecticut, USA). Both are in the pGEX-2T vector. The ear domain of α-adaptin N-terminally tagged with GST was gifted from R. G. W. Anderson (University of Texas Southwestern Medical Centre, Texas, USA). It contains residues 701 – 938 of α-adaptin and is in pGEX-2T vector. The SH3 domain of endophilin II (residues 307 –368) N-terminally tagged with GST in the pGEX-2T vector was gifted by P. McPherson (McGill University, Canada). The full length amphiphysin I N-terminally His-tagged construct was gifted by H.T. McMahon (MRC Laboratory of Molecular Biology, Cambridge, UK). It is in the pET-15b vector. The C-terminus of synaptophysin (residues 225 –308) C-terminally tagged with GST was made by O. Jupp and is in pGEX-4T-1 vector.

2.1.4 Peptides

The following peptides were synthesized by Genemed Synthesis Inc. (San Francisco, America). RRMKWKK corresponds to the minimal internalisation sequence from penetratin residues 52 – 58 (Fischer et al. 2000).

Table 1 – Details of the peptides

Peptide name	Peptide sequence	Description
$AP2_{624-644}$	RRM KWK KQG DLL GDL LNL DLG PPV NVP Q	Clathrin interaction site (ter Haar et al. 2000)
CytC	RRM KWK KKL IGV LSS LFP PK	Hsc 70 interaction site with cytochrome c (Morgan et al. 2001)
$DynI_{832-840}$	RRM KWK KQV PSR PNR AP	Amphiphysin interaction site (Shupliakov et al. 1997)
$DynI_{769-784}$AA	RRM KWK KPA GRR APT SAP TPQ RR	Phosphomimetic peptide with Cdk5 phosphorylation sites (Tan et al. 2003) substituted (S774A + S778A)
$DynI_{769-784}$EE	RRM KWK KPA GRR EPT SEP TPQ RR	Phosphomimetic peptide with Cdk5 phosphorylation sites (Tan et al. 2003) substituted (S774E + S778E)
$DynI_{769-784}$AA Cys	CPA GRR APT SAP TPQ RR	Cysteine tagged phosphomimetic peptide with S774A + S778A
$SynI_{585-600}$	RRM KWK KRQ GPP QKP PGP AGP IR	p85 subunit of PI3K interaction site (Cousin et al. 2003)
$SJ_{1101-1110}$	RRM KWK KEP KRP PPP RP	Endophilin interaction site (Cestra et al. 1999)
$Syp_{257-274}$	RRM KWK KYG PQD SYG PQG GYQ PDY G	Dynamin interaction region (Daly and Ziff 2002)

2.1.5 Antibodies

Antibodies were purchased from the following companies as indicated in the table below.

Table 2 – Details of the antibodies used

Antibody	Company	Western blot dilution
α-adaptin	Sigma-Aldrich	1 : 1000
Amphiphysin I (N-19)	Santa Cruz Biotechnology	1 : 500
Clathrin heavy chain (C-20)	Santa Cruz biotechnology	1 : 250
Dynamin I (C-16)	Santa Cruz biotechnology	1 : 1000
Dynamin I P-774	Gift from P. J. Robinson	1 : 1000
Dynamin I P-778	Gift from P. J. Robinson	1 : 1000
Endophilin I (S-20)	Santa Cruz Biotechnology	1 : 1000
Synapsin Ia/Ib	Santa Cruz Biotechnology	1 : 250
Synaptojanin I (N-15)	Santa Cruz Biotechnology	1 : 500
Synaptophysin (SVP38)	Santa Cruz Biotechnology	1 : 100
Syndapin I	BD Biosciences	1 : 2000
anti-sheep/goat	Sigma-Aldrich	1 : 10000
anti- rabbit	Sigma-Aldrich	1 : 10000
anti-mouse	Sigma-Aldrich	1 : 10000

2.2 Synaptosome preparation

Synaptosomes are isolated nerve terminals and are the simplest system containing all of the proteins necessary for SV exocytosis and endocytosis (Nicholls 1993). Population measurements of neurotransmitter release and SV membrane turnover can be assayed in parallel with biochemical studies making synaptosomes an ideal system to study the molecular mechanisms of synaptic transmission. The main disadvantage of the synaptosome system is that they do not contain a nucleus and therefore DNA and protein expression cannot be manipulated. Thus for overexpression or gene silencing studies cultured neurons such as cerebellar granule cells or hippocampal neurons are better systems.

Synaptosomes are only functional for up to 6 hours after preparation (Nicholls 1993) and therefore it is important to take several precautions during the preparation procedure to ensure that healthy and functional synaptosomes are purified. It is essential that the time between extraction of the rat brain and homogenisation is kept to a minimum and that the whole preparation procedure is carried out on ice and using chilled rotors. Crude P2 synaptosomes were sufficient for most biochemical procedures but for fluorescence experiments, electron microscopy and some experiments where a more pure synaptosome preparation was required, percoll purified synaptosomes were used.

2.2.1 Crude P2 synaptosomes

Crude P2 synaptosomes were prepared as illustrated in figure 2.1A. Sprague-Dawley rats of at least two months old were killed by stunning and cervical dislocation. The forebrain was rapidly dissected and isolated into ice-cold 1 X sucrose solution (0.32 M sucrose, 1 mM EDTA, 5 mM Tris pH 7.4). After rinsing in the sucrose solution, the forebrain was transferred to a tube containing 9 ml of sucrose solution and minced with scissors. This was then transferred to a glass, Teflon coated, 30 ml homogeniser (Wheaton) and homogenised with at least six up and down strokes at 700 rpm. No more than two rats were killed at once to keep the time between dissection and homogenisation to a minimum.

Homogenates were pooled and centrifuged at 1075 x *g* (3000 rpm) for 10 min. All spins were carried out using a Sorval (RC26 plus) centrifuge at 4 °C with an SS-34

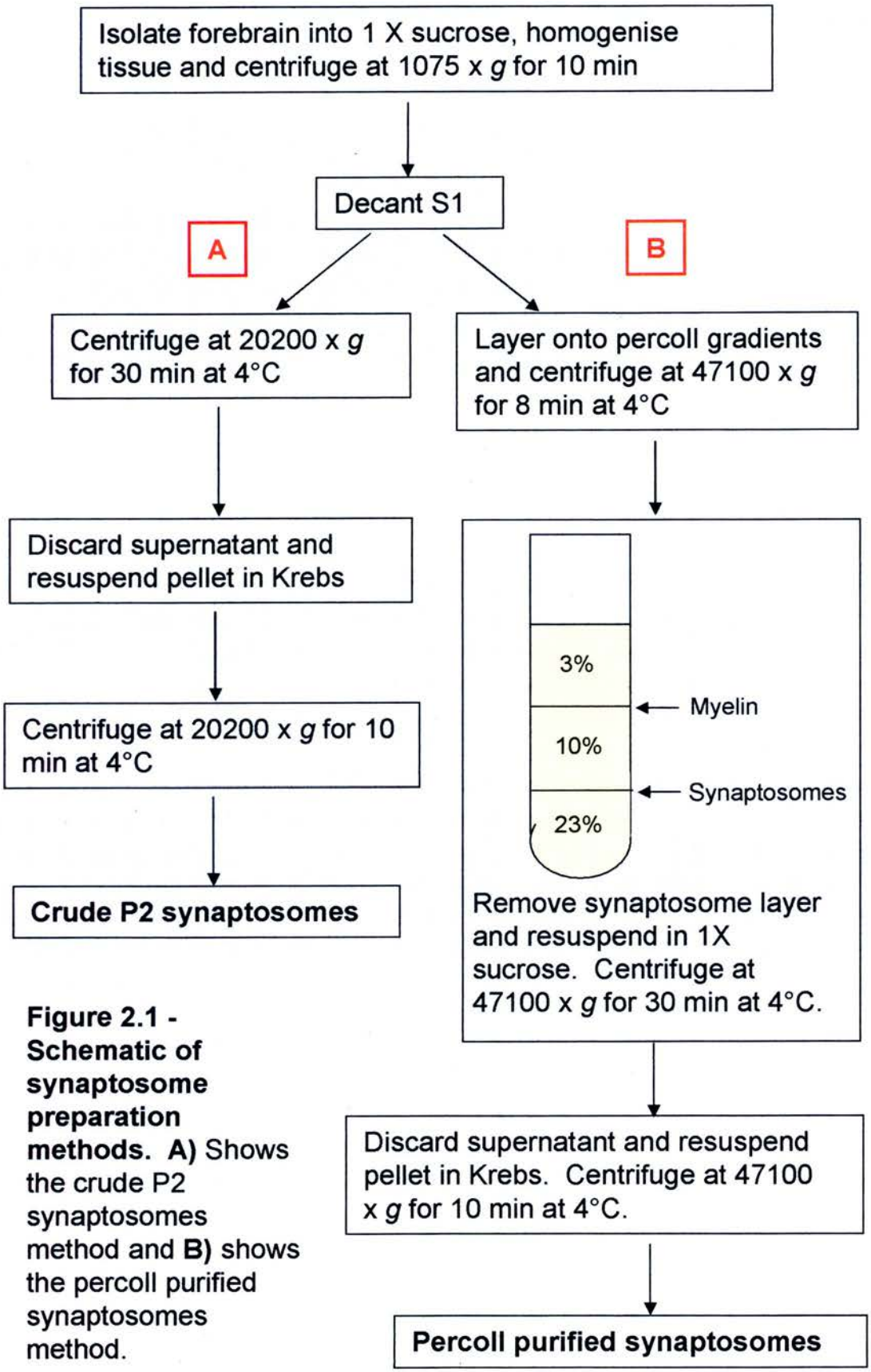

Figure 2.1 - Schematic of synaptosome preparation methods. A) Shows the crude P2 synaptosomes method and **B)** shows the percoll purified synaptosomes method.

rotor. After centrifuging, a red-tinted pellet is formed with a looser white pellet on the top. The supernatant contains the synaptosomes and the pellet contains red blood cells, mitochondria and other debris. When pouring off the supernatant, care was taken not to pour off the loose white pellet. The decanted supernatant (S1) was stored on ice. To ensure maximum recovery of synaptosomes, the pellet (P1) was resuspended in another 9 ml of 1 X sucrose and centrifuged for a further 10 min at 1075 x *g*. This supernatant was combined with the previous supernatant (S1) and spun at 20200 x *g* (13 000 rpm) for 30 min to pellet the synaptosomes. The supernatant (S2) was discarded and the pellet (P2) was resuspended in Krebs-like buffer (118.5 mM NaCl, 4.7 mM KCl, 1.18 mM $MgSO_4$, 10 mM glucose, 1 mM Na_2HPO_4, 20 mM HEPES, pH 7.4 with saturated Tris base) and centrifuged for a further 10 min at 20200 x *g*.

The supernatant was discarded and the pellet resuspended in $+Ca^{2+}$ Krebs-like buffer (Krebs-like buffer plus 1.3 mM $CaCl_2$) to an appropriate concentration for use, typically 3 mg/ml as estimated by Bradford Assay.

2.2.2 Percoll purified synaptosomes

The protocol for percoll purified synaptosomes (illustrated in figure 2.1B) is based on the method of Dunkley *et al* (1986) and is identical to that for crude P2 synaptosomes (section 2.2.1) up to the stage where the S1 fractions were combined. Instead of spinning the S1, it is layered onto pre-prepared percoll gradients. This is to separate the synaptosomes from the myelin and mitochondria.

Usually, four gradients are required for one rat forebrain. The gradients were prepared by pipetting 3 ml of 23 % percoll into a centrifuge tube and layering 3 ml of 10 % percoll onto the 23 % percoll layer using a peristaltic pump. This was repeated with a further 3 ml of 3 % percoll. The percoll solutions contained 0.32 M sucrose, 1 mM EDTA and 5 mM Tris pH 7.4 and the appropriate volume of percoll, v/v. The poured gradients were stored at 4 °C until use.

The S1 synaptosomes were loaded onto the gradients using a cut off 1 ml pipette tip and spun at 47100 x *g* (20 000 rpm) for 8 min with constant braking for the deceleration. After centrifugation the gradients took on the appearance illustrated in figure 2.1B with the myelin at the 3 –10 % interface, the synaptosome fraction at the 10-23 % interface and dense membranous material such as mitochondria pelleted at the bottom. The fractions were recovered using a pipette-aid with a cut off P200 tip. The myelin layer was removed and discarded and the synaptosome layer removed into a fresh ice-cold centrifuge tube and diluted at least four fold with ice-cold 1 X sucrose solution. This solution was then centrifuged at 47100 x *g* for 30 min. The supernatant was carefully discarded from the loose pellet and the pellet resuspended in Krebs-like buffer. This was recentrifuged at 47100 x *g* for 10 min. The supernatant was discarded and the pellet resuspended in $+Ca^{2+}$ Krebs-like buffer. The percoll purified synaptosomes were then aliquoted to the appropriate concentration, typically 1 mg/ml for fluorescence and 2 mg/ml for biochemistry, and stored on ice until use.

2.3 Fluorescence assays

Bulk phase fluorescence assays are a convenient and effective method to monitor the kinetics and magnitude of SV exocytosis and endocytosis in synaptosomes. The fluorimeter used to collect all the data was a Spex Fluoromax (Spex Industries Inc, New Jersey, USA) with a modified chamber incorporating a thermostatically controlled cuvette chamber to maintain the temperature at 37 °C and a magnetic stirrer.

2.3.1 Glutamate release assay

Synaptosomes from the forebrain are 90 % glutamatergic (Nicholls 1993) making glutamate an ideal neurotransmitter to monitor the extent of SV exocytosis. The assay used was based on that devised by Nicholls and Sihra (1986) and uses glutamate dehydrogenase, which couples the oxidation of glutamate to oxo-glutarate with the reduction of $NADP^+$ to NADPH (fig 2.2A). NADPH is fluorescent when excited at 340 nm and so the generation of NADPH, and hence the release of glutamate, was measured by an increase in fluorescence at the emission wavelength of 460 nm. Glutamate dehydrogenase only detects the glutamate released because it does not enter the synaptosomes.

Glutamate release has to be measured in the presence and absence of extracellular Ca^{2+} because the electrogenic Na^+/glutamate symporter reverses direction upon membrane depolarisation and hence pumps glutamate out of the synaptosomes. This release is termed the Ca^{2+}-independent release and is subtracted from the glutamate

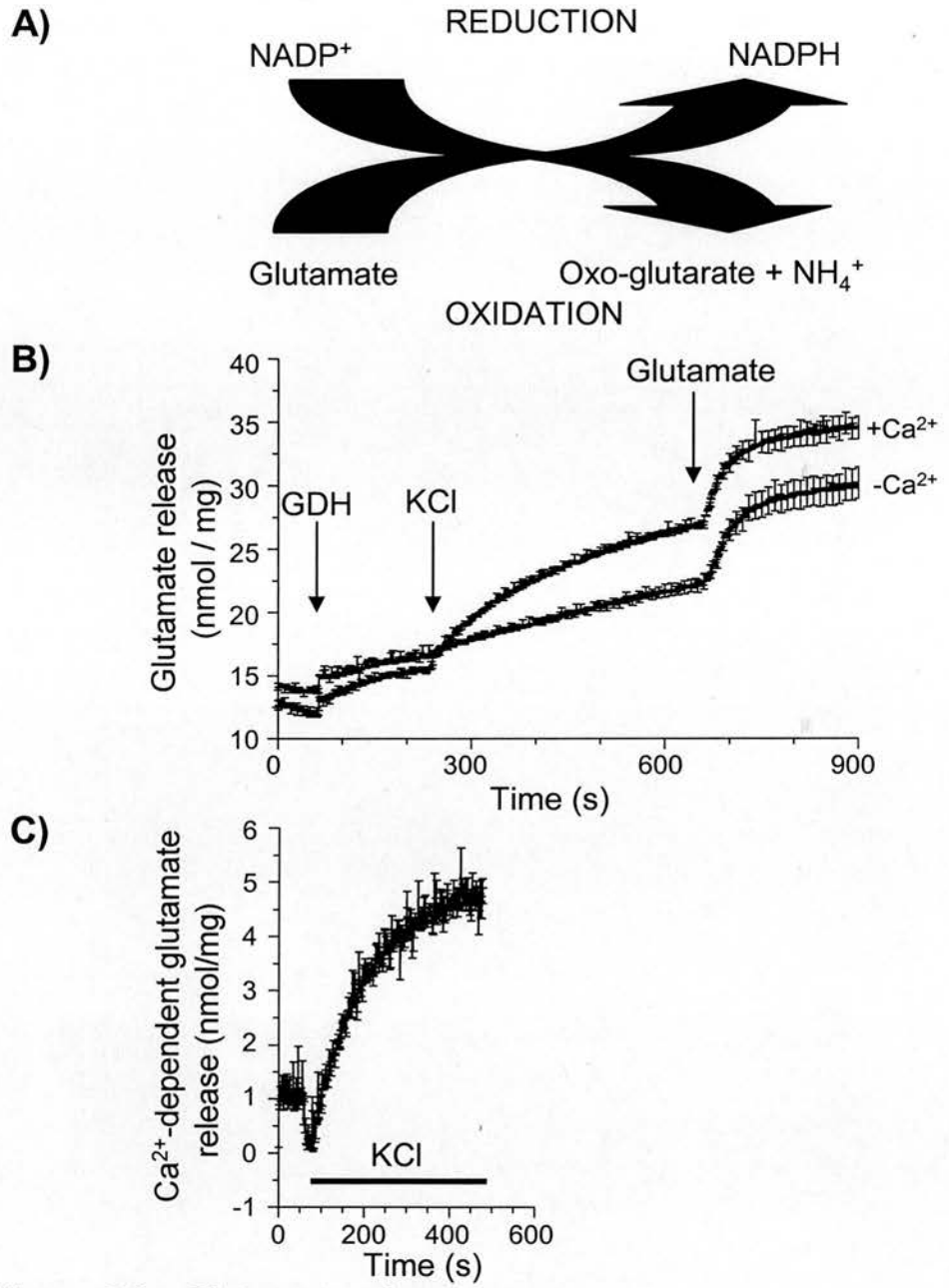

Figure 2.2 – Glutamate release assay.

A) Diagram illustrating the glutamate dehydrogenase reaction used in the glutamate release assay. **B)** Glutamate release assay traces ± Ca^{2+}. The glutamate dehydrogenase (GDH), stimulant, in this case KCl, and glutamate addition points are indicated with arrows. ($n \geq 3 \pm SEM$). **C)** Ca^{2+}-dependent glutamate release trace calculated from the raw traces aligned in **B**. The decrease in fluorescence upon KCl addition is a commonly observed artifact of the assay. Bar denotes the presence of KCl.

release in the presence of Ca^{2+} to get the Ca^{2+}-dependent release and therefore the glutamate released due to exocytosis (Nicholls et al. 1987).

Percoll purified synaptosomes (0.6 mg) were resuspended in either 1 ml of $-Ca^{2+}$ Krebs-like buffer (supplemented with EGTA to a final concentration of 1 mM) or 1 ml of $+Ca^{2+}$ Krebs-like buffer and preincubated for 15 min ± 40 μM cyclosporin A or 30 min ± 100, 250 or 500 μM penetratin peptides as indicated at 37 °C. After the preincubation period, the synaptosomes' suspension was added to a cuvette containing either 1 ml of prewarmed $-Ca^{2+}$ Krebs-like buffer or $+Ca^{2+}$ Krebs-like buffer, and 2 mM $NADP^+$ (final concentration 1 mM). The synaptosomes were placed in a stirred chamber in the fluorimeter and after 1 min 50 units of glutamate dehydrogenase were added. After a further 3 min, the synaptosomes were stimulated with the addition of either 30 mM KCl or 1 mM 4-AP. The glutamate released was measured for 7 min before addition of 4 nmol glutamate. This was added to act as an internal control to standardise the amount of glutamate dehydrogenase added.

The data was collected using dm3000 version 3.2 software (Spex Industries Inc, New Jersey, USA) and analysed using Microsoft Excel and GraphPad Prism. Figure 2.2B shows an example of a glutamate release raw trace with the points of addition of the glutamate dehydrogenase, stimulant and glutamate indicated. Following addition of the glutamate dehydrogenase it was not unusual to see an increase in the fluorescence. This is probably due to the leakage of glutamate from damaged synaptosomes. In fact, the extent of basal glutamate release is a very good indication of synaptosome viability. The individual raw traces were firstly normalised for the

4 nmol of glutamate added and then lined up at an arbitrary value at the point of stimulation. The traces in the absence of Ca^{2+} were then subtracted from those in the presence of Ca^{2+} and the result displayed as the Ca^{2+}-dependent release from 1 mg of synaptosomes (fig 2.2C). The assay was linear over all concentrations tested (Nicholls et al. 1987).

2.3.2 SV turnover assay

This assay uses the fluorescent dye, FM2-10, which is a member of a family of styryl dyes (Betz et al. 1996). These dyes are extremely useful tools for studying SV recycling because they are impermeant to membranes and are more fluorescent in a lipophilic environment, i.e. membrane bound, than in solution. Thus they stain membranes in an activity-dependent manner (Betz et al. 1996). The properties of these dyes are confined by different parts of the molecule. Figure 2.3A shows the structure of the styryl dyes using FM2-10 as an example. The dyes are amphipathic with a hydrophilic, positively charged head group and a hydrophobic tail, linked together with a double bond bridging region. The different styryl dyes differ in the size of the head group, the length of the tail and the number of double bonds in the centre region of the molecule (Betz et al. 1996).

The head group determines the membrane permeability: a small alkyl group which is monocationic is membrane-permeable while a much larger head group with a dicationic charge, such as FM2-10, is not membrane permeable (Betz et al. 1996). This means that FM2-10 will insert into the outer leaflet of the plasma membrane without passing through. The tail determines the staining properties of the dyes and

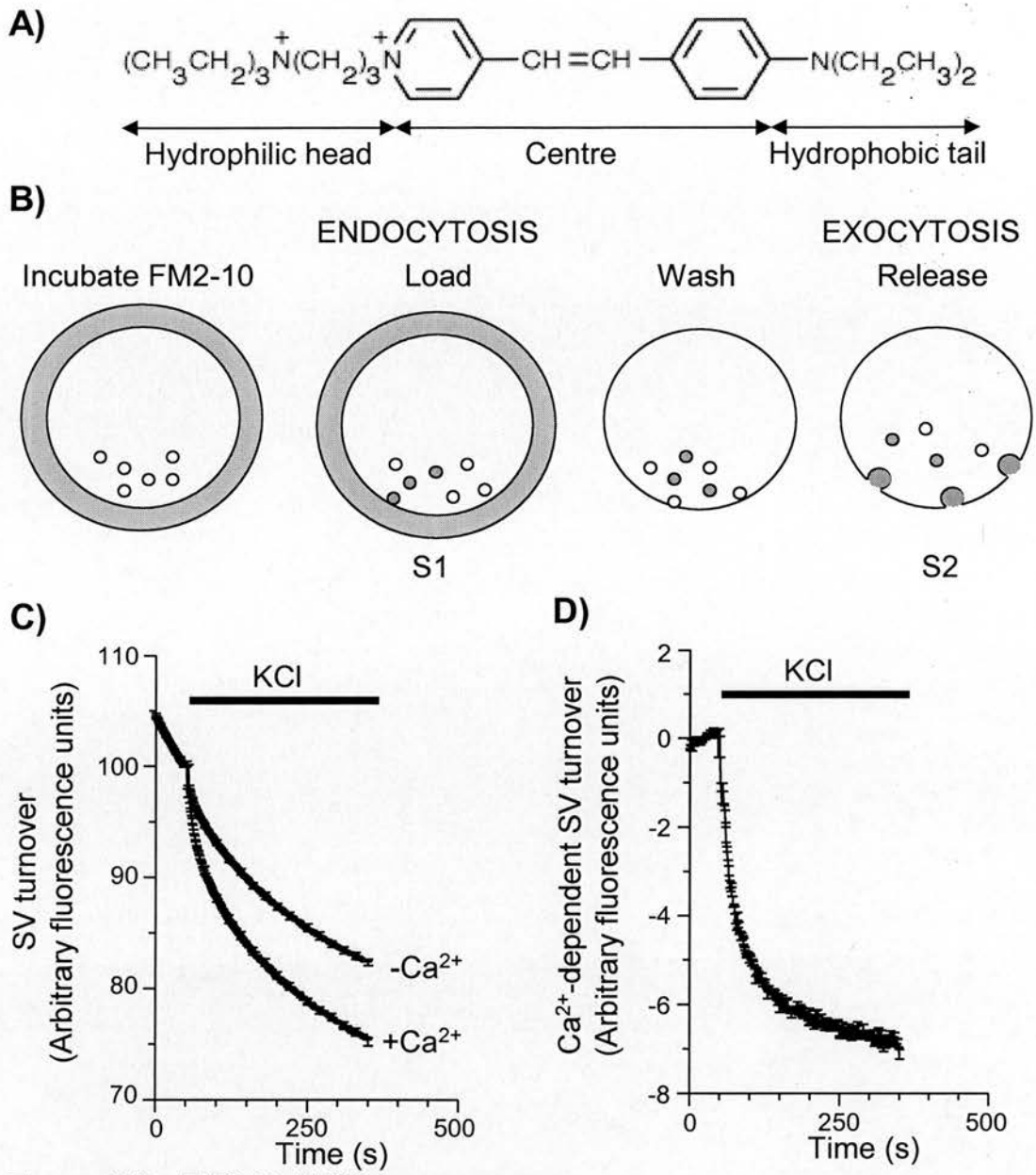

Figure 2.3 - FM2-10 SV turnover assay

A) Structure of FM2-10 showing the hydrophilic head group and hydrophobic tail. (Adapted from Molecular Probes data sheet) **B)** Schematic of the FM2-10 SV turnover assay showing the four stages: incubation with FM2-10 to allow dye insertion into the membrane, internalisation of the dye, washing to remove non-internalised dye and stimulation to release the internalised dye. (Adapted from Marks and McMahon, 1998) **C)** Aligned traces obtained ± Ca^{2+} ($n \geq 3 \pm$ SEM). **D)** Ca^{2+}-dependent trace calculated by subtracting the $-Ca^{2+}$ trace from the $+Ca^{2+}$ trace. Bar denotes the presence of KCl in **C + D**.

usually consists of two aliphatic hydrocarbon chains which vary in length depending on the molecule. The dyes with short tails, such as FM2-10, are less lipophilic and thus fluoresce less brightly than those with longer tails. However, the dyes with longer tails, such as FM3-25, bind with higher affinity to the plasma membrane and although staining the membrane more brightly, cannot be washed off the plasma membrane, making them more useful for labelling of structures rather than for monitoring membrane turnover (Betz et al. 1996).

The spectral properties of the dyes are determined by the double bond bridging region. The greater the number of double bonds, the longer the excitation and emission wavelengths thus the emission wavelength for FM1-43 and FM2-10, which have only one double bond, is in the green part of the spectrum where as for FM4-64, which has three double bonds, it is in the red part of the spectrum. The emission wavelength of the dyes however, are unaffected by the head group size and tail length (Betz et al. 1996).

Styryl dyes are also only weakly fluorescent in an aqueous environment and increase in fluorescence dramatically when in a lipophilic environment (Betz et al. 1996). This means that the fluorescence of the plasma membrane or labelled vesicles, can be monitored with little interference from any dye present in solution making the dyes excellent tools for labelling recycling SV (Betz et al. 1996; Cousin and Robinson 1999).

The styryl dye used for this assay was FM2-10, because it is the most hydrophilic of the dyes and thus has the shortest half-time in the membrane – 0.7 s for FM2-10 compared to 2.7 s for FM1-43 and 5.9 s for FM1-84 (Ryan et al. 1996). A short half-life is important for accurate quantification of SV turnover because the dye has to fully dissociate from the SV membrane upon exocytosis. Non-internalised dye can also be washed off the plasma membrane easily allowing more accurate determination of the amount of internalised dye (Cousin and Robinson 1999).

The assay is illustrated in figure 2.3B. It is important to use percoll-purified synaptosomes because FM2-10 binds to myelin. By removing this contaminant the signal to noise ratio is greatly improved. Percoll-purified synaptosomes (0.6 mg) are pre-incubated in 1 ml of either $-Ca^{2+}$ or $+Ca^{2+}$ Krebs-like buffer for either 15 min (± 40 μM cyclosporin A) or 30 min (± 100, 250 or 500 μM peptides) at 37 °C, where indicated. After preincubation 100 μM FM2-10 was added to allow insertion into the outer leaflet of the plasma membrane. After 1 min, exocytosis was stimulated by the addition of 30 mM KCl for 2 min. The FM2-10 was internalised by compensatory endocytosis ("loading") during this period. The synaptosomes were immediately pelleted at 13400 x *g* (12 000 rpm) for 1 min and the pellet resuspended in $+Ca^{2+}$ Krebs-like buffer supplemented with 1 mg/ml BSA to wash off any non-internalised, extracellularly bound FM2-10. This step was repeated and the pellet resuspended in 1 ml of $+Ca^{2+}$ Krebs-like buffer. The resuspended pellet was added to a cuvette containing 1 ml of $+Ca^{2+}$ Krebs-like buffer and placed in the stirred cuvette holder in the fluorimeter. The synaptosomes were then stimulated after 3 min with a standard stimulus of 30 mM KCl to release the accumulated dye, since the background

fluorescence was too high to simply measure the fluorescence and use this as a readout for endocytosis. This was observed as a decrease in fluorescence as the FM2-10 departitions from the plasma membrane into the aqueous environment. This decrease in fluorescence is an indication of the amount of dye internalised during the initial stimulation (Marks and McMahon 1998; Cousin and Robinson 1999). The synaptosome pellet is resuspended in $+Ca^{2+}$ Krebs-like buffer irrespective of whether the sample was loaded in $-Ca^{2+}$ or $+Ca^{2+}$ conditions to ensure that unloading conditions are the same for all samples. This means that any observed difference in fluorescence is due to dye loading (endocytosis) and not unloading.

The synaptosomes were excited at 488 nm and emission recorded at 540 nm. This is because FM2-10 has a peak emission wavelength of 540 nm in synaptosomes (data not shown). The data was collected using dm3000 version 3.2 software and analysed using Microsoft Excel and Graph Pad Prism. The raw traces were individually normalised to an arbitrary value of 100 at the point of stimulation. This normalisation was performed to align the traces allowing comparison between conditions. Examples of aligned raw traces in the presence and absence of Ca^{2+} are shown in figure 2.3C. The assay was performed in the presence and absence of Ca^{2+} because there is a small Ca^{2+}-independent decrease in fluorescence on stimulation, possibly due to a slight voltage dependence of the dye (Marks and McMahon 1998). Therefore, the values in the absence of Ca^{2+} were subtracted from the release in the presence of Ca^{2+} to give the Ca^{2+}-dependent release (figure 2.3D).

The SV turnover assay can be modified to investigate exocytosis. In this case, synaptosomes are loaded with a standard protocol and then the unloading conditions are varied depending on the experiment. Specifically, 0.6 mg of percoll purified synaptosomes was resuspended in 1 ml of $+Ca^{2+}$ Krebs-like buffer. As before, the synaptosomes were incubated with 100 μM FM2-10 for 1 min and loaded with a 30 mM KCl stimulus. After 2 min the synaptosomes were pelleted and washed twice in $+Ca^{2+}$ Krebs-like buffer supplemented with 1 mg/ml BSA. This time the pellet was resuspended in 1 ml of either $+Ca^{2+}$ or $-Ca^{2+}$ Krebs-like buffer. The synaptosomes were then incubated for 30 min at 37 °C ± the indicated concentration of peptides. The tubes were wrapped in foil during the incubation to minimise photobleaching of the FM2-10. The synaptosomes were then added to a cuvette containing 1 ml of either $+Ca^{2+}$ or $-Ca^{2+}$ Krebs-like buffer and placed into the fluorimeter. The excitation wavelength was 488 nm and the emission recorded at 540 nm as before. Exocytosis was stimulated with 30 mM KCl and the fluorescence recorded for 5 min. The data was analysed in the same manner as for the previous SV turnover assay.

The SV turnover assay only provides an estimate of SV endocytosis and thus the parameter called retrieval efficiency was used. Retrieval efficiency takes into consideration the prior amount of exocytosis and thus is a more accurate reflection of the amount of SV endocytosis. Retrieval efficiency was calculated as the amount of endocytosis/exocytosis where endocytosis was defined as the total Ca^{2+}-dependent decrease in fluorescence from FM2-10-labelled synaptosomes and exocytosis as the Ca^{2+}-dependent glutamate release after 2 min of stimulation (Cousin and Robinson

1998). Where the FM2-10 exocytosis assay was used, exocytosis was defined as the total Ca^{2+}-dependent fluorescence decrease from stimulated FM2-10 labelled synaptosomes.

2.3.3 Internalisation assay

A limitation of the FM2-10 endocytosis assay is that a block at any stage of the SV recycling pathway would be reflected as a block of SV endocytosis. The internalisation assay (Marks and McMahon 1998; Di Paolo et al. 2002), can distinguish between a block in SV retrieval and an inhibition of later stages such as uncoating or trafficking. The principle of the assay is the same as the endocytosis assay, but instead of stimulating the release of the internalised dye, the synaptosomes are hypotonically lysed and the SVs crudely purified by centrifugation. SVs are not lysed by this treatment and thus the fluorescence detected in the supernatant is due to the internalised vesicles. Simplistically, if inhibition occurred during SV retrieval, then the fluorescence would be less than control, since fewer SVs were retrieved. Alternatively, if SV uncoating or trafficking were perturbed then the fluorescence would be the same as control since SV retrieval was unaffected.

Percoll purified synaptosomes (0.6 mg) were resuspended in 1 ml of either + Ca^{2+} or –Ca^{2+} Krebs-like buffer, pre-incubated with drugs or peptides and loaded with 100 μM FM2-10 in an identical manner to the SV turnover assay (2.3.2). The synaptosomes were then washed twice with +Ca^{2+} Krebs-like buffer supplemented with 1 mg/ml BSA Krebs buffer. The synaptosomes were then lysed in 1 ml of 20 mM ice-cold Tris (pH 7.4) and supplemented with 150 mM KCl to restore the

ionic concentration. The lysed synaptosomes were then vortexed for 10 s and centrifuged at 13400 x *g* (12 000 rpm) for 2 min to pellet the membranous debris. The supernatant was removed to a fresh eppendorf tube and stored on ice until all samples were collected. The samples were wrapped in foil to prevent photobleaching. Once all the samples were generated, the initial fluorescence of each sample was measured in the fluorimeter (excitation 488 nm, emission 540nm). Again, each experiment was done in the presence and absence of Ca^{2+} and the Ca^{2+}-dependent FM2-10 accumulated was calculated by subtracting the value in the absence of Ca^{2+} from that in the presence of Ca^{2+}.

2.4 DNA / protein expression and purification

2.4.1 Preparation of competent cells

Competent cells for both the TOP10 and BL21 RIL strains were prepared using the following method (Promega 1996).

A scrape from competent cells in the –70 °C freezer was used to inoculate 5 ml of LB medium (10 g bacto-tryptone, 5 g yeast extract, 10 g NaCl, made up to 1 l with distilled water, pH 7 with NaOH) and incubated overnight at 37 °C with shaking at 225 rpm. The following day 1 ml of the overnight culture was used to seed 100 ml of sterile LB medium plus 20 mM filter sterilised $MgSO_4$. The $MgSO_4$ increases cell growth rate and transformation efficiency (Hanahan 1983). The cells were grown with shaking at 37 °C until they reached an optical density of 0.4 – 0.6 at a wavelength of 600 nm.

The cells were then pelleted by centrifugation at 5000 x *g* for 5 min at 4 °C in sterile 250 ml centrifuge bottles. (A Beckmann Avanti J-25 centrifuge with JL16.250 rotor was used for these spins). The supernatant was discarded and the cells resuspended in 40 ml of filter sterilised ice-cold transformation buffer 1 (TFB1, 30 mM KAcetate, 10 mM $CaCl_2$, 50 mM $MnCl_2$, 100 mM RbCl, 15 % glycerol, pH 5.8 with 1 M acetic acid). The cells were then incubated on ice for 5 min. The cells were again centrifuged at 5000 x *g* for 5 min at 4 °C. The supernatant was discarded and the cells resuspended in 4 ml of filter sterilised ice-cold transformation buffer 2 (TFB2, 10 mM MOPS, 75 mM $CaCl_2$, 10 mM RbCl, 15 % glycerol, pH 6.5 with 1 M KOH). The TFB1 and TFB2 both contain Ca^{2+} salts and rubidium which increase the transformation efficiency by allowing the cells to take up DNA (Hanahan 1983). The cells were incubated on ice for 30 min and then aliquoted, 200 µl / sterile eppendorf, snap frozen in dry ice and stored at –70 °C until use.

2.4.2 Transformation of competent cells

The TOP10 competent cells were mainly used for the production of DNA and the BL21 RIL competent cells for protein expression. Both were transformed by the same method (Promega 1996).

Competent cells were defrosted on ice and approximately 10 ng of DNA added. The DNA was mixed by swirling with a pipette tip and not by pipetting so as not to shear the DNA. The cells were incubated on ice for 30 min to allow the DNA to adhere to the outside of the cells. After this, the cells were heat shocked at 42 °C for 45 s. This stimulates the cells to take up the DNA. The cells were then left on ice for

2 min before 250 µl of LB medium was added and the cells incubated at 37 °C with shaking for 30 min to allow cell recovery. Following this, 100 µl of the cells were spread on agar plates (LB media + 1.5 % select-agar) containing the appropriate antibiotic and left in the 37 °C incubator overnight for colonies to form.

2.4.3 Glycerol Stocks

A single colony from the plate containing the transformed bacteria was picked using a pipette tip and used to seed a 5ml LB culture plus antibiotic. This was grown at 37°C with shaking until an optical density of 0.6 at 600 nm was reached. At this point the cells are in growth phase and have not entered stationary phase. 900 µl of the culture was added to 100 µl of autoclaved glycerol and mixed by pipetting. The culture was then snap-frozen in dry ice and stored at -70 °C, where scrapes were used to seed cultures for either DNA production (TOP10s) or protein expression (BL21s).

2.4.4 DNA production and purification

A scrape from the glycerol stock was used to seed a 5 ml LB medium culture plus relevant antibiotic (usually 0.1 mg/ml ampicillin). This was in turn used to seed a 100 ml LB culture plus antibiotic overnight. This culture was then used to perform a maxi-prep of the DNA plasmid as detailed in the Qiagen manual (Qiagen 2000).

Briefly, the cells were pelleted and lysed in an alkaline cell lysis solution and the genomic DNA, protein, cell debris and SDS precipitated. The plasmid DNA in the cleared lysate was bound by an anion-exchange resin in low-salt and pH conditions and washed to remove any contaminants, in particular carbohydrate from the

bacteria. The plasmid DNA was then eluted from the resin in a high salt wash and precipitated, desalted using isopropanol and finally precipitated using 70 % ethanol. The concentration of the DNA was estimated by measuring the absorbance at 260 nm in a spectrophotometer and applying the following formula:

$$[\text{DNA}] = \frac{\text{Abs}_{260} * \text{DNA multiplication factor} * \text{dilution factor}}{1000}$$

Where the Abs_{260} is the absorbance at 260 nm. the DNA multiplication factor is 50 for double stranded DNA and the dilution factor is the amount the DNA was diluted by (usually 100 fold dilution).

2.4.5 Expression of GST-fusion proteins

A 5 ml overnight culture set up from a scrape from the appropriate glycerol stock was used to seed a 250 ml culture of LB media plus antibiotic. This was incubated at 37 °C with shaking until an optical density of between 0.6 and 0.8 at a wavelength of 600 nm was reached. Optical densities of above 0.8 mean that the bacteria have entered stationary growth which results in reduced protein expression.

All of the constructs used are based on the *lac* promoter and so require the addition of 1 mM IPTG to induce the expression of the fusion protein. IPTG is a non-metabolisible compound that performs the same role as the natural inducer, allolactose. It binds to the lactose repressor molecule, preventing its binding to the promotor region and so allowing the polymerase to bind and transcribe the gene – in this case the fusion protein sequence.

After induction, the bacteria were left to produce protein at 37 °C with shaking for 3 hours before the culture was centrifuged at 5000 x *g* for 5 min at 4 °C. The pellet was resuspended in 14 ml of saline tris EDTA (STE) buffer (100 mM Tris, 150 mM NaCl, 1 mM EDTA, pH 8). The bacteria were again centrifuged at 5000 x *g* for 5 min. The supernatant was discarded and the pellet left to air dry before storage at -70 °C.

The frozen pellets were thawed on ice and resuspended in 40 ml of ice cold STE buffer plus 1 mM PMSF, to inhibit proteases. To break down the bacterial cell wall 3.33 mg of lysozyme (for 250 ml of culture volume) was added and the culture incubated on ice for 30 min. To this 200 µl of 1 M DTT and 4.5 ml of 10 % triton X-100 were added. The suspension was then sonicated 6 times for 30 s on ice with a 30 s break between each sonication. The lysate was centrifuged at 17230 x *g* (12 000 rpm) for 5 min at 4 °C and the supernatant, containing the expressed fusion protein, was incubated with pre-prepared glutathione-sepharose 4B beads for at least an hour at 4 °C with tumbling to allow binding of the GST-tag to the sepharose beads.

The glutathione-sepharose beads were prepared by washing 3 ml of beads in 20 ml of PBS (137 mM KCl, 4 mM KCl, 20 mM Na_2HPO_4, NaH_2PO_4 to pH to 7.3) and centrifuging at 50 x *g* (500 rpm) for 5 min to pellet the beads. The beads were then blocked in 20 ml of PBS plus 0.1 % triton X-100 and centrifuged as above and finally washed in 20 ml of PBS.

After incubation of the beads with the lysate, the beads were spun down at 50 x *g* (500 rpm) and the supernatant removed. The beads were then washed 5 times in PBS , once in PBS supplemented with 350 mM NaCl (final concentration 500 mM NaCl) to reduce non-specific binding, and a further twice in PBS before being resuspended in PBS to make a 50 % slurry. The beads were stored at 4 °C until use. The amount of fusion protein bound to the beads was estimated by running on an SDS gel.

Where the purified fusion protein was required without the glutathione sepharose beads, for example for an *in vitro* binding assay, the PBS was removed from the beads by centrifugation at 50 x *g* (500 rpm) for 5 min. The beads were then incubated with 5 ml of glutathione elution buffer (10 mM glutathione, 50 mM Tris, pH 8) with rotation for 20 min at 4 °C. The beads were again pelleted at 50 x *g* for 5 min and the supernatant collected. The amount of protein eluted from the beads was determined by Bradford assay and SDS-PAGE. The eluted proteins were then cleaned to remove the glutathione. This was achieved by passing the protein solution through a desalting column. Bio-gel P-6DG beads were hydrated by incubation with distilled water for 15 min. Columns were packed with the hydrated beads and then centrifuged at 210 x *g* (1400 rpm) for 1 min to remove the water from the beads. The protein solution (200 µl per ml of hydrated beads) was added to the columns and the columns again centrifuged at 210 x *g* for 1 min. The flow through contained the protein while the glutathione and other salts were retained in the column.

2.4.6 Expression of His-tagged fusion proteins

The amphiphysin I full length construct is His-tagged and so was purified differently to the GST-fusion proteins. A poly-His tag binds with high affinity to nickel and so can be purified using nickel coated agarose beads. It is important to ensure that none of the solutions used contain EDTA or EGTA since both chelate divalent metal ions and thus would remove the nickel from the beads. Other compounds such as DTT were avoided since this reduces the nickel ions decreasing the binding capacity of the beads. β-mercaptoethanol was used instead to prevent disulphide cross-linkages. The bound His-tagged proteins were eluted from the nickel beads by incubation with imidazole-containing solutions. The imidazole binds the nickel beads with higher affinity than the His-tag and thus competes with the His-tagged protein facilitating elution from the beads (Qiagen 2003).

An overnight seed culture was used to seed a 250 ml LB plus antibiotic culture. Once an optical density of 0.6 at 600 nm was achieved, protein expression was induced with the addition of 1 mM IPTG for 3 hours, as for GST-fusion proteins. After the induction period, the bacteria were centrifuged at 5000 x g for 5 min to pellet the bacteria. The pellet was resuspended in breaking buffer (100 mM HEPES, 500 mM KCl, 5 mM $MgCl_2$, 2 mM β-mercaptoethanol, pH 8) and centrifuged once more at 5000 x g for 5 min. The supernatant was discarded and the pellet stored at -70 °C until use. The pellet was thawed on ice and resuspended in 40 ml of ice-cold breaking buffer supplemented with an EGTA-free protease inhibitor tablet and 1 mM PMSF. To this 3.33 mg of lysozyme (for 250 ml culture volume) was added and the suspension incubated on ice for 30 min. After the incubation period 4 ml of 10 %

triton-X100 was added and the lysate sonicated on ice 6 x 30 s times with 30 s intervals between each sonication. The lysate was then centrifuged at 17230 x *g* (12 000 rpm) for 5 min and the supernatant incubated with pre-prepared nickel agarose beads for at least an hour with rotation at 4 °C. The nickel beads were pre-prepared by washing 1 ml of beads in 20 ml of breaking buffer. The beads were then pelleted by centrifugation at 50 x *g* (500 rpm) for 5 min.

After the incubation period, the beads and approximately a tenth of the bacterial lysate were transferred into a 5 ml Qiagen capped disposable column. The frit was pushed down the column until it was slightly above the beads. The cap was removed from the bottom of the column and the bacterial lysate allowed to pass through. The frit prevents the beads drying out since the fluid level does not drop below it. The remains of the bacterial lysate was passed through the column to increase recovery of the His-tagged protein. The beads were then washed with 40 ml of wash buffer (50 mM imidazole, 20 mM HEPES, 200 mM KCl, 2 mM β-mercaptoethanol, 10 % glycerol, pH 7.4). The imidazole was present to reduce non-specific binding. Once the wash buffer had passed through the column, the cap was replaced and 6 ml of elution buffer (wash buffer plus imidazole to a final concentration of 150 mM) was added. The elution buffer was incubated with the beads with rotation for 15 min at 4 °C. The cap was then removed from the column and the eluate collected. The concentration of eluted protein was determined by Bradford assay and by running a sample of the protein on an SDS gel.

For use in an *in vitro* binding assay, the purified amphiphysin I was cleaned by dialysis to remove the imidazole. Since the volume of the protein solution was small, a Slide-A-Lyzer® cassette was used. The protein solution was injected into the cassette with a syringe and 18 gauge needle. The excess air was withdrawn to ensure that the protein solution was in contact with the maximum membrane area. The cassette was then floated in 1l of dialysis solution (in this case binding buffer, 20 mM HEPES, 150 mM KCl) for approximately 6 hours and the dialysis solution changed and left overnight at 4 °C. The cassette was then emptied. A syringe was filled with a volume equal to the volume of protein solution injected into the cassette initially, and injected into the cassette. The cassette was then rotated to allow the air to rise and the protein solution removed from underneath. The amount of cleaned protein was determined by Bradford assay and SDS-PAGE.

2.5 Biochemical techniques

2.5.1 GST-fusion protein pulldown assay

The GST-pulldown assay is a powerful method to identify *in vitro* binding partners of a particular protein. A protein, or a domain of a protein, is fused to gluathione S-transferase (GST) and coupled to glutathione sepharose beads. These beads can then be incubated with a lysate, in this case a synaptosome lysate, and proteins which bind to the fusion protein can be extracted and identified. This technique is therefore useful for identifying potential protein-protein interactions.

GST-pulldown assays were carried out using ProbeQuant G-50 spin columns (Amersham) to increase recovery of the proteins of interest and to improve reproducibility (Brymora et al. 2001). This method removes the need for multiple washes and microfuge steps and the associated pitfalls of aspirating all the supernatant without removing the beads because the wash solutions are spun through the column (fig. 2.4).

The protocol is summarised in figure 2.5. Experiments were performed using 3 mg/ml P2 synaptosomes. The synaptosomes were incubated at 37 °C in $+Ca^{2+}$ Krebs-like buffer and stimulated where indicated by the addition of 30 mM KCl. The synaptosomes were then vortexed and spun down in a microfuge for 1 min. The Krebs-like buffer was aspirated and the synaptosome pellet resuspended in 200 µl of ice-cold lysis buffer (1 % Triton X-100, 25 mM Tris, 150 mM NaCl, 1 mM EGTA, 1 mM EDTA, 20 µg/ml leupeptin, 1 mM PMSF, 1 mM $ZnSO_4$, pH 7.4 plus 1 protease inhibitor tablet per 25 ml lysis buffer). The lysis reaction was allowed to continue for 15 min with samples on ice and vortexed every 5 min. The lysates were spun in a chilled microfuge at 18890 x *g* (13 000 rpm) for 5 min and 175 µl of the supernatant incubated with pre-prepared ProbeQuant G-50 microcolumns containing the washed GST fusion protein coupled to GSH beads. The beads and lysate were incubated with rotation for 1 hr at 4 °C.

The GST-fusion protein columns were prepared by firstly emptying the ProbeQuant G-50 microcolumns and washing them thoroughly with distilled water. The appropriate volume of GST-fusion protein bead slurry was added to each column

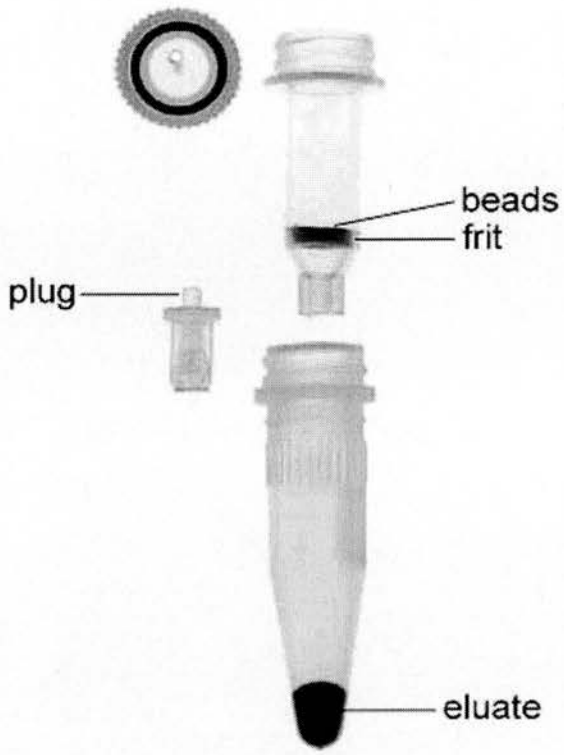

Figure 2.4 – Spin column for pulldown assays and immunoprecipitations

Image illustrates the ProbeQuant G-50 columns which fit inside a 2 ml eppendorf tube. The columns have a plug which positively displaces air from under the sample, reducing the likelihood of leakage from the sample below the frit. The frit also remains intact during the boiling of the sample preventing the sample becoming contaminated with beads. Figure taken from Brymora *et al*, 2001.

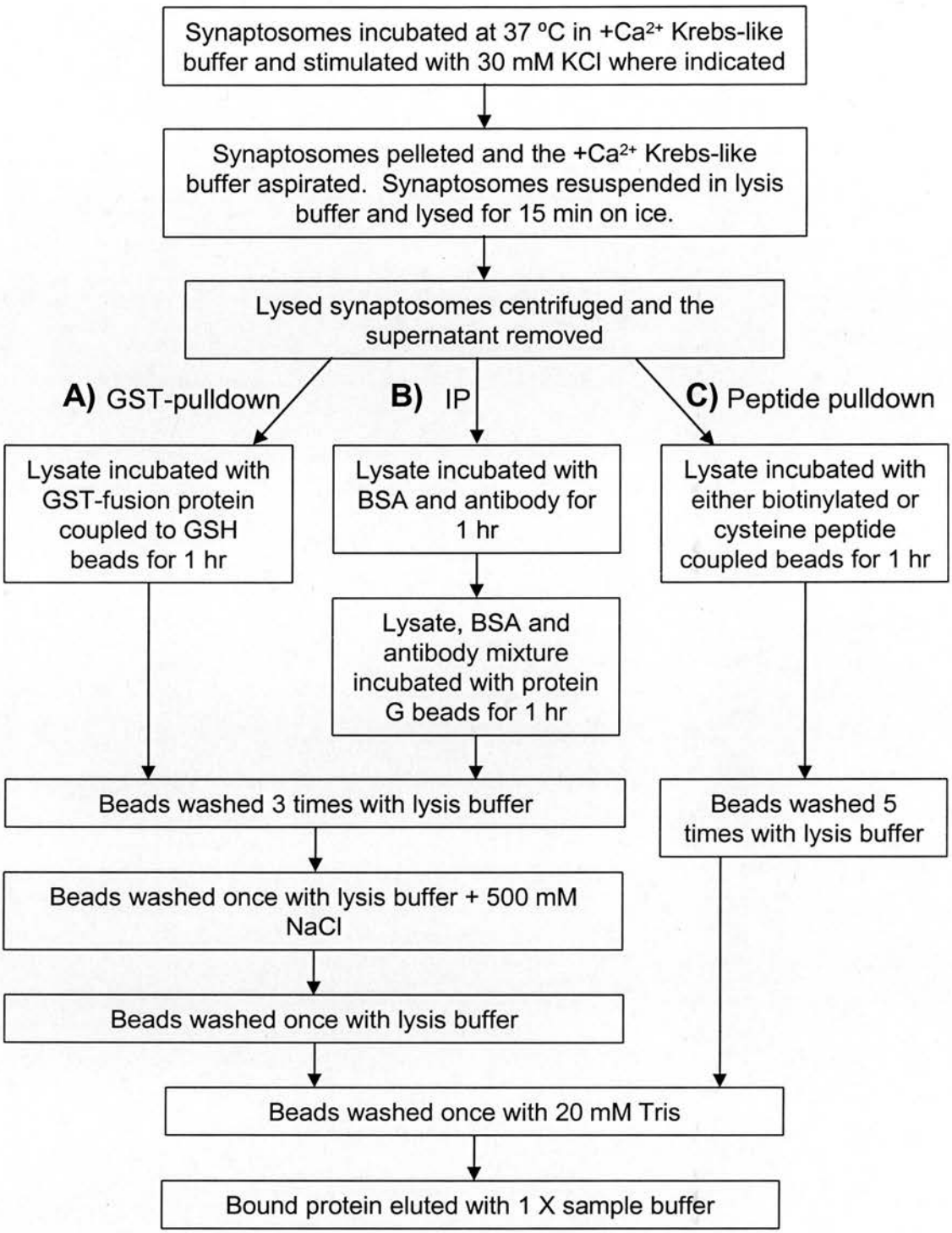

Figure 2.5 – Overview of the GST-pulldown, immunoprecipitation and peptide pulldown protocols

Flow chart illustrating **A)** the GST-pulldown assay protocol, **B)** the immunoprecipitation (IP) protocol and **C)** the peptide pulldown assay protocol.

(typically between 20 and 300 µl, depending on the efficiency of the protein expression and coupling reaction). The columns were unplugged and inserted into 2 ml eppendorf tubes in a chilled microfuge rotor. The PBS in the slurry was spun through the column at 870 x *g* (2800 rpm) for 10 s. The spin speed was slow to prevent the beads becoming crushed. The flow through in the 2 ml eppendorf was removed and the beads were washed with 500 µl of chilled lysis buffer and spun for a further 10 s at 870 x *g*. The tubes were then replugged and 50 µl of lysis buffer was added to the beads. The columns were stored at 4 °C until use.

After incubation with the lysate the columns were unplugged and inserted into 2 ml eppendorf tubes in the chilled microfuge. They were spun at 870 x *g* for 10 s and the flow through discarded. All of the washes were carried out with ice-cold solutions. The beads were washed three times with 500 µl of lysis buffer, once with 500 µl of lysis buffer plus NaCl (final concentration 500 mM), once again with 500 µl of lysis buffer and finally with 500 µl of 20 mM Tris, pH 7.4. The columns were then replugged and a sufficient volume of 1X sample buffer (67 mM Tris, 9.3 % glycerol, 2 mM EGTA, 67 mM SDS, bromophenol blue, 12 % β-mercaptoethanol) added to cover all of the beads, typically 30 µl. The columns were then vortexed and boiled for 5 min before being unplugged and inserted into fresh 1.5 ml eppendorfs and spun at 18890 x *g* (13 000 rpm) for 10 min. The eluted samples were stored at –20 °C until analysed by SDS-PAGE.

In some experiments the synaptosomes were lysed in lysis buffer plus 2 mM $CaCl_2$ and with the EDTA and EGTA omitted. The beads for these samples were prepared

by washing in lysis buffers containing 2 mM $CaCl_2$, as well as all of the washes following incubation with the synaptosome lysate. This was to ensure that any Ca^{2+}-dependent interactions were not lost during any of the washes.

2.5.2 Immunoprecipitation of proteins

Immunoprecipitation is used to determine *in vivo* interactions of a protein of interest. The protein of interest is specifically extracted from a cell lysate by an antibody thus pulling out the protein and importantly, binding partners within the lysate. This technique is superior to GST-pulldown assays since it extracts endogenous protein-protein interactions. The antibody is bound to an insoluble matrix, in this case protein G covalently linked to sepharose beads. Bound proteins can then be eluted using SDS sample buffer.

The protocol is summarised in figure 2.5B. P2 synaptosomes (3 mg/ml) or percoll synaptosomes (2 mg/ml) were incubated at 37 °C in $+Ca^{2+}$ Krebs-like buffer and stimulated with 30 mM KCl where indicated. The synaptosomes were lysed in an identical manner as for the GST-pulldown assay (2.5.1). The synaptosome lysate was removed into a fresh eppendorf and 175 µl of 50 mg/ml BSA was added to decrease non-specific binding. The appropriate volume of antibody, typically between 6 – 10 µl, was then added and the samples vortexed. The eppendorfs were incubated with rotation for 1 hr at 4 °C.

Whilst the samples were incubating, the protein G beads were prepared. ProbeQuant G-50 columns were emptied and washed with distilled water as for the GST-

pulldown assay (2.5.1). A 25 % protein G bead solution in PBS slurry (200 µl) was added to the columns. The columns were unplugged and placed inside 2 ml eppendorfs in a chilled rotor. The columns were spun at 870 x *g* (2800 rpm) for 10 s to remove the PBS. The beads were then washed with 500 µl of lysis buffer and covered with 50 µl of lysis buffer as for the GST-beads. The columns were stored at 4 °C until use.

After 1 hr, the whole of the antibody-sample solution was added to the plugged columns containing the protein G beads and incubated, with rotation, at 4 °C for a further hour. The columns were then unplugged and inserted into 2 ml eppendorf columns in the chilled microfuge. They were spun at 870 x *g* for 10 s and the flow through discarded. The beads were then washed in an identical manner to the beads in the GST-pulldown assay and the bound proteins eluted with 30 µl of 1 X sample buffer. The samples were boiled, spun into fresh 1.5 ml eppendorfs and stored at -20 °C until analysis, as above.

For some IPs the protocol was modified to include a further incubation with peptides to disrupt complexes formed on the beads. Following incubation with the antibody and the protein-G beads, the beads were washed but instead of elution with 1 X sample buffer, 175 µl of lysis buffer plus the indicated concentration of peptide were added. The columns were then incubated for 1 hr with rotation at 4 °C. The flow through was saved and the beads washed as before. The bound samples were eluted with 1 X sample buffer.

2.5.3 Peptide pulldown assays

Peptides N-terminally tagged with either biotin or a free cysteine residue, were used to determine the binding targets of the peptide sequence in synaptosomes. Biotin binds to streptavidin with high affinity and so the biotin tag was used to couple the peptides to streptavidin-coated sepharose beads. The free cysteine was used to couple peptides to Sulpholink® beads. Sulpholink® beads also have a free cysteine residue and so under oxidising conditions disulphide bonds form, covalently coupling the peptide to the beads. Cysteine-tagged peptides have the advantage that following coupling of the peptide, the remaining cysteine residues on the beads can be blocked by reaction with cysteine in solution. This reduces the amount of non-specific binding, allowing easier identification of potential peptide binding partners. The overall protocol for the peptide pulldown assays is summarised in figure 2.5C.

2.5.3.1 Biotinylated peptide pulldown assay

ProbeQuant G-50 columns were used for the peptide pulldown assays. The columns were washed out as before and the streptavidin sepharose beads added. The biotinylated peptide was coupled to the beads by incubating 250 µM peptide with the streptavidin beads for 1 hr with rotation at 4 °C. Following the incubation period, the beads were washed with 500 µl of lysis buffer. The beads were then covered with 50 µl of lysis buffer and stored at 4 °C until use.

Percoll purified synaptosomes (2 mg/ml) were stimulated with 30 mM KCl where indicated and lysed as for the GST-pulldown assay (2.5.1). The 175 µl of cleared lysate was then incubated with the biotinylated peptide coupled to the streptavidin

coated beads for 1 hr with rotation at 4 °C. The beads were then washed in an identical manner to the GST-pulldown assay except that the lysis buffer plus 500 mM NaCl wash was omitted. The bound proteins were eluted with 1 X sample buffer and stored at -20 °C until analysis.

2.5.3.2 Cysteine-linked peptide pulldown assay

The cysteine-tagged peptides were coupled to Sulpholink® gel using a modified version of the method supplied by Pierce. The Sulpholink gel® was equilibriated to room temperature and 500 µl of the slurry pipetted into empty, washed ProbeQuant G-50 columns. The beads were equilibrated by washing four times with 500 µl of coupling buffer (50 mM Tris, 5 mM EDTA, pH 8.5). The lyophilised cysteine tagged peptides were solubilised in coupling buffer and 1 mg/ml was added to each column – control columns with only coupling buffer were also prepared. The columns were mixed end-over-end for 15 min at room temperature and then left to stand for 30 min at room temperature. The columns were then washed three times with 500 µl of coupling buffer. The remaining cysteine residues on the beads were then blocked by incubating the beads with 50 mM cysteine solution (pH 8.5) for 15 min end-over-end and a further 30 min standing at room temperature. The blocked columns were then washed six times with 500 µl of wash buffer (1 M NaCl) and twice with 500 µl of PBS. The beads were covered with PBS and the columns stored at 4 °C until use.

The peptide pulldown assay was conducted like the GST-fusion protein assay, although the lysis buffer plus 500 mM NaCl wash was omitted. The volume of the

beads is also much greater and so typically 150 µl of sample buffer was used to cover the beads and consequently the final sample volume was much larger. This was concentrated down by evaporation using heating at 95 °C before analysis by SDS-PAGE.

2.5.4 Synaptosome lysis experiments

Lysates derived from synaptosomes pre-incubated in the absence and presence of cyclosporin A were used to determine the phosphorylation status of proteins such as dynamin I. Percoll purified synaptosomes (0.3 mg) were resuspended in 50 µl of $+Ca^{2+}$ Krebs-like buffer and incubated in a water bath at 37 °C for 15 min ± 40 µM cyclosporin A. The basal samples were prepared by the addition of 50 µl of $+Ca^{2+}$ Krebs-like buffer and stimulated samples were prepared by the addition of 50 µl of $+Ca^{2+}$ Krebs-like buffer supplemented with 60 mM KCl (final concentration 30 mM KCl). Both basal and stimulated samples were fixed by the addition of 50 µl of 3 X sample buffer (0.2 M Tris pH 6.8, 28 % glycerol, 6 mM EGTA, 200 mM SDS, bromophenol blue, β-mercaptoethanol) and boiled for 5 min. The samples were stored at -20 °C until analysis by western blotting.

2.5.5 SDS gel electrophoresis

Samples generated from the above procedures were analysed by SDS-PAGE on 7.5 %, 10 % or 15 % poly-acrylamide SDS gels. Gels were stained with either coomassie or silver stain. The gel system used to cast and run the gels was the Protean 3 system (Bio-Rad, California, USA).

The table below shows the recipes used for one mini-gel.

Table 2.1 – Recipies for the SDS-PAGE gels

	Separating gel			Stacking gel
	7.5 %	10 %	15 %	
0.5 mM Tris buffer pH 6.8	-	-	-	500 µl
1.5 mM Tris buffer pH 8.8	1 ml	1 ml	1 ml	-
30 % Acrylamide/Bis solution 37.5:1	1 ml	1.3 ml	2 ml	300 µl
10 % SDS	40 µl	40 µl	40 µl	20 µl
dH_20	2 ml	1.7 ml	1 ml	1.2 ml
10 % APS	14 µl	14 µl	14 µl	20 µl
TEMED	3 µl	3 µl	3 µl	2 µl

The separating gel was left to set after overlaying with butanol to ensure the gel set level. Once set, the butanol was poured off and the stacking gel added. The stacking gel recipe was the same regardless of the % of the separating gel. Gels were run in running buffer (25 mM Tris, 200 mM glycine, 10 % SDS) at 140 V for approximately 1.5 hr. The gels were then stained in coomassie G-250 (50 % methanol, 10 % acetic acid, 40 % distilled water, 0.25 % coomassie G-250) for approximately 15 min and subsequently destained (50% methanol, 10 % acetic acid, 40 % distilled water).

Where bands were to be cut out for MALDI-TOF analysis, gels were stained with coomassie R-250 (17 % ammonium sulphate, 3 % phosphoric acid, 0.1 % coomassie R-250, 34 % methanol, 45.9 % distilled water) and destained using distilled water. These gels were handled as little as possible, and during staining and destaining were

in containers with lids to minimise contamination from keratin. Bands were cut out on top of a light box using clean scalpel blades for each band and put in methanol washed eppendorfs.

Where greater sensitivity was required the gels were silver stained using a method based on that of Wray *et al* (1981). After running the gel, it was fixed in 50 % methanol for one hour and then washed three times in distilled water for 5 min each. The gel was then stained (0.05 M $AgNO_3$, 0.02 M NaOH, NH_4OH enough to dissolve Ag precipitate) for 30 min and washed again three times for 5 min each in distilled water. The gel was then put in developer solution (0.24 mM citric acid monohydrate, 6 mM formaldehyde) before stopping the reaction with 50 % methanol.

2.5.6 Western blotting

To detect the presence of a specific protein or state of a protein, for example phosphorylation state, some samples were analysed by western blotting. After running an SDS-PAGE gel the samples were transferred on to nitrocellulose membrane by passing an electric current through the gel. This transfers the proteins from the gel onto the membrane. The membrane was then incubated with antibodies to a given protein and the presence of the antibody detected by chemoluminescence.

Proteins were transferred from the SDS-PAGE gel to nitrocellulose membrane using a Bio-rad mini-transblotting cell. The transfer was performed using chilled transfer buffer (960 mM glycine, 25 mM tris) and run at 100 V for 90 min or at 30 V

overnight. The sandwich was then dismantled and the membrane air dried for approximately 20 s. The membrane was then stained with ponceau S solution (0.1 % ponceau S in 5 % acetic acid) to check that the gel had transferred correctly to the membrane. Ponceau S stain is water soluble and so the membrane was then destained in water and blocked in PBS plus 5 % skimmed milk and 0.5 % PVP-40 for at least one hour. Blocking the membrane with a protein solution (milk) ensures that the whole surface of the membrane has protein bound, reducing non-specific binding of the antibodies to the membrane in subsequent steps.

After washing with PBS, the membrane was incubated with the appropriate antibody (diluted in PBS plus 0.5 % PVP-40) for at least three hours, washed several times with PBS and incubated with the appropriate secondary antibody (again diluted in PBS plus 0.5 % PVP-40) for one hour. The secondary antibody is coupled to horseradish peroxidase (HRP) and thus can react with the peroxide in the chemoluminescence reagent. The membrane was again washed several times in PBS before being covered with chemoluminescent solution for 5 min and exposed to photographic film. The reaction by the HRP on the secondary antibody releases light which is detected by the photographic film. On some occasions a GeneGnome system (Syngene, Cambridge, UK) was used instead of film where the signal was very strong and a short exposure was required. The software used to take the image was GeneSnap Version 6.05 (Syngene).

Some of the western blot exposures were analysed by densitometry. The blots were firstly scanned using a Bio-rad GS-710 scanner and analysed using Quantity 1

software (Bio-rad). An area was drawn around the largest band of interest and the same box size copied across the other bands. Boxes were also drawn in blank sections of each lane to be used for background readings. The density of each box was recorded by the software. The reading from the background boxes was subtracted from the band boxes. The density of the bands after correction for background could then be used for comparison and further analysis.

2.5.7 $^{45}Ca^{2+}$ overlay assay

The $^{45}Ca^{2+}$ overlay assay is a useful tool to determine if proteins or protein domains can bind Ca^{2+}. The protocol used was based on a protocol devised by Maruyama *et al* (1984) and modified by Liu *et al* (1996). Firstly samples of purified proteins (1 μg) were run on an SDS-PAGE gel. A 15 % gel was used since the protein domains of interest were mostly under 40 kDa and a 15 % gel would resolve these proteins better than a 7.5 or 10 % gel. The gel was then transferred onto nitrocellulose membrane as for western blotting (2.5.6) and following transfer ponceau S stained to ensure transfer was complete. The membrane was then destained with distilled water and washed twice with 5 mM imidazole (pH 7.4) for 5 min each. This step is to strip off any divalent cations present on the membrane.

The membrane was then incubated in 10 ml of overlay buffer (5 mM imidazole, 60 mM KCl, 5 mM $MgSO_4$, pH 7.4). To this 1 μCi/ml $^{45}Ca^{2+}$ was added and incubated with rocking for 30 min at room temperature. The membrane was then washed in 30 % ethanol for 10 min and then in 30 % ethanol for a further 1 min. The

membrane was then air dried and taped into a film cassette for autoradiography. The film was typically left for 2 days before developing.

2.5.8 *In vitro* binding assay

An *in vitro* binding assay was used to determine if two proteins interacted directly. One of the proteins was GST-tagged to allow purification on GSH coated beads. The binding assay was carried out using the ProbeQuant G-50 columns as used previously for GST-pulldowns. GSH beads were washed in PBS, blocked in PBS + 0.1 % Triton X-100 and washed again in PBS. The PBS was removed and the beads resuspended in PBS to make a 50 % slurry. The slurry was pipetted into empty columns (40 µl).

The binding assay was conducted in binding buffer (20 mM HEPES, 150 mM KCl, 1 mM DTT, 0.05 % Tween, pH 7.4) with the addition of either 2 mM $CaCl_2$ for $+Ca^{2+}$ samples or 2 mM EGTA for $-Ca^{2+}$ samples. The concentration of the protein with the GST-tag was kept constant at 200 nM and the concentration of the other protein was serially diluted from 500 µM to 15.63 µM.

The proteins in the binding assay buffer were incubated with the blocked GSH beads with rotation for 2 hr at 4 °C. Following the incubation, the beads were washed in a similar manner to the GST-pulldown assay (2.5.1) five times with 400 µl of binding buffer supplemented with either 2 mM $CaCl_2$ for the $+Ca^{2+}$ samples or 2 mM EGTA for the $-Ca^{2+}$ samples. The bound proteins were then eluted in 40 µl of 1 X sample buffer and stored at -20 °C until analysis.

The samples generated from the *in vitro* binding assay were run on a 10 or 15 % SDS-PAGE gel and transferred. The samples were blotted for the protein of interest which was serially diluted and, as a loading control, for GST. The exposures were then analysed by densitometry. The density was expressed as % binding saturation to allow comparison between conditions.

2.6 Electron microscopy

Percoll-purified synaptosomes (0.15 mg) were incubated ± 40 μM cyclosporin A for 15 min at 37 °C and stimulated, where indicated, for 2 min with 30 mM KCl. The pellets were then resuspended in fixative (0.1 M NaCacodylate, 2 mM $CaCl_2$, 3 % glutaraldehyde) for 1 hour and pelleted. The pellet was then washed 3 times in cacodylate buffer (0.1 M NaCacodylate, 2 mM $CaCl_2$) by resuspending the pellet and centrifuging. The pellet was then resuspended in stain (2 % OsO_4) for 1 hour, spun down and finally cacodylate buffer layered on the top of the pellet. The samples were then transferred to Steven Mitchell (Electron microscope facility, University of Edinburgh) for further processing. The samples were dehydrated for 10 min in each of 50 % acetone, 70 % acetone, 90 % acetone and 100 % acetone. The samples were infiltrated with a 50:50 mix of araldite and acetone and baked in a 60 °C oven overnight. The samples were then embedded in resin for 48 hr at 60 °C before sectioning and mounting onto grids. The grids were viewed using a Philips CM12 electron microscope.

2.7 Cerebellar granule neuron experiments

Synaptosomes are a very powerful system for studying the molecular mechanisms of SV recycling since they are the simplest system containing all the proteins necessary for neurotransmission. However, they do not contain a nucleus and so transfection of mutant proteins and protein domains is not possible. For this sort of study cerebellar granule neurons (CGNs) are a better system to work with since they can be readily cultured and can be transfected.

2.7.1 CGN preparation and culture

CGNs were provided by Dr. M. Cousin but were prepared as follows. The cerebellum from 7 day old Sprague-Dawley rats were extracted and minced using a McIlwain tissue chopper. The chopped tissue was then incubated with trypsin to dissociate the cells. After trypsinisation, soy bean trypsin inhibitor (SBTI) was added to inhibit the trypsin and DNase was added to prevent the cell solution becoming viscous. The cells were pelleted by centrifugation and the cell pellet resuspended in approximately 1.5 ml of buffer containing SBTI and DNase. The cells were triturated using pipettes of decreasing bore size to fully dissociate the cells. The cell suspension was then layered onto Earle's balanced salt solution (EBSS) and centrifuged to remove any debris resulting from trituration. The pellet was resuspended in approximately 2 ml culture medium (Minimal Essential Medium (MEM) containing Earle's Salts plus 10% (v/v) foetal calf serum, 25 mM KCl, 30 mM glucose, 2 mM glutamine, 100 U/ml penicillin and 100 µg/ml streptomycin) and the cells counted using a haemocytometer. The volume of the suspension was then adjusted so that 100 µl of the suspension contained $2.5x10^6$ cells. An aliquot of

100 µl was then pipetted onto coverslips which had been pretreated with poly-D-lysine and placed into culture dishes. The coverslips were then placed in the incubator (37 °C, 5 % CO_2) for an hour before a further 2-3ml of culture media was added to each well. After 24 hr, the media was replaced with 2ml of culture media supplemented with 10 µM cytosine arabinoside. The cytosine arabinoside inhibits cell division and thus prevents other cell types present in the culture, such as astrocytes, multiplying.

2.7.2 Calcium phosphate transfection of CGNs

CGNs were transfected 7 days after culturing using calcium phosphate precipitation. The DNA to be transfected forms a precipitate with the calcium phosphate which when added to the cells is internalised. The DNA can then become incorporated into the nucleus of the CGNs and the protein of interest expressed.

Conditioned media from the cells was aspirated from the culture wells and placed into a CO_2 incubator. The cells were washed twice with MEM to remove all traces of serum from the cells. The cells were then incubated in 1 ml of MEM at 37 °C, 5 % CO_2 for 1 hr.

During this incubation period the DNA precipitate was prepared. For each well usually 5.75 µg of DNA was used. The 5.75 µg of DNA was added to a tube containing 2.25 µl of 2.5 M $CaCl_2$ and the required volume of distilled water to bring the total volume up to 22.5 µl. After vortexing, this solution was then added drop wise to 22.5 µl of 2X HEPES buffered saline (HeBS, 300 mM NaCl, 10 mM KCl,

1.5 mM $Na_2HPO_4.12H_2O$, 15 mM D-glucose, 50 mM HEPES, pH 7.14) while the HeBS was stirred on a vortex. The solution was then incubated at room temperature for at least 30 min in the dark.

Once the precipitate and cell incubation periods were over, 45 µl of precipitate suspension was added drop wise to the centre of each well. The dish was then agitated to fully disperse the DNA. The cells were incubated for 30 – 40 min at 37 °C, 5 % CO_2. After this incubation period, the cells were washed twice with MEM solution and then 2 ml of the original conditioned media was added to each well. The cells were analysed usually 2 days after transfection.

2.7.3 Imaging of CGNs with styryl dyes

SV turnover in CGNs transfected with eGFP-tagged constructs was monitored using a similar assay protocol to the SV turnover assay in synaptosomes (2.3.2). The styryl dye FM4-64 was used instead of FM2-10 because it is red-shifted and thus emitted fluorescence can be measured in the red spectrum simultaneously with the green fluorescence of the eGFP-tagged construct. The CGNs were loaded with FM4-64 using a KCl stimulus to evoke exocytosis and subsequent endocytosis. The extracellularly bound FM4-64 was then washed off the cells and the internalised FM4-64 released by a further stimulation with KCl. Again, the stimulation-dependent release of the FM4-64 was taken as an estimate of the amount of dye internalised and of SV turnover. The kinetics of unloading were also investigated since, once normalised, will reflect any effect on exocytosis.

Neurons were removed from culture medium and left to repolarise for 10 min in incubation medium (170 mM NaCl, 3.5 mM KCl, 0.4 mM KH_2PO_4, 20 mM *N*-tris[hydroxy-methyl]-methyl-2-aminoethane-sulphonic acid (TES), 5 mM $NaHCO_3$, 5 mM glucose, 1.2 mM Na_2SO_4, 1.2 mM $MgCl_2$, 1.3 mM $CaCl_2$, pH 7.4). Neurons were then loaded with FM4-64 by evoking SV turnover using KCl stimulation medium (incubation medium supplemented with 50 mM KCl and 10 μM FM4-64, 50 mM NaCl being removed to maintain osmolarity) for 2 min. Cells were washed with incubation medium and after 15 min the FM4-64 was unloaded from the cells by stimulation with 50 mM KCl. FM4-64 unloading was visualised using a Zeiss axiovert TV-100 epifluorescence microscope using a x43 oil immersion objective at 550 nm excitation and > 575 nm emission. Transfected neurons were visualised at 480 nm excitation and a band pass filter of 510 – 550 nm. The stimulus-dependent decrease in fluorescence intensity of FM4-64 loaded nerve terminals was visualised using a Hamamatsu Orca-ER CCD digital camera (Japan) and offline imaging software (Compix Imaging Systems, USA).

The stimulation-dependent fluorescence drop was quantified by drawing regions of interest, corresponding to the nerve terminals, and the fluorescence in that area recorded over time. Regions of interest were drawn around puncta from transfected CGNs as well as non-transfected CGNs in the same field of view to act as an internal control. Figure 2.6A shows some of the raw data obtained from a control experiment with untransfected CGNs. The initial fluorescence of each puncta begins at different levels and thus the fluorescence drops also start at different initial values. The first stage of the analysis is to normalise the start point of the drop at the point of

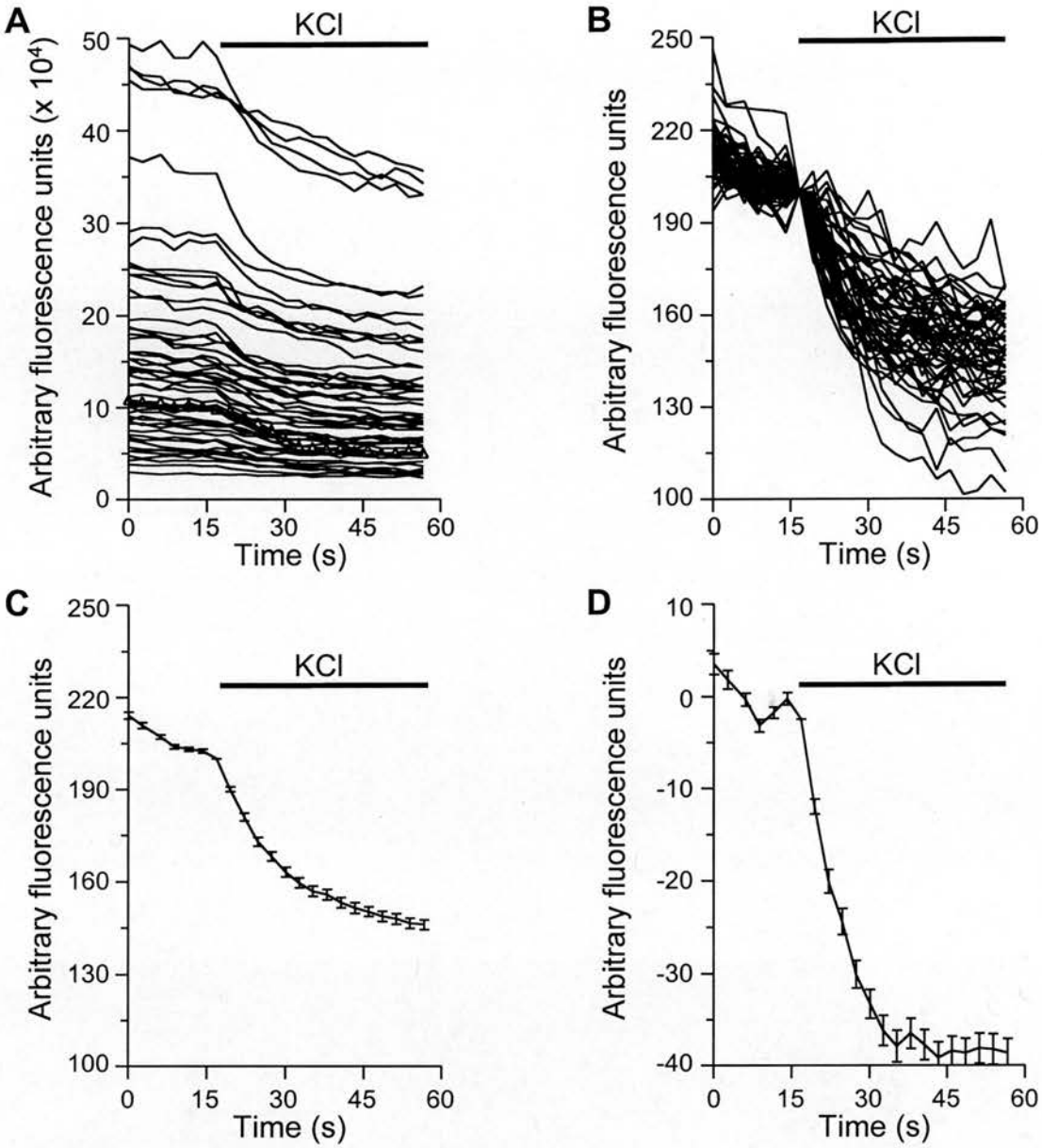

Figure 2.6 – Analysis stages for SV turnover assay in cerebellar granule neurons (CGNs)

A) The fluorescence drop from individual nerve terminals in CGNs loaded with FM4-64 upon stimulation with 50 mM KCl. **B)** The data from **A** with the start point of the fluorescence drop normalised to an arbitrary value. **C)** The average fluorescence drop. **D)** The average fluorescence drop following normalisation for the decay of the FM4-64. ($n \geq 87 \pm$ SEM, where error bars are shown) Bar denotes the presence of KCl.

stimulation to an arbitrary fluorescence value. Some of the individual normalised traces can be seen in figure 2.6B. Note that the start point for the drop upon stimulation is the same for all traces and that although the start point is normalised, the size of drop varies depending on the response of the individual nerve terminals. The average stimulation dependent fluorescence drop can now be calculated by taking the mean of the individual drops (fig 2.6C).

The fluorescence of the styryl dyes decay when exposed to the light and therefore part of the fluorescence drop is due to the bleaching of the dye. Several experiments were run to determine the decay of the dye and curves to fit the decays generated. The average stimulation-dependent fluorescence drop curve is then normalised by subtraction of the decay curve which best matches the slope and rate of the decay. This means that the calculated fluorescent drop is entirely attributed to the stimulation-dependent release of the dye (fig 2.6D).

The kinetics of release can be used to determine if there is any effect on exocytosis. By normalising the start and end point of the fluorescence drop between 1 and 0, respectively, the curve displayed is independent of dye accumulation and reflects only the rate of release, and thus, exocytosis. From this curve the time taken for the fluorescence to drop by 50 % ($t_{1/2}$) was determined (fig 2.7) since the unloading rate is linear.

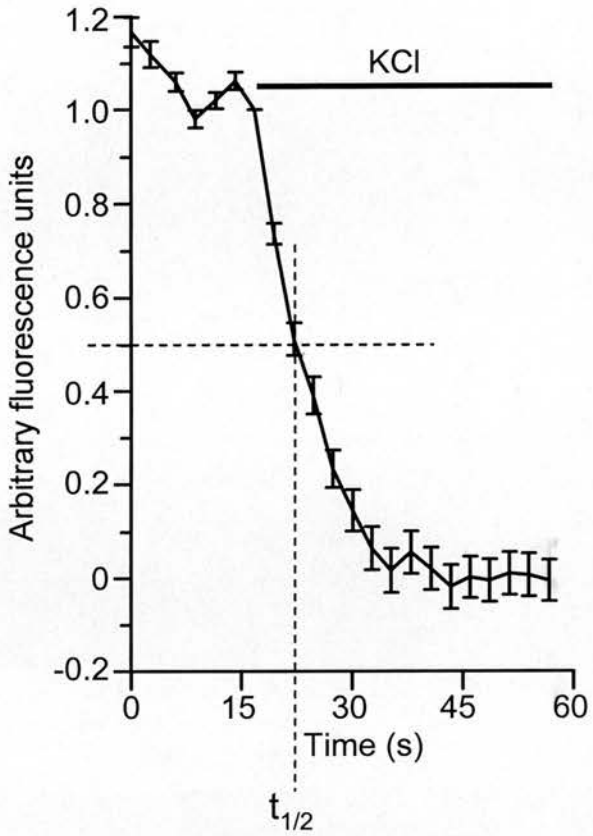

Figure 2.7 – Kinetic analysis of unloading of CGNs

Graph showing the average fluorescence drop corrected for FM4-64 decay with the start and end points of the drop normalised between 1 and 0. The point for the fluorescence to drop by 50 % ($t_{1/2}$) is marked. Bar denotes the presence of KCl.

CHAPTER 3

PENETRATIN MEDIATED PEPTIDE DELIVERY TO STUDY SV TRAFFICKING

3.1 Introduction

Biological membranes are impermeable to hydrophilic molecules and so the inability to transport these molecules across the plasma membrane has limited the use of peptides to study cellular function *in vivo*. The discovery that a 60 amino acid sequence known as the homeobox was able to translocate across membranes (Joliot et al. 1991) began research into harnessing this as a method to carry oligonucleotides and polypeptides into cells. The most studied cell penetrating peptide is a truncated form of the homeodomain known as penetratin. However, several other cell penetrating peptides have been discovered including Tat-derived peptides (originally isolated from a transcription factor involved in HIV replication), arginine rich sequences and signal-sequence based peptides (Lindgren et al. 2000; Futaki et al. 2001). Myristolation of peptides has also been used successfully to make peptide sequences membrane permeant (Marks and McMahon 1998).

3.2 The penetratin sequence

Research into cell penetrating peptides began with work on proteins involved in the regulation of neuronal morphological development and differentiation. These proteins were termed homeotic proteins and exerted their effect by binding to DNA sequences in the promotors and enhancers of target genes (Doe and Scott 1988). The region responsible for DNA binding is a 60 amino acid stretch known as the homeobox (Prochiantz 1996; Derossi et al. 1998). To investigate the role of this region, a peptide consisting of these 60 amino acids was synthesised and incubated with neurons during cell dissociation and before cell plating (Joliot et al. 1991). This allowed the peptide to passively diffuse into the neurons as a consequence of neurite

damage. Following a period in culture, a dramatic effect on cell morphology was observed as a result of the transcription factor activity of the homeobox sequence of the peptide. Interestingly, the same effect was seen when the peptide was incubated with the cells in culture after plating. This meant that the peptide sequence itself was able to translocate across the plasma membrane and accumulate in the nuclei of the cells without the need for permeabilisation of the cells.

The homeobox consists of three α-helices with one β-turn between helices two and three (fig 3.1, Derossi et al. 1998). Mutation of residues in the β-turn prevented DNA binding of the peptide but not translocation. Mutation, however, of two tryptophan residues in the third helix to phenylalanines did prevent translocation, indicating that the third helix was essential for internalisation (Le Roux et al. 1993; Derossi et al. 1994; Derossi et al. 1998). The generation of a peptide consisting solely of the sixteen C-terminal amino acids, corresponding to the third helix, showed internalisation with comparable properties to the full length homeodomain, confirming that the third helix was sufficient for translocation. This sequence was termed penetratin (Derossi et al. 1994; Derossi et al. 1998).

To determine the minimum sequence required for translocation, the penetratin sequence was truncated from both the C-terminus and the N-terminus (Fischer et al. 2000). C-terminal truncation of even one residue produced a peptide unable to cross the lipid bilayer efficiently. However, truncation at the N-terminal side of up to eight residues maintained approximately 60 % of control activity. This produced the

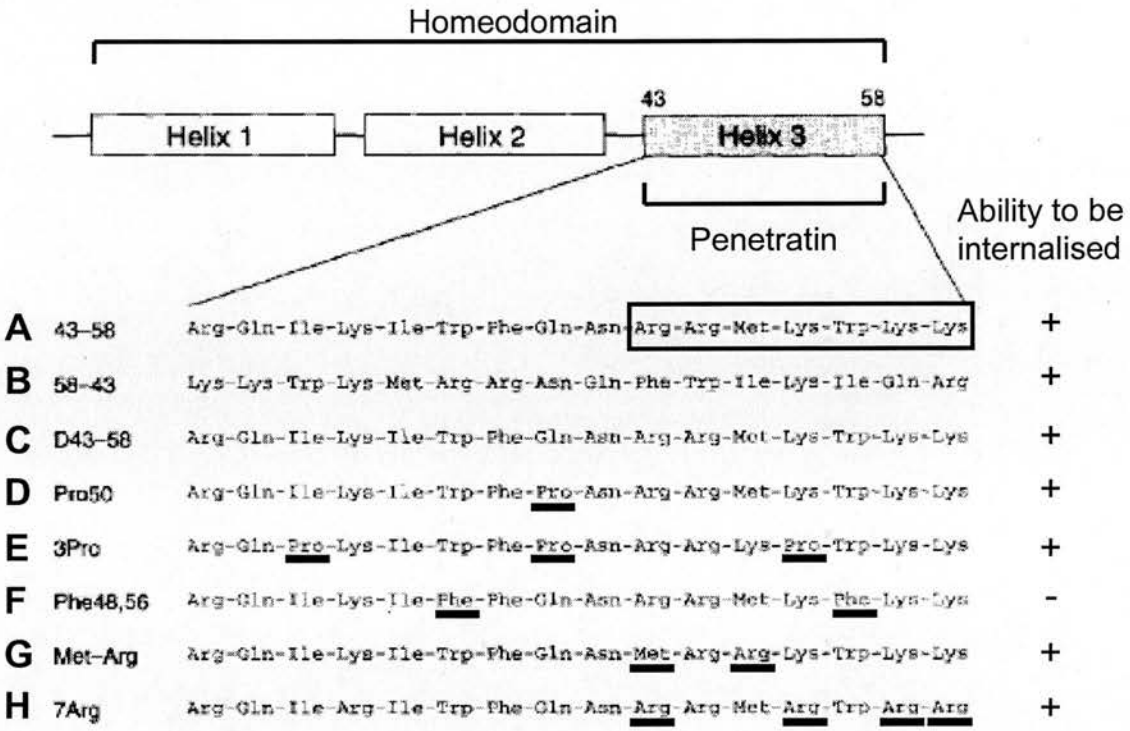

Figure 3.1 – Sequence of penetratin

Illustration showing that penetratin is derived from the third helix of the homeodomain. **(A)** Amino acid sequence, in the three letter code, for penetratin along with the mutant forms **(B to H)** designed to determine the requirements for internalisation. The mutated residues have been underlined. The ability for each peptide to be internalised is indicated (+ represents peptide that can be internalised and – represents a peptide which cannot). The boxed in sequence displays the minimum sequence required for translocation across the plasma membrane (Fischer *et al*, 2000). Figure adapted from Derossi *et al*, 1998.

shortened sequence – Arg-Arg-Met-Lys-Trp-Lys-Lys. It is this sequence which was utilised for peptide tagging in this thesis.

3.3 Mechanism of translocation

The method of penetratin translocation is still under investigation with several possible routes suggested. Studies with the entire homeodomain and with the penetratin sequence showed that the peptides were internalised at 4 °C as well as 37 °C and that the process could not be saturated, implying that the peptides were not being taken into the cell via endocytosis (Joliot et al. 1991; Derossi et al. 1994; Christiaens et al. 2004). Internalisation in the presence of endocytosis inhibitors was also observed reinforcing the theory of uptake by a non-endocytosis dependent process (Lindgren et al. 2004; Nakase et al. 2004).

Melittin, from bee venom, forms transient pores in the plasma membrane to mediate internalisation. Penetratin, however, does not internalise via a pore forming mechanism since vesicles loaded with a fluorescent dye show leakage of the dye in the presence of melittin but not in the presence of penetratin (Thoren et al. 2000).

Mutations in the penetratin sequence were made to determine if specific requirements such as charge, hydrophobicity and secondary structure were important for internalisation in an effort to elucidate the molecular mechanism (fig 3.1, Prochiantz 1996; Derossi et al. 1996; Derossi et al. 1998). Peptides synthesised with the reverse sequence (fig 3.1B) and composed entirely of D enantiomers (fig 3.1C) were effectively internalised, showing that chiral recognition between the peptide

and a cell surface receptor was not required. Proline residues were introduced to the sequence (fig 3.1 D and E) in order to break up the α-helicity but again, these versions of penetratin were efficiently internalised proving that a helix conformation is not an essential requirement. Interestingly, although both peptides were efficiently internalised, the proline mutants were not translocated to the nucleus to the same extent (Derossi et al. 1996). Mutation of tryptophans 48 and 56 to phenylalanine (fig 3.1F, Derossi et al. 1994; Prochiantz 1996; Derossi et al. 1996) did prevent internalisation, implying that the tryptophan residues had a specific role in the process in addition to maintaining amphiphilicity. Tryptophan 56 is likely to be the more important since tryptophan 48 is not as highly conserved across species. Mutation of the surrounding residues did not affect internalisation (fig 3.1G and H, Derossi et al. 1998) confirming that these two tryptophan residues were the important residues in the internalisation process.

From all of this data, the inverted micelle model for peptide internalisation was proposed (Prochiantz 1996; Derossi et al. 1996; Derossi et al. 1998). This is illustrated in figure 3.2. The positively charged amino acids in the penetratin sequence interact directly with the negatively charged phospholipids and aggregate on the surface of the membrane, destabilising it. Work studying the intrinsic tryptophan fluorescence of the peptide indicated that the tryptophan residues inserted into the bilayer, which could promote a change in the organisation of the lipids to an inverted micelle (Christiaens et al. 2002). The peptide, including the cargo, would be accommodated inside the hydrophilic cavity of the inverted micelle, before releasing the peptide into the cytoplasm. The model was tested with phosphorus 31 NMR and

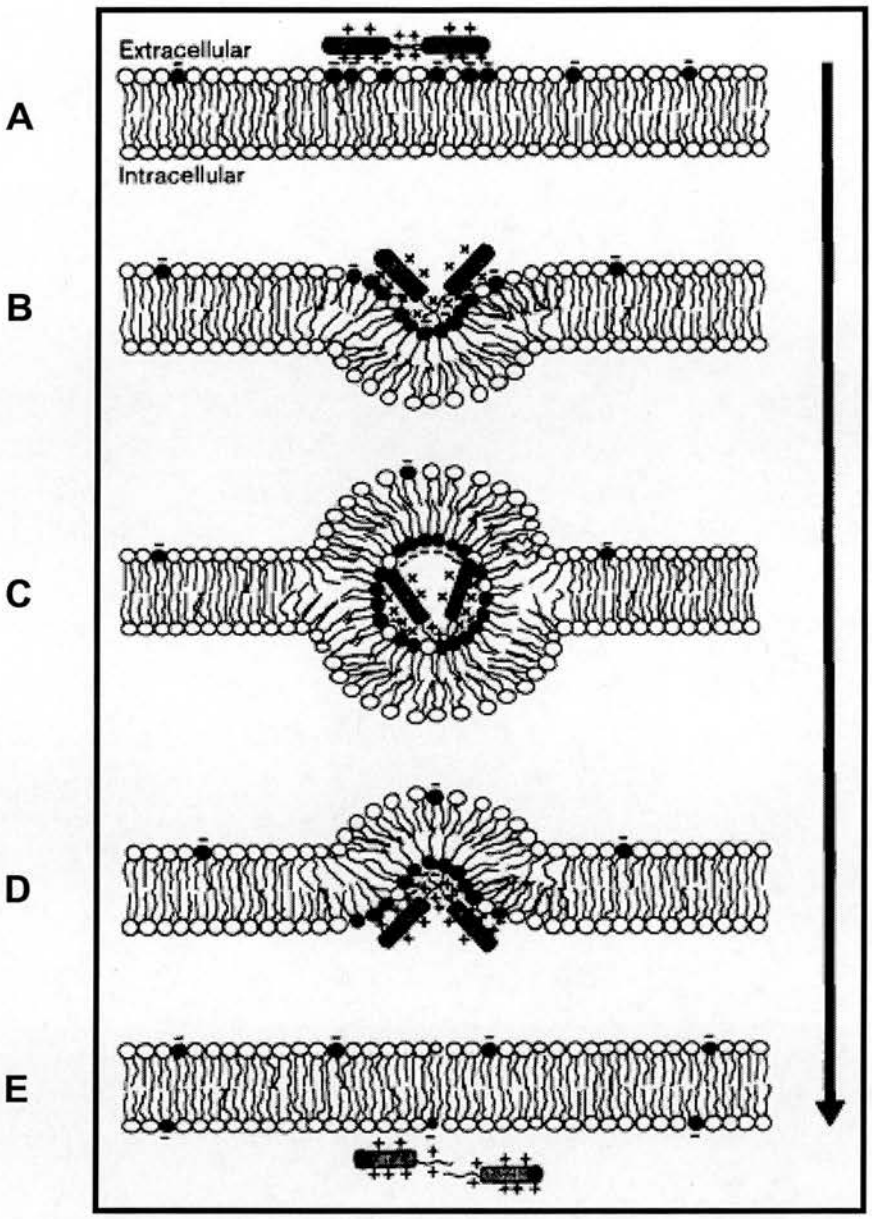

Figure 3.2 – Proposed translocation mechanism of penetratin

(A) The positively charged peptide associates with the negatively charged phospholipids in the membrane. **(B)** The increased concentration of peptide destabilises the membrane along with insertion of the conserved tryptophan into the membrane. **(C)** An inverted micelle is formed with the peptide contained in the hydrophilic cavity. **(D and E)** The peptide is released on the other side of the membrane. Figure adapted from Prochiantz, 1996.

inverted micelles were only formed by the wild type penetratin peptides and not by the phenylalanine mutant peptides lacking the tryptophan residues (Prochiantz 1996).

The inverted micelle model has no requirement for a surface receptor and therefore the peptide movement is not unidirectional. This was observed by Thorén *et al* (2000) using a form of penetratin tagged with a fluorescent reporter and incubated with liposomes. Internal fluorescence of the liposomes increased with time and following dilution with buffer, the intravesicular fluorescence decreased, implying the peptide was able to translocate back out until a new equilibrium was reached.

Proteins of up to a hundred amino acids are internalised efficiently by penetratin but larger cargo cannot always be internalised. This agrees with the inverted micelle model where the cargo has to be contained in the cavity and thus limits the size capable of membrane translocation. However, the homeoproteins themselves are exceptions to this (Prochiantz 1996; Derossi et al. 1998).

There have been other models of internalisation proposed such as membrane thinning where the peptide aggregates cause perturbation of the lipid bilayer, decreasing the surface tension and allowing the peptide to pass through the membrane (Magzoub et al. 2002). Macropinocytosis has also been proposed (Nakase et al. 2004), although the inverted micelle model remains the most popular with the field.

3.4 Strategy to use penetratin as a tool to investigate SV endocytosis

Penetratin does not appear to depend fully on classical endocytosis to be taken into the cell (Prochiantz 1996; Derossi et al. 1998; Lindgren et al. 2000) and thus it is an ideal tool for studying *in vivo* protein-protein interactions involved in endocytosis in nerve terminals. SV endocytosis involves a cascade of many protein-protein interactions and therefore the aim of these experiments was to disrupt specific interactions at different stages of the SV cycle to determine, firstly, if the interaction was essential for SV recycling and secondly, what effect disruption of one interaction had on the other interactions in the cascade.

Peptides were designed from known interaction motifs between proteins involved at different stages in the SV lifecycle (fig 3.3). The peptides were all N-terminally tagged with the shortened form of penetratin which translocates with almost the same efficiency as full length penetratin (Fischer et al. 2000). These peptides were then used in assays of SV recycling to determine if perturbation of specific interactions had an effect on SV exocytosis or endocytosis. GST-fusion protein pulldown assays were also used to determine the specificity of the peptides and to investigate whether perturbation of an interaction early in SV endocytosis, say at nucleation, had any effect on the protein-protein interactions thought to occur later in the process, say at fission.

This chapter shows that penetratin tagging of peptides is an effective way of delivering peptides into synaptosomes. The peptides were functional since inhibition of SV exocytosis and endocytosis was observed. This was not due to the penetratin

A

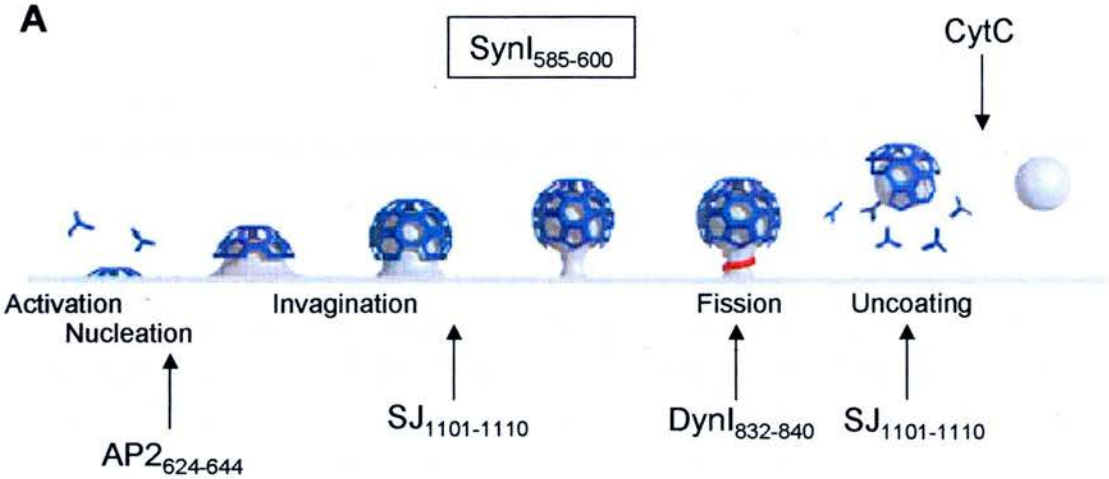

B

Peptide name	Peptide sequence	Description
$AP2_{624-644}$	RRM KWK KQG DLL GDL LNL DLG PPV NVP Q	AP2 / Clathrin interaction
$SJ_{1101-1110}$	RRM KWK KEP KRP PPP RP	Synaptojanin / Endophilin interaction
$DynI_{832-840}$	RRM KWK KQV PSR PNR AP	Dynamin I / Amphiphysin interaction
CytC	RRM KWK KKL IGV LSS LFP PK	Cytochrome c / Hsc 70 interaction
$SynI_{585-600}$	RRM KWK KRQ GPP QKP PGP AGP IR	p85 / Synapsin I interaction

Figure 3.3 – Strategy to block SV endocytosis

(A) Schematic showing the stages of SV endocytosis (activation, nucleation, invagination, fission and uncoating). The arrows denote the points at which the peptides are designed to act. Note that $SynI_{585-600}$ was designed to inhibit vesicle trafficking and not at a stage in the generation of a vesicle. Figure adapted from Gad *et al*, 2000. **(B)** Table listing the names of the peptides, the sequence of each of the peptide (in the single letter amino acid code) and the interaction each was designed to inhibit.

tag since differential effects were observed depending on the peptide. Pulldown assays with domains of endocytosis proteins confirmed that the peptides were able to inhibit protein-protein interactions, although some of the peptides with more generic sequences, such as the proline rich peptides, were not totally specific.

3.5 Penetratin peptides can specifically inhibit SV exocytosis or endocytosis depending on the sequence

To determine if any of the peptides had an effect on SV exocytosis or endocytosis, SV recycling was assayed in synaptosomes using the styryl dye, FM2-10, to measure synaptic vesicle turnover and a glutamate release assay was used to measure exocytosis.

SV turnover was first assayed. Synaptosomes were pre-incubated for 30 min plus or minus Ca^{2+} and in the absence and presence of peptide. The synaptosomes were stimulated with 30 mM KCl to evoke exocytosis and subsequent endocytosis. Endocytosis will result in the internalisation of the dye. The extent of internalisation is then estimated by a second maximal stimulus which unloads all the FM2-10 accumulated during the first stimulation (Cousin and Robinson 2000b). A decrease in SV turnover could be explained by either an inhibition of exocytosis or endocytosis, since both have to be active for dye internalisation to occur. To differentiate between exocytosis and endocytosis, the effect of the peptides was examined using an enzyme-coupled fluorescence assay which measures glutamate release. This is a good estimate of exocytosis since more than 90% of central synapses are glutamatergic (Nicholls 1993).

A more accurate method of quantifying the amount of endocytosis in these assays is by the parameter called the retrieval efficiency (Cousin et al. 2001). It is the amount of SV turnover divided by the amount of exocytosis after 2 min and therefore takes into account any effects of the prior round of exocytosis. A value of less than one indicates a specific block in endocytosis.

3.5.1 AP2/clathrin interaction

The heterotetrameric adaptor protein, AP2, is involved in the nucleation of SV endocytosis (Slepnev and De Camilli 2000). The β2 subunit binds to clathrin at two sites: one on the ear domain and one on the hinge region, thus localising clathrin to sites of SV endocytosis (Slepnev and De Camilli 2000). It is this region on the β2 ear domain containing a 'clathrin box', which the $AP2_{624-644}$ peptide sequence was extracted from (ter Haar et al. 2000) and thus is predicted to disrupt the AP2-clathrin interaction and arrest SV endocytosis at an early stage.

Figure 3.4B shows the effect of different concentrations of $AP2_{624-644}$ peptide on SV turnover. The concentration of $AP2_{624-644}$ peptide used for further study was 500 μM. The $AP2_{624-644}$ peptide inhibited SV turnover by 84 % (16.5 % ± 23.6 % of control, fig 3.4C) and had no significant effect on Ca^{2+}-dependent glutamate release (99.6 % ± 8.8 % of control, fig 3.4D). The retrieval efficiency was calculated to be 0.16 ± 0.18 (fig 3.4E) and therefore the $AP2_{624-644}$ peptide inhibited SV endocytosis, as predicted.

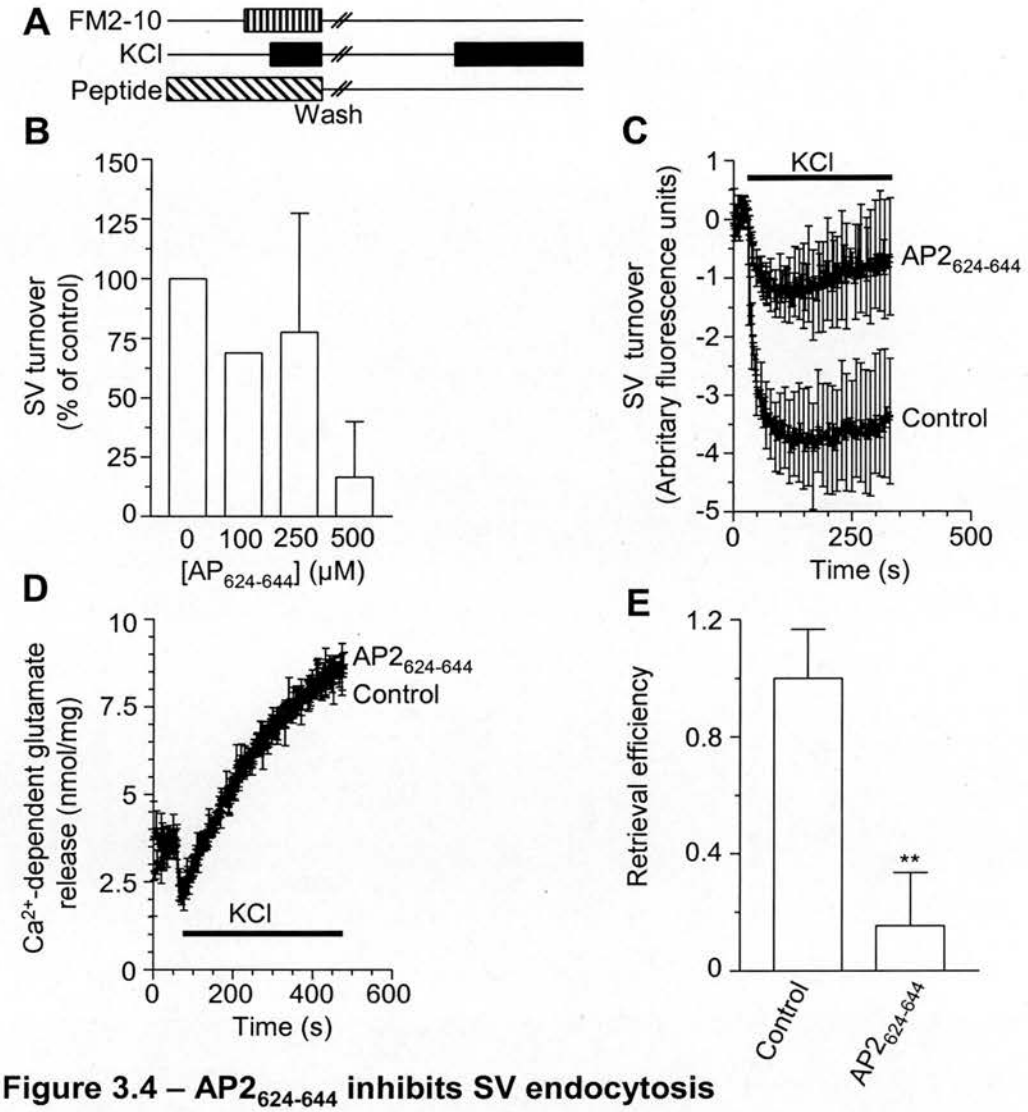

Figure 3.4 – $AP2_{624-644}$ inhibits SV endocytosis

(A) Schematic illustrating the SV turnover assay protocol. **(B)** Synaptosomes were incubated with the indicated [$AP2_{624-644}$ peptide] ± Ca^{2+} for 30 minutes prior to loading with FM2-10. The Ca^{2+}-dependent FM2-10 unloading (SV turnover) is displayed. (n = 1 for 100 μM, ≥ 3 ± SEM for 250 and 500 μM) **(C)** Ca^{2+}-dependent SV turnover for 500 μM $AP2_{624-644}$ (n ≥ 3 ± SEM). **(D)** Ca^{2+}-dependent glutamate release from control or peptide treated synaptosomes stimulated with 30 mM KCl (n ≥ 3 ± SEM). Bar in **C** and **D** denotes the presence of KCl. **(E)** Retrieval efficiency calculated as the amount of endocytosis, **C**, divided by the amount of exocytosis after 2 minutes of stimulation, **D**. Student's t-test was performed (**p < 0.01).

3.5.2 Endophilin/synaptojanin

Endophilin and synaptojanin have been implicated in both invagination and uncoating. The SH3 domain of endophilin can bind to the PRD domain of dynamin I but binds with higher affinity to the PRD domain of synaptojanin (Slepnev and De Camilli 2000). Endophilin null mutants displayed a diffuse localisation of synaptojanin but synaptojanin null mutants displayed normal synaptic localisation of endophilin, suggesting that a role of endophilin is to localise synaptojanin to sites of SV endocytosis (Schuske et al. 2003). The $SJ_{1101\text{-}1110}$ peptide sequence is taken from residues 1101-1110 of the PRD domain of synaptojanin. This region is thought to correspond to the endophilin binding site and thus this peptide should disrupt the synaptojanin-endophilin interaction (Cestra et al. 1999; Gad et al. 2000) and block SV endocytosis at an intermediate stage or during uncoating.

The effect of different concentrations of $SJ_{1101\text{-}1110}$ peptide on SV turnover is shown in figure 3.5A. There was not a significantly larger inhibition above 250 μM and thus the peptide was used at this concentration. The $SJ_{1101\text{-}1110}$ peptide inhibited SV turnover (48.4 % ± 17 % of control, fig 3.5B) but had no significant effect on glutamate release (97.0 % ± 4.6 % of control, fig 3.5C). The retrieval efficiency was calculated as 0.5 ± 0.1 (fig 3.5D) confirming the hypothesis that the $SJ_{1101\text{-}1110}$ peptide inhibits SV endocytosis.

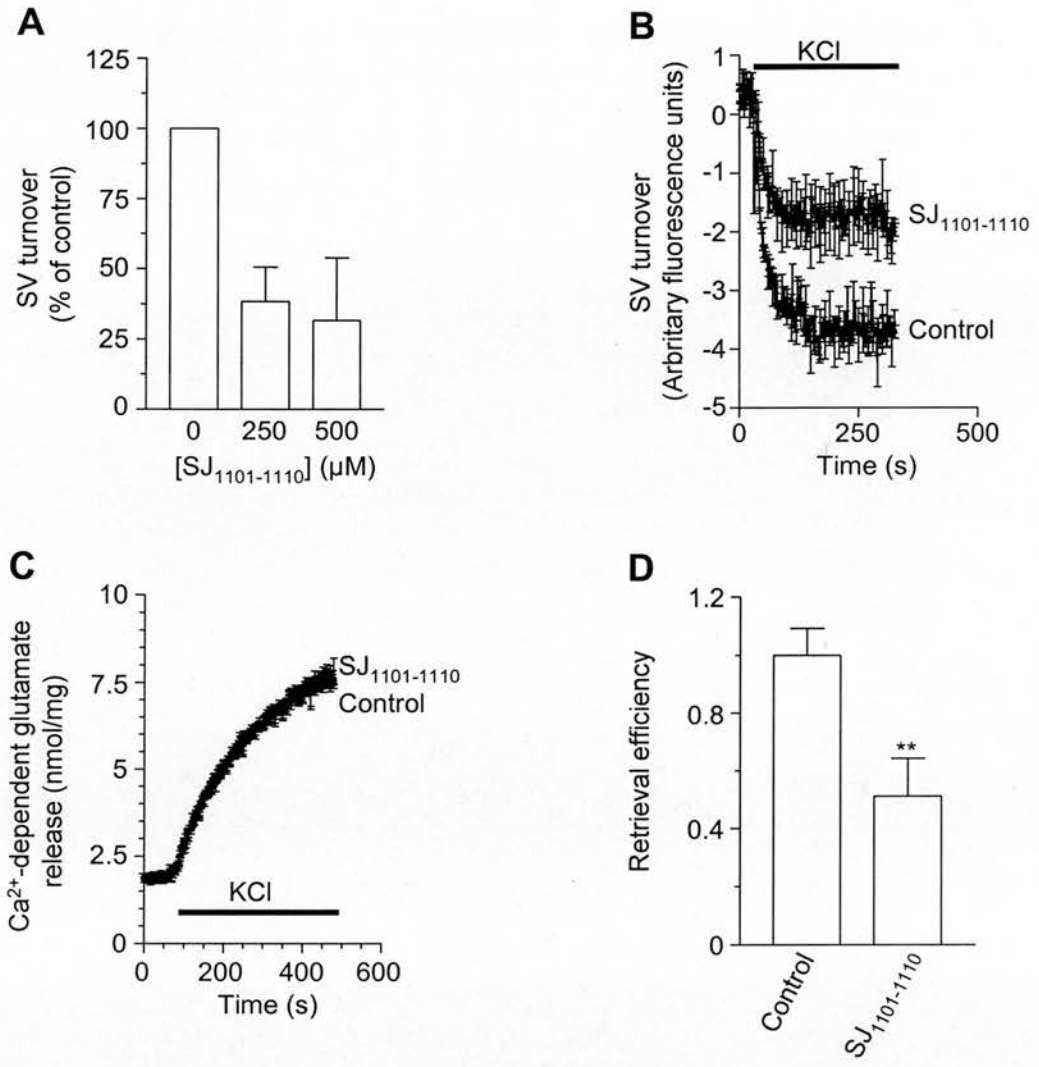

Figure 3.5 – $SJ_{1101-1110}$ inhibits SV endocytosis

(A) Synaptosomes were incubated with the indicated [$SJ_{1101-1110}$ peptide] ± Ca^{2+} for 30 minutes prior to loading with FM2-10. Ca^{2+}-dependent FM2-10 unloading (SV turnover) is displayed. (n ≥ 2 ± SD) **(B)** Average Ca^{2+}-dependent SV turnover for 250 μM $SJ_{1101-1110}$ peptide (n ≥ 3 ± SEM). **(C)** Ca^{2+}-dependent glutamate release from control or peptide treated synaptosomes stimulated with 30 mM KCl (n ≥ 3 ± SEM). Bar in **B** and **C** denotes the presence of KCl. **(D)** Retrieval efficiency calculated as the amount of endocytosis, **B**, divided by the amount of exocytosis after 2 minutes of stimulation, **C**. Student's t-test was performed (**$p < 0.01$).

3.5.3 Dynamin I/amphiphysin I interaction

The main role of amphiphysin I is proposed to be to localise dynamin I to the neck of a deeply invaginated pit. A peptide consisting of residues 828 – 842 of the PRD of dynamin I inhibited binding of dynamin I to the SH3 domain of amphiphysin I and inhibited SV endocytosis at the stage of invaginated clathrin-coated pits (Shupliakov et al. 1997). This peptide sequence was shortened to encompass only the PXRPXR binding site for amphiphysin plus a few flanking residues and thus consists of residues 832 – 840 of the PRD of dynamin I. This peptide would be expected to inhibit the dynamin I – amphiphysin interaction, preventing dynamin I recruitment to sites of SV endocytosis and therefore inhibition of SV endocytosis at a late stage.

Increasing concentrations of $DynI_{832-840}$ peptide showed a concentration dependent inhibition of SV turnover (fig 3.6A). The largest inhibition was seen with 500 μM and therefore, the peptide was used at this concentration. SV turnover was inhibited by the $DynI_{832-840}$ peptide by 75 % (25 % ± 10.2 % of control, fig 3.6B). There was a slight inhibition of glutamate release (78.4 % ± 8.2 % of control, fig 3.6C) but this is not enough to account for the inhibition seen in the SV turnover assay. This is highlighted in the retrieval efficiency of 0.32 ± 0.1 (fig 3.6D), indicating an inhibition of SV endocytosis.

3.5.4 Hsc70/cytochrome c interaction

Hsc70 is important for uncoating of the SVs following retrieval. The CytC peptide is taken from the sequence of cytochrome c which binds to the substrate domain of

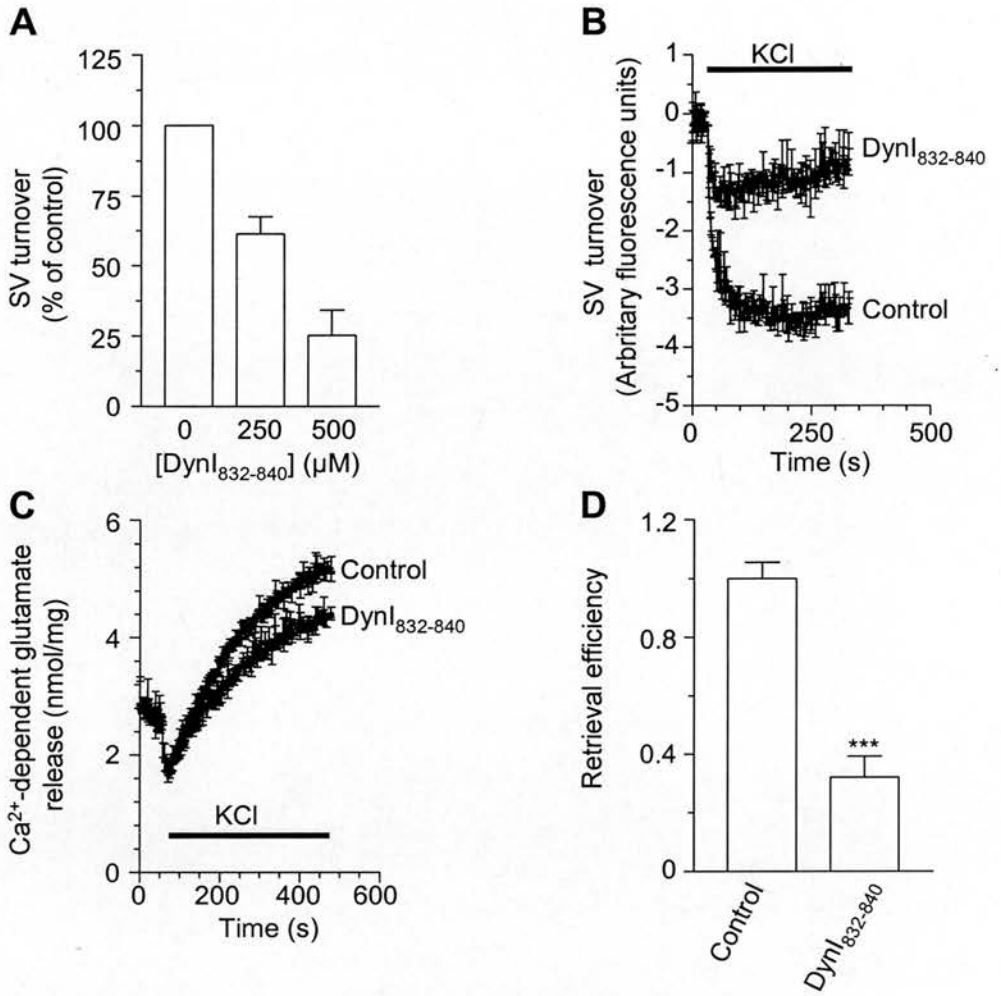

Figure 3.6 – $DynI_{832-840}$ inhibits SV endocytosis

(A) Ca^{2+}-dependent FM2-10 unloading from synaptosomes pre-incubated for 30 minutes with the indicated [$DynI_{832-840}$ peptide] and stimulated with 30 mM KCl ($n \geq 3 \pm SEM$). **(B)** Ca^{2+}-dependent SV turnover traces for 500 μM $DynI_{832-840}$. **(C)** Synaptosomes were pre-incubated with ± 500 μM $DynI_{832-840}$ peptide ± Ca^{2+} for 30 minutes prior to assaying. Ca^{2+}-dependent glutamate release from control or peptide treated synaptosomes stimulated with 30 mM KCl is displayed ($n \geq 3 \pm SEM$) Bar in **B** and **C** denotes presence of KCl. **(D)** Retrieval efficiency for $DynI_{832-840}$ calculated from the values represented in **B** and **C**. Student's t-test was applied (***$p < 0.001$).

Hsc70 and inhibits uncoating of clathrin coated vesicles (Morgan et al. 2001). This peptide would therefore be predicted to inhibit SV endocytosis during uncoating.

The CytC peptide (250 μM) showed a substantial block of SV turnover (10.9 % ± 19.2 % of control, fig 3.7A). At higher concentrations, the CytC peptide abolished SV turnover (data not shown). This peptide, however, inhibited glutamate release by 75 % (25.5 % ± 1.5 % of control, fig 3.7B). The retrieval efficiency was not significantly different to control (1.1 ± 0.2, fig 3.7C). Thus, it can be concluded that the inhibition by the CytC peptide in SV turnover is due to an inhibition in SV exocytosis and not SV endocytosis.

The block of SV exocytosis may originate from toxicity of the peptide to the synaptosomes. This was tested by assaying glutamate release before synaptosome stimulation with 30 mM KCl. If the synaptosomes are damaged and the plasma membrane is compromised, increased extracellular glutamate will be observed. Figure 3.7D shows the extent of extracellular glutamate accumulated by addition of glutamate dehydrogenase (GDH) in the presence and absence of the CytC peptide. Under control conditions, there is a slight increase in fluorescence upon GDH addition, which is routinely observed, but when the synaptosomes are preincubated with CytC peptide, in the presence or absence of Ca^{2+}, there is five times the increase in fluorescence. Therefore, the increase in fluorescence in the presence of the CytC peptide may indicate that it has compromised synaptosome viability. No other peptide tested increased the fluorescence upon addition of GDH, suggesting that the CytC peptide sequence is responsible for cell toxicity.

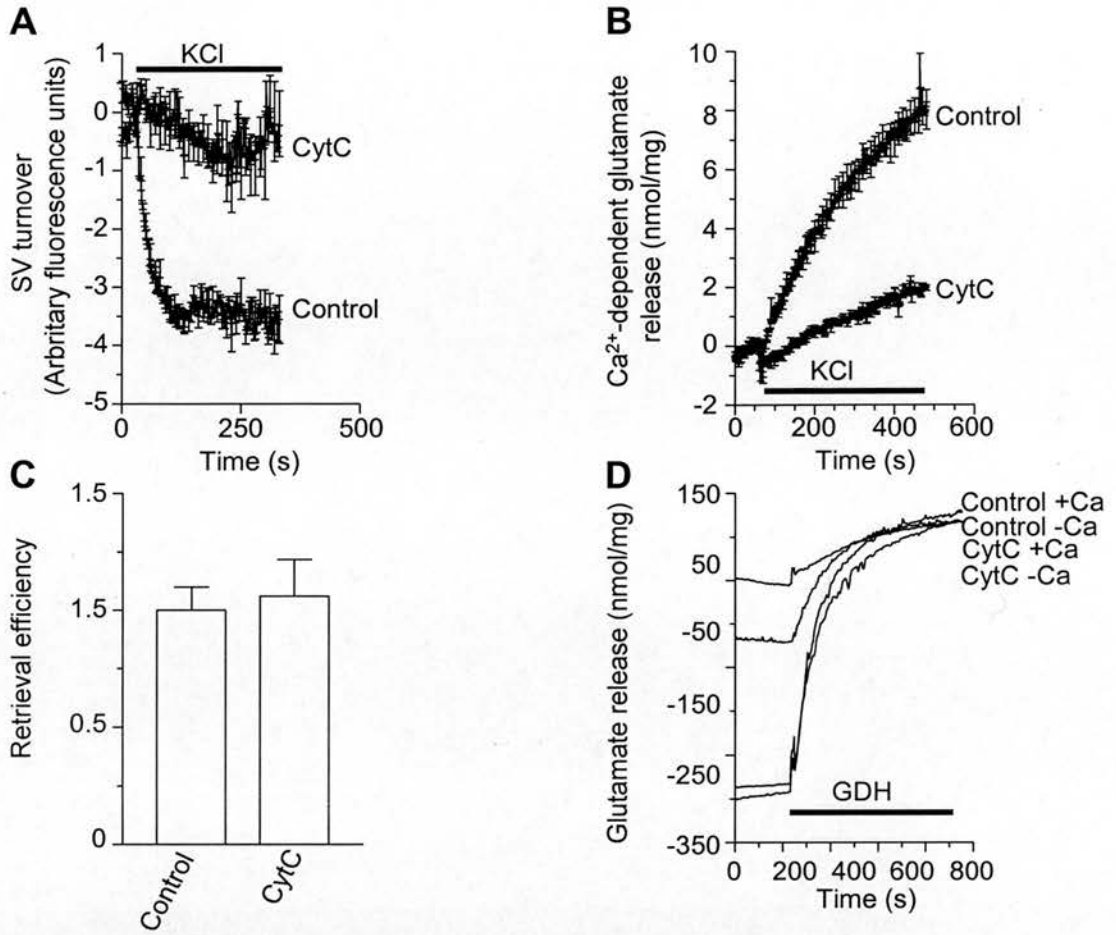

Figure 3.7 – CytC peptide inhibits SV exocytosis

(A) Synaptosomes were incubated ± 250 µM CytC peptide ± Ca^{2+} for 30 minutes prior to loading with FM2-10. Ca^{2+}-dependent FM2-10 unloading (SV turnover) is displayed ($n \geq 3 \pm$ SEM). **(B)** Ca^{2+}-dependent glutamate release from control or peptide treated synaptosomes stimulated with 30 mM KCl ($n \geq 3 \pm$ SEM). **(C)** Retrieval efficiency calculated as the amount of endocytosis, **A**, divided by the amount of exocytosis after 2 minutes of stimulation, **B**. **(D)** Example traces showing the glutamate release from synaptosomes ± 250 µM CytC peptide ± Ca^{2+}, following addition of glutamate dehydrogenase (GDH, n = 1). Bar in **B** and **C** denotes the presence of KCl and the bar in **D** denotes the presence of (GDH).

3.5.5 Synapsin I/p85 interaction

Synapsin associated PI3 kinase activity has a role in the delivery of SVs from the reserve pool to the RRP (Cousin et al. 2003). These proteins interact via a PRD – SH3 interaction. The $SynI_{585-600}$ peptide is taken from the PRD domain of synapsin I and contains the PXXP binding motif for the SH3 domain of the p85, a subunit of PI3 kinase. Since this peptide is designed to inhibit the interaction between synapsin I and p85, it would be predicted to inhibit SV exocytosis and have no effect on SV endocytosis.

The $SynI_{585-600}$ peptide inhibited SV turnover by 28 % (71.8 % ± 9.4 % of control, fig 3.8A). The $SynI_{585-600}$ peptide also inhibited glutamate release, and hence exocytosis, by a comparable amount (72.5 % ± 1.2 % of control, fig 3.8B). Therefore, when the retrieval efficiency was calculated the $SynI_{585-600}$ peptide was not significantly different to control ($SynI_{585-600}$ peptide retrieval efficiency was 0.96 ± 0.1, fig 3.8C). This confirms that the $SynI_{585-600}$ peptide inhibits SV exocytosis with no detectable effect on SV endocytosis.

3.6 Penetratin peptides can inhibit specific interactions

All of the peptides tested inhibit SV exocytosis or SV endocytosis (figs 3.4 – 3.8). Since the peptide sequences were designed to inhibit a specific interaction, the most logical explanation is that the peptides are inhibiting SV turnover by disrupting protein-protein interactions. This hypothesis was tested using GST-fusion proteins of endocytosis domains and analysing the binding partners in the absence and presence of the peptides. The fusion proteins used were the SH3 domain of

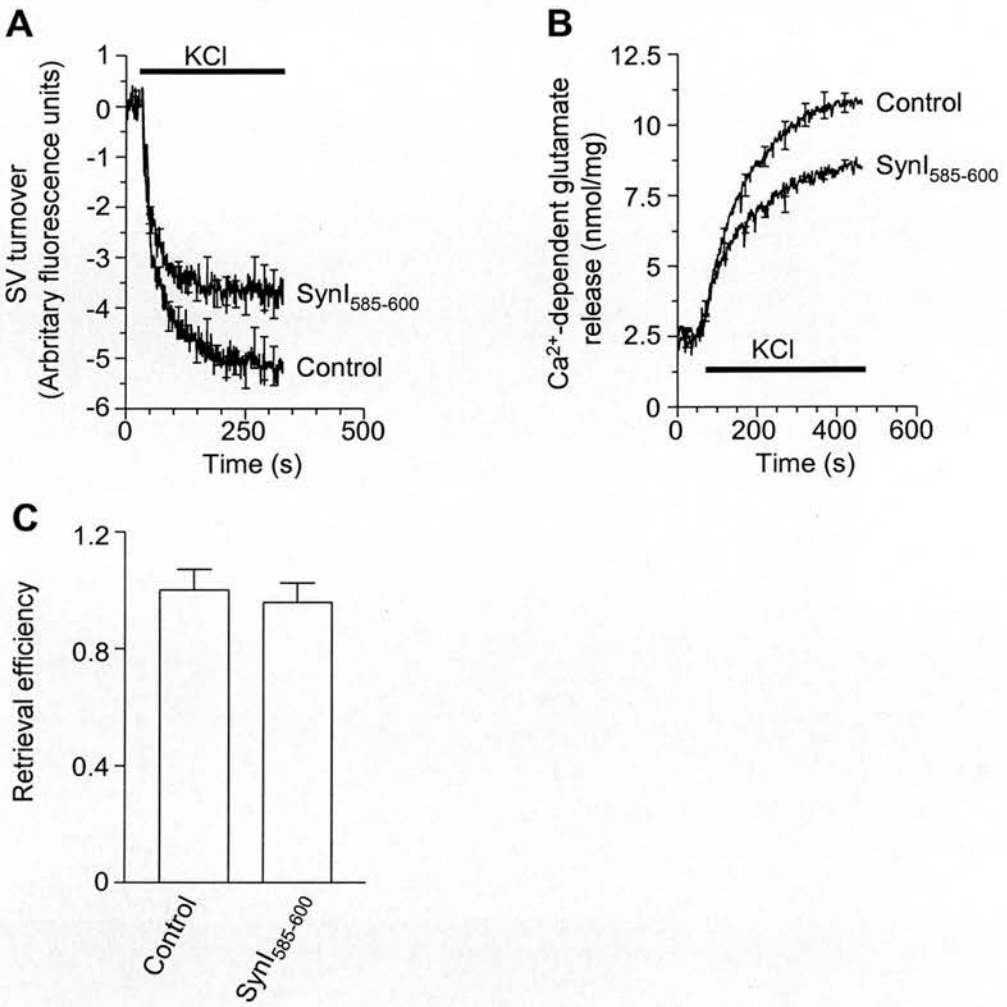

Figure 3.8 – $SynI_{585-600}$ peptide inhibits SV exocytosis

(A) Ca^{2+}-dependent FM2-10 unloading from synaptosomes pre-incubated ± 400 µM $Syn_{585-600}$ peptide ($n \geq 3 \pm SEM$). **(B)** Ca^{2+}-dependent glutamate release stimulated with 30 mM KCl from synaptosomes pre-incubated ± 400 µM $Syn_{585-600}$ peptide prior to assaying ($n = 3 \pm SEM$). Experiment performed by M. Cousin: data taken from Cousin *et al*, 2003. Bar in **A** and **B** denotes the presence of KCl. **(C)** Retrieval efficiency calculated as the amount of endocytosis, **A**, divided by the amount of exocytosis after 2 min stimulation, **B**.

amphiphysin I, the SH3 domain of p85, the ear domain of the α2 subunit of AP2 and the SH3 domain of endophilin II.

The GST-SH3 domain of amphiphysin I binds to dynamin I and synaptojanin (Grabs et al. 1997) and incubation with a similar peptide taken from the PRD of dynamin I prevents binding of dynamin I to the SH3 domain of amphiphysin I (Shupliakov et al. 1997). Therefore, incubation with the $DynI_{832-840}$ peptide should inhibit dynamin I binding. Synaptosome lysates ± 2 mM $DynI_{832-840}$ were incubated with the SH3-domain of amphiphysin I (fig 3.9A). Four times as much peptide was used in the pulldown compared to the functional studies to ensure that the interaction was inhibited. The level of fusion protein was also higher than the levels of the amphiphysin SH3 domain in the synaptosomes and therefore more peptide was required to block the dynamin I binding sites. (The same logic was applied to the other pulldowns (fig 3.9B and fig 3.10A, B and C) and thus the concentration of peptide used to inhibit the *in vitro* interactions is much greater than that required for the functional studies). Dynamin I and synaptojanin were both present in the absence of the peptide. In the presence of the $DynI_{832-840}$ peptide, dynamin I binding was dramatically reduced. Synaptojanin binding appeared unaffected.

To test the ability of the $SynI_{585-600}$ peptide to inhibit the synapsin I-PI3 kinase interaction, a GST-fusion protein of the SH3 domain of p85 (subunit of PI3 kinase) was used. In the absence of the $SynI_{585-600}$ peptide, synapsin Ia and b, dynamin I and synaptojanin were extracted from synaptosome lysates (fig 3.9B). In the presence of

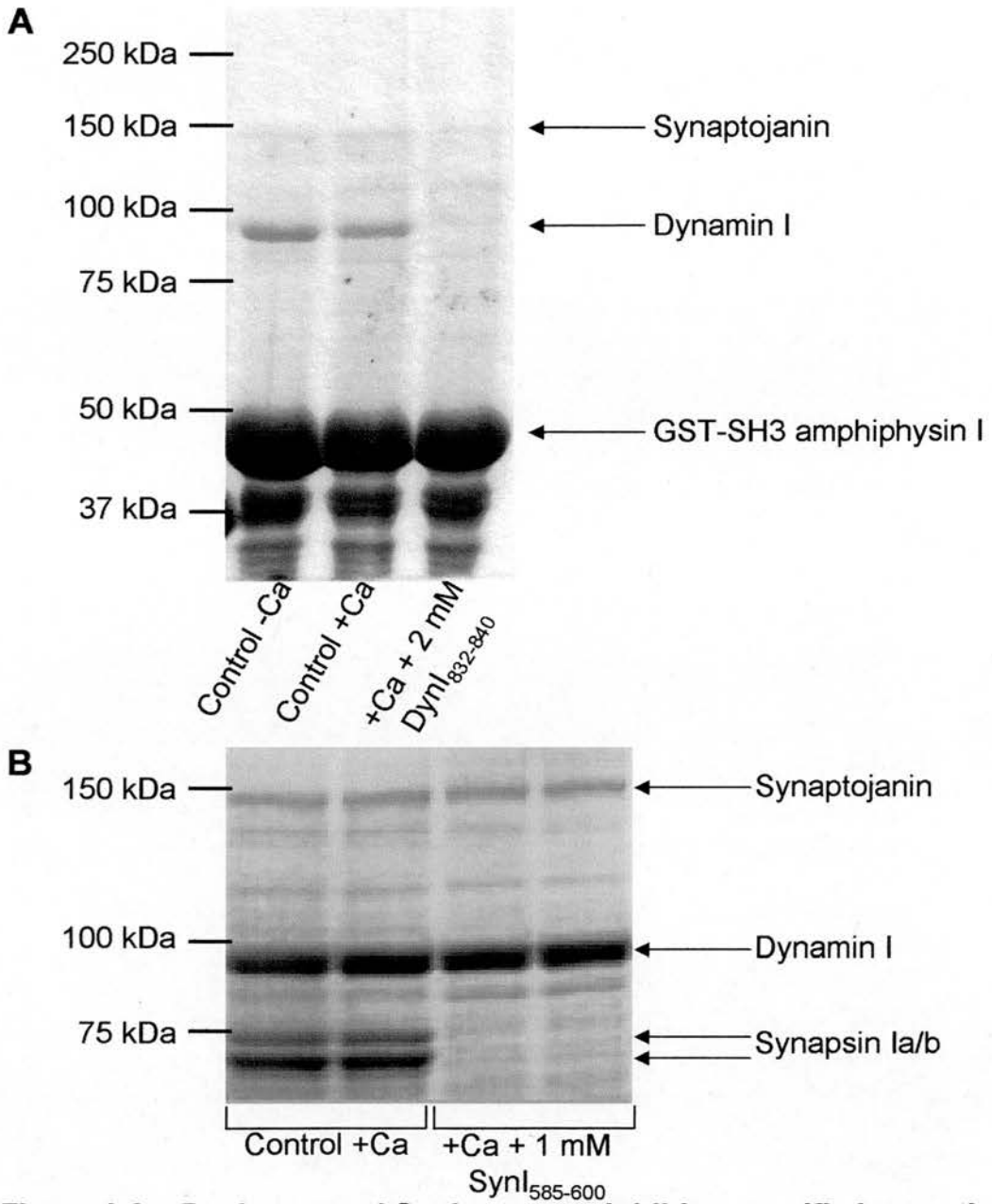

Figure 3.9 – $Dynl_{832-840}$ and $Synl_{585-600}$ can inhibit a specific interaction

(A) Synaptosomes were lysed ± Ca^{2+}. The lysates were incubated with the GST-SH3 domain of amphiphysin I coupled to GSH beads. The bound proteins were eluted, separated by SDS-PAGE and the gels coomassie stained. **(B)** Coomassie gel of the proteins extracted from synaptosome lysates incubated with the SH3 domain of p85 fused to GST ± 1 mM $Synl_{585-600}$. (Experiment performed in collaboration with the P. Robinson lab.: taken from Cousin *et al*, 2003). Arrows indicate eluted proteins identified by molecular weight **(A**, and previously by western blot**)** and MALDI-TOF **(B)**.

the $SynI_{585-600}$ peptide, however, only dynamin I and synaptojanin were present showing that synapsin binding was specifically competed off.

Pulldown experiments from bovine brain extract with the GST-α2 ear domain of AP2 identified AP180, amphiphysin and dynamin I as being associated with this region (Wang et al. 1995). Clathrin binds to the β2-ear and hinge domains (Slepnev and De Camilli 2000). To investigate whether the $AP2_{624-644}$, $SJ_{1101-1110}$ and CytC peptides affected the pattern of proteins extracted by the GST-α2 ear domain fusion protein, the peptides were incubated with synaptosome lysates and fusion protein. None of the peptides appear to have altered the pattern of proteins extracted with the GST-α2 ear domain of AP2 (fig 3.10A).

Endophilin and amphiphysin both bind to dynamin I and synaptojanin although endophilin preferentially binds to synaptojanin and amphiphysin binds dynamin I with higher affinity (Slepnev and De Camilli 2000). The $DynI_{832-840}$ peptide reduces binding of dynamin I to the SH3 domain of amphiphysin while binding of synaptojanin is unaffected (fig 3.9A). To test if the $SJ_{1101-1110}$ peptide had a similar effect on synaptojanin binding, the peptide was incubated with the GST-SH3 domain of endophilin (fig 3.10B) and GST-SH3 domain of amphiphysin (fig 3.10C). There is a general decrease in the amount of protein pulled down by the SH3 domain of endophilin in the presence of the $SJ_{1101-1110}$, probably due to unequal protein loading, but the $SJ_{1101-1110}$ peptide did inhibit the binding of synaptojanin to the SH3 domain of endophilin as well as disrupting the binding of dynamin I (fig 3.10B). However,

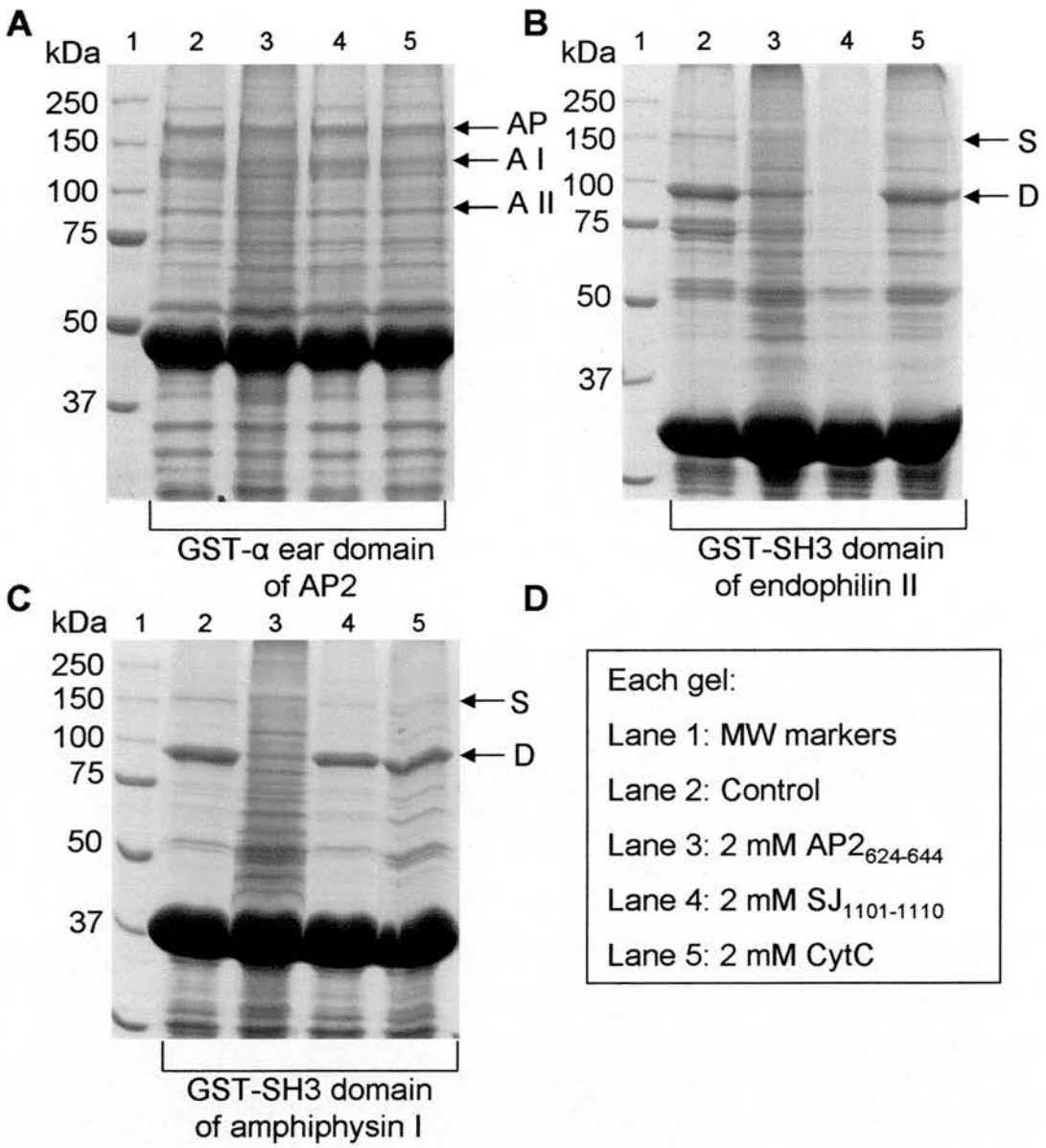

Figure 3.10 – Peptides block different interactions

Synaptosome lysates were incubated with the GST-α ear domain of AP2 **(A)**, GST-SH3 domain of endophilin II **(B)** or the GST-SH3 domain of amphiphysin I **(C)** ± 2 mM of the indicated peptide **(D)**. Extracted proteins were run on 10 % acrylamide gels and coomassie stained. Proteins are abbreviated to AP (AP180), A I (Amphiphysin I), A II (Amphiphysin II), D (Dynamin I) and S (Synaptojanin) and were identified by molecular weight (and previously by western blot during construct characterisation). N = 1.

the binding of dynamin I and synaptojanin to the SH3 domain of amphiphysin were unaffected by the $SJ_{1101-1110}$ peptide (fig 3.10C).

Intriguingly, incubation of the $AP2_{624-644}$ peptide with the GST-SH3 domain of amphiphysin competes off binding of dynamin I and synaptojanin (fig 3.10C). The effect is not as dramatic as with the GST-SH3 domain of endophilin but the amount of dynamin I bound is less than control (fig 3.10B).

The CytC peptide had no visible impact on any of the proteins extracted by the three fusion proteins tested (fig 3.10A - C).

3.8 Discussion

This chapter shows that penetratin tagging of peptides is an effective method to deliver peptides across the plasma membrane of synaptosomes. All of the peptides tested inhibited SV exocytosis or SV endocytosis and several were able to inhibit specific protein-protein interactions involved in these processes.

Translocation versus endocytosis

The exact internalisation mechanism of penetratin linked peptides is still under investigation, however, studies at 4 °C, mutations removing the chirality of the peptide and the use of endocytosis inhibitors suggests that endocytosis is not the principal route of uptake into cells (Joliot et al. 1991; Derossi et al. 1994; Thoren et al. 2000; Magzoub et al. 2002; Christiaens et al. 2004; Lindgren et al. 2004; Nakase et al. 2004). However, a study by Richard *et al* (2002) showed that cell fixation

caused an artifactual uptake of Tat and arginine rich peptides and that these peptides showed inhibition of uptake at 4 °C. The kinetics of uptake were similar to the styryl dye FM4-64 and fluorescent imaging showed the peptide localisation to be punctate and colocalised to endocytic markers. If the inverted micelle model of peptide uptake is correct however, it is perhaps not surprising that fluorescence was detected in intracellular compartments since the peptides would be able to cross any lipid membrane and would not require to be endocytosed to reach an endosome, for example.

The amino acid composition and charge of Tat and arginine peptides is markedly different from the penetratin sequence and could therefore have an effect on the method of uptake. Indeed they have different kinetics of uptake (Hallbrink et al. 2001) and different effects on lipid membranes (Thoren et al. 2005). The Tat peptides were able to promote vesicle fusion where as the penetratin peptides promoted vesicle aggregation. In a recent comparative study it was proposed that arginine rich peptides and penetratin peptides were internalised by distinct mechanisms (Nakase et al. 2004): penetratin uptake was unaffected by macropinocytosis inhibitors and did not induce a significant rearrangement of the actin cytoskeleton, which is indicative of internalisation by this route, in contrast to the arginine peptide.

The functional data presented in this chapter, while not proving an internalisation mechanism, is compatible with a predominantly non-endocytosis uptake mechanism. Synaptosomes require to be stimulated, and thus undergo exocytosis, before

endocytosis can occur. The synaptosomes were preincubated for 30 min with the peptides prior to stimulation and loading of the FM2-10. They undergo only one round of stimulation during which the FM2-10 is loaded. If it was the case that the peptide was only taken up via endocytosis, the peptide would have to be taken up in the same round as the FM2-10. Since inhibition of dye loading was seen with several of the peptides, and thus inhibition of endocytosis, the peptides must have already been present inside the synaptosomes prior to stimulation. This suggests that peptide internalisation, at least in part, is not endocytosis dependent.

Functional effects of the peptides on SV recycling

The $AP2_{624-644}$, $SJ_{1101-1110}$ and $DynI_{832-840}$ peptides all specifically inhibited SV endocytosis (fig 3.4 -3.6) and the CytC and $SynI_{585-600}$ peptides inhibited exocytosis (fig 3.7 and 3.8). No two peptides had the same profile, with some exerting more of an effect than others. This implies that the penetratin sequence itself is unlikely to be responsible for the effects on SV turnover since the inhibitions are not uniform. This could, however, be tested directly by using a peptide consisting solely of the shortened penetratin sequence and assaying the effect on SV turnover.

The $AP2_{624-644}$, $SJ_{1101-1110}$, $DynI_{832-840}$ and the CytC peptides were all predicted to inhibit SV endocytosis since the peptide sequences were designed to inhibit interactions important at different stages in this process. The $AP2_{624-644}$, $SJ_{1101-1110}$ and $DynI_{832-840}$ peptides did inhibit SV endocytosis but the CytC peptide blocked SV exocytosis (fig 3.7) to such an extent that an effect on SV endocytosis was indistinguishable. The block of exocytosis is compatible with a previous study

where injection of this peptide inhibited synaptic transmission (Morgan et al. 2001) but the most likely explanation is that the CytC peptide is toxic to the synaptosomes. This is indicated by the increase in extracellular glutamate prior to synaptosome stimulation in the glutamate release assay (fig 3.7D). To confirm this hypothesis other markers of synaptosome viability such as the ability to maintain ATP levels and the Ca^{2+} profile could be assayed (Cousin et al. 1995). The CytC peptide binds to the substrate binding domain of Hsc70 (Morgan et al. 2001), and therefore it is possible that the peptide could bind to the substrate binding domains of other ATPases in synaptosomes, compromising viability.

The $DynI_{832\text{-}840}$ peptide showed a slight inhibition of exocytosis, although it was not quite significant as judged by a two-way ANOVA. An inhibition of exocytosis is not surprising since PRD-SH3 domain interactions are involved in many cellular processes and so this peptide may be having a non-specific effect on exocytosis. However, the $SJ_{1101\text{-}1110}$ peptide, which also contains an SH3 binding PRD motif, did not have a similar effect on exocytosis and on the evidence from the pulldown experiments (fig 3.9 and 3.10) appeared to be less specific than the $DynI_{832\text{-}840}$ peptide. A second explanation for the inhibition in the exocytosis assay by the $DynI_{832\text{-}840}$ peptide is that dynamin I has a role in exocytosis as well as endocytosis (see chapter 5 for a discussion on this topic).

The peptides were designed to arrest different stages of SV endocytosis to pull out the protein complexes assembled at that point. The different peptides can inhibit SV exocytosis or endocytosis and can inhibit predicted protein interactions. However,

electron microscopy will be required to determine which stage of SV endocytosis the peptides act at since the peptides should produce different membrane morphologies. For example, the $AP2_{624-644}$ peptide is predicted to inhibit SV endocytosis at an early stage, and therefore $AP2_{624-644}$ treated synaptosomes would be predicted to have a dramatically reduced number of SVs as well as plasma membrane ruffling. These features are indicative of the SVs having fused with the plasma membrane but been unable to be retrieved. The $DynI_{832-840}$ peptide should block SV endocytosis at a much later stage and so evidence of deeply invaginated clathrin-coated pits at the plasma membrane would be expected.

Specificity of the peptides

The specificity of the peptides was tested using pulldown experiments with GST-fusion proteins of domains of endocytosis proteins. The amphiphysin SH3 domain binds to dynamin I and synaptojanin (Grabs et al. 1997). In the presence of the $DynI_{832-840}$ peptide, binding of dynamin I was inhibited but synaptojanin was not illustrating the specificity of this peptide, since both synaptojanin and dynamin I interact via proline rich sequences. The $SynI_{585-600}$ peptide showed a similar specificity for the p85-synapsin interaction since binding of dynamin I and synaptojanin were unaffected by incubation with the peptide.

Although the $SJ_{1101-1110}$ peptide disrupted the interaction between synaptojanin and the SH3 domain of endophilin, it also inhibited the binding of dynamin I. This is in contrast to the $DynI_{832-840}$ peptide which only disrupted the interaction of dynamin I with the SH3 domain of amphiphysin. A possible explanation for this non-

specificity is that there is some debate over the endophilin binding site on synaptojanin. Originally the binding site was mapped to residues 1102 – 1110 (Cestra et al. 1999) and it is this site that the peptide was designed from. Further research using truncated versions of the synaptojanin PRD showed that endophilin bound to the region immediately C-terminal to the first binding site (residues 1112-1130; Gad et al. 2000). This region contains two putative endophilin binding motifs and either one was sufficient for endophilin binding. The same experiment conducted with the first identified binding sequence (residues 1102 – 1110) failed to purify endophilin (Ringstad et al. 2001) implying that these residues did not contain the binding site. It is possible therefore, that the peptide used in this chapter, while not containing the endophilin binding site, may be similar enough to disrupt PRD-SH3 domain interactions, explaining the lack of specificity but still causing an inhibition of SV endocytosis. It would be interesting to see if a peptide composing of the 1112 – 1230 residues could specifically inhibit the synaptojanin-endophilin SH3 domain interaction without affecting the dynamin I-endophilin SH3 domain interaction.

The SH3 domain of amphiphysin is unusual amongst SH3 domains because it has a large patch of negative electrostatic potential on the surface (Owen et al. 1998). This patch explains the substrate specificity of the SH3 domain of amphiphysin for a PXRPXR binding motif in PRDs rather than a more conventional class two PXXPXR motif since it contains two basic arginine residues (Owen et al. 1998). Amphiphysin recognises the sequence PSRPNR in the PRD of dynamin I and PSRPIR in the PRD of synaptojanin (Owen et al. 1998) - both of which conform to

the PXRPXR consensus. This site in synaptojanin is distinct to the site bound by the SH3 domain of endophilin, above. The $SJ_{1101-1110}$ peptide, however, does not contain a PXRPXR motif, explaining why binding of dynamin I and synaptojanin to the SH3 domain of amphiphysin was unaffected by this peptide. Interestingly, the $DynI_{832-840}$ peptide, which does contain a PXRPXR motif, did not affect synaptojanin binding to the SH3 domain of amphiphysin, suggesting that the flanking sequences may also have a role in substrate recognition.

The specificity of the $AP2_{624-644}$ peptide for the clathrin interaction was unable to be directly tested since clathrin binds to the ear domain and hinge region of β2 subunit of AP2 and the GST-fusion construct in the laboratory was for the ear domain of the α2 subunit and therefore not expected to extract clathrin in any great amount. The peptide was however, incubated with three different constructs to determine if there was any change to the pattern of extracted proteins. There was no effect with the ear domain of the α2 subunit but dynamin I and synaptojanin binding to the SH3 domain of amphiphysin was inhibited. The effect was less dramatic with the SH3 domain of endophilin. The inhibition of these interactions was quite unexpected since the $AP2_{624-644}$ peptide was designed to inhibit the AP2-clathrin interaction. On closer inspection of the peptide sequence, however, the $AP2_{624-644}$ peptide contains a region with the sequence PPVNVP. This is not an ideal proline motif for dynamin I or synaptojanin binding but may be close enough to disrupt these interactions. This could explain why the binding of dynamin I and synaptojanin to the SH3 constructs were affected. The $AP2_{624-644}$ peptide also contains a lot of basic, positively charged lysine residues. Since the SH3 domain of amphiphysin has a much larger negative

electrostatic patch than other SH3 domains, this may explain why the peptide had a more pronounced inhibition on dynamin I and synaptojanin binding to the amphiphysin SH3 domain than the endophilin SH3 domain.

The original theory behind this work was to identify different protein complexes in SV endocytosis. Now that the peptides have been characterised with assays of SV recycling and GST-pulldowns, immunoprecipitations can be undertaken to further investigate the *in vivo* complexes involved in SV endocytosis.

Conclusions

Penetratin tagging of peptides is an efficient method to deliver peptides across the plasma membrane of synaptosomes. Usage in cells may be limited however since the peptides can localise to the nucleus. Since synaptosomes do not have a nucleus this problem was bypassed. Some versions of the penetratin sequence have prolines introduced which allow translocation into the cytoplasm but not the nucleus, and thus may be a better tag for use in cells (Derossi et al. 1996).

The specificity of the peptides was entirely dependent on the sequence. The $SynI_{585-600}$ and $DynI_{832-840}$ peptides were specific for the interactions they were designed for but the $SJ_{1101-1110}$ and probably the $AP2_{624-644}$ peptides were not. The flanking regions around the binding site sequences are likely to be as important as the binding site sequence themselves.

Overall, the use of penetratin tagged peptides is an excellent tool to study the effect of protein sequences on SV recycling *in vivo* as well as in a more biochemical approach to studying protein-protein interactions.

CHAPTER 4

Ca^{2+}-DEPENDENT DYNAMIN I INTERACTIONS: ROLES FOR SYNAPTOPHYSIN AND AMPHIPHYSIN I

4.1 Introduction

SV exocytosis and endocytosis are stimulated by Ca^{2+} influx into the nerve terminal following depolarisation of the plasma membrane by an action potential. Therefore many proteins implicated in SV recycling are regulated directly by binding Ca^{2+}, or indirectly through Ca^{2+}-dependent interactions. Dynamin I is one such protein.

Dynamin I can be regulated directly by Ca^{2+}; with the PRD domain forming at least part of the binding site (Liu et al. 1996). The GTPase activity of dynamin I is inhibited by relatively high levels of Ca^{2+} (IC_{50} of 30 μM) as well as the ability of dynamin I to vesiculate phospholipids, suggesting a role for Ca^{2+} binding of dynamin I in endocytosis (Liu et al. 1996; Cousin 2000).

Dynamin I interactions, both with phospholipids and other proteins, are also regulated by Ca^{2+}. The binding of dynamin I to phospholipids is stimulated in the presence of Ca^{2+} (Liu et al. 1994a), thus possibly facilitating the translocation of dynamin I to the plasma membrane from the cytosol upon nerve terminal stimulation. Calcineurin binds to dynamin I in a Ca^{2+}-dependent manner thus possibly targeting the essential phosphatase to the sites of endocytosis (Lai et al. 1999). Dynamin I also interacts with the integral SV protein synaptophysin in a Ca^{2+}-dependent manner (Daly et al. 2000; Daly and Ziff 2002). Disruption of this interaction by injection of the synaptophysin C-terminus into the squid giant axon inhibited SV recycling (Daly et al. 2000), thus underlying the importance of this putative interaction in SV recycling.

Synaptophysin is the most abundant SV protein, making up 7 % of the total vesicle membrane protein (Janz and Südhof 1998) yet the function of this protein remains largely unknown. Since the function and regulation of dynamin I is essential for SV recycling and disruption of the synaptophysin dependent interaction inhibits SV turnover (Daly et al. 2000), the dynamin I-synaptophysin interaction was studied in more detail.

4.2 Synaptophysin

Synaptophysin was discovered in 1985 as a 38 kDa integral SV membrane protein which was expressed in brain tissue and the adrenal gland. More specifically, immunohistochemical staining of brain sections found synaptophysin localised mainly to nerve terminals but also to the Golgi apparatus (Jahn et al. 1985; Wiedenmann and Franke 1985). When expressed in cell lines, including non-neuronal lines, synaptophysin was targeted to small translucent vesicles, similar to SVs, and so it was concluded that this molecule contains all the information necessary for targeting to vesicles without the requirement of a chaperone (Leube et al. 1989).

Synaptophysin has four transmembrane domains with cytosolic N- and C-termini (Sudhof et al. 1987; Johnston and Sudhof 1990; Valtorta et al. 2004). The molecule has two intravesicular loops which can form disulphide bonds and covalently link neighbouring synaptophysin molecules to form oligomeric structures (Johnston and Sudhof 1990). The first loop also harbours an N-glycosylation site (Leube et al. 1989). The C-terminus contains ten tyrosine-rich repeats (Sudhof et al. 1987;

Valtorta et al. 2004), nine of which conform to the degenerate pentapeptide sequence YG(P/Q)QG (Daly and Ziff 2002).

Synaptophysin is highly phosphorylated on tyrosine residues and is one of the major phosphotyrosine proteins in SVs (Pang et al. 1988; Valtorta et al. 2004). The kinase responsible for the tyrosine phosphorylation was found to be c-src since the phosphorylation was intravesicular and c-src is associated with SVs (Valtorta et al. 2004). Incubation with tyrphostin AG789, an inhibitor of c-src amongst other tyrosine kinases, prevents phosphorylation of synaptophysin during a long-term potentiation stimulation paradigm, suggesting that tyrosine phosphorylation of synaptophysin is important *in vivo*, at least for synaptic plasticity (Mullany and Lynch 1998). Synaptophysin can also be phosphorylated by Ca^{2+}-calmodulin-dependent protein kinase II on serine residues (Valtorta et al. 2004). Despite synaptophysin being heavily phosphorylated, the role for the phosphorylation has yet to be elucidated.

4.3 Potential roles for synaptophysin

Synaptophysin has been used as a molecular marker for SVs and nerve terminals since its discovery but the function of this highly abundant protein is still controversial. Overexpression of synaptophysin in *Xenopus* embryos increased the efficacy of spontaneous and evoked transmitter release (Alder et al. 1995) and injection of antibodies or antisense RNA against synaptophysin inhibited transmitter secretion at neuromuscular synapses and in a reconstituted oocyte system, respectively, (Alder et al. 1992a; Alder et al. 1992b; Valtorta et al. 2004) implying a

role for synaptophysin in the regulation of transmitter release. However, the synaptophysin knock out mouse was viable and fertile and exhibited no changes in the architecture of the brain or changes in synaptic transmission and plasticity (McMahon et al. 1996). This implies that synaptophysin was not essential for neurotransmitter release.

A possible explanation for the lack of effect seen in the knock out mouse is that synaptophysin function is redundant. Synaptoporin (or synaptophysin II) is an isoform of synaptophysin which is also found enriched in SVs as well as a ubiquitously expressed isoform known as pantophysin (Sugita et al. 1999). There is also another family of related integral SV proteins known as the synaptogyrins, which have the same overall structure as the synaptophysins with four transmembrane regions and a cytoplasmic C-terminal tail which is tyrosine phosphorylated. Synaptogyrin I is expressed neuronally and its homologue, cellugyrin, is ubiquitously expressed (Janz and Südhof 1998; Sugita et al. 1999).

Synaptoporin is not tyrosine phosphorylated and has a much more restricted distribution in the brain than either synaptophysin and synaptogyrin (Janz et al. 1999). Synaptogyrins have also been implicated in the regulation of Ca^{2+}-dependent exocytosis in PC12 cells (Sugita et al. 1999). The synaptogyrin knock out mouse, like the synaptophysin knock out mouse, was viable and fertile and without any changes in synaptic transmission (Janz et al. 1999). The double knock out of synaptophysin and synaptogyrin was again normal with regards to survival, brain architecture and synaptic release, but it did have impaired short and long term

potentiation, indicating that these proteins could compensate for each other and had a role in synaptic plasticity (Janz et al. 1999).

Another study looked at the effects in the rod photoreceptors in synaptophysin knock out mice (Spiwoks-Becker et al. 2001). These cells were chosen because they do not express significant levels of synaptoporin, which could compensate for synaptophysin. In these mice, secretion was normal but the morphology of the synapses was not. Significantly fewer SVs were seen in the knock out mice and this was reduced further during periods of high stimulation. A higher number of clathrin coated vesicles and the persistence of vacuoles were also observed, indicating a reduction in SV recycling and a role for synaptophysin in this process. A similar phenotype was observed in electron micrographs of giant squid axons injected with the C-terminus of synaptophysin (Daly et al. 2000). Thus synaptophysins have roles in either synaptic plasticity or SV recycling.

4.4 Molecular mechanism of synaptophysin action

Synaptophysin seems to have a role in the regulation of synaptic transmission rather than an essential role in the process. Many putative roles have been proposed based on properties of synaptophysin studied *in vitro*. Thomas and colleagues (1988) first proposed that synaptophysin could act as a channel protein. They showed that synaptophysin existed as a hexamer and that on reconstitution into a lipid bilayer, the purified synaptophysin displayed voltage sensitive channel activity (Thomas et al. 1988). An antibody against one of the pentapeptide repeats in the C-terminal tail of synaptophysin also blocked channel activity in SVs (Thomas et al. 1988; El Far and

Betz 2002; Yin et al. 2002) and further studies on this putative channel reconstituted in a bilayer showed that increasing the Ca^{2+} concentration on the 'cytosolic' side increased the conductance and open probability (El Far and Betz 2002; Yin et al. 2002). The 'kiss and run' mode of vesicle recycling is thought to proceed via a fusion pore and it has been proposed that synaptophysin forms part of this pore (Pennuto et al. 2002; Valtorta et al. 2004).

Synaptophysin binds specifically to cholesterol rather than to phosphatidylcholine or phosphatidylinositol (Thiele et al. 2000). Since cholesterol is enriched at areas of the plasma membrane often referred to as rafts, it is possible that synaptophysin may aid the formation of domains in the plasma membrane enriched in SV constituents and high in cholesterol (Martin 2000). Cholesterol allows a high degree of membrane curvature and thus may promote vesicle formation. Cholesterol depletion was found to inhibit synaptic-like microvesicle biogenesis but had little effect on total endocytic activity (Thiele et al. 2000), suggesting a role in membrane trafficking for synaptophysin. Synaptophysin interacts with the γ-subunit of the AP1 complex involved in the budding of vesicles from the trans-Golgi network (Horikawa et al. 2002). This role is consistent with the observed staining of synaptophysin at the Golgi complex (Jahn et al. 1985; Wiedenmann and Franke 1985) and further implicates synaptophysin in the biogenesis of vesicles.

Synaptophysin forms hetero-oligomers with synaptobrevin, one of the SNARE proteins essential for exocytosis, as well as both proteins forming homo-oligomers (Calakos and Scheller 1994; Pennuto et al. 2002). The binding site for

synaptophysin was localised to the C-terminal transmembrane region of synaptobrevin allowing the cytosolic N-terminal chain to interact with the other SNARE proteins (Yelamanchili et al. 2005). Fluorescence resonance energy transfer (FRET) studies showed that the homo- and hetero-synaptophysin and synaptobrevin complexes were dynamic (Pennuto et al. 2002). Upon stimulation, synaptophysin dissociates from synaptobrevin (Pennuto et al. 2002; Reisinger et al. 2004), suggesting that synaptophysin may sequester synaptobrevin until needed for fusion or that it may deliver synaptobrevin to the sites of exocytosis (Valtorta et al. 2004). This view is supported by evidence that overexpression of synaptophysin with synaptobrevin can target synaptobrevin correctly to SVs. Synaptobrevin overexpressed alone displayed a diffuse distribution (Pennuto et al. 2003). However, another study found that stimulation increased the amount of synaptophysin associated with synaptobrevin as well as increasing the abundance of both synaptophysin and synaptobrevin homo-multimers (Khvotchev and Sudhof 2004). Although the results are conflicting, what is clear is that these complexes are dynamically regulated in parallel with SV recycling.

The C-terminal cytoplasmic domain of synaptophysin containing the tyrosine repeats binds dynamin I in a Ca^{2+}-dependent manner (Daly et al. 2000; Daly and Ziff 2002). Progressive deletion of the tyrosine repeats resulted in a reduction of dynamin I binding (Daly and Ziff 2002). The interaction between dynamin I and synaptophysin also requires high levels of Ca^{2+} (100 – 250 μM), suggesting that it could only occur at the active zone (Daly and Ziff 2002). Injection of a GST-fusion of the C-terminus of synaptophysin had a profound inhibitory effect on SV recycling in the squid giant

axon (Daly et al. 2000). It inhibited transmitter release during high frequency stimulation and electron microscopy showed a reduction in the size of the total vesicle pool and in the number of docked vesicles as well as an increase in the number of clathrin coated vesicles (Daly et al. 2000). This was interpreted as an inhibition of a non-clathrin dependent form of endocytosis which was required during high frequency stimulation to replenish the vesicle pools rapidly, although an inhibition of vesicle uncoating cannot be totally ruled out.

Despite many years of research the exact function of synaptophysin has remained elusive. Synaptophysin does however appear to have a function in the regulation of SV recycling whether that is during exocytosis, endocytosis or vesicle trafficking. The regulated interaction with dynamin I (Daly et al. 2000; Daly and Ziff 2002) is of particular interest since dynamin I is essential for SV endocytosis and to this end the interaction was further investigated.

This chapter shows that overexpression of the C-terminus of synaptophysin in cerebellar granule neurons (CGNs) inhibited SV endocytosis and that a peptide designed from this region inhibited SV turnover in synaptosomes. GST-pulldowns with the C-terminus of synaptophysin (Syp C-term-GST) extracted dynamin I but also a more prominent band identified as amphiphysin I by western blot. Both interacted in a Ca^{2+}-dependent manner. Further investigation of these interactions showed that dynamin I and amphiphysin I bound independently of each other and that, *in vitro*, amphiphysin I could bind to the C-terminus of synaptophysin. These

results suggest that synaptophysin has a potential role in SV endocytosis and its interaction with dynamin I and amphiphysin I could also contribute.

4.5 The C-terminus of synaptophysin inhibits SV endocytosis in nerve terminals of cerebellar granule neurons

Since synaptophysin has a putative role in SV endocytosis, the effect of overexpressing the full length protein and the C-terminus in cerebellar granule neurons (CGNs) was investigated. The C-terminally eGFP-tagged constructs were transfected into CGNs and SV recycling monitored using the styryl dye, FM4-64. FM4-64 was used rather than FM2-10 because it emits fluorescence in the red spectrum, thus enabling simultaneous monitoring of green (eGFP) and red (FM4-64) fluorescence.

CGNs were loaded with FM4-64 using a similar protocol to the loading of FM2-10 in synaptosomes (see chapters 3, 5 and later in this chapter). CGNs were stimulated with 50 mM KCl in the presence of 10 μM FM4-64 for two minutes to evoke exocytosis and subsequent endocytosis which internalises the FM4-64. CGNs were then washed to remove any extracellularly bound FM4-64 before stimulating exocytosis once more with a 50 mM KCl stimulus for 30 s to unload the dye. Any effect on SV turnover would be reflected in a change in the amount of dye accumulated and unloaded.

Figure 4.1 shows CGNs transfected with full length synaptophysin-eGFP. Panel 4.1A shows the overlay image of the CGNs loaded with FM4-64 (red) and those

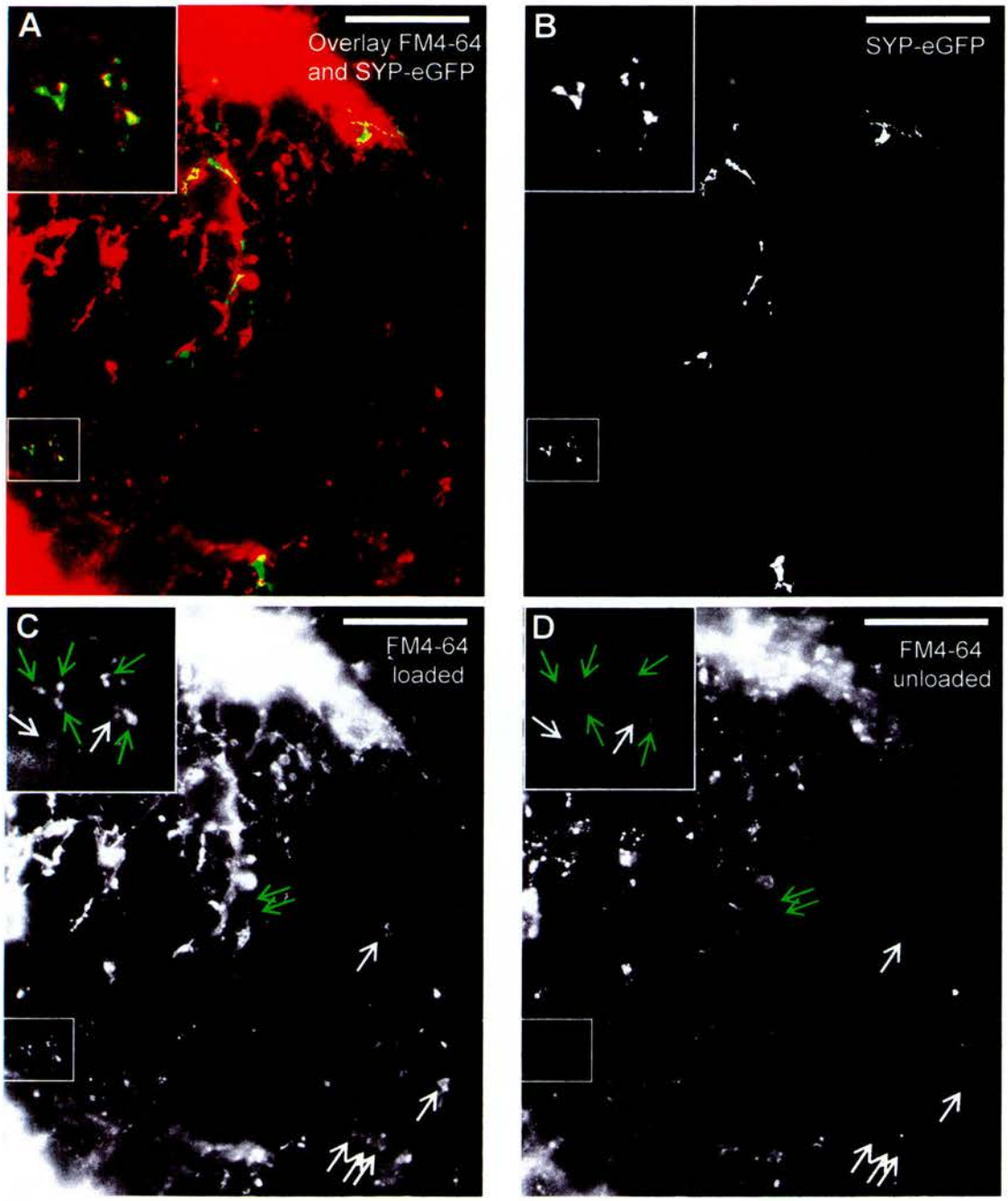

Figure 4.1 – Full length synaptophysin-eGFP has no effect on SV turnover in CGNs

(A) Overlay image of CGNs loaded with FM4-64 (red) and synaptophysin-eGFP transfected neurites (eGFP-SYP, green). **(B)** Monochrome image of SYP-eGFP transfected neurites. **(C)** FM4-64 loaded neurites before and **(D)** after stimulation with 50 mM KCl. **(A-D)** Boxed area in each field is magnified in the inset. Scale bar is 5 µM. White and green arrows indicate nerve terminals of untransfected and transfected CGNs, respectively. Field shown is representative of 4 separate experiments.

which are transfected (green). Loading of FM4-64 between transfected and non-transfected CGNs is comparable - reflected in the extent of loading in figure 4.1C. Unloading of FM4-64 between transfected and non-transfected CGNs in the same field (compare the monochrome images from the red channel in fig 4.1C before stimulation and 4.1D after stimulation) is also comparable. The enlarged section in each panel clearly demonstrates transfected neurites (fig 4.1A and B) which load FM4-64 (fig 4.1 C) and unload FM4-64 upon stimulation (fig 4.1D). Thus in gross terms full length synaptophysin-eGFP has no effect on SV turnover.

The same experiment was conducted with CGNs transfected with C-terminus synaptophysin-eGFP (fig 4.2). Again, FM4-64 loading is in red and the transfected neurites are in green (fig 4.2A). In this instance less FM4-64 seems to be accumulated in the transfected nerve terminals. However, the unloading of the dye was not affected since both untransfected and transfected CGNs lost FM4-64 on stimulation (fig 4.2D).

To prove that a reduction in SV turnover occurred, unloading of FM4-64 from full length synaptophysin-eGFP and C-terminus synaptophysin- eGFP nerve terminals was quantified. This was performed by selecting regions of interest around each nerve terminal, both transfected and non-transfected in the same field, and recording the extent of the fluorescence loss from these regions during stimulation. Example traces showing a typical time course of unloading in one experiment are shown in figure 4.3A for the full length synaptophysin- eGFP and in figure 4.3B for the C-terminus synaptophysin- eGFP. The fluorescence drop for the full length

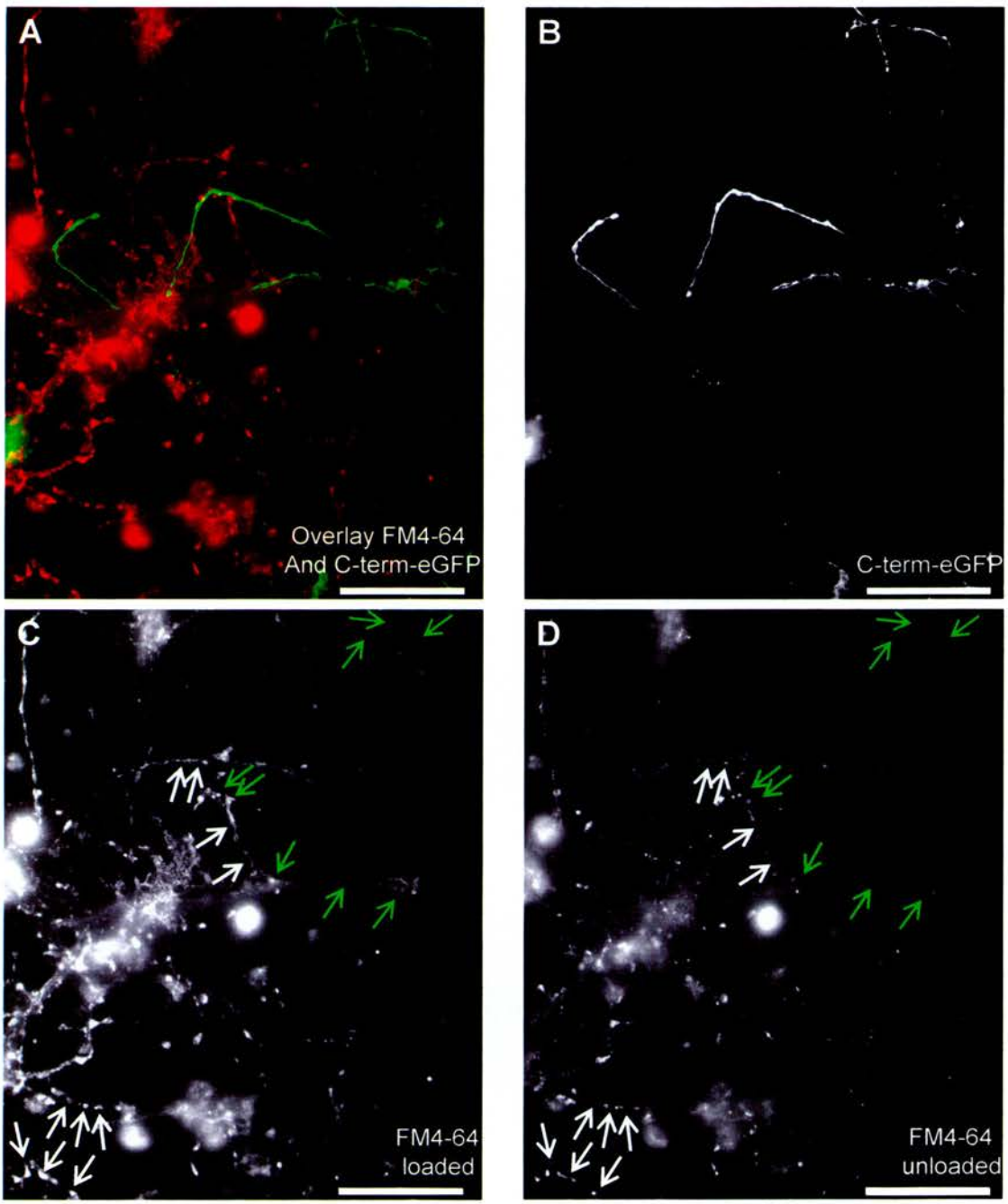

Figure 4.2 – C-terminus synaptophysin-eGFP reduces SV turnover in CGNs

(A) Overlay image of CGNs loaded with FM4-64 (red) and C-terminus synaptophysin-eGFP transfected neurites (C-term-eGFP, green). **(B)** Monochrome image of C-term-eGFP transfected neurites. **(C)** FM4-64 loaded neurites before and **(D)** after stimulation with 50 mM KCl. Scale bar is 5 μM. White and green arrows indicate nerve terminals of untransfected and transfected CGNs, respectively. Field shown is representative of 4 separate experiments.

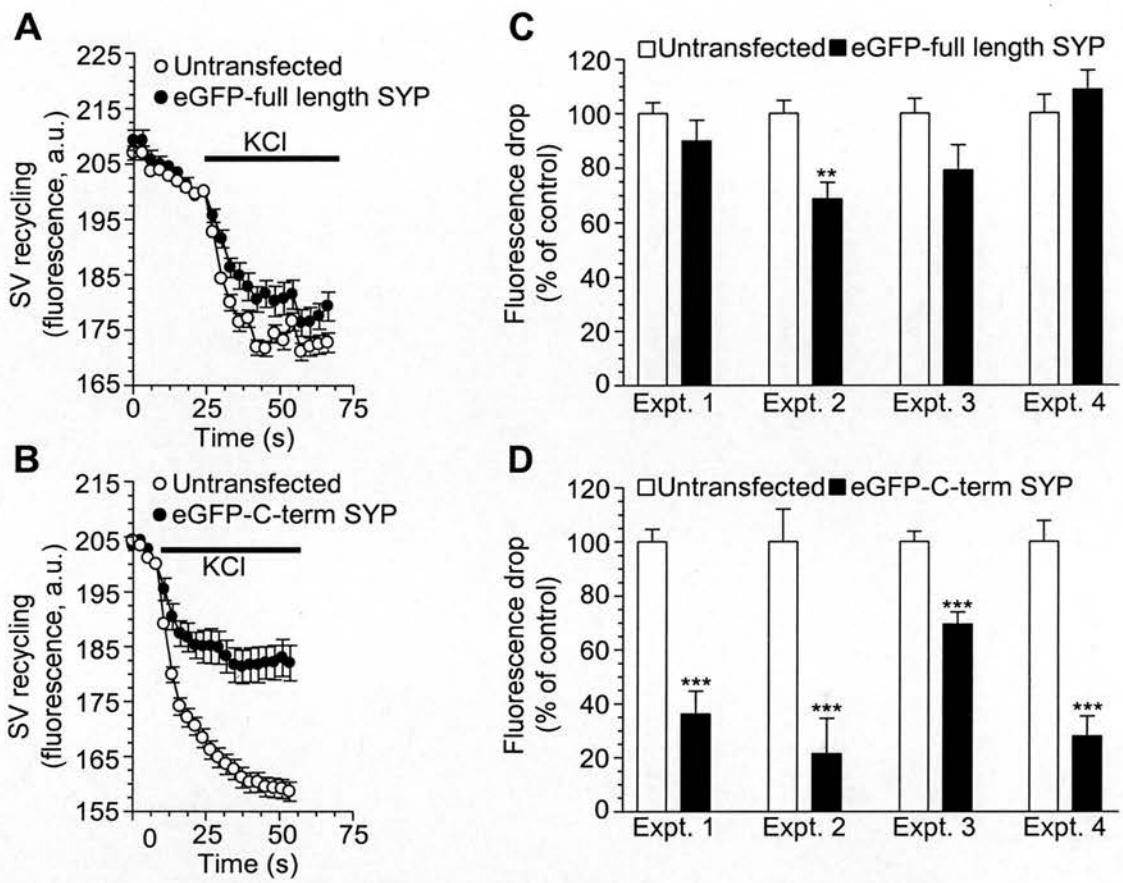

Figure 4.3 – Overexpression of the C-terminus of synaptophysin inhibits SV turnover in CGNs

Example average trace of the fluorescence drop upon stimulation with 50 mM KCl for CGNs transfected with full length synaptophysin-eGFP (SYP) **(A)** or C-terminus (C-term) SYP-eGFP **(B)**. Closed circles represent transfected CGNs and open circles represent untransfected CGNs in the same field and the bar denotes the presence of KCl for both **A** and **B**. Average fluorescence drops, as a % of untransfected CGNs in the same field, from 4 separate experiments with CGNs transfected with either full length SYP-eGFP **(C)** or C-term SYP-eGFP **(D)**. Open bars represent untransfected CGNs and closed bars represent transfected CGNs in **C** and **D** ($n \geq 12$ for transfected nerve terminals and $n \geq 33$ for untransfected nerve terminals for each experiment ± SEM). Significance in **C** and **D** was determined by Student's t-test for each experiment (**$p<0.01$, ***$p<0.0001$).

synaptophysin construct is very similar to that of the untransfected nerve terminals in the same field (fig 4.3A). The C-terminus of synaptophysin construct however, shows a marked inhibition (fig 4.3B). Thus the C-terminus has reduced SV turnover in CGNs.

The average fluorescence drop for the two synaptophysin constructs varied between experiments although there was generally no statistical difference between the transfected full length synaptophysin CGNs and the untransfected controls (fig 4.3C). Similarly, the CGNs transfected with the C-terminus of synaptophysin showed variation with inhibition ranging from 30 – 70 % of control but in all cases the inhibition was extremely significant (fig 4.3D).

The overall average, i.e. all four experiments combined (fig 4.5A), showed an unexpected inhibition of 26 % (73.9 ± 7.2 % of control) for the full length synaptophysin-eGFP construct (see discussion) and a inhibition of 61 % (38.4 ± 8.9 % of control) for the C-terminus synaptophysin- eGFP. Thus overexpressing the C-terminal portion of synaptophysin is 2.5 times as effective at inhibiting SV turnover as overexpressing the full length synaptophysin, suggesting this region may have a role in SV recycling.

The inhibition in SV turnover observed with the synaptophysin C-terminus could be a result of either an inhibition of SV exocytosis or endocytosis because FM4-64 loading and unloading involves both. To delineate between the two possibilities, the data was reanalysed to examine the kinetics of unloading. By normalising the start

and end points of the fluorescence drop between 1 and 0, the unloading values are now independent of dye accumulation and reflect only the rate at which the vesicles were released. The kinetics of release is therefore a measure of exocytosis, assuming that SVs mix randomly after SV endocytosis.

Example time courses of the kinetics of unloading for the full length synaptophysin-eGFP (fig 4.4A) and the C-terminus synaptophysin- eGFP (fig 4.4B) constructs are shown. The rate of unloading is not significantly different from control untransfected CGNs in the same field for either construct. The time taken for the fluorescence to drop by 50 % ($t_{1/2}$) expressed as a % of control is shown for all of the experiments (fig 4.4C and D) as well as the combined average of these experiments (fig 4.5B). This analysis shows that there is no statistically significant difference in the kinetics of unloading, and therefore exocytosis, between each of the constructs and control untransfected CGNs. Thus the inhibition seen in the synaptophysin C-terminus transfected nerve terminals in the SV turnover assay (fig 4.5A) is due to an inhibition in SV endocytosis, implicating synaptophysin, and in particular, the C-terminal tail in this process.

4.6 A peptide designed from the C-terminal tail of synaptophysin inhibits SV endocytosis in synaptosomes

The C-terminal tail of synaptophysin contains nine degenerate pentapeptide repeats, each starting with a tyrosine residue (fig 4.6, Daly and Ziff 2002; Valtorta et al. 2004). These repeats are thought to be the site where dynamin I binds to

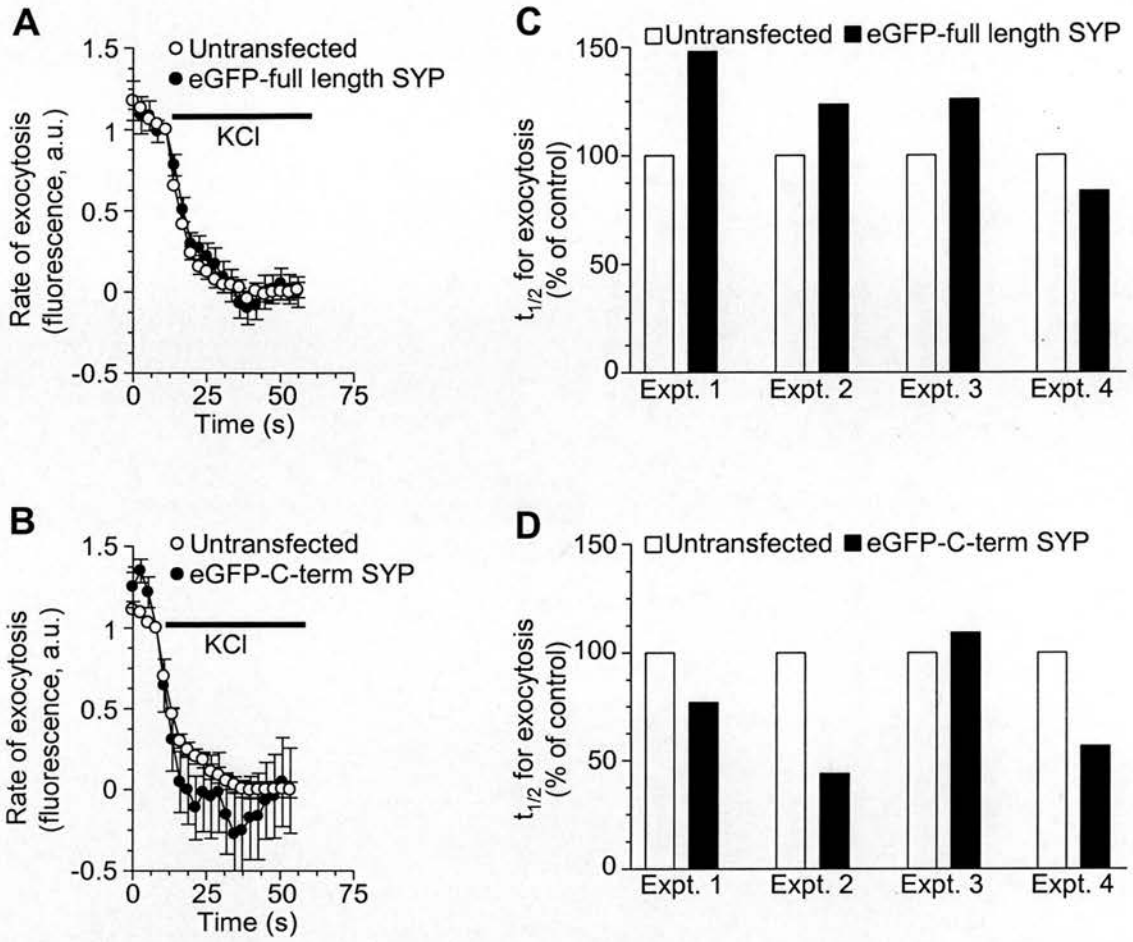

Figure 4.4 – Neither synaptophysin construct significantly inhibits exocytosis in CGNs

The start and end points of the fluorescence drop in fig 4.3 were normalised to examine exocytosis. Example average trace of the rate of exocytosis for CGNs transfected with full length synaptophysin (SYP)-eGFP **(A)** or C-terminus (C-term) SYP-eGFP **(B)**. Closed circles represent transfected CGNs and open circles represent untransfected CGNs in the same field and the bar denotes the presence of KCl for both **A** and **B**. The time taken for the fluorescence to reach half of the original level ($t_{1/2}$), as a % of the $t_{1/2}$ for untransfected CGNs in the same field, for 4 separate experiments with CGNs transfected with full length SYP-eGFP **(C)** or C-term SYP-eGFP **(D)**.

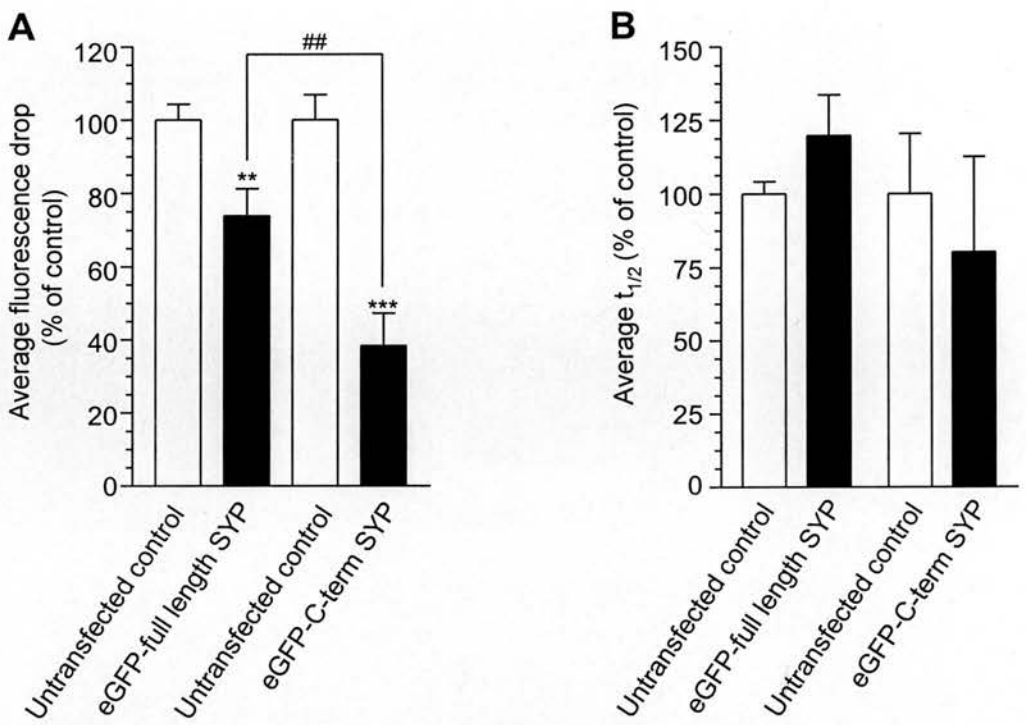

Figure 4.5 – Over-expression of the C-terminus of synaptophysin inhibits SV endocytosis but not SV exocytosis in CGNs

(A) Overall average of the fluorescence drop from the 4 experiments (fig 4.3C and D) for both CGNs transfected with full length SYP-eGFP and C-term SYP-eGFP, as a % of control (Overall, $n \geq 64$ for transfected nerve terminals and $n \geq 229$ for untransfected nerve terminals). Significance determined by applying students t-test for each condition (** $p < 0.01$, ***$p < 0.001$ compared to control, $^{\#\#}p < 0.01$ compared to transfected full length SYP-eGFP). **(B)** Average $t_{1/2}$ from the 4 experiments (fig 4.4C and D) for both CGNs transfected with full length SYP-eGFP and C-term SYP-eGFP, as a % of control. Significance determined by applying students t-test for each condition (all $p > 0.05$). Open bars represent untransfected CGNs and closed bars represent transfected CGNs for **A and B**.

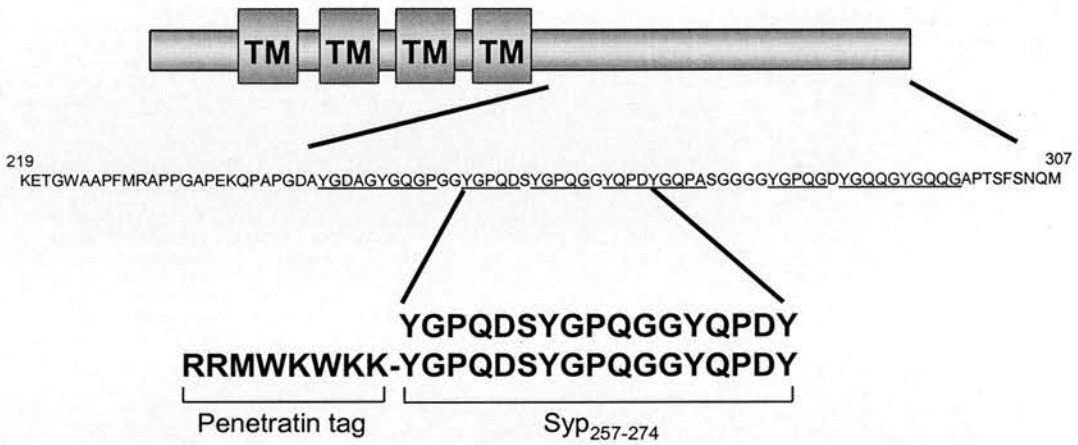

Figure 4.6 – Synaptophysin structure and peptide design

Schematic of the domain structure of synaptophysin showing the four transmembrane (TM) regions. The N and C-terminal tails are both cytosolic. The sequence of the C-terminal tail is shown in single amino acid code. The C-terminal tail contains nine repeats of a degenerate pentapeptide sequence with the consensus YG(P/Q)QG. These repeats are underlined. The blown up region shows the sequence from residues 257 – 274 of the C-terminal tail from which the peptide sequence was taken. The sequence of the peptide including the N-terminal penetratin tag for delivery in to the cytosol is also shown.

synaptophysin (Daly et al. 2000; Daly and Ziff 2002). This is because truncation of synaptophysin from the C-terminus, and therefore progressively deleting these repeats, reduced the binding of dynamin I (Daly and Ziff 2002). Therefore, this region was used to design a peptide to inhibit the dynamin I-synaptophysin interaction. Amino acids 257- 274 were selected because they encompassed three of the central tyrosine repeats (fig 4.6). The penetratin sequence was included N-terminal to the peptide sequence to facilitate entry into the cytosol.

The effect of this peptide ($Syp_{257-274}$) on SV recycling was investigated in synaptosomes with the FM2-10 SV turnover assay. Synaptosomes were pre-incubated with varying concentrations of peptide from 100 – 500 μM and were loaded with FM2-10 using the standard protocol (illustrated fig 4.7A). To determine the amount of FM2-10 accumulated the synaptosomes were unloaded with a 2 min stimulus of 30 mM KCl. The amount of SV turnover inhibited by the $Syp_{257-274}$ peptide expressed as a % of control is shown in figure 4.7B. The $Syp_{257-274}$ peptide inhibited SV turnover by 60 % (40.2 ± 28.3 % of control) at 250 μM and this did not increase with higher concentrations of peptide (fig 4.7B). Figure 4.7C shows the effect of 250 μM of $Syp_{257-274}$ peptide on SV turnover. The effect of $Syp_{257-274}$ on SV exocytosis was investigated using the glutamate release assay. There was no significant difference between peptide treated synaptosomes and control synaptosomes (fig 4.7D), indicating that the peptide does not inhibit exocytosis. To better quantify the effect of the $Syp_{257-274}$ peptide on SV endocytosis the retrieval efficiency (endocytosis / exocytosis) was calculated. A value of less than one

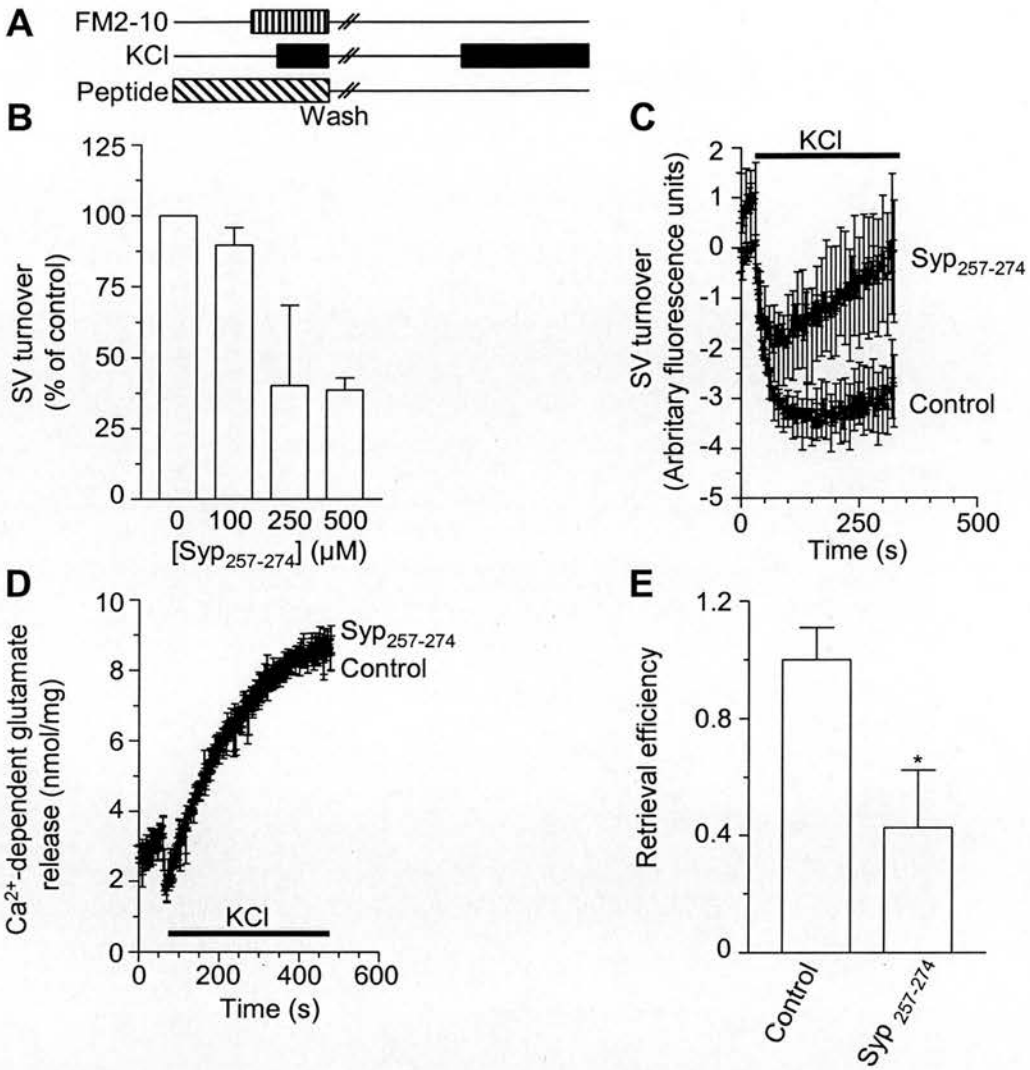

Figure 4.7 – $Syp_{257-274}$ peptide inhibits SV endocytosis

(A) Schematic illustrating the SV turnover assay protocol. **(B)** Synaptosomes were incubated with the indicated concentrations of $Syp_{257-274}$ peptide ± Ca^{2+} for 30 minutes prior to loading with FM2-10. The Ca^{2+}-dependent FM2-10 unloading (SV turnover) in response to a 2 min stimulus with 30 mM KCl is displayed ($n \geq 3 \pm SEM$). **(C)** Average Ca^{2+}-dependent SV turnover traces for 250 μM $Syp_{257-274}$. **(D)** Ca^{2+}-dependent glutamate release from control or peptide treated (250 μM) synaptosomes stimulated with 30 mM KCl. ($n \geq 3 \pm SEM$). Bar in **C** and **D** denotes the presence of KCl. **(E)** Retrieval efficiency calculated as the amount of endocytosis, **C**, divided by the amount of exocytosis after 2 minutes of stimulation, **D**. Student's t-test was performed (*$p < 0.05$).

indicates a specific block of SV endocytosis. The retrieval efficiency for the $Syp_{257-274}$ peptide was calculated as 0.4 ± 0.2 (fig 4.7E), confirming that the $Syp_{257-274}$ peptide inhibits SV endocytosis, agreeing with the previous finding that the C-terminus of synaptophysin has a role in SV endocytosis.

It would have been interesting to examine the effect of the $Syp_{257-274}$ peptide on SV recycling in CGNs, but this experiment was not conducted because penetratin-tagged peptides are likely to accumulate in the nucleus of cells. This is because the penetratin sequence is derived from that of a transcription factor (Joliot et al. 1991), so may cause mislocalisation from the cytosolic/plasma membrane target interactions.

4.7 Dynamin I and amphiphysin I bind to the C-terminus of synaptophysin in a Ca^{2+}-dependent manner

The C-terminus of synaptophysin appears to have a functional role in SV endocytosis when overexpressed in primary neuronal culture and a peptide designed to inhibit the dynamin I-synaptophysin interaction also inhibits SV endocytosis in isolated nerve terminals. Therefore the interactions of this region were explored in more detail using GST-pulldown assays. Dynamin I has been shown to bind to the C-terminus of synaptophysin in a Ca^{2+}-dependent manner (Daly and Ziff 2002) so this interaction was investigated first. Synaptosomes lysed in the presence of either 2 mM $CaCl_2$ or 1 mM EGTA plus 1 mM EDTA were incubated with the synaptophysin C-terminus-GST (Syp C-term-GST) coupled to GSH beads. The extracted proteins were separated by SDS-PAGE and stained by coomassie. A band of the correct molecular

weight for dynamin I (approximately 100 kDa) bound in a Ca^{2+}-dependent manner (fig 4.8). However, a more prominent band running between the 100 and 150 kDa markers was also extracted in the presence of Ca^{2+} (fig 4.8). The levels of the Syp C-term-GST were equal for all conditions so different amounts of fusion protein were not responsible for the binding in the presence of Ca^{2+} (fig 4.8).

A likely candidate for the higher molecular weight band is amphiphysin I, since it runs at 125 kDa on an SDS-PAGE gel, and can bind dynamin I (Slepnev and De Camilli 2000). The samples were thus blotted for dynamin I and amphiphysin I. Both proteins were present only in the plus Ca^{2+} lanes (fig 4.9), suggesting that the two bands extracted with the Syp C-term-GST in the presence of Ca^{2+} were dynamin I and amphiphysin I. Interestingly, the amount of amphiphysin I extracted upon stimulation in the presence of Ca^{2+} decreases, perhaps reflecting an overall change in protein dynamics during stimulation.

Amphiphysin I is known to bind to GST in the presence of Ca^{2+} (H. Falconer, personal communication) and so the experiment was repeated but with GST as well as the Syp C-term-GST coupled to GSH beads. Again the extracted proteins were analysed by coomassie stained gel. The band identified as amphiphysin I by molecular weight does appear to bind to the GST control in the presence of Ca^{2+} but not nearly as strongly as to the Syp C-term-GST (fig 4.10). The dynamin I band may also be detectable in the GST control, but again, not to the same extent as the Syp C-term-GST. The amounts of fusion proteins were equal between conditions and so not responsible for the differences in binding (fig 4.10).

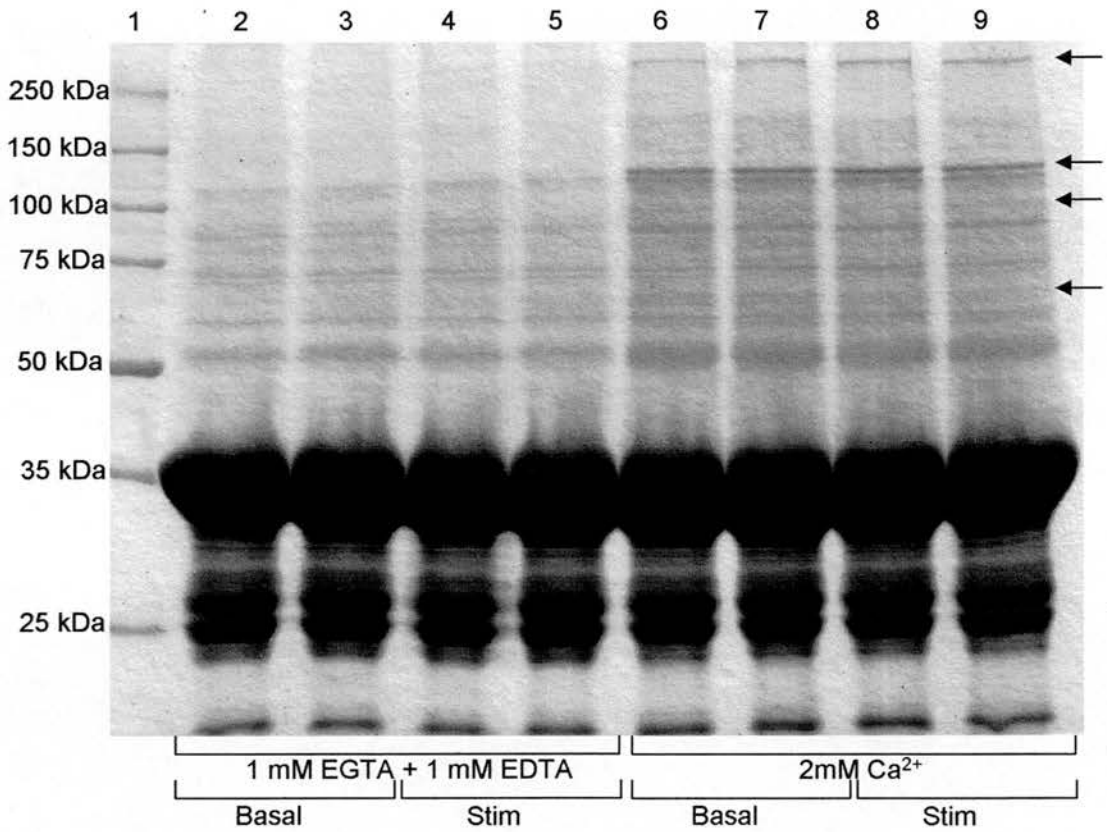

Figure 4.8 – The C-terminus of synaptophysin has Ca^{2+}-dependent binding partners

Basal (lanes 2, 3, 6 and 7) or stimulated (stim) with 30 mM KCl (lanes 4, 5, 8 and 9) synaptosomes were lysed in lysis buffer with either 1 mM EGTA + 1 mM EDTA (lanes 2 – 5) or 2 mM $CaCl_2$ (lanes 6 – 9) and incubated with GSH beads coupled to the Syp C-term-GST. The bound samples were separated by SDS-PAGE (10 % gel) and coomassie stained. The arrows indicate proteins bound in a Ca^{2+}-dependent manner. Gel representative of $n \geq 3$.

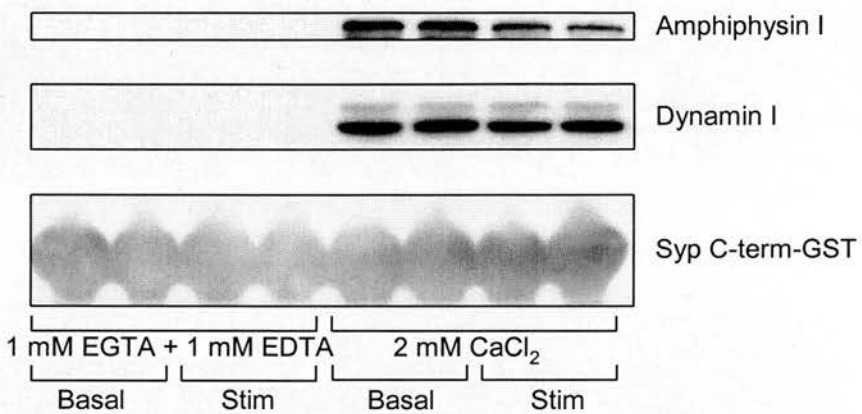

Figure 4.9 – The C-terminus of synaptophysin extracts dynamin I and amphiphysin I in a Ca^{2+}-dependent manner

Proteins extracted from lysates made from synaptosomes under basal and stimulated (stim, with 30 mM KCl) conditions by the Syp C-term-GST were western blotted for dynamin I and amphiphysin I. The amount of Syp C-term-GST is shown from cross-reaction with the secondary antibody. Blots representative of $n \geq 2$.

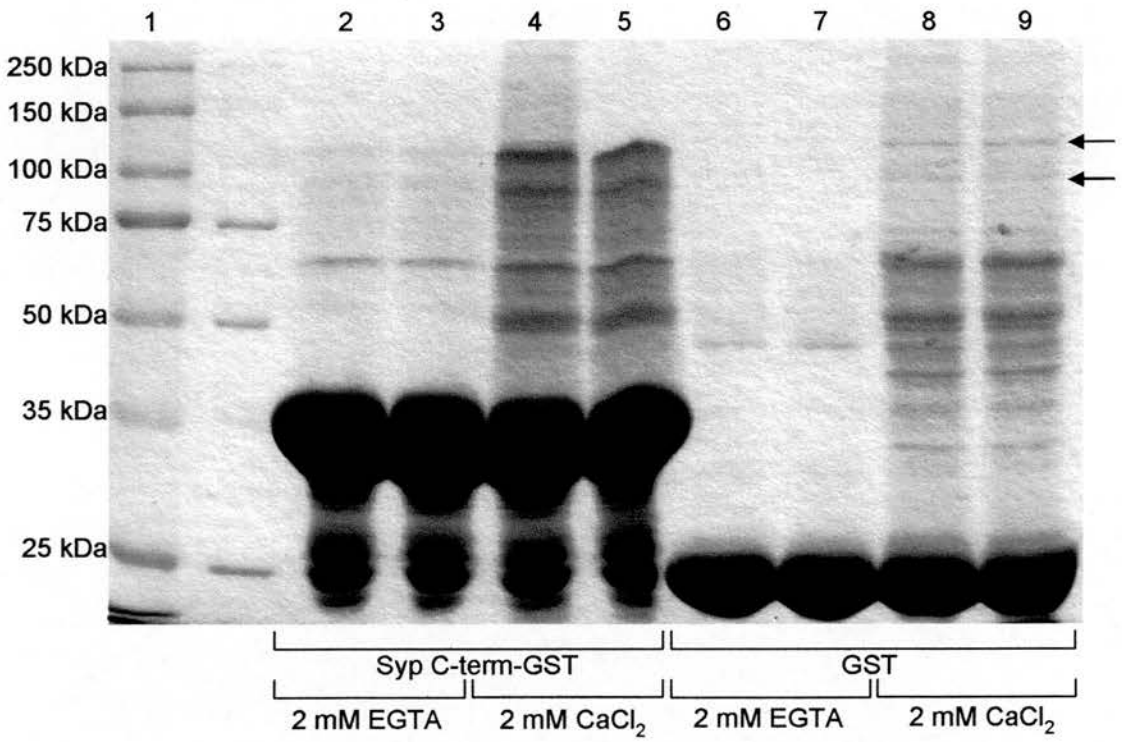

Figure 4.10 – Ca^{2+}-dependent binding of dynamin I and amphiphysin I to GST is not responsible for extraction by Syp C-term-GST

Synaptosomes were lysed in lysis buffer with either 1 mM EGTA + 1 mM EDTA (lanes 2, 3, 6 and 7) or 2 mM $CaCl_2$ (lanes 4, 5, 8 and 9) and incubated with GSH beads coupled to Syp C-term-GST (lanes 2 – 5) or GST (lanes 6 – 9). The bound samples were separated by SDS-PAGE (10 % gel) and coomassie stained. The arrows indicate dynamin I and amphiphysin I as identified by molecular weight. Gel is representative of $n \geq 2$.

4.8 Dynamin I and amphiphysin I bind independently to the C-terminus of synaptophysin

The $Syp_{257-274}$ peptide was designed to disrupt the dynamin I-synaptophysin interaction and so to test this, the $Syp_{257-274}$ peptide was incubated with synaptosomes lysed in the presence of 2 mM Ca^{2+} and the Syp C-term-GST coupled to the GSH beads. The bound samples were blotted for dynamin I. The Syp C-term-GST incubated with the $Syp_{257-274}$ peptide extracted less dynamin I than the control lane without peptide (M. Cousin, personal communication), suggesting that the $Syp_{257-274}$ peptide can disrupt the dynamin I-synaptophysin interaction. A band of greater molecular weight than dynamin I was also reduced upon peptide binding (M. Cousin, personal communication). This band could be amphiphysin I but this cannot be confirmed because the membrane was not blotted with amphiphysin I antibody.

Dynamin I and amphiphysin I bind to the C-terminus of synaptophysin in a Ca^{2+}-dependent manner (fig 4.8 – 4.10) and the $Syp_{257-274}$ peptide disrupts binding of at least dynamin I (M. Cousin, personal communication). Since dynamin I and amphiphysin I interact with each other, either could be indirectly binding synaptophysin via the other or they could be binding to synaptophysin independently. To test these possibilities the dynamin I-amphiphysin I interaction was disrupted using the $DynI_{832-840}$ peptide (fig 3.9A) during pulldown assays with Syp C-term-GST. The presence of the $DynI_{832-840}$ peptide did not alter the amount of dynamin I or amphiphysin I extracted by the Syp C-term-GST in the presence of Ca^{2+} (fig 4.11A lanes 3 and 4). This was confirmed by blotting the samples for dynamin I and amphiphysin I. Both were present in the sample incubated with the

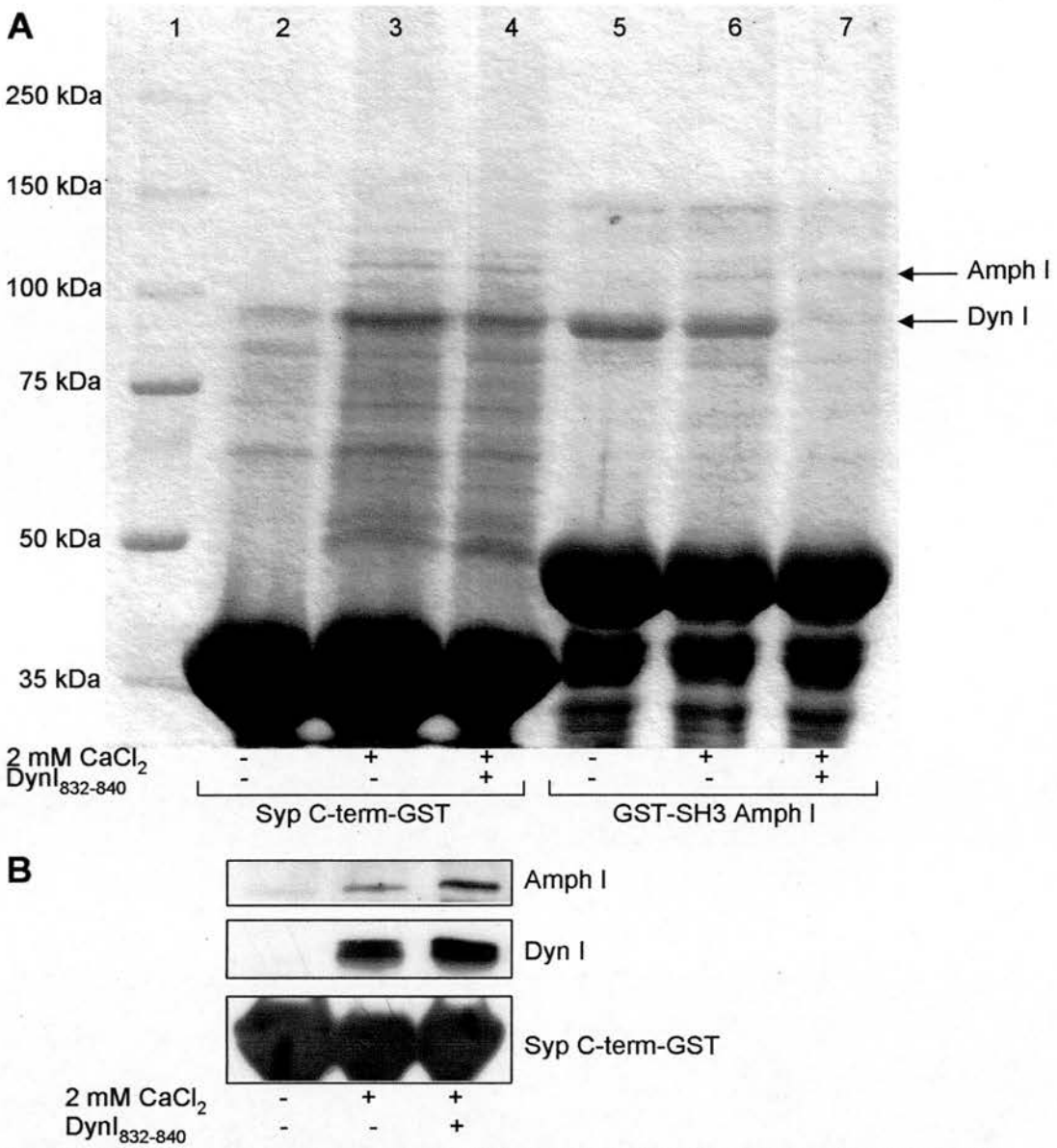

Figure 4.11 – Dynamin I and amphiphysin I bind independently to the the C-terminus of synaptophysin

(A) Synaptosomes lysed in the presence of either 1 mM EGTA + 1 mM EDTA or 2 mM $CaCl_2$ were incubated firstly with GSH beads coupled to Syp C-term-GST ± 3 mM $DynI_{832-840}$ peptide. This peptide disrupts the dynamin I-amphiphysin I interaction (fig 3.9). The flow through was then incubated with GSH beads coupled to GST-SH3 of amphiphysin I (GST-SH3 Amph I). All the bound samples were separated by SDS-PAGE (7.5 % gel) and coomassie stained. **(B)** Some of the bound Syp C-term-GST samples were western blotted for amphiphysin I and dynamin I. The Syp C-term-GST is shown from cross-reaction of the secondary antibody. Experiment n = 2.

$DynI_{832-840}$ peptide (fig 4.11B), suggesting that dynamin I and amphiphysin I bind independently to the C-terminus of synaptophysin.

To prove that the dynamin I-amphiphysin I interaction was disrupted by the $DynI_{832-840}$ peptide, the flow through from the Syp C-term-GST was incubated with GST-SH3 amphiphysin I coupled to GSH beads. In the presence of the $DynI_{832-840}$ peptide dynamin I extraction was abolished (fig 4.11A lanes 6 and 7) and thus the dynamin I-amphiphysin I interaction was disrupted.

4.9 Amphiphysin I binds to the C-terminus of synaptophysin *in vitro* but not via the SH3 domain

The dynamin I-synaptophysin interaction is already published (Daly and Ziff 2002) but this is the first demonstration of a putative amphiphysin I-synaptophysin interaction. To show that these two proteins do interact directly an *in vitro* binding assay was conducted. GSH beads were incubated with either GST or Syp C-term-GST and a range of concentrations of purified His-tagged full length amphiphysin I in the presence of 2 mM $CaCl_2$ or 2 mM EGTA. His-tagged amphiphysin I was used to ensure that the GSH beads were not binding both fusion proteins. In the presence of Ca^{2+} amphiphysin I binds to both GST and Syp C-term-GST. However, amphiphysin I binds Syp C-term-GST at much lower concentrations compared to GST indicating a specific interaction (fig 4.12A). In the absence of Ca^{2+} amphiphysin I again bound to both the GST and Syp C-term-GST but this time there was no disparity when amphiphysin I concentrations were lower (fig 4.12B). Importantly amphiphysin I binding to the synaptophysin C-terminal tail was greatly

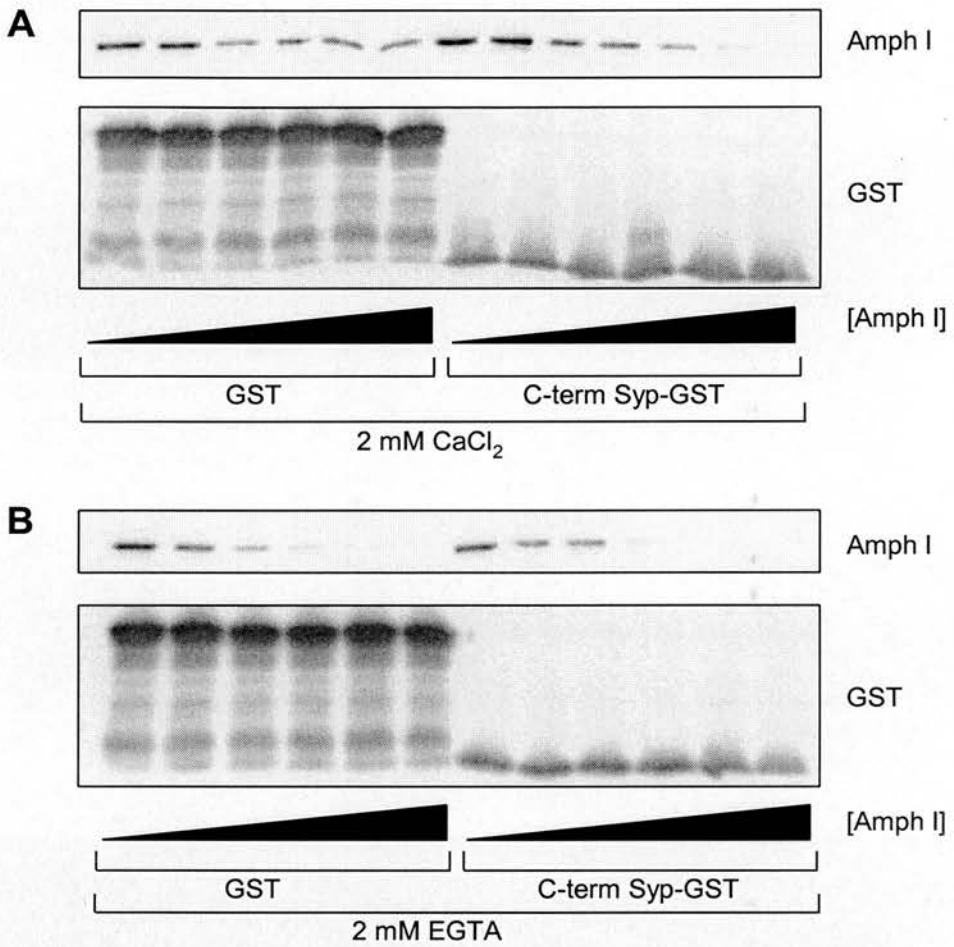

Figure 4.12 – Amphiphysin I binds the C-terminus of synaptophysin directly *in vitro*

GSH beads were incubated with either 200 nM Syp C-term-GST or 200 nM GST and His-amphiphysin I (Amph I) serially diluted from 0.5 µM to 15.6 nM. The experiment was performed in duplicate with one set incubated in buffer containing either 2 mM $CaCl_2$ **(A)** or 2 mM EGTA **(B)**. The samples were separated by SDS-PAGE (10 % gels) and western blotted for amphiphysin I (Amph I) and GST. Experiment representative of n =2.

increased in the presence of Ca^{2+} compared to GST. This is borne out by densitometric analysis of the blots (fig 4.13). At low concentrations of amphiphysin I, binding to the Syp C-term-GST remains at approximately 50% of saturated binding compared to less than 10% for the other conditions. At higher concentrations (> 150 nM) of amphiphysin I, there is an element of non-specific binding detected with all conditions. Taken together, this implies that the interaction is direct.

To determine which part of amphiphysin was responsible for binding to synaptophysin, synaptosomes lysed in the presence of 2 mM $CaCl_2$ or 1 mM EGTA plus 1 mM EDTA were incubated with GST-SH3 amphiphysin I or GST coupled to GSH beads. Synaptophysin was not detected with either fusion protein (fig 4.14), indicating that amphiphysin I does not bind to synaptophysin via its SH3 domain.

4.10 Amphiphysin I and the C-terminus of synaptophysin I bind Ca^{2+}

The dynamin I-synaptophysin and amphiphysin I-synaptophysin interactions are both Ca^{2+}-dependent and therefore at least one of the proteins may bind Ca^{2+}, causing a conformational change which enables the interaction. To determine if any of the proteins bind Ca^{2+}, a $^{45}Ca^{2+}$ overlay assay was performed. The purified fusion proteins were separated by SDS-PAGE and transferred to nitrocellulose membrane. The membrane was then incubated with $^{45}Ca^{2+}$. Autoradiography of the membrane revealed that the synaptophysin C-terminus, amphiphysin I SH3 domain and full length amphiphysin I all bound Ca^{2+} (fig 4.15). Interestingly the PRD of dynamin I did not bind Ca^{2+}. Neither did GST (fig 4.15). Thus binding of Ca^{2+} by either

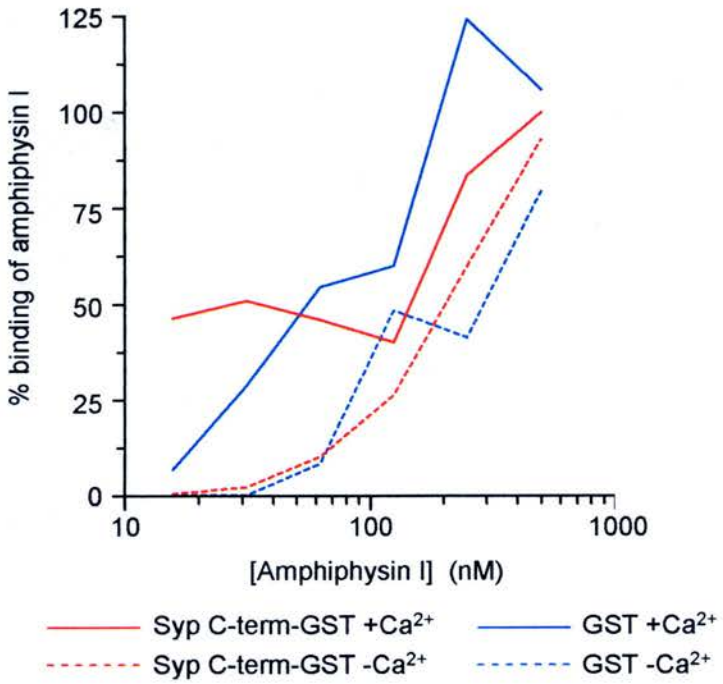

Figure 4.13 – Quantitative analysis of the binding of amphiphysin I to the C-terminus of synaptophysin *in vitro*

Densitometry was performed on the western blot in fig 4.12. The binding of amphiphysin I, expressed as a % of saturated binding, is shown for each of the conditions. Binding to Syp C-term-GST is shown in blue and binding to GST in red. Solid lines show binding in presence of 2 mM $CaCl_2$ and dashed lines show binding in the presence of 2 mM EGTA.

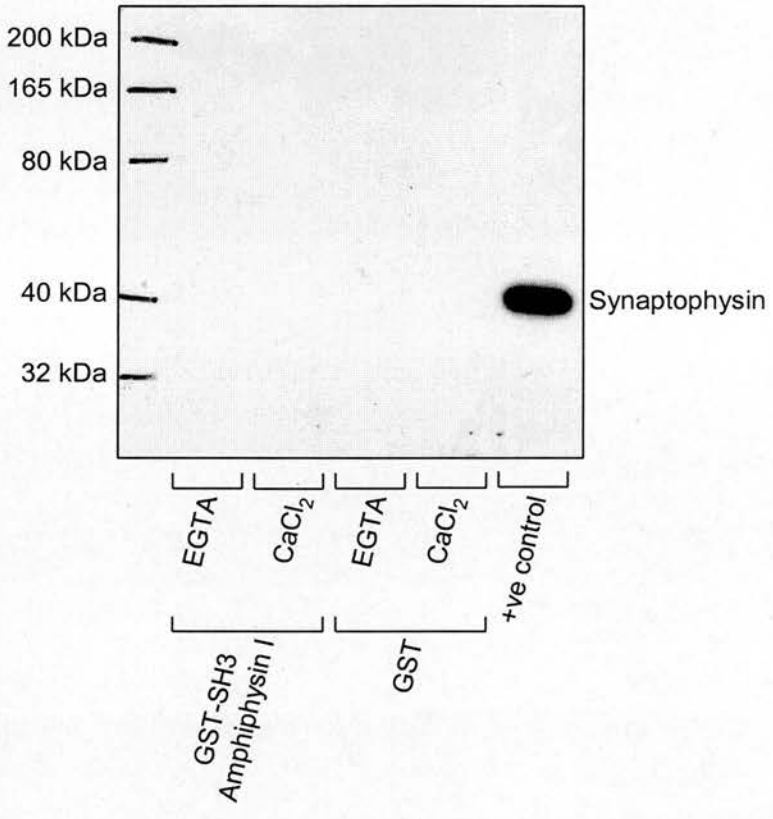

Figure 4.14 – Synaptophysin does not bind to the SH3 domain of amphiphysin I

Synaptosomes lysed in lysis buffer containing 1 mM EGTA + 1 mM EDTA (EGTA) or 2 mM $CaCl_2$ ($CaCl_2$) were incubated with GSH beads coupled to GST-SH3 amphiphysin I. The bound samples were western blotted and probed for synaptophysin. Experiment n = 1.

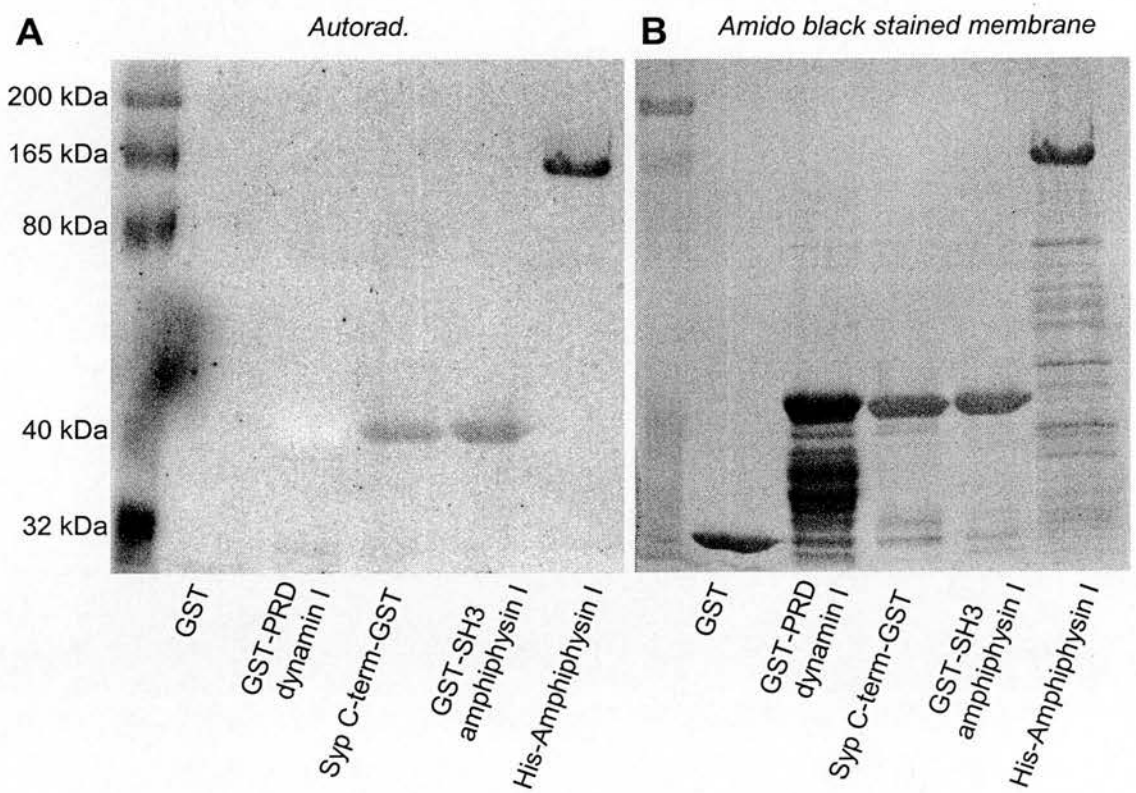

Figure 4.15 – Amphiphysin I and the C-terminus of synaptophysin bind Ca^{2+}

A 15 % gel with 4 µg of GST, GST-PRD dynamin I, Syp C-term-GST, GST-SH3 amphiphysin I and His-full length amphiphysin I was transferred onto nitrocellulose membrane. The membrane was overlayed with 10 µCi of $^{45}Ca^{2+}$ and washed. The dried membrane was exposed by autoradiography **(A)** and subsequently stained with amido black to display the protein levels **(B)**. Experiment n = 1.

synaptophysin or amphiphysin I could stimulate the interaction. Protein levels were equal as shown by amido black staining of the membrane (fig 4.15B).

4.11 Discussion

This chapter shows that overexpression of the C-terminus of synaptophysin or disruption of interactions mediated by the C-terminus of synaptophysin inhibits SV endocytosis. Dynamin I was previously shown to bind to the C-terminus of synaptophysin in a Ca^{2+}-dependent manner but this chapter shows that amphiphysin I also binds to the C-terminus of synaptophysin in a Ca^{2+}-dependent manner at least *in vitro*, further linking synaptophysin to a role in SV endocytosis.

Overexpression of synaptophysin

Synaptophysin has been used as a SV marker since its discovery in 1985 but only recently has it been used as a marker of SVs in real time. This was made possible by the tagging of synaptophysin with fluorescent variants of GFP. Experiments with full length synaptophysin-eGFP in hippocampal neurons showed that the fluorescent protein was targeted to SVs and had no effect on synapse density, neurite length or the number of SVs per terminal (Pennuto et al. 2002; Pennuto et al. 2003). Work by a separate group showed that synaptophysin-eGFP was again localised to synapses and colocalised with FM4-64 puncta (Li and Murthy 2001). They showed also that the synaptophysin-eGFP had no effect on the rate of exocytosis and interpreted this as the synapses being functionally normal.

In agreement with Li and Murthy (2001), this chapter shows that there was no difference in the rate of exocytosis from full length synaptophysin-eGFP and control untransfected cells (fig 4.5B). There was also no effect of the C-terminus synaptophysin-eGFP construct on exocytosis (fig 4.5B). However, both constructs significantly inhibited SV endocytosis (fig 4.5A). This inhibition is likely to be an underestimate, since only nerve terminals which loaded and unloaded with FM4-64 were included in the analysis. Nerve terminals where endocytosis was completely inhibited by the overexpression of either construct would not have been taken into consideration. The slight inhibition observed with overexpression of the full length synaptophysin-eGFP (fig 4.5A) may well be due to disruption of the relative amounts of synaptophysin and synaptobrevin homo- and hetero-multimers. These complexes are very dynamic and thus the equilibrium may be altered by overexpression of synaptophysin. Inhibition of SV endocytosis was not addressed by Li and Murphy (2001) since they normalised the release of dye at the start and end points of stimulation and therefore were looking at the rate of exocytosis, which is independent of the amount of dye accumulated.

Another group using a secretion assay in PC12 cells, where the stimulated release of a cotransfected hormone was used to monitor exocytosis, did observe a small inhibition of exocytosis when synaptophysin was cotransfected (Sugita et al. 1999). This system is not ideal however since hormones are thought to be packaged into dense core vesicles and synaptophysin is localised to small, translucent SVs (Valtorta et al. 2004).

The C-terminus of synaptophysin is involved in SV recycling

Overexpression of the C-terminus of synaptophysin inhibits SV endocytosis 2.5 times more effectively than overexpression of full length synaptophysin (fig 4.5A). This correlates well with the injection of the C-terminus into the giant squid axon where a block of endocytosis was also observed (Daly et al. 2000). They postulated that a clathrin-independent form of endocytosis had been inhibited since they saw an increase in the number of clathrin-coated vesicles away from the active zone, with uncoated vesicles directly behind them. The increase in coated vesicles was said to result from a block in clathrin-independent endocytosis resulting in a shift to fully clathrin-dependent endocytosis, thus increasing the number of coated vesicles observed. This block in endocytosis could also be explained by a block in SV uncoating. To delineate between these two possibilities the FM2-10 internalisation assay (see chap 5.2) could be used. This assay can differentiate between a block in SV retrieval and a block following scission of the SV, for example during uncoating or vesicle trafficking.

The SV turnover assay performed in this chapter only provides information about the total turnover of vesicles and not the method of retrieval but it is interesting to note that SV endocytosis was not completely inhibited (fig 4.3B and D and fig 4.5A) and so could reflect another functional recycling pathway which was unaffected by synaptophysin. The $Syp_{257-274}$ peptide, similarly, did not completely inhibit SV endocytosis, even at higher concentrations (fig 4.7B and C). Thus synaptophysin may be central to one SV recycling pathway but not another.

Ca^{2+}-dependent interactions of synaptophysin

Dynamin I was extracted from a pulldown assay using the C-terminus of synaptophysin in a Ca^{2+}-dependent manner (fig 4.8 – 10), agreeing with Daly and Ziff (2002). However, another band of higher molecular weight identified as amphiphysin I was also extracted (fig 4.8 – 10). The difference between the proteins extracted in this chapter and those from Daly and Ziff (2002) may be due to differences in lysis buffers, since the lysis buffer used in this thesis contained three times as much salt as that used by Daly and Ziff. This may have created a different electrostatic environment and be responsible for the discrepancy. Another possible explanation is that the GST tags were on different ends of the C-terminus of synaptophysin. The construct used by Daly and Ziff (2002) had the GST-tag N-terminal to the synaptophysin sequence and the construct used here was C-terminally tagged. The tag being on the different end of the coding sequence may have masked part of the binding site and therefore extracted less from the synaptosome lysate.

Daly and Ziff (2002) commented that they had been unable to reconstitute a Ca^{2+}-dependent interaction between the C-terminus of synaptophysin and purified dynamin I and postulated that this was due to the absence of another protein present in the lysate which aided this interaction. The data in this chapter points to amphiphysin I as having a potential role here since it was extracted in a Ca^{2+}-dependent manner from a Syp C-term-GST pulldown assay. Purified amphiphysin I can also bind to the C-terminus of synaptophysin *in vitro* (fig 4.12 – 4.13), supporting this idea.

However, the Syp C-term-GST pulldown assay in the presence of the $DynI_{832-840}$ peptide suggests that dynamin I and amphiphysin I can bind independently to the C-terminus of synaptophysin (fig 4.11) and so perhaps all three proteins are part of a larger complex. This could be tested using *in vitro* binding assays with all three proteins. An *in vivo* method to test this hypothesis employs fluorescence resonance energy transfer (FRET) by fluorescently labelling the proteins in pairs and monitoring the FRET signal (Pennuto et al. 2002). If dynamin I and amphiphysin I do bind independently of one another, each should produce a FRET signal with synaptophysin.

Amphiphysin I and synaptophysin can bind Ca^{2+}

In order to gain insight into the mechanism of the dynamin I-synaptophysin and amphiphysin I-synaptophysin interactions, the ability of the proteins to bind Ca^{2+} was analysed. The PRD of dynamin I did not bind Ca^{2+} (fig 4.15) which is interesting because full length dynamin I bound Ca^{2+} and digestion of the C-terminal tail prevented this (Liu et al. 1996). It is possible that the C-terminal PRD requires another part of the molecule to form part of the binding site for Ca^{2+}.

Full length His-tagged amphiphysin I and the GST-SH3 domain of amphiphysin I bound Ca^{2+} in the $^{45}Ca^{2+}$ overlay assay (fig 4.15). The Syp C-term-GST also bound Ca^{2+} (fig 4.15) in agreement with previous experiments using the same $^{45}Ca^{2+}$ overlay assay (Rehm et al. 1986). However, another study that investigated Ca^{2+} binding using equilibrium dialysis showed that synaptophysin did not bind Ca^{2+} (Brose et al. 1992). The implication of this is that if synaptophysin does not bind

Ca^{2+} then dynamin I and amphiphysin I must. Both dynamin I and amphiphysin I can potentially bind Ca^{2+} although in light of the conflicting Ca^{2+} binding results for synaptophysin, further experiments using different techniques, such as a gel retardation assay (Liu et al. 1996), a change in intrinsic tryptophan or tyrosine fluorescence upon Ca^{2+} binding or equilibrium dialysis (Vogel 2002) will be necessary to confirm the Ca^{2+} binding ability of any of the proteins. It is also interesting to note that although the amphiphysin SH3 domain can bind Ca^{2+} (fig 4.15), synaptophysin does not bind to the SH3 domain (fig 4.14). Perhaps the binding of Ca^{2+} to the SH3 domain causes a conformation change unmasking the synaptophysin binding site. Certainly the SH3 domain of amphiphysin I has been postulated to bind back on itself to bind the central PRD (Farsad et al. 2003), and thus Ca^{2+} binding may open up the amphiphysin molecule enabling binding to synaptophysin. This could be investigated further by using a truncated version of amphiphysin lacking the SH3 domain and determining whether or not synaptophysin can still interact with amphiphysin and if so, if the interaction remains Ca^{2+} dependent.

What is the role of the dynamin I and amphiphysin I Ca^{2+} regulated interactions with synaptophysin?

Synaptophysin has been implicated in several stages of the vesicle lifecycle from the biogenesis of vesicles to fusion of vesicles with the plasma membrane (Valtorta et al. 2004). This chapter shows evidence that synaptophysin has a role in SV endocytosis and that it is mediated by Ca^{2+}-dependent interactions with dynamin I and/or amphiphysin I.

Synaptophysin is involved with the targeting of synaptobrevin to SVs (Pennuto et al. 2003). In the presence of Ca^{2+} synaptobrevin no longer binds to synaptophysin and therefore sets up the possibility that synaptophysin could be involved in the delivery of synaptobrevin to the SNARE complex for exocytosis (Daly and Ziff 2002). Following dissociation from synaptobrevin, synaptophysin would be able to bind to dynamin I and amphiphysin I and recruit these endocytosis proteins to the sites of SV retrieval (Valtorta et al. 2004). However, stimulation increases the formation of synaptophysin-synaptobrevin multimers (Khvotchev and Sudhof 2004) and thus it would be interesting to investigate if dynamin I and amphiphysin I can bind to these multimers or if these complexes are mutually exclusive.

The dynamin I-synaptophysin interaction also occurs only at high concentrations of Ca^{2+} (Daly and Ziff 2002). The implications of this are two-fold: firstly, dynamin I GTPase activity would be inhibited at these concentrations (Liu et al. 1996) and so fission of the vesicle neck would be unlikely and secondly, concentrations of Ca^{2+} high enough to promote these interactions would only occur at the active zone (Cousin 2000; Daly and Ziff 2002). This suggests that either synaptophysin serves to recruit dynamin I although the high Ca^{2+} would prevent endocytosis until after exocytosis was finished (Daly and Ziff 2002) or dynamin I and synaptophysin are involved in a clathrin independent form of endocytosis, such as 'kiss and run', which occurs at the active zone (Daly et al. 2000).

The role of amphiphysin I may be to serve as an adapter protein to recruit other cytosolic factors to the sites of endocytosis. Many proteins interact via SH3 domain

–PRD interactions (Slepnev and De Camilli 2000) and so amphiphysin I may recruit other proteins involved in endocytosis, regardless of the mode of endocytosis.

What is clear is that the most abundant SV protein, synaptophysin, may have several roles in SV trafficking including SV endocytosis as shown in this chapter and that dynamin I, and possibly amphiphysin I, function is regulated by Ca^{2+}.

CHAPTER 5

ROLE OF THE PHOSPHORYLATION OF SERINES 774 AND 778 IN DYNAMIN I FUNCTION

5.1 Introduction

The dephosphins (dynamin I, amphiphysin I, amphiphysin II, AP180, eps15, epsin, synaptojanin I and PIPKIγ) are essential for the formation and scission of SVs in endocytosis (Cousin and Robinson 2001). The dephosphins undergo a cycle of phosphorylation where they are co-ordinately dephosphorylated upon nerve terminal stimulation by the Ca^{2+}/calmodulin-dependent phosphatase, calcineurin, and following termination of stimulation, are rephosphorylated by their endogenous kinases to reset the system (Cousin and Robinson 2001). Dephosphorylation and the rephosphorylation of the dephosphins are both essential for further rounds of SV endocytosis to occur (Cousin and Robinson 2001).

Calcineurin dephosphorylates all of the dephosphins and is essential for SV endocytosis (Marks and McMahon 1998; Cousin and Robinson 2001). There is not an equivalent kinase which re-phosphorylates all of the dephosphins after stimulation, however. Cdk5 activity is essential for the maintenance of SV endocytosis and although many of the dephosphins, for example amphiphysin, are *in vitro* substrates (Chen et al. 1999; Floyd et al. 2001; Tomizawa et al. 2003) only dynamin I, synaptojanin and PIPKIγ so far appear to be *in vivo* substrates (Tan et al. 2003; Lee et al. 2004).

The *in vivo* phosphorylation sites for dynamin I have been identified by mass spectrometry as serines 774 and 778 in the PRD (Tan et al. 2003; Larsen et al. 2004). These sites are dephosphorylated in intact nerve terminals in a stimulation dependent

manner and rephosphorylation of these sites can be inhibited by the selective Cdk5 inhibitor, roscovitine (Tan et al. 2003).

It is known that calcineurin and Cdk5 are essential for SV endocytosis but they act on multiple substrates. Therefore, the aim was to determine if the specific dephosphorylation and rephosphorylation of dynamin I was essential for SV endocytosis, and if so, investigating the mechanism of its control. To do this, phosphomimetic peptides against the *in vivo* phosphorylation sites of dynamin I were used. This chapter shows that a peptide mimicking dephosphorylated dynamin I was nearly four times more effective at inhibiting SV endocytosis than a peptide mimicking phosphorylated dynamin I, indicating that there is an essential role for these phosphorylation sites in endocytosis. Further experiments to probe the function of the phosphorylation sites identified the endocytosis protein syndapin I as a stimulation-dependent binding partner to this region. This interaction was investigated using GST-pulldown assays with the PRD of dynamin I, immunoprecipitations (IPs) with both dynamin I and syndapin I antibodies and complementary studies with the phosphomimetic peptides.

5.2 Calcineurin is essential for SV endocytosis and dephosphorylation of dynamin I on serines 774 and 778

Ca^{2+} influx through voltage-gated Ca^{2+}channels following nerve terminal stimulation acts as the signal for exocytosis at the active zone. In the endocytic zones adjacent to the active zone at the plasma membrane, the lower Ca^{2+} concentration acts as the trigger for calcineurin to dephosphorylate the dephosphins (Cousin 2000).

Cyclosporin A, a selective inhibitor of calcineurin, inhibits SV endocytosis (Marks and McMahon 1998; Cousin et al. 2001). This is confirmed in figure 5.1. Synaptosomes were pre-incubated for 15 min plus or minus extracellular Ca^{2+} and in the absence and presence of 40 μM cyclosporin A. SV turnover was measured first using the FM2-10 SV turnover assay (fig 5.1B). Cyclosporin A inhibited SV turnover by 70 % (29.8 % ± 10.8 % of control, fig 5.1A) in agreement with previous studies (Marks and McMahon 1998; Cousin et al. 2001).

The effect of cyclosporin A on exocytosis was determined using the glutamate release assay. Cyclosporin A had no significant effect on Ca^{2+}-dependent glutamate release (104.2 % ± 17.2 % of control, fig 5.1C), again, in agreement with previous studies (Nichols et al. 1994; Marks and McMahon 1998; Cousin et al. 2001; Baldwin et al. 2003).

A more accurate method of quantifying the amount of endocytosis in these assays is by the parameter called the retrieval efficiency (SV turnover divided by exocytosis). The retrieval efficiency was calculated to be 0.3 ± 0.1 (fig 5.1D) and therefore cyclosporin A inhibited SV endocytosis.

Since the FM2-10 SV turnover assay uses unloading of dye to monitor endocytosis, it does not distinguish between an inhibition of SV retrieval from the plasma membrane or a subsequent trafficking defect before exocytosis. To delineate between these two possibilities an internalisation assay was used. It is a modified version of the SV turnover assay but instead of stimulating the release of

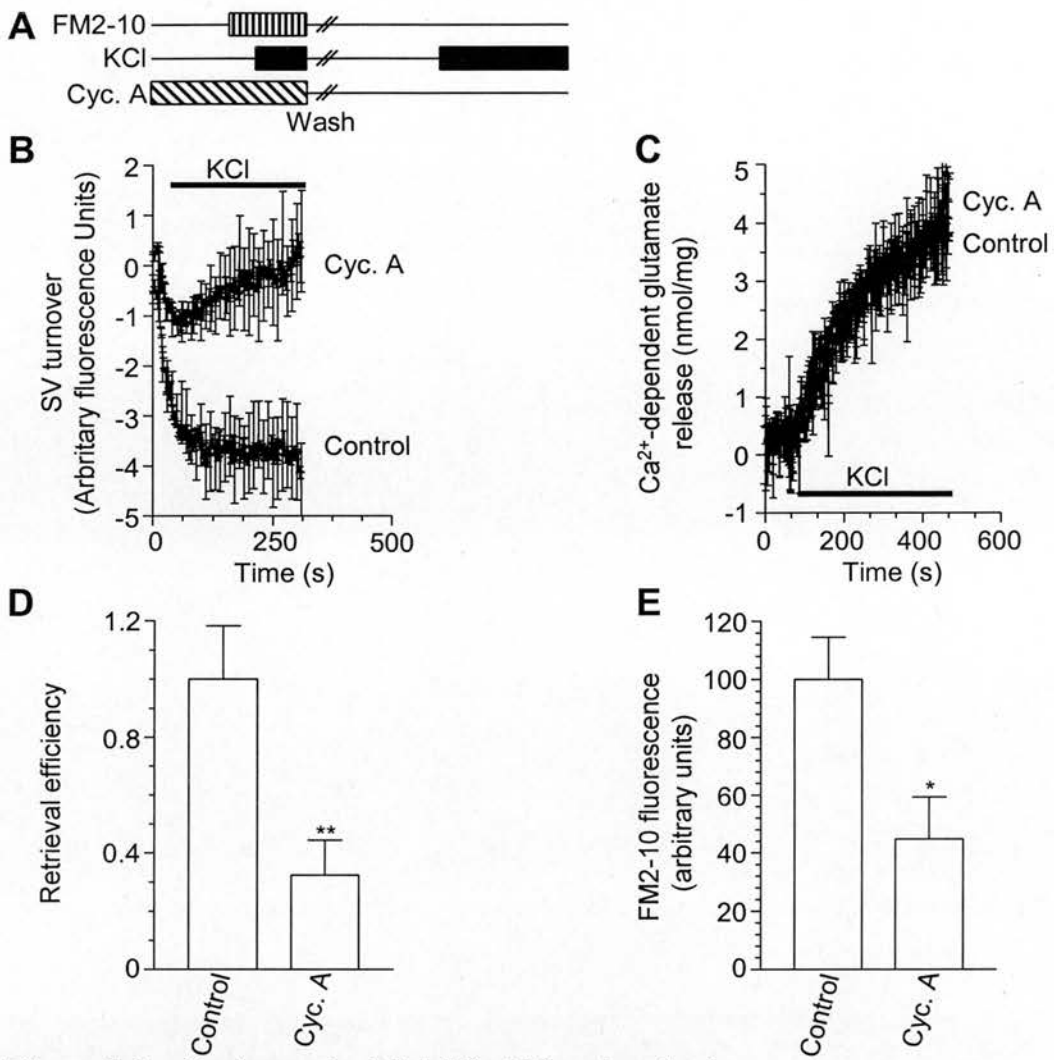

Figure 5.1 – Cyclosporin A inhibits SV endocytosis

(A) Protocol for SV turnover assay. **(B)** Ca^{2+}-dependent FM2-10 unloading from synaptosomes pre-incubated for 15 min plus or minus 40 µM cyclosporin A (Cyc. A) and stimulated with 30 mM KCl (n = 2 ± SD for all conditions). **(C)** Glutamate release from synaptosomes treated with or without 40 µM Cyc. A and stimulated with 30 mM KCl. Traces are Ca^{2+}-dependent (n = 3 ± SEM). In both **B** and **C** bar denotes KCl stimulation. **(D)** Retrieval efficiency for Cyc. A treated synaptosomes. Calculated from Ca^{2+}-dependent FM2-10 unloading divided by Ca^{2+}-dependent glutamate release after 2 min. Values are normalised to control. **(E)** Internalised fluorescence from control synaptosomes and synaptosomes treated with 40 µM Cyc. A for 15 minutes. Values are Ca^{2+}-dependent and normalised to control. (n ≥ 3 ± SEM) In **D** and **E** student's t test has been applied (*p < 0.05, **p < 0.01)

accumulated dye, the synaptosomes were hypotonically lysed following dye loading. The SVs were then crudely purified by centrifugation and the fluorescence of the supernatant, containing the SVs, measured. If there is no inhibition in this assay, then the observed inhibition of SV endocytosis (fig. 5.1B and D) would be due to a recycling defect. If there is an inhibition, then that indicates that there was a block in SV endocytosis prior to vesicle scission. Cyclosporin A inhibited dye uptake by 55 % (44.8 ± 14.5 %, fig 4.1E), confirming a block in SV endocytosis at the vesicle retrieval stage.

In order to gain insight as to which stage of SV retrieval was inhibited, the morphology of basal, stimulated and cyclosporin A-treated synaptosomes was examined by electron microscopy. Figure 5.2A shows a typical synaptosome under basal conditions full of SVs and a few dense core vesicles. It also has an intact plasma membrane and contains a mitochondrion. Figure 5.2B shows a synaptosome after a two minute stimulation with 30mM KCl. The overall morphology does not change from basal. Figure 5.2C shows a synaptosome after pre-incubation with 40μM cyclosporin A and a two minute stimulation with 30mM KCl. Extensive vesicle depletion can be seen and the absence of any intermediate vesicle profiles indicates a block early in endocytosis. This is consistent with inhibition of calcineurin.

The functional and morphological data in figures 5.1 and 5.2 have shown that calcineurin activity is required for endocytosis. The dephosphins, including

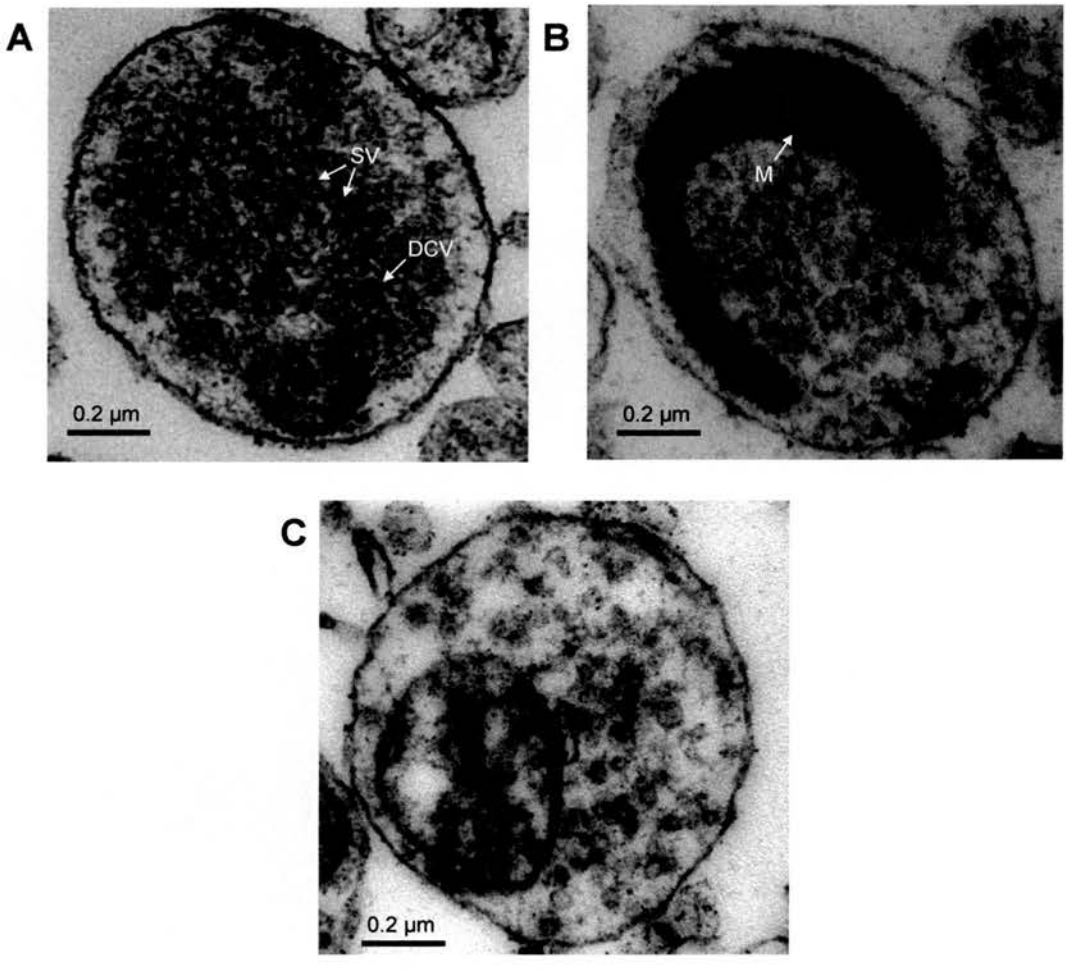

Figure 5.2 – Cyclosporin A inhibits SV endocytosis at an early stage

(A) Typical synaptosome under basal conditions. **(B)** Synaptosome after stimulation with 30 mM KCl for 2 min. **(C)** Synaptosome treated with 40 µM cyclosporin A and stimulated with 30 mM KCl for 2 min. Arrows indicate synaptic vesicles (SV), dense core vesicles (DCV) and a mitochondrion (M). Scale bar represents 0.2 µm. Pictures are representative of synaptosomes in the field.

dynamin I, are the substrates for calcineurin and therefore cyclosporin A should be able to block the dephosphorylation.

This has been shown using radiolabelled phosphate - in the presence of cyclosporin A the level of phosphorylated dynamin I did not decrease upon stimulation (Marks and McMahon 1998). The *in vivo* phosphorylation sites for dynamin I are serines 774 and 778 in the PRD (Tan et al. 2003; Larsen et al. 2004) and so using phosphospecific antibodies raised against these phosphorylated residues, the effect of cyclosporin A on dephosphorylation of these sites of dynamin I, specifically, was investigated. Lysates were made from basal and stimulated synaptosomes in the absence and presence of 40 μM cyclosporin A. The lysates were probed with phosphospecific antibodies to serines 774 and 778 (fig. 5.3). On depolarisation, phosphorylation decreases at both sites. In the presence of cyclosporin A this decrease is inhibited, showing that calcineurin is responsible for the dephosphorylation of the *in vivo* sites. The total amount of dynamin I in each condition is equal since probing with a pan dynamin I antibody shows no difference between the samples. Thus the decrease is not due to a lower level of dynamin I present in the stimulated sample. Since calcineurin activity is essential for SV endocytosis and the dephosphorylation of serines 774 and 778 by calcineurin can be inhibited by cyclosporin A, this implies a role for these phosphorylation sites in SV endocytosis.

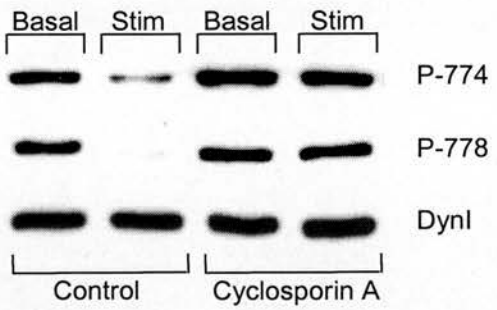

Figure 5.3 – Dynamin I is dephosphorylated by calcineurin at serines 774 and 778 upon depolarisation

Synaptosome lysates were blotted for total dynamin (DynI), phosphoserine 774 (P-774) and phosphoserine 778 (P-778). Lysates were prepared from either basal or stimulated (30 mM KCl) synaptosomes ± 15 min preincubation with 40 μM cyclosporin A as indicated.

5.3 SV endocytosis is inhibited by phosphomimetic peptides encompassing the dynamin I phosphorylation sites

The role of the phosphorylation status of the individual dephosphins is unknown and cannot be investigated using drugs or methods which inhibit or interfere with calcineurin or Cdk5 because both have multiple substrates. To investigate the role of dynamin I phosphorylation specifically, phosphomimetic peptides were designed from the PRD of dynamin I which encompass the phosphorylation sites (fig 5.4). Serines 774 and 778 were substituted with either alanine residues ($DynI_{769\text{-}784}AA$), to mimic dephosphorylated dynamin I, or glutamic acid residues ($DynI_{769\text{-}784}EE$), to mimic phosphorylated dynamin I. Both peptides have the penetratin sequence N-terminal to the dynamin I sequence to facilitate entry into the cytosol of the synaptosomes (Chapter 3).

The effect of the phosphomimetic peptides on SV turnover was assayed using FM2-10 (fig 5.1A). Figure 5.5B shows the effect of different concentrations of the phosphomimetic peptides on SV turnover. The synaptosomes were pre-incubated with the peptides for 30 min prior to assaying. $DynI_{769\text{-}784}AA$ and $DynI_{769\text{-}784}EE$ cause a concentration-dependent inhibition of SV turnover. However, $DynI_{769\text{-}784}AA$ is much more potent than $DynI_{769\text{-}784}EE$ as demonstrated in Fig 5.5B. The concentration of 250 μM was selected since this highlighted the difference between the peptides. At 250 μM, $DynI_{769\text{-}784}AA$ inhibited SV turnover by 43 % (57.1 % ± 2 % of control) compared to 20 % (81.1 % ± 2.4 % of control) with $DynI_{769\text{-}784}EE$ (fig 5.5C). This data shows that both peptides inhibit SV turnover but that $DynI_{769\text{-}784}AA$ peptide does so more efficiently. At higher concentrations (500 μM) both peptides

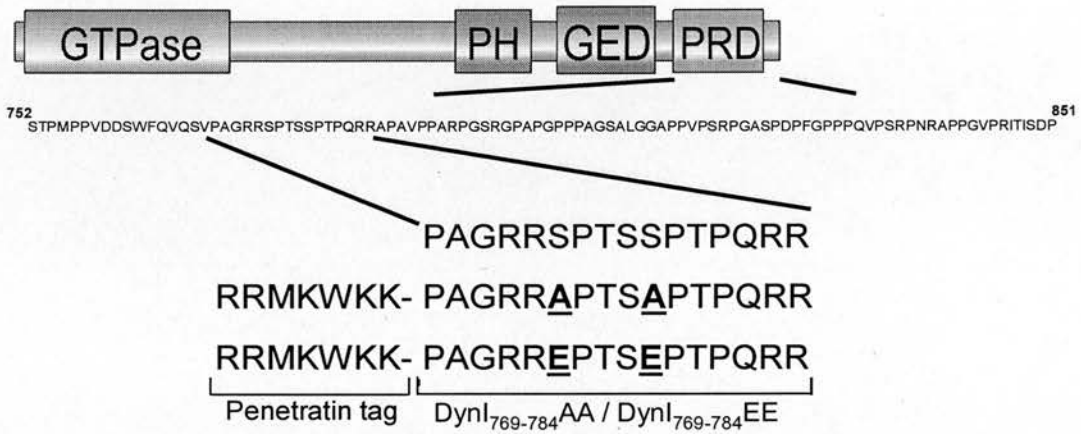

Figure 5.4 – Dynamin I structure and peptide design

Schematic of the domain structure of dynamin I showing the GTPase domain, pleckstrin homology (PH) domain, GTPase effector domain (GED) and the proline rich domain (PRD) with the sequence of the PRD in the single amino acid code. The expanded region shows the sequence from residues 769 – 784 of the PRD from which the phosphomimetic peptide sequences were based. The sequence of each of the peptides is shown including the N-terminal penetratin tag for delivery into the cytosol. Serines 774 and 778 were substituted to either alanine ($DynI_{769-784}AA$) or to glutamic acid ($DynI_{769-784}EE$).

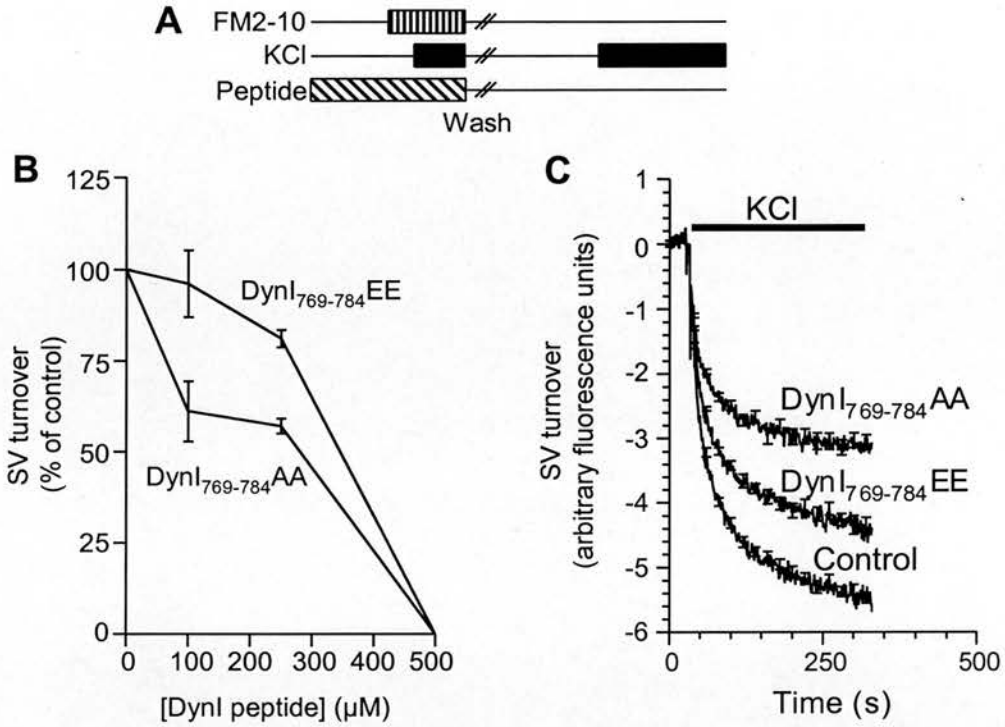

Figure 5.5 – $DynI_{769-784}AA$ and $DynI_{769-784}EE$ inhibit SV turnover in a concentration dependent manner

(A) Schematic illustrating the SV turnover assay protocol. **(B)** Synaptosomes were incubated ± peptide and ± Ca^{2+} for 30 minutes prior to FM2-10 loading. Ca^{2+}-dependent FM2-10 unloading (SV turnover), is displayed as a % of control, in response to a 2 min stimulation with 30 mM KCl ($n = 1$ for 500 μM traces, $n \geq 3 \pm$ SEM for 100 and 250 μM traces). **(C)** Average Ca^{2+}-dependent endocytosis traces for 250 μM $DynI_{769-784}AA$ or $DynI_{769-784}EE$ peptide, shown as data points in figure 5.5B. All curves are significantly different from each other ($p < 0.001$) as determined by two-way ANOVA using a Bonferroni post-hoc test ($n \geq 3 \pm$ SEM for all conditions). The bar denotes the presence of KCl.

abolish SV turnover indicating the essential requirement for this region of the PRD in SV endocytosis.

Glutamate release was used to monitor the effect of the phosphomimetic peptides on exocytosis. Both peptides inhibited glutamate release to a small but non-significant extent ($DynI_{769\text{-}784}AA$ was 92.5 ± 8.4 % of control and $DynI_{769\text{-}784}EE$ was 90.2 ± 9.5 % of control, fig 5.6A), indicating that the inhibition of SV turnover (fig 5.5C) was not an indirect effect of an inhibition in exocytosis.

Another method of measuring exocytosis uses a modified version of the FM2-10 SV turnover assay (fig 5.6B). Instead of pre-incubating synaptosomes with peptides and then loading with dye, the synaptosomes are loaded with a standard 30 mM KCl stimulus and then incubated with the peptides for 30 min before unloading. This protocol ensures that endocytosis is unaffected by peptide addition and thus any effect on exocytosis will be reflected in the amount of released dye during the second stimulus. Interestingly, both peptides showed a significant inhibition of exocytosis of approximately 20 % ($DynI_{769\text{-}784}AA$ – 81.1 ± 4.1 % of control and $DynI_{769\text{-}784}EE$ – 82.3 ± 4.2 % of control, fig 5.6C). This suggests the PRD of dynamin I may also play a role in exocytosis.

The SV turnover assay has two exocytosis steps – one to stimulate dye loading (S1) and a second to release the loaded dye (S2, see protocol in fig 5.1A). The previous two experiments estimate the amount of glutamate and FM2-10 (fig 5.6A and fig 5.6C respectively) released during S1 stimulation. An important control, however, is

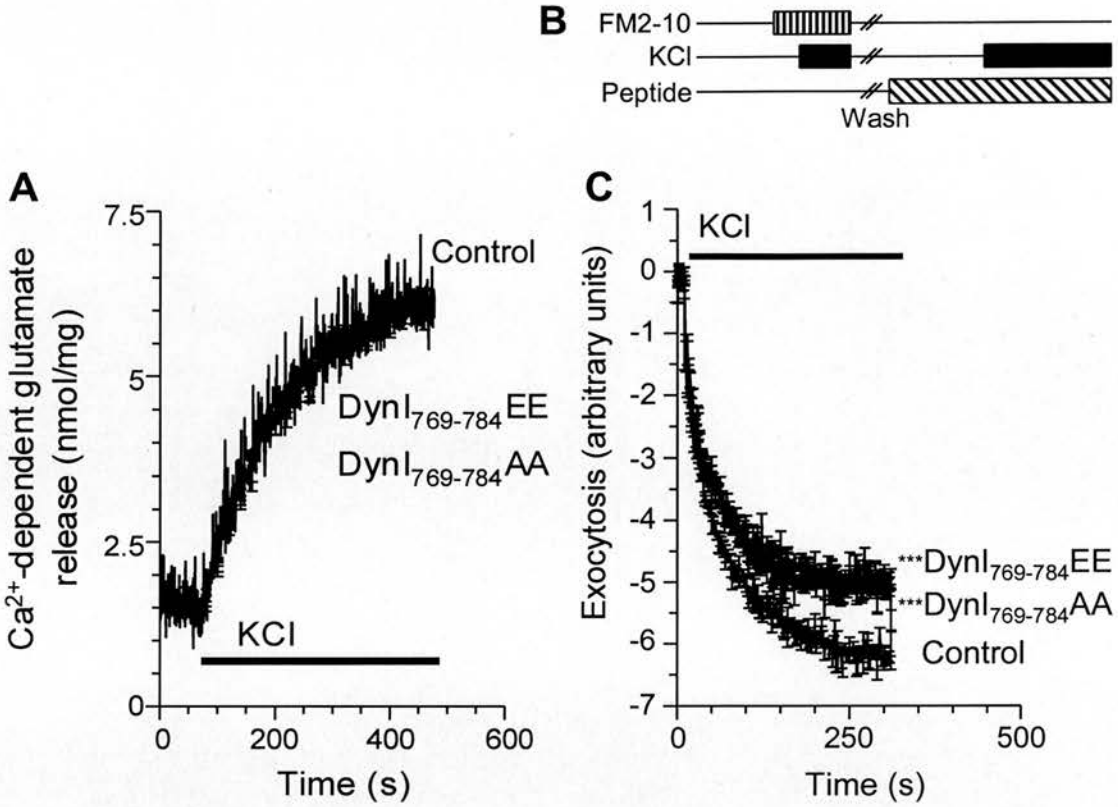

Figure 5.6 - $DynI_{769-784}AA$ and $DynI_{769-784}EE$ do not affect glutamate release but inhibit FM2-10 unloading

(A) Synaptosomes were preincubated ± 250 µM of either peptide and ± Ca^{2+} for 30 minutes prior to assaying. Ca^{2+}-dependent glutamate release from control or peptide treated synaptosomes stimulated with 30 mM KCl is displayed ($n \geq 3$ ± SEM for all conditions). **(B)** The schematic represents the FM2-10 exocytosis assay protocol. **(C)** Synaptosomes were loaded with FM2-10 using a 30 mM KCl stimulation for 2 min. The synaptosomes were then incubated for 30 min at 37°C ± 250 µM of either $DynI_{769-784}AA$ or $DynI_{769-784}EE$. Exocytosis was measured by the fluorescence released upon stimulation with another 30 mM KCl stimulation. Peptide traces are both significantly different to the control trace (***$p < 0.001$) as determined by two-way ANOVA using a bonferroni post-hoc test ($n \geq 3$ ± SEM for all conditions). Bar denotes presence of KCl in both A and C.

to measure exocytosis at S2, since inhibition at this stage would impact on the turnover readout. Neither peptide showed any significant effect on glutamate release (fig 5.7A) at S2, confirming that the inhibition of SV turnover observed with $DynI_{769-784}AA$ was due to a block in SV endocytosis.

To more accurately quantify the amount of endocytosis in these assays retrieval efficiency was calculated (amount of SV turnover divided by the amount of exocytosis). When this value is calculated using glutamate release as a measure of exocytosis, $DynI_{769-784}AA$ is nearly 4 times more effective at inhibiting SV endocytosis (fig 5.7B) than $DynI_{769-784}EE$ (0.62 ± 0.01 for $DynI_{769-784}AA$ and 0.90 ± 0.01 for $DynI_{769-784}EE$). Retrieval efficiency can also be calculated using the FM2-10 exocytosis assay. Using these values the retrieval efficiency for $DynI_{769-784}AA$ is 0.71 ± 0.03 and the retrieval efficiency for $DynI_{769-784}EE$ is not significantly different from control (0.99 ± 0.03), again emphasizing the selectivity of $DynI_{769-784}AA$ compared to $DynI_{769-784}EE$.

To determine at which stage of SV recycling the phosphomimetic peptides were acting, the amount of FM2-10 incorporated into vesicles was measured using the SV internalisation assay. $DynI_{769-784}AA$ produced an inhibition of 35 % (64.9 ± 5.5 % of control) where as $DynI_{769-784}EE$ did not significantly block dye internalisation (90.7 ± 7.1 % of control, fig 5.8). This confirms that $DynI_{769-784}AA$ inhibits the process of SV endocytosis whereas $DynI_{769-784}EE$ has little effect. Taken together these results show that phosphorylation of serines 774 and 778 on dynamin I is essential for its

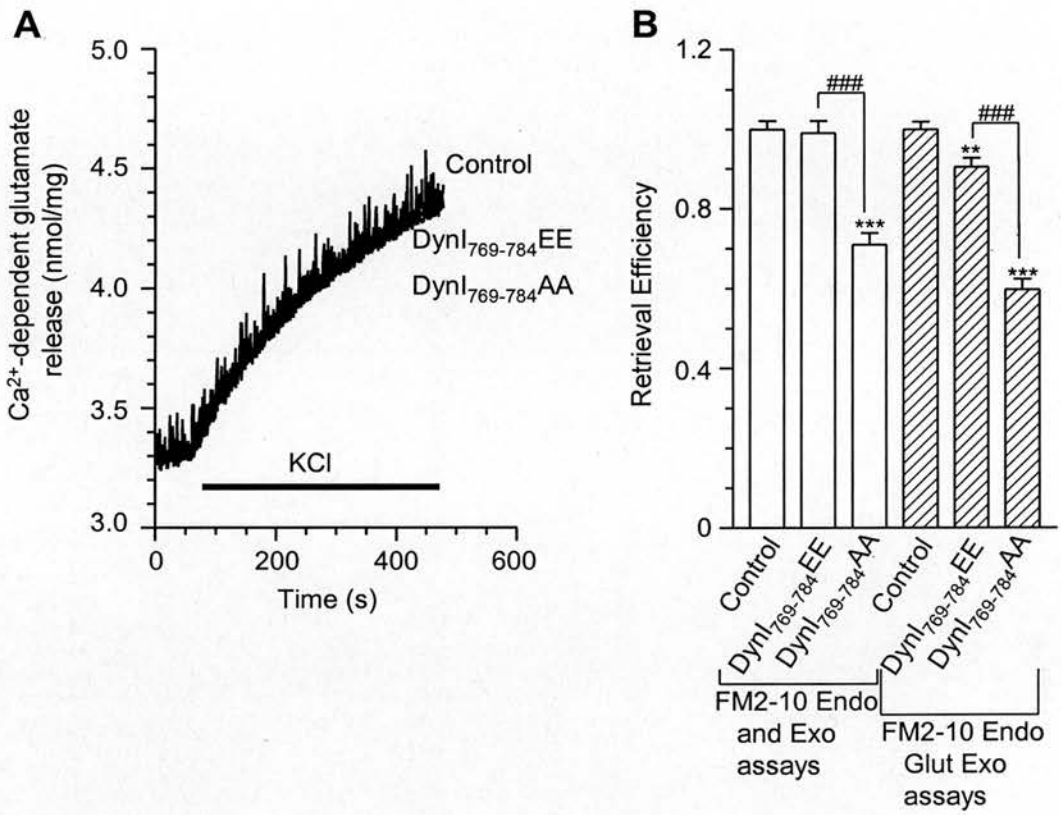

Figure 5.7 - Dynl$_{769-784}$AA significantly inhibits SV endocytosis

(A) Glutamate release from synaptosomes pre-incubated ± 250 μM Dynl$_{769-784}$AA or Dynl$_{769-784}$EE and stimulated twice with 30 mM KCl. Trace represents the S2 stimulus (n = 1 for all conditions). Bar denotes presence of KCl. **(B)** Retrieval efficiency calculated as the amount of endocytosis, from figure 5.5C, divided by the amount of exocytosis after 2 min of stimulation from figure 5.6. Open bars show retrieval efficiency calculated using the FM2-10 exocytosis assay (fig 5.6C). Hashed bars show retrieval efficiency calculated using the glutamate release exocytosis assay (fig 5.6A). One-way ANOVA was applied (*p values are compared to control, #p values are compared to each other. **$p < 0.01$, ***$p < 0.001$ and ###$p < 0.001$).

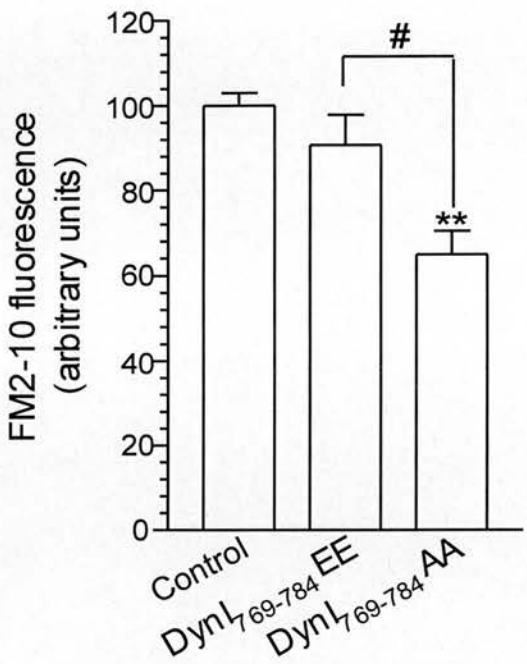

Figure 5.8 – $DynI_{769-784}AA$ inhibits SV endocytosis not trafficking

Synaptosomes pre-incubated with 250 µM of either $DynI_{769-784}AA$ or $DynI_{769-784}EE$ were loaded as in the FM2-10 SV turnover assay, before being hypotonically lysed. The SVs were crudely purified and the fluorescence measured. Fluorescence values are Ca^{2+}-dependent and normalised to control (n = 3). One-way ANOVA was applied (**P<0.01 compared to control, #P<0.05 $DynI_{769-784}AA$ compared to $DynI_{769-784}EE$.)

function in SV endocytosis and that the $Dyn_{769\text{-}784}AA$ peptide acts in a dominant negative manner.

5.4 Effect of cyclosporin A and the phosphomimetic peptides on SV turnover stimulated by different mechanisms

KCl stimulation operates by producing a clamped depolarisation of the plasma membrane and thus increasing the probability of opening the voltage dependent Ca^{2+} channels causing a localised Ca^{2+} increase at active zones (Cousin and Robinson 2000b). However, exocytosis can be stimulated by different mechanisms. The potassium channel antagonist 4-aminopyridine (4-AP) works by increasing the excitability of the plasma membrane. The compound inhibits K_A^+ channels in the plasma membrane which usually correct spontaneous depolarisations and prevent the action potential reaching threshold. When blocked the spontaneous depolarisations are not compensated for, leading to the propagation of repetitive action potentials (Tibbs et al. 1996; Cousin and Robinson 2000b; Baldwin et al. 2003). Inhibition of dephosphorylation by cyclosporin A had little effect on KCl stimulated glutamate release (fig 5.1C), but can potentiate glutamate release stimulated with 1 mM 4-AP (Nichols et al. 1994; Sihra et al. 1995; Baldwin et al. 2003). This was confirmed by measuring glutamate release stimulated by 1 mM 4-AP following incubation with 40 μM cyclosporin A (fig 5.9A). Cyclosporin A increased glutamate release by 60.1 ± 7.6 %, illustrating that different methods of stimulation evoke different responses in the same system.

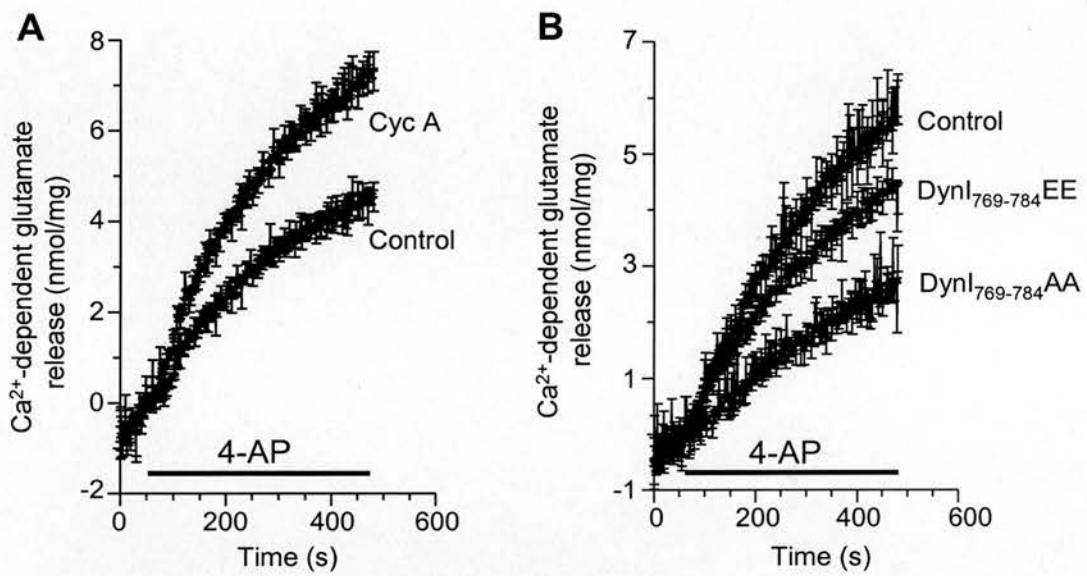

Figure 5.9 – Effect of cyclosporin A and the phosphomimetic peptides on synaptosomes stimulated with 4-AP

(A) Ca^{2+}-dependent glutamate release from control synaptosomes and synaptosomes pre-incubated with 40 µM cyclosporin A (Cyc. A) for 15 min and stimulated with 1 mM 4-aminopyridine (4-AP) ($n \geq 3 \pm$ SEM). Traces are significantly different as determined by two-way ANOVA ($p > 0.001$) **B)** Synaptosomes were pre-incubated for 30 min with 250 µM of either $DynI_{769\text{-}784}AA$ or $DynI_{769\text{-}784}EE$ and stimulated with 1 mM 4-AP. Ca^{2+}-dependent glutamate released was then measured ($n \geq 3 \pm$ SEM). All conditions are statistically significant ($p > 0.001$) as determined by a two-way ANOVA. In **A** and **B** the bar denotes the presence of 4-AP.

Since cyclosporin A enhanced glutamate release stimulated by 4-AP, the effect of the phosphomimetic peptides were also investigated to see if the effect was due to dynamin I dephosphorylation. Both peptides inhibited 4-AP stimulated exocytosis, with the $DynI_{769\text{-}784}AA$ peptide being more effective than the $DynI_{769\text{-}784}EE$ peptide (fig 5.9B). $DynI_{769\text{-}784}AA$ inhibited glutamate release by 53 % (47.0 ± 6.1 % of control) and $DynI_{769\text{-}784}EE$ by 25 % (75.4 ± 8.0 % of control), thus illustrating that this region of dynamin I and its phosphorylation status has an essential, but possibly different role, in vesicle recycling when stimulation is evoked by 4-AP compared to KCl.

5.5 Identification of a binding partner for residues 769-784 of dynamin I

The functional data shows that there is an essential role for residues 769-784 of the PRD of dynamin I in SV endocytosis and that the phosphorylation status of serines 774 and 778 is important in the regulation of SV turnover. Since the $DynI_{769\text{-}784}AA$ peptide showed significant inhibition of SV turnover and the $DynI_{769\text{-}784}EE$ peptide had very little effect (fig 5.5 – 5.9), this implies that the $DynI_{769\text{-}784}AA$ peptide is binding to another protein and inhibiting a protein-protein interaction crucial for SV recycling. Thus the $DynI_{769\text{-}784}AA$ peptide was chosen to be used as bait in a pulldown assay, from synaptosome lysates, to identify any binding partners of this region of dynamin I in its dephosphorylated state.

To make a $DynI_{769\text{-}784}AA$ column the peptide was N-terminally tagged with biotin instead of penetratin to enable coupling to streptavidin conjugated sepharose beads. Basal and stimulated synaptosome lysates were incubated with streptavidin beads in

the absence and presence of the biotinylated peptide. The beads were washed and bound proteins eluted and separated by SDS-PAGE. To increase the sensitivity the gel was silver stained (fig 5.10). A number of non-specific bands were apparent on the gel and in the presence of the peptide several bands disappear, but in lane 4 (stimulated lysate plus biotinylated peptide) an extra band at approximately 60 kDa was seen (p60). Thus a candidate binding partner was identified.

To decrease the amount of non-specific binding and therefore increase the likelihood of finding a genuine interaction, the peptide pulldown assay was modified to use Sulpholink® beads. The beads covalently couple to cysteine-tagged peptides and the remaining unbound sites on the beads can be blocked with free cysteine, therefore reducing non-specific binding to the beads. $DynI_{769\text{-}784}AA$ was N-terminally tagged with a cysteine residue and coupled to the beads. As before, basal and stimulated synaptosomes lysates were incubated with the beads in the absence and presence of the cysteine-tagged $DynI_{769\text{-}784}AA$. Proteins eluted from the column were separated by SDS-PAGE and silver stained (fig 5.11A). There was much less non-specific binding evident compared to the biotinylated method (fig 5.10) and again, there were bands which only appeared in the stimulated lysate plus peptide lane. This time there were two bands at approximately 60 kDa (i and ii on the gel, fig 5.11A). In an attempt to identify the bands they were cut out and sent for MALDI-TOF analysis. Unfortunately, after multiple attempts, the bands were unable to be identified using this approach.

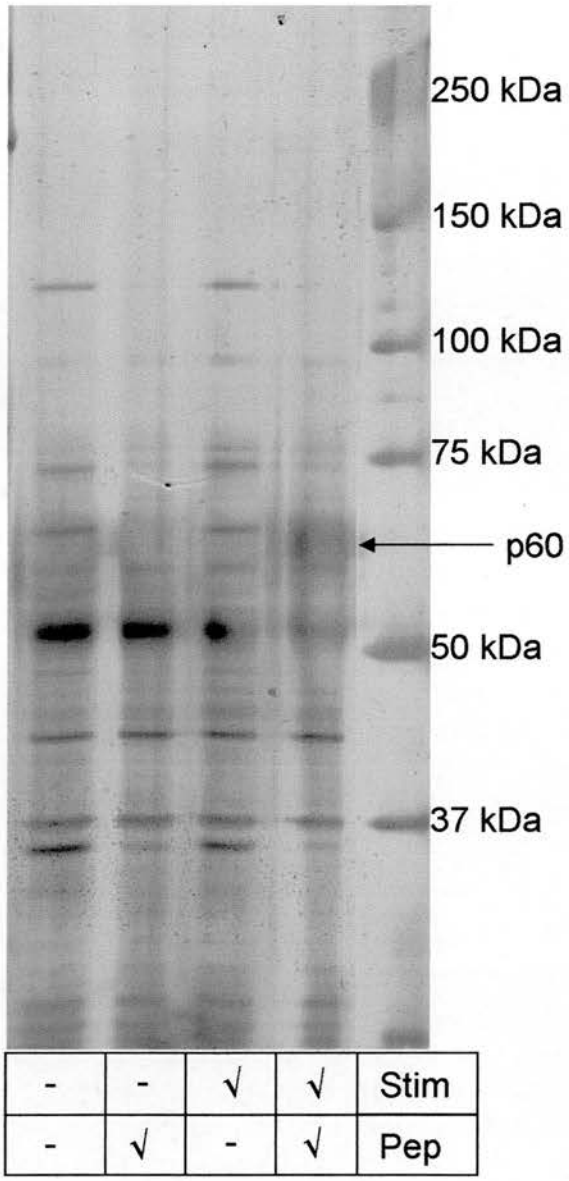

Figure 5.10 – Protein extracted from synaptosome lysate with biotinylated $Dynl_{769-784}AA$

N-terminal biotinylated $Dynl_{769-784}AA$ peptide was coupled to steptavidin sepharose beads. Synaptosome lysates either basal (lanes 1 + 2) and stimulated (lanes 3 + 4) were incubated with either streptavidin beads alone (lanes 1 + 3) or with steptavidin beads plus peptide (lanes 2 + 4). The eluted bound protein samples were run on a 7–15% acrylamide gradient gel which was subsequently silver stained. Arrow indicates an additional band at approximately 60 kDa in the stimulated lysates plus peptide lane. Experiment n =1.

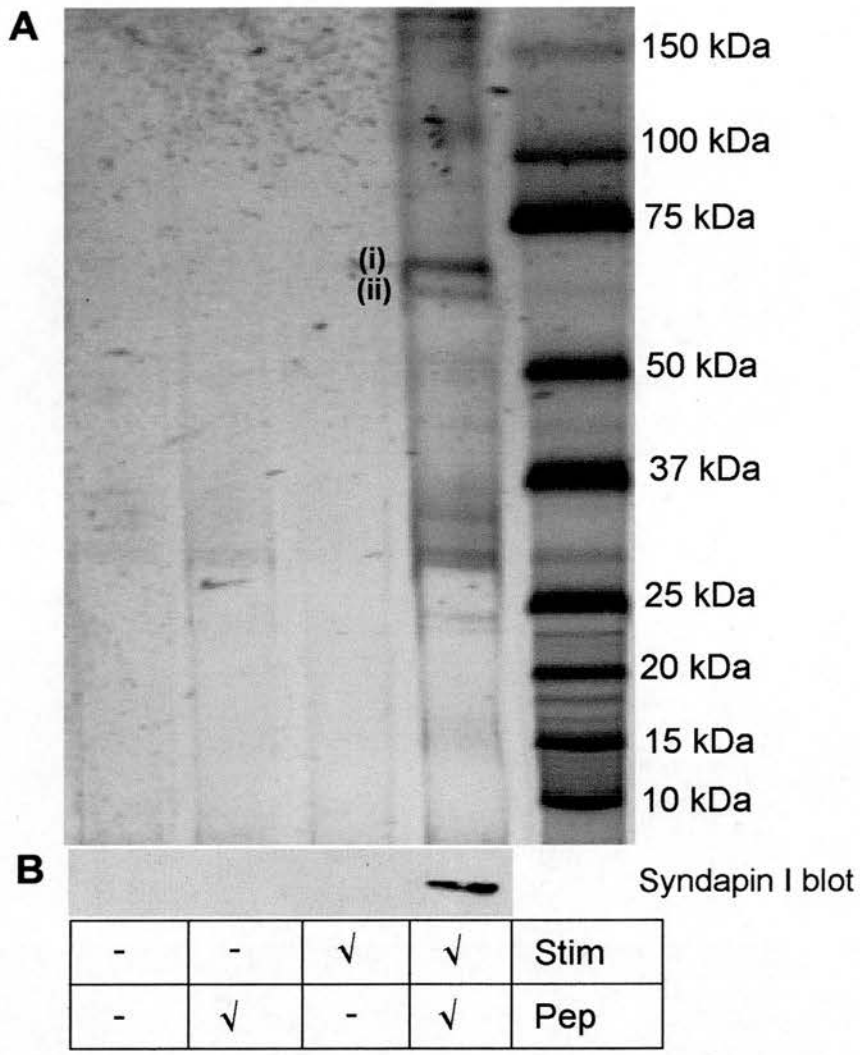

Figure 5.11 – Syndapin I extracted from synaptosome lysates by Cys-Dynl$_{769-784}$AA

Basal (lanes 1 + 2) and stimulated (lanes 3 + 4) synaptosome lysates were incubated with Sulpholink® beads alone (lanes 1 + 3) and with Sulpholink® beads which had been coupled to cys-Dynl$_{769-784}$AA peptide (lanes 2 + 4). The eluted bound proteins were run on a precast 8-16% gradient gel and silver stained **(A)** or blotted with anti-syndapin I antibody **(B)**. Bands i and ii were sent for MALDI-TOF analysis but were unable to be identified. Gel and blot representative of 3 and 2 replicates respectively.

A search of the literature for proteins involved in endocytosis with a molecular weight of approximately 60 kDa yielded very few proteins - most are over 90 kDa. Syndapin I, however, is a 55 kDa protein thought to function as a link between the endocytic machinery and the actin cytoskeleton (Qualmann et al. 1999; Slepnev and De Camilli 2000). It is expressed only in the brain and contains a C-terminal SH3 domain known to bind to dynamin I, synaptojanin and N-WASP (Qualmann et al. 1999). The SH3 domain of syndapin I has also been shown to inhibit receptor-mediated endocytosis suggesting an essential role in the process (Qualmann and Kelly 2000). Syndapin I, therefore, seems like a likely candidate for the binding partner of the $DynI_{769\text{-}784}AA$ peptide seen in both the biotinylated peptide and the cysteine-tagged peptide pulldown assays. Some of the remaining cysteine-tagged peptide pulldown assay samples were transferred to nitrocellulose and blotted for syndapin I (fig 5.11B). The only lane which gave a positive result with the syndapin I antibody was the stimulated lysate plus peptide lane. Thus the protein, p60, which bound the $Dyn_{769\text{-}784}AA$ peptide, may be the essential endocytic protein syndapin I.

5.6 $DynI_{769\text{-}784}AA$ increases protein binding to the PRD of dynamin I rather than inhibiting it

The PRD of dynamin I is responsible for many protein-protein interactions and is the region implicated in the binding to syndapin I (Qualmann et al. 1999). To confirm that the $DynI_{769\text{-}784}AA$ peptide disrupts syndapin I-dynamin I interactions, competitive assays were performed. If syndapin I did bind to dynamin I at residues 769 - 784, binding should be competed off with increasing concentrations of peptide. The PRD fused to GST was expressed in BL21 competent cells and coupled to

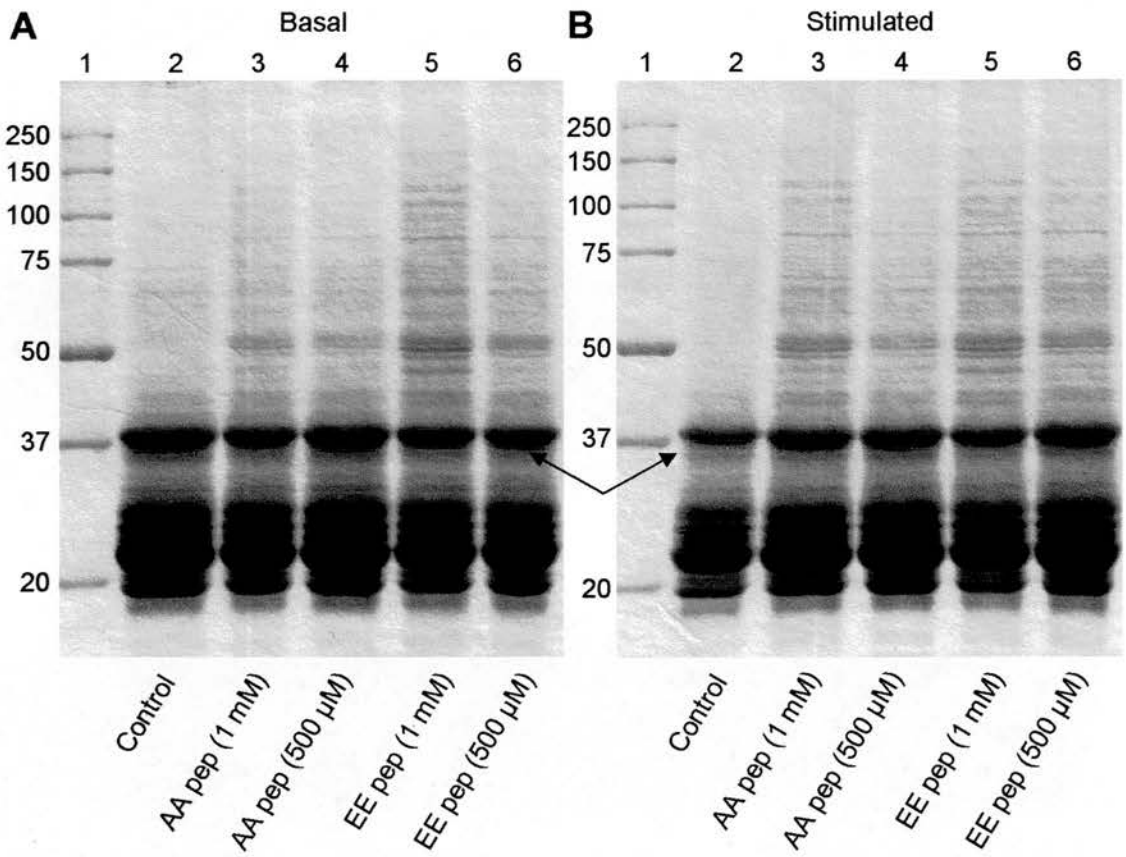

Figure 5.12 – Both peptides increase the total amount of protein binding to the PRD of dynamin I from basal and stimulated synaptosome lysates

Basal **(A)** or stimulated **(B)** synaptosome lysates were incubated with GSH beads coupled to GST-PRD and the indicated concentration of $DynI_{769\text{-}684}$AA (lanes 3 and 4, both gels) or $DynI_{769\text{-}784}$EE (lanes 5 and 6, both gels). Samples were separated by SDS-PAGE (10% gel) and coomassie stained. Arrows indicate the GST-PRD fusion protein. Representative of n =2 samples.

glutathione sepharose (GSH) beads. This fusion protein binds many endocytic proteins (Slepnev *et al*, 1998). Basal (fig 5.12A) and stimulated (fig 5.12B) synaptosome lysates were incubated with the indicated concentrations of $DynI_{769-784}AA$ and $DynI_{769-784}EE$ peptides before incubation with the GST-PRD column. Proteins retained on the column were separated by SDS-PAGE. Both peptides increased total amount of protein bound, rather than specifically reducing the interaction of a particular protein. There was no difference in the binding between basal lysates and stimulated lysates but the amount of binding appears to be concentration dependent with more binding the greater the concentration of either peptide.

To confirm that the increase in binding was of endocytic proteins and not non-specific binding, some of the samples were western blotted for syndapin I and amphiphysin I (fig 5.13). Both proteins show an increase in binding with the addition of either peptide confirming the amount of endocytosis proteins bound to GST-PRD were increased. All the samples have equal amounts of GST-PRD and so an increase in GST protein does not account for the increase in global binding.

5.7 Dynamin I interacts with syndapin I in a stimulation dependent manner *in vivo*

Pulldown assays are an excellent method to investigate protein interactions but are an *in vitro* assay. To determine whether dynamin I and syndapin I interact *in vivo* in nerve terminals, immunoprecipitations (IPs) were used.

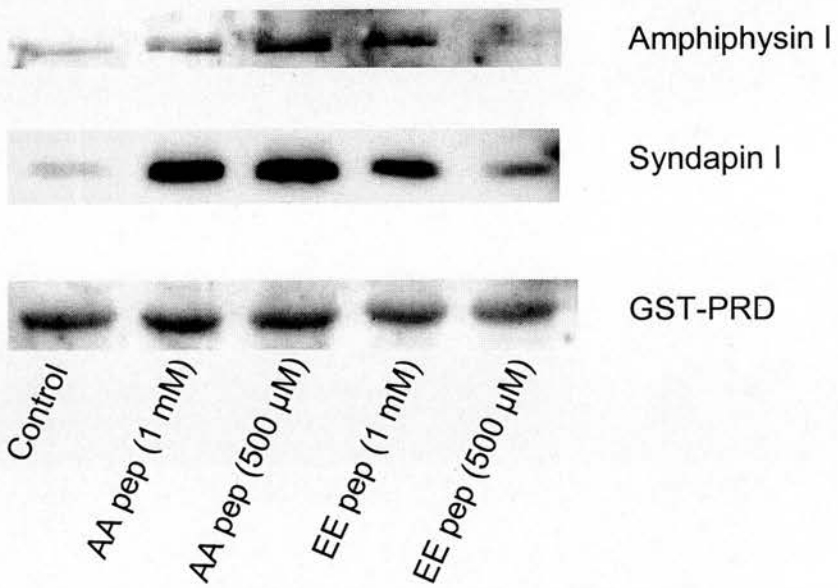

Figure 5.13 – Both peptides increase amount of syndapin I and amphiphysin I bound to dynamin I GST-PRD

Stimulated samples treated as for figure 5.12 were western blotted and probed for syndapin I and amphiphysin I. Both show an increase in binding with the addition of peptide. Amount of GST-PRD shown from cross-reaction of secondary antibody. Experiment n =1.

Reciprocal IPs were carried out using antibodies against dynamin I and syndapin I. The antibodies were incubated with basal and stimulated synaptosome lysates and the samples blotted for dynamin I and syndapin I (fig 5.14A). When the IP was carried out using dynamin I antibodies, similar amounts of syndapin I was extracted regardless of stimulation. However, when syndapin I was immunoprecipitated, the amount of dynamin I extracted increased in the stimulated lysate samples. The amount of primary protein immunoprecipitated in both IPs was equal, suggesting that the increase in dynamin I binding to syndapin I was stimulation dependent.

To investigate whether this stimulation dependent interaction was due to dynamin I dephosphorylation on stimulation, reciprocal IPs were carried out from synaptosomes which had been treated with 40 μM cyclosporin A prior to lysis (fig 5.14B). Again, there was no difference in the amount of syndapin I extracted when the IP antibody was against dynamin I. Importantly however, there was no increase in the amount of dynamin I isolated from the syndapin I IP where dephosphorylation was blocked by cyclosporin A. This implies that the phosphorylation status of dynamin I is important for its interaction with syndapin I *in vivo*.

To determine whether the $DynI_{769\text{-}784}AA$ peptide can disrupt the stimulation-dependent interaction between dynamin I and syndapin I, 2 mM $DynI_{769\text{-}784}AA$ was incubated in the lysate along with the antibody. The syndapin I IP samples were again blotted for dynamin I. The level of dynamin I increases upon stimulation, as before, and increases further in the stimulated sample incubated with the peptide (fig 5.15A). The syndapin I levels were equal (fig 5.15B) and so any effect in the amount

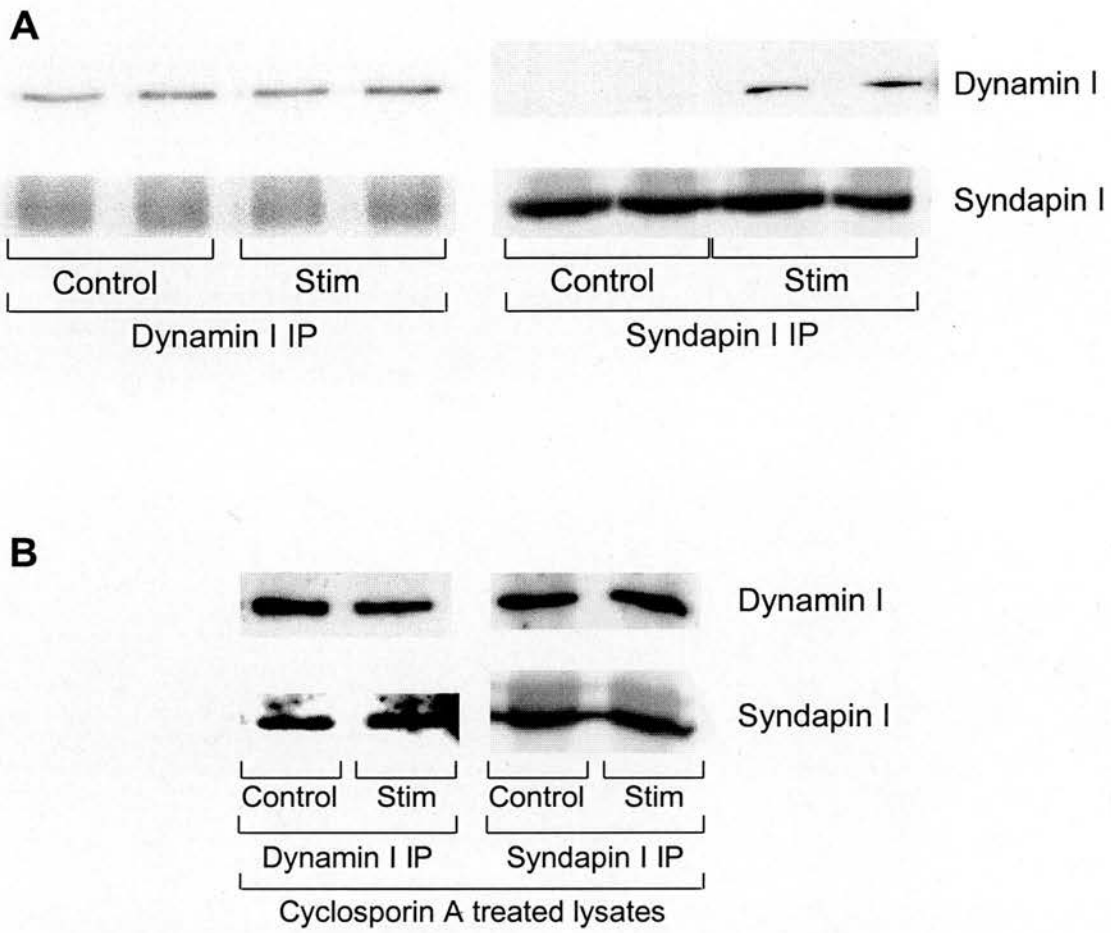

Figure 5.14 – Dynamin I interacts with syndapin I in a stimulation-dependent manner *in vivo*.

(A) Samples from reciprocal immunoprecipitations (IPs) from control and stimulated synaptosome lysates were blotted for dynamin I and syndapin I. Control represents basal synaptosomes and stim represents synaptosomes stimulated with 30 mM KCl. **(B)** Synaptosomes incubated with 40 μM cyclosporin A for 15 min were lysed and subjected to reciprocal IPs. Samples were again blotted for dynamin I and syndapin I. For **A** and **B** blots are representative of ≥ 3 experiments.

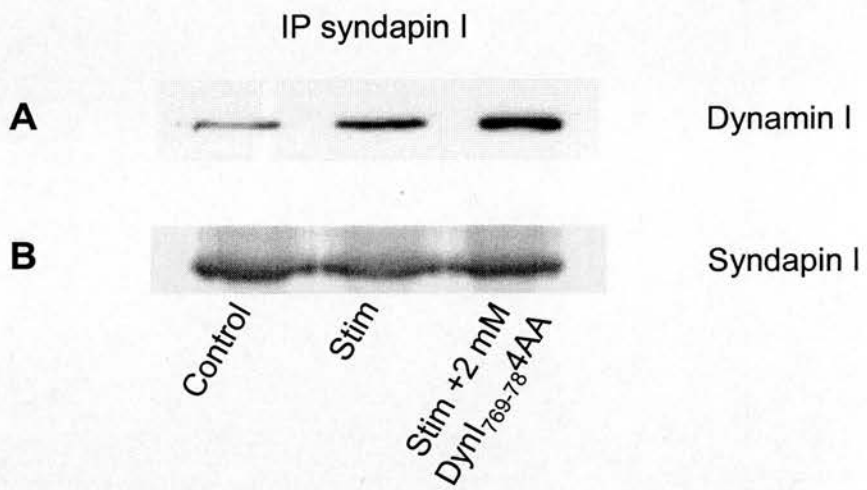

Figure 5.15 – Dynl$_{769-784}$AA peptide increases dynamin I binding to syndapin I *in vivo*

IP, using a syndapin I antibody, from control and stimulated (stim) synaptosome lysates incubated plus or minus 2 mM Dynl$_{769-784}$AA. Samples were blotted for dynamin I **(A)** and syndapin I **(B)**. Experiment n =1.

of dynamin I is due to the conditions and not the quantity of syndapin I immunoprecipitated. This agrees with the PRD-GST pulldown data where addition of the peptide increased the amount of binding.

5.8 DynI$_{769-784}$AA inhibits the dynamin I-syndapin I interaction

Incubating the DynI$_{769-784}$AA peptide with synaptosome lysates prior to pulldown with the GST-PRD or in a syndapin I IP, increased the amount of syndapin I and dynamin I binding, respectively. This implied that the peptide was facilitating formation of a complex and thus to use the peptide as a competitive inhibitor of the interaction, the IP protocol was modified so that the peptide was incubated with the protein bound on the antibody rather than in the lysate (fig 5.16). The theory behind the modification is that the peptide should be able to compete off binding of syndapin I or dynamin I from a pre-formed complex on the beads.

Using the modified protocol, the dynamin I-syndapin I interaction was investigated with IPs. Synaptosome lysates were incubated with the dynamin I or syndapin I antibodies and IgG beads. The beads were washed and then incubated with 2 mM DynI$_{769-784}$ peptide. The bound samples and the through samples were analysed by western blot. In the dynamin I IP the amount of syndapin I bound to dynamin I is slightly reduced after peptide treatment. However, the amount of dynamin I in this sample is also decreased (fig 5.17A), due to an unequal immunoprecipitation possibly caused by fewer protein G beads or less antibody reducing the amount of dynamin I extracted. Despite this, there is a substantial elution of syndapin I in the through sample for the peptide incubation (fig 5.17A), showing that the peptide is

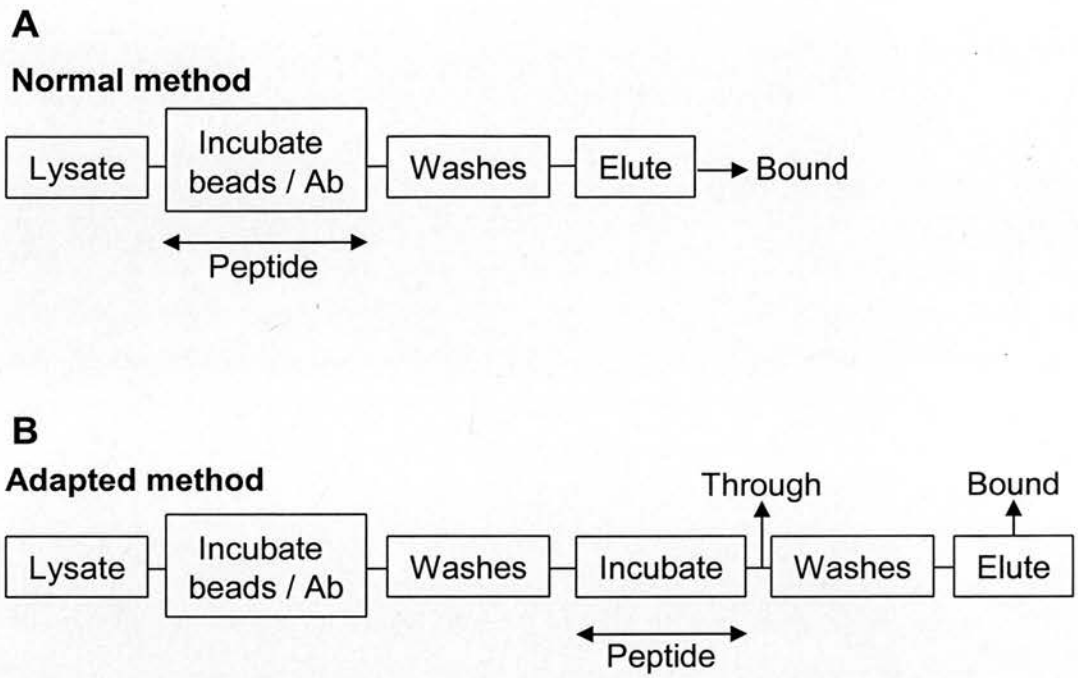

Figure 5.16 The normal and adapted IP protocols

Schematic of the normal **(A)** and adapted **(B)** IP protocol with ↔ representing points of peptide incubation and → representing the points where samples were obtained.

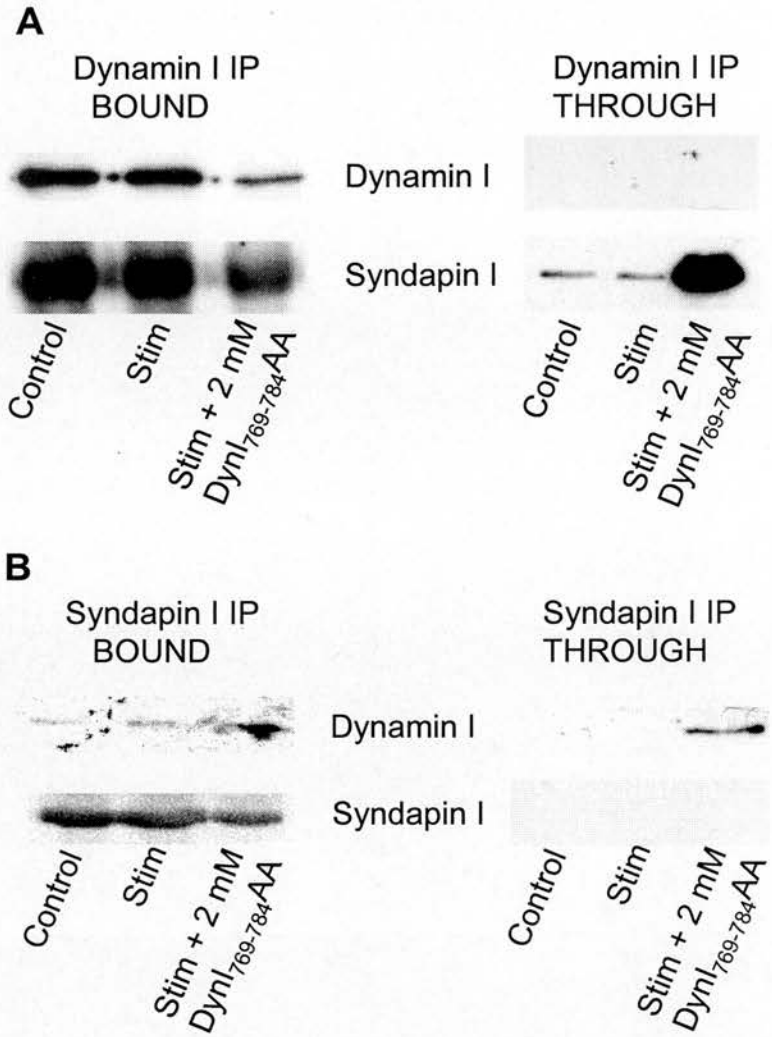

Figure 5.17 – Dynl$_{769-784}$AA can inhibit the interaction between dynamin I and syndapin I *in vivo*

(A) The bound and through samples from dynamin I IPs conducted using the adapted protocol (fig. 5.16B) from control and stimulated (stim) synaptosome lysates ± 2 mM Dynl$_{769-784}$AA peptide were blotted for syndapin I and dynamin I. Representative of two independent experiments. **(B)** The reciprocal IPs using syndapin I antibody were performed and the bound and through samples were again blotted for syndapin I and dynamin I.

capable of disrupting the dynamin I-syndapin I interaction. The through sample was also probed for dynamin I. There was no elution detected, which is as predicted since all the dynamin I would be expected to be bound to the IP antibody.

The reverse experiment was carried out with syndapin I IPs and although there was no obvious change in the levels of dynamin I in the bound samples, again the peptide facilitated the elution of dynamin I (fig 5.17B). There was no syndapin I detected in the through (fig 5.17B).

Several proteins are predicted to bind to the PRD of dynamin I (Okamoto et al. 1997; Slepnev et al. 1998; Slepnev and De Camilli 2000). Amphiphysin binds to the PRD at a motif further to the C-terminus than the peptide (residues 833-838 of dynamin I, Grabs et al. 1997). If the peptide was non-specifically eluting all of the proteins bound to dynamin I, amphiphysin I would be expected to be eluted too. The through sample was probed for amphiphysin I (fig 5.18A) but there was no elution detected. There was also no elution of endophilin and p85 (catalytic subunit of PI3 kinase) detected (fig 5.18A), which also bind this PRD, implying that the peptide is specifically eluting syndapin I. Figure 5.18B shows that amphiphysin I, p85 and endophilin were extracted from a dynamin I IP and therefore were bound to the complex prior to peptide incubation.

Taking both the dynamin I IP data and the syndapin I IP data together, the $DynI_{769\text{-}784}AA$ peptide is capable of disrupting the dynamin I-syndapin I interaction

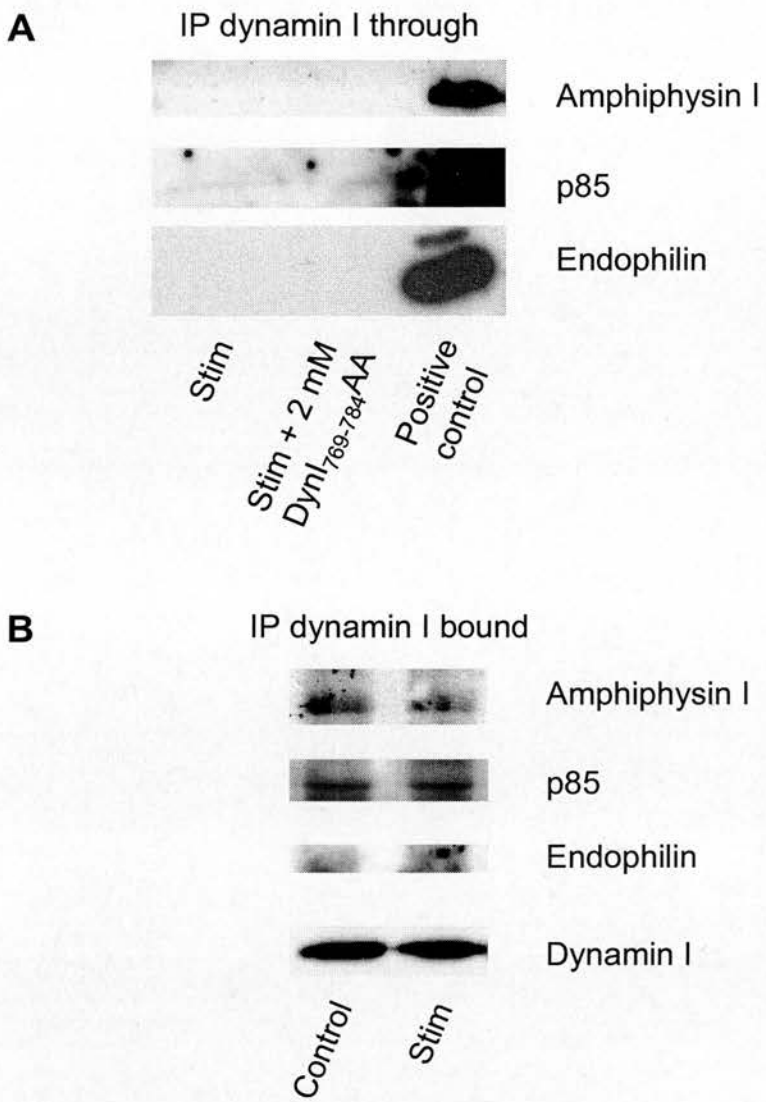

Figure 5.18 – Dynl$_{769-784}$AA does not elute other dynamin I PRD interacting proteins

(A) The through samples from dynamin IPs conducted using the adapted protocol (fig. 5.16B) from control and stimulated synaptosome lysates ± 2 mM Dynl$_{769-784}$AA peptide were blotted for amphiphysin I, p85 and endophilin. Representative of two independent experiments. **(B)** Dynamin I IP's from control and stimulated synaptosome lysates. The samples were probed for amphiphysin I, p85, endophilin and dynamin I.

specifically, showing a physiological role for this region of dynamin I from residues 769 – 785.

5.9 Discussion

A cycle of dephosphorylation and rephosphorylation is required for the maintenance of SV endocytosis. This chapter shows that the dephosphorylation of dynamin I, specifically on serines 774 and 778, has an essential role in SV endocytosis and that the region encompassing these sites from residues 769 – 784 forms at least part of an interaction motif for syndapin I which interacts with dynamin I in a stimulation-dependent manner.

Calcineurin inhibition by cyclosporin A

Figures 5.1 and 5.2 confirmed that calcineurin activity was essential for SV endocytosis and figure 5.3 showed, for the first time, that calcineurin dephosphorylates serines 774 and 778 in the PRD of dynamin I. All of these experiments used the drug cyclosporin A. Cyclosporin A functions by binding to cyclophilin and this complex potently inhibits calcineurin activity (Liu et al. 1991; Rusnak and Mertz 2000; Bandyopadhyay et al. 2004; Zhang et al. 2004). Since the interaction is not direct it could be argued that the effect seen on SV endocytosis was mediated by cyclophilin and not calcineurin. This is unlikely to be the case since SV turnover assays conducted using another proposed inhibitor of calcineurin, cypermethrin, yielded the same results (Smillie et al. 2005).

A number of cyclosporin A derivatives are being synthesised to mimic the conformational change of cyclosporin A upon cyclophilin binding in order to create a version of cyclosporin A which binds directly to calcineurin (Zhang et al. 2004). Use of these derivatives to inhibit calcineurin could alleviate the issues created by the requirement of cyclophilin for cyclosporin A mediated calcineurin inhibition.

Roles for dynamin I phosphorylation in SV recycling

The peptide mimicking the dephosphorylated state of dynamin I ($DynI_{769\text{-}784}AA$) significantly inhibited SV turnover, specifically at the vesicle retrieval stage. This is in contrast to the peptide mimicking the phosphorylated state of dynamin I ($DynI_{769\text{-}784}EE$) which did not significantly inhibit SV endocytosis (fig 5.5 – 5.8). The inhibition in retrieval efficiency for the $DynI_{769\text{-}784}AA$ peptide, and thus endocytosis, is approximately 30 % (taking the retrieval efficiencies for FM2-10 exocytosis assay, fig 5.7B) which is in good agreement with the inhibition of approximately 35 % seen in the internalisation assay (fig 5.8). This shows that the inhibition seen in the SV turnover assay was entirely attributable to an inhibition in SV retrieval.

One explanation for the disparity between the peptides is that the $DynI_{769\text{-}784}AA$ peptide is internalised more efficiently than the $DynI_{769\text{-}784}EE$ peptide since the $DynI_{769\text{-}784}EE$ peptide is less positively charged. This is unlikely since the endocytosis inhibition data is in agreement with experiments using full length eGFP-tagged wild-type dynamin I and constructs with the same phosphomimetic mutations as the peptides. These constructs were transfected into CGNs and using a similar protocol to figures 5.1A and 5.5, SV turnover was assayed with styryl dyes to

determine the effect of dynamin I phosphorylation on SV recycling (V. Anggono, personal communication). Wild-type dynamin I had no effect compared to control untransfected cells. Both the double alanine and double glutamic acid substitutions inhibited SV endocytosis. Once again, the double alanine substitution was more potent than the double glutamic acid mutant, confirming a phosphorylation-dependent role for dynamin I in SV endocytosis.

Although the evidence in this chapter points towards a role for dynamin I phosphorylation in SV endocytosis, there may also be a role for the PRD in SV exocytosis. Exocytosis was monitored by two different assays: measurement of glutamate release (fig 5.6A) and measurement of FM2-10 dye released (fig 5.6B). The FM2-10 release assay is probably the more accurate of the two since it labels all of the vesicles that are recycling. The glutamate release assay only approximates the amount of exocytosis since not all the vesicles that fuse with the plasma membrane contain glutamate, although 90 % of synapses are glutamatergic (Nicholls 1993).

The glutamate release assay showed a statistically insignificant inhibition of 10 % with both peptides whereas the FM2-10 release fluorescence assay showed a significant inhibition of approximately 20 % for both peptides. The $DynI_{769\text{-}784}AA$ peptide, however, does not inhibit SV exocytosis more potently than the $DynI_{769\text{-}784}EE$, unlike in the SV endocytosis assays.

Experiments conducted with the eGFP-tagged constructs harbouring the double mutations also showed a non-significant inhibition of SV exocytosis of

approximately 20 % (V. Anggono, personal communication) corroborating the data obtained from the FM2-10 exocytosis assay with the peptides (fig 5.6B). Taken together, this implies that there is a potential role of the PRD of dynamin I in exocytosis which is not phosphorylation dependent.

Evidence for such a role has been published for dynamin II, the ubiquitously expressed isoform of dynamin I. Dynamin II is essential for receptor-mediated endocytosis (Urrutia et al. 1997). However, it also has a role in constitutive and regulated hormone secretion, or exocytosis, in neuroendocrine cells (Yang et al. 2000). Secretion was inhibited by knock-down of dynamin II expression with antisense RNA and by transfection of dynamin II with a mutated PH domain or lacking the SH3 domain. Work with the *shibire* mutation in *Drosophila* has implicated dynamin I with a role in exocytosis as well as the well characterised role in endocytosis. *Shibire* synapses under intense stimulation exhibited a rapid depression within 20 ms which was too fast to be due to vesicle depletion and thus suggests a defect in the refilling of the RRP, and hence exocytosis (Kawasaki et al. 2000).

Another interpretation of the discrepancy in the exocytosis assay results is that phosphorylation of dynamin I may have a role in non-glutamate exocytosis, thus explaining the larger inhibition seen in the FM2-10 release assay. Experiments using munc13-1 knock out mice (Augustin et al. 1999) or mutant munc13-1 (Rhee et al. 2002) showed that release from glutamatergic neurons was almost totally inhibited but release from GABAergic neurons was unaffected by loss of wild type munc13-1.

Another protein involved in exocytosis, SNAP-25, was found only at glutamatergic synapses, and to have a role in neuronal excitability (Verderio et al. 2004). These cases demonstrate that there may be multiple vesicle release mechanisms which are transmitter-specific.

Thus, use of phosphomimetic substitutions of serines to alanines and glutamic acid residues in conjunction with assays of SV recycling have shown that there is a role for dynamin I phosphorylation in SV endocytosis as well as a potential role for dynamin I in exocytosis.

Role for dynamin I in 'kiss and run' vesicle recycling

4-AP and KCl stimulate glutamate release by two different mechanisms. KCl stimulation causes a clamped depolarisation of the plasma membrane whilst 4-AP inhibits the K^+ channels responsible for preventing spontaneous membrane depolarisations and therefore propagates action potentials. 4-AP stimulation thus mimics a more physiological stimulation since it evokes an exocytic response via action potentials (Nicholls 1993; Cousin and Robinson 2000b; Baldwin et al. 2003).

Inhibition of calcineurin by either cyclosporin A (Nichols et al. 1994; Baldwin et al. 2003; fig 5.9A) or FK506 (Sihra et al. 1995) enhances Ca^{2+}-dependent glutamate release stimulated with 1 mM 4-AP. However, stimulation with 30 mM KCl (Nichols et al. 1994; Baldwin et al. 2003; fig 5.1B)or 0.3 mM 4-AP (Baldwin et al. 2003) in the presence of cyclosporin A, does not. Moreover, the amount of FM2-10 released, in the presence of cyclosporin A, was unaltered regardless of whether

stimulation was by KCl or 4-AP. This discrepancy with 1 mM 4-AP stimulation was interpreted as being a transition to 'kiss and run' where a fusion pore could open sufficiently to release glutamate but not enough to allow departition of the FM2-10 from the membrane (Cousin and Robinson 2000b; Baldwin et al. 2003).

The effect of the phosphomimetic peptides on 1 mM 4-AP stimulated glutamate release was investigated in order to determine if there was a role for dynamin I phosphorylation in 4-AP stimulated release. Both peptides inhibited Ca^{2+}-dependent release (fig 5.9B). The $DynI_{769\text{-}784}AA$ peptide inhibited release more potently than the $DynI_{769\text{-}784}EE$ (fig 5.9B), implying that dynamin I phosphorylation may also control dynamin I function in 'kiss and run'.

There is mounting evidence of a role for dynamin I in 'kiss and run'. Experiments conducted by Holroyd *et al* (2002) using fluorescence microscopy in PC12 cells showed that dynamin I was associated with a population of secretory granules which fused and internalised at the same point. The recapture was inhibited by GTPγS and peptides that blocked dynamin I function (Holroyd et al. 2002). In chromaffin cells a dynamin I-dependent 'kiss and run' process which was inhibited by expression of the SH3 domain of amphiphysin and by GTPγS, where as a dynamin I independent 'kiss and run' process controlled by protein kinase C was unaffected (Graham et al. 2002). Experiments using anti-dynamin I antibodies also confirmed a role for dynamin I in 'kiss and run' in chromaffin cells (Artalejo et al. 2002).

A role for dynamin I in 'kiss and run' was also proposed in *Drosophila*. Endophilin knock out larvae were found to be able to sustain release at 15 – 20 % of the normal rate during high frequency stimulation only. This was attributed to 'kiss and run' since at low stimulation frequencies the larvae were unable to load FM1-43 at synapses. When the endophilin knock out was combined with the *shibire* temperature sensitive mutation (i.e. mutation in dynamin I), the larvae were unable to maintain release at any level, implicating dynamin I in the 'kiss and run' process (Verstreken et al. 2002).

Dynamin I and its phosphorylation regulation may therefore have a role in 'kiss and run' as well as the better characterised clathrin-mediated mode of vesicle retrieval.

Syndapin I and dynamin I interact *in vivo* in a stimulation dependent manner

The $DynI_{769\text{-}784}AA$ peptide, but not the $DynI_{769\text{-}784}EE$ peptide, was able to inhibit SV endocytosis. This implies that there is a phosphorylation dependent binding partner for the region of dynamin I from residues 769 – 784.

Using the $DynI_{769\text{-}784}AA$ peptides on columns, proteins of approximately 60 kDa were isolated (p60, fig 5.10 and 5.11). Blotting suggested that at least one of these was syndapin I. Unfortunately the extracted proteins were unable to be identified by MALDI-TOF analysis. The gels were silver stained to increase sensitivity since the quantity of material involved was small and so this may have reduced the efficiency of protein elution from the gel pieces as well as the lack of material impeding the identification.

Since the tagged peptides are mimicking dephosphorylated dynamin I, i.e. the form of dynamin I found following stimulation, then the binding partner would be expected to be extracted from both basal and stimulated synaptosome lysates. However, both tagged peptides isolated proteins of approximately 60 kDa only from the stimulated lysates in the presence of the peptide (fig 5.10 and fig 5.11). This suggests that the binding partner may also be modified in a stimulation dependent manner or perhaps is released from another protein upon stimulation, making it available to bind to dynamin I.

The case that syndapin I may be p60 is strengthened by evidence from pulldowns using GST tagged dynamin I PRD with parallel phosphomimetic mutations. Syndapin I was identified by MALDI-TOF only to bind to the wild type PRD and the double alanine mutant PRD. There was no binding, however, to the double glutamic acid mutant PRD (V. Anggono, personal communication), suggesting that syndapin I binds only to dephosphorylated dynamin I.

It is possible for syndapin I to undergo a stimulation-dependent modification, such as phosphorylation or dephosphorylation, which enables it to bind to dephosphorylated dynamin I and thus explain why syndapin I was found only in the stimulated lysate plus peptide lanes (fig 5.10 and 5.11). Syndapin I can be phosphorylated by several kinases *in vitro* including PKC and casein kinase 2 (Plomann et al. 1998; Kessels and Qualmann 2004). It has also been shown to be a substrate for an inositol hexakisphosphate-regulated protein kinase and that inositol hexakisphosphate-

dependent phosphorylation of syndapin I increases the affinity for dynamin I two to three fold *in vitro* (Hilton et al. 2001; Kessels and Qualmann 2004).

To investigate this further and the putative effect of syndapin I phosphorylation on SV endocytosis, mapping the phosphorylation site would be important. Once located, it could be mutated with a similar strategy to the dynamin I phosphorylation sites and the effect on SV endocytosis investigated.

The endophilin SH3 domain has also been published to bind to the PRD domain of dynamin I at two sites with differing affinities. The low affinity site overlaps with the amphiphysin SH3 domain binding site at the C-terminus of the dynamin I PRD and the high affinity binding site was localised to the N-terminus of the PRD, near the dynamin I *in vivo* phosphorylation sites. Interestingly, phosphorylation of the dynamin I PRD with Cdk5 prevented binding of the SH3 domain of endophilin, suggesting that it was phosphorylation-dependent (Solomaha et al. 2005). However, studies with the GST-full length endophilin and *in vivo* phosphorylated dynamin I failed to show any phosphorylation dependent binding, implying that the results with the SH3 domain were unique to the isolated SH3 domain. The same experiments showed that phosphorylation of dynamin I prevented binding to GST-full length syndapin I, further suggesting that syndapin I is the physiological phosphorylation dependent binding partner to dynamin I (V. Anggono, unpublished observations).

Logically, by adding a competitive peptide to inhibit an interaction, it would be expected to compete off a binding partner. However, when the $DynI_{769\text{-}784}AA$ was

incubated in the lysate with either the GST-PRD or during the IPs (figs 5.12 – 5.13 and 5.15), an increase in the total amount of protein was seen, with increasing concentration of peptide. It appears as though the peptide is facilitating the formation of a complex, rather than preventing a specific interaction.

Dynamin I and syndapin I are published to interact via the PRD of dynamin I and the SH3 domain of syndapin I (Qualmann et al. 1999). The $DynI_{769-784}AA$ peptide does not contain a traditional PXXP SH3 domain recognition sequence, implying that syndapin I may have more than one dynamin I binding site. The peptide may bind to one site which then causes a conformation change enabling syndapin I to bind to dynamin I at another site. Syndapin I can form oligomers and is found as part of high molecular weight complex (Qualmann et al. 1999) and so the peptide, and dynamin I *in vivo*, may facilitate the formation of this complex and thus explain the increase in total endocytosis protein binding seen in figures 5.12- 5.13 and 5.15. The role of this complex may be to concentrate all the proteins required for SV endocytosis at the site of vesicle formation where they are required. Mapping of the binding site on syndapin I for dynamin I would aid investigation into this area.

Modification of the pulldown / IP protocol so that the $DynI_{769-784}AA$ peptide was incubated after the interacting proteins had been extracted allowed the complex to form and so the peptide was then able to inhibit a specific interaction. The $DynI_{769-784}AA$ peptide was able to elute syndapin I and dynamin I from dynamin I and syndapin I IP's, respectively (fig 5.17). Other SH3 domain containing proteins were

not eluted (fig 5.18A) showing the specificity of this peptide for the dynamin I-syndapin I interaction.

None of the experiments performed thus far have shown a stimulation-dependent interaction *in vivo*. However, the amount of dynamin I extracted from a syndapin I IP increased upon stimulation and was blocked by cyclosporin A (fig 5.14). There was not an equivalent increase in the amount of syndapin I extracted from a dynamin I IP upon stimulation. A possible reason for this discrepancy could be due to the fact that the majority of dynamin I (90 %) is in the dephosphorylated state in nerve terminals at rest (Liu et al. 1994a). The dynamin I antibody will be able to bind both the phosphorylated and dephosphorylated forms and so any differences in the interactions due to stimulation-dependent dephosphorylation will be overshadowed by the majority of the dynamin I pool which remains unchanged.

To fully understand the role of the dynamin I-syndapin I interaction, further investigation into the interaction itself would be required. This could be evaluated through *in vitro* binding assays. Experiments with phosphorylation mutants of both dynamin I and syndapin I as well as *in vitro* Cdk5 phosphorylated dynamin I could also be used to show that this is a direct interaction and that it is regulated by phosphorylation. *In vivo* interactions could be observed in real time in living cells by imaging fluorescently labelled versions of the two proteins. If dynamin I and syndapin I were tagged with appropriate fluorophores, FRET and fluorescence lifetime imaging (FLIM) analysis would be excellent tools to examine how and when these proteins interact in a cell under physiological conditions. This has already been

shown to be possible in cultured neurons with tagged synaptophysin and synaptobrevin (Pennuto et al. 2002).

What is the role of dynamin I phosphorylation?

This chapter has shown that the dephosphorylation of serines 774 and 778 of dynamin I is essential for SV endocytosis and that residues 769 – 784 are important for syndapin I binding but what is the role of this stimulation-dependent interaction?

It has long been postulated that actin may have several roles in SV endocytosis, from providing a force to complete the fission reaction to simply propelling the newly formed vesicles away from the plasma membrane (Qualmann et al. 2000; Shupliakov et al. 2002; Merrifield 2004). Experiments conducted by Merrifield *et al* (2002) using total internal reflection (TIRF) microscopy in conjunction with epifluorescence microscopy showed that dynamin I was recruited to clathrin coated structures followed by N-WASP, Arp2/3 and actin. N-WASP is known to bind to the SH3 domain of syndapin I (Qualmann et al. 1999) and to activate the Arp2/3 complex stimulating localised actin polymerisation. Therefore, a possible model for the dynamin I-syndapin I interaction could be to localise the actin machinery to the endocytosis machinery at the site of vesicle fission (Kessels and Qualmann 2004). This is summarized in figure 5.19 which shows dynamin I binding to PIP_2 on the plasma membrane as the coated pit is invaginating. Syndapin I oligomerises and these oligomers can bind to dynamin I and N-WASP, localising N-WASP and the Arp2/3 complex to the neck of the invaginated coated pit. Since the Arp2/3 complex can nucleate actin filament polymerisation, this cascade of protein-protein

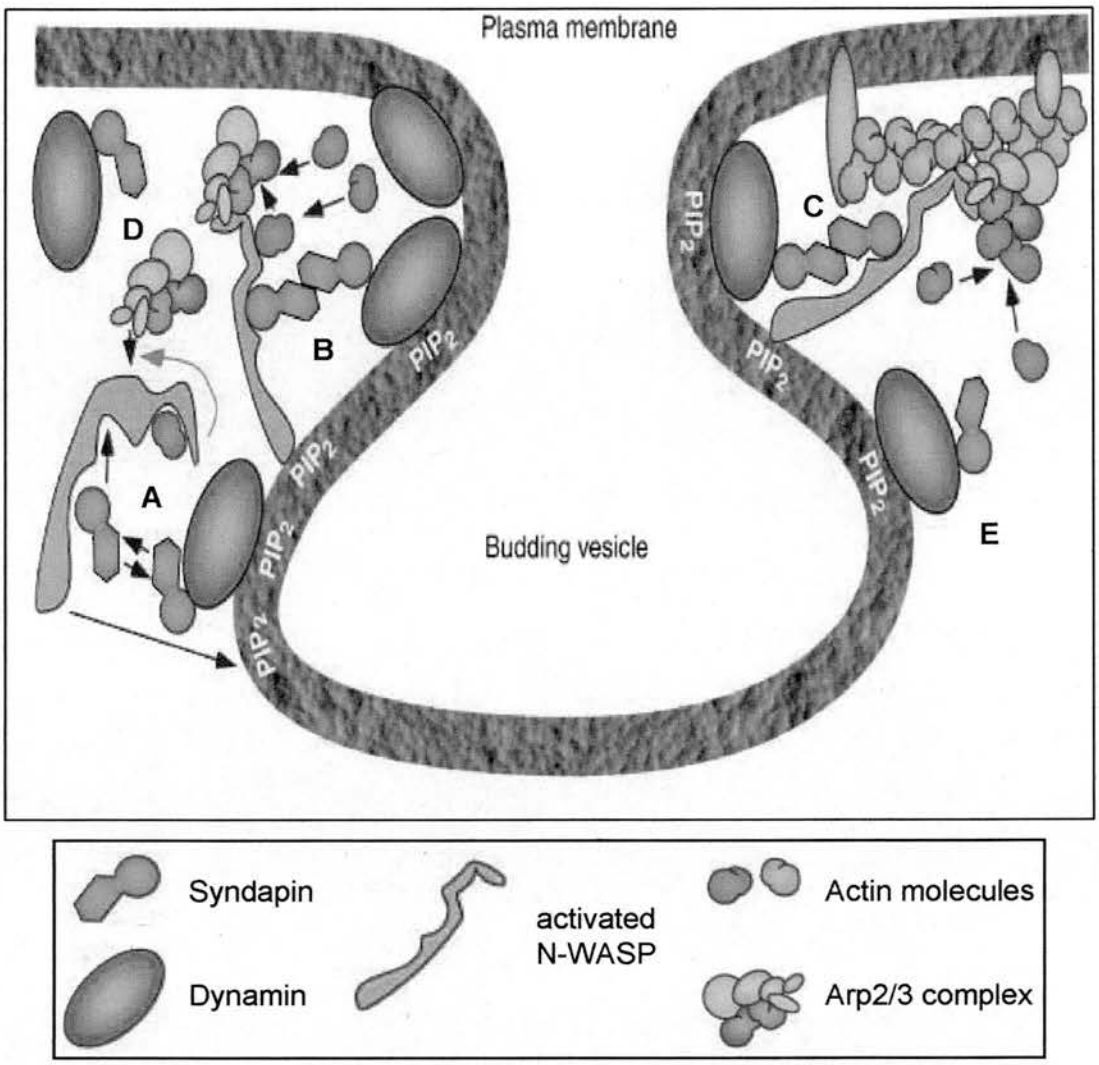

Figure 5.19 – Connection of the endocytosis machinery to the actin polymerisation machinery via the dynamin I-syndapin I interaction

(A) Dynamin I localises to regions of PIP_2 on the plasma membrane as the pit is invaginating. Syndapin I can bind to dynamin I bringing in N-WASP and the activated Arp2/3 complex. **(B)** As the pit becomes deeply invaginated, dynamin I accumulates at the neck of the pit bringing with it the syndapin complex and localising actin polymerisation at the neck. Actin filaments can be generated *de novo* **(B)** or as branches of existing filaments **(C)**. Dynamin I-syndapin I oligomers could form in the cytosol before **(D)** or after **(E)** dynamin I localisation at the membrane. Figure taken from Kessels and Qualmann, 2004.

interactions localises actin filament polymerisation to the neck of a forming vesicle where the force generated by the forming actin filaments could be used in the fission reaction, or the cytoskeletal network created used to transport the newly retrieved vesicles away from the sites of endocytosis.

The role of dynamin I dephosphorylation and the stimulation-dependent interaction with syndapin I may be to temporally and spatially regulate actin polymerisation so that actin filaments are only generated once vesicle formation is sufficiently advanced and at the stage where force generation or transport is required.

CHAPTER 6

GENERAL DISCUSSION

6.1 Introduction

SV recycling is essential for the maintenance of synaptic transmission and involves cascades of tightly regulated protein-protein and protein-lipid interactions. This ensures that SV exocytosis and endocytosis proceed in a temporally and spatially controlled manner. Several mechanisms of SV retrieval exist including 'kiss and run', clathrin-coated vesicle retrieval and bulk endocytosis. It is likely that all of these mechanisms occur in the nerve terminal and probably more than one method of retrieval will be evoked at any one time. The molecular mechanism determining which pathway is triggered has not been resolved to date although several models have been postulated. The most commonly held suggestion is that the RRP is recycled by a rapid mode of endocytosis, which may be 'kiss and run', and that the reserve pool, when mobilised, is recycled by a slower, possibly clathrin-mediated route. Certainly at hippocampal synapses the SVs in the RRP seem to be closer to the active zone than those in the reserve pool (Schikorski and Stevens 2001). However, at the frog neuromuscular junction this is not the case since the RRP SVs appear to be distributed throughout the nerve terminal and are not necessarily near the active zone, suggesting that there are other, perhaps biochemical factors determining SV entry into the RRP (Rizzoli and Betz 2004).

Ca^{2+} has been postulated to be the trigger for mobilising reserve pool SVs (Kuromi and Kidokoro 2005). During low frequency stimulation, Ca^{2+}-influx would be sufficient to trigger exocytosis of the RRP and subsequent internalisation of these vesicles. During tetanic stimulation, Ca^{2+} influx would last for longer and thus be able to increase the Ca^{2+} concentration further from the plasma membrane and

trigger the mobilisation of the reserve pool. Certainly Ca^{2+} is essential for both exocytosis and endocytosis in nerve terminals although the reserve pool mobilisation theory is speculation.

The interactions of several proteins involved in SV exocytosis and endocytosis are regulated either directly or indirectly by Ca^{2+}. This thesis showed that a complex containing synaptophysin, dynamin I, and amphiphysin I forms in the presence of Ca^{2+} and that dynamin I and amphiphysin I can associate independently with synaptophysin. The role of these interactions may be to localise dynamin I and amphiphysin I to sites of SV retrieval.

Dynamin I and amphiphysin I are both dephosphins and as such are dephosphorylated upon nerve terminal stimulation by calcineurin and rephosphorylated by their kinase(s) following SV endocytosis. The role of the phosphorylation status of dynamin I, specifically, was addressed in this thesis. Dephosphorylation of dynamin I is essential for SV endocytosis and syndapin I was identified as a stimulation-dependent binding partner. The role of this interaction may be to localise and activate actin polymerisation at sites of SV endocytosis away from the active zone during the fission and trafficking stages.

6.2 Model of action

The data presented in this thesis confirm an essential role for dynamin I in SV retrieval. The Ca^{2+}-dependent interaction between dynamin I and synaptophysin was already postulated to have a role in SV retrieval (Daly et al. 2000; Daly and Ziff

2002). The data presented in chapter 4 confirmed that the C-terminus of synaptophysin had a role in SV endocytosis and that this was potentially mediated via putative Ca^{2+}-dependent interactions with dynamin I and amphiphysin I. Calcineurin and Cdk5 are both essential to maintain consecutive rounds of stimulation (Marks and McMahon 1998; Cousin et al. 2001; Tan et al. 2003) and therefore the data in chapter 5 showing an essential role for the phosphorylation status of one of their substrates, dynamin I, is in agreement with this. The identification of syndapin I as a stimulation-dependent binding partner is also compatible with a role for syndapin I in endocytosis since over-expression of the SH3 domain has been shown to inhibit receptor-mediated endocytosis (Qualmann and Kelly 2000). A possible interpretation of the data presented in this thesis is proposed in the following model.

The first assumption of this model is that the RRP is recycled by a rapid mode of SV endocytosis taking place at the active zone, potentially 'kiss and run'. The reserve pool of SVs is recycled by a slower mechanism occurring on the periphery of the active zone, most probably by a clathrin-mediated mechanism following full fusion. The second assumption is that the rapid 'kiss and run' pathway is predominantly evoked by low frequency stimulation and that at high frequency or during prolonged stimulation the slower clathrin-mediated pathway is also required to retrieve the excess membrane.

The model is summarised in figure 6.1. Under conditions of low stimulation, the concentration of Ca^{2+} at the active zone is high, inducing exocytosis. Synaptophysin

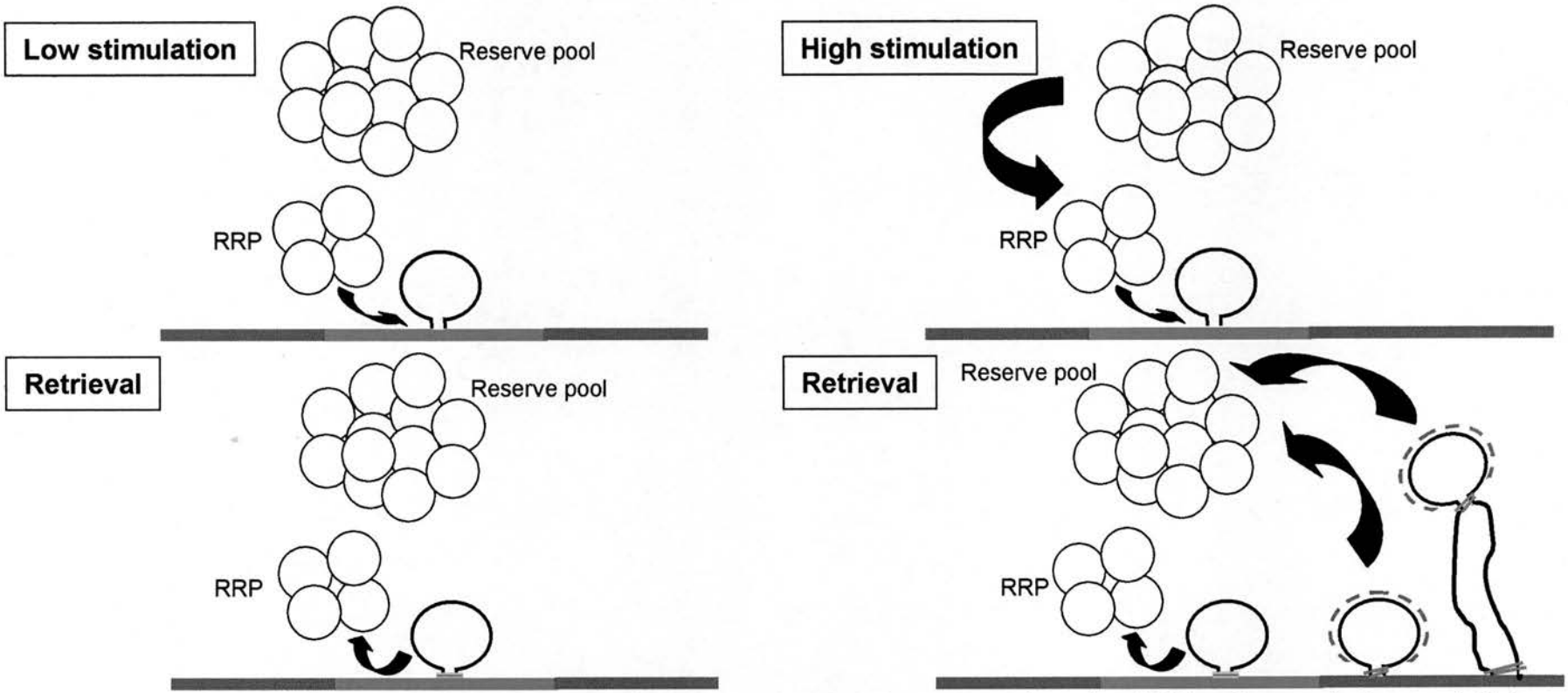

Figure 6.1 – Model for SV recycling pathways Schematic showing the proposed mode of SV cycling under low and high stimulation conditions. During low frequency stimulation, the RRP fuse with the active zone (red region) and are retrieved by a rapid form of endocytosis possibly involving a synaptophysin, amphiphysin I and dynamin I complex (blue and magenta box). During high frequency stimulation, the reserve pool is recruited and SV endocytosis proceeds via full fusion as well. SVs are then retrieved by rapid endocytosis and clathrin-mediated endocytosis (green coated SV). Dynamin I is represented by magenta lines. During intense stimulation, SVs may also be retrieval by bulk endocytosis.

binds to synaptobrevin in the absence of Ca^{2+} and so upon Ca^{2+} influx would dissociate (Daly and Ziff 2002), freeing synaptobrevin to interact in the SNARE complex. Concomitantly, in the presence of the increased Ca^{2+}, synaptophysin can bind to dynamin I and amphiphysin I at the site of vesicle fusion. Synaptophysin may also form part of the fusion pore complex, localising dynamin I and amphiphysin I to the neck of the vesicle. In turn they may either form part of the mechanism to rapidly retrieve the SV or act as adaptors to localise the machinery that does.

In support of this hypothesis, both dynamin I and synaptophysin have been suggested to have a role in 'kiss and run' and in particular, the synaptophysin-dynamin I interaction (Daly et al. 2000). Inhibition of this interaction by injection of a peptide designed from the C-terminus of synaptophysin, inhibited SV recycling in the giant squid axon. Specifically, there was an increase in clathrin coated vesicles thought to be a result of a switching of all SV recycling to the clathrin-mediated pathway.

Under conditions of intense stimulation, the reserve pool is required and full fusion predominantly occurs. The prolonged stimulation increases the Ca^{2+} transient in the nerve terminal, activating several proteins, including calcineurin, leading to dephosphorylation of the dephosphins and the retrieval of vesicles outside the active zone where the Ca^{2+} concentration is lower and thus not inhibiting the GTPase activity of dynamin I. The dephosphorylation of dynamin I allows its translocation to the plasma membrane as well as the stimulation dependent interaction with syndapin I. Syndapin I stimulates actin polymerisation via interactions with N-

WASP and the arp2/3 complex. Thus, actin is localised to the neck of the forming vesicle.

Under conditions of intense stimulation, bulk endocytosis may also be required to retrieve all of the vesicle membrane quickly. This is thought to occur via bulk internalisation of areas of the plasma membrane outside of the active zone by a clathrin-independent mechanism, although dynamin I and other proteins which can induce membrane curvature such as epsin, endophilin and amphiphysin, may have a role. SVs can then bud off of the internalised membrane via a clathrin and dynamin I dependent mechanism (Royle and Lagnado 2003).

6.3 Retrieval and fission of the SV

The GTPase activity of dynamin I is well documented as being essential for the fission step of clathrin-mediated SV endocytosis (Slepnev and De Camilli 2000). However, if dynamin I is at the active zone, for example during participation in 'kiss and run', the Ca^{2+} concentration may inhibit the GTPase activity, suggesting that this activity may not be essential for rapid vesicle retrieval. In contradiction, studies using the *shibire* mutant show an inhibition of neurotransmission within 20 ms, thought to be too fast for a defect in SV endocytosis to have occurred (Kawasaki et al. 2000). The *shibire* mutant has a mutation in the GTPase domain of dynamin I suggesting this activity is required for either exocytosis or very rapid retrieval of SVs.

Amphiphysin I can tubulate liposomes with its N-terminal BAR domain. BAR domains are found in a variety of proteins and are domains which can sense membrane curvature. A subset of proteins, such as amphiphysin I, have a BAR domain at the N-terminus. These BAR domains have an amphipathic helix at the extreme N-terminus which upon insertion into the membrane can induce curvature (Peter et al. 2004). The Ca^{2+}-dependent interaction with synaptophysin, may serve to localise amphiphysin I where the N-BAR domain can aid in the recapture of a vesicle following a transient fusion event with the plasma membrane. As the Ca^{2+} concentration returns to basal levels, amphiphysin I would dissociate from synaptophysin, allowing perhaps a more conventional role in the targeting of dynamin I for clathrin-mediated retrieval.

Syndapin I also has a BAR domain although it is located in the central part of the molecule (Peter et al. 2004). Following association with dephosphorylated dynamin I, the BAR domain of syndapin I may also bind to the neck region of the forming vesicle since BAR domains lacking the N-terminal helix tend to bind highly curved membranes (Peter et al. 2004). Syndapin I may therefore have a more direct role in vesicle fission over and above localising actin polymerisation.

6.4 The role of dynamin I phosphorylation

The majority of dynamin I in the nerve terminal is in the dephosphorylated state bound to the plasma membrane (Robinson et al. 1994). This pool of dynamin I is not accessible for phosphorylation (Liu et al. 1994a) and so therefore probably does not participate in the regulated phosphorylation cycle of dynamin I involved in SV

endocytosis. Although dynamin I and synaptophysin can interact in a Ca^{2+}-dependent manner, the interaction does not seem to be stimulation dependent (fig 4.7-8) suggesting that the phosphorylation status of dynamin I is not as important. Potentially, therefore, it could be the membrane bound pool of dynamin I which could be involved in the rapid 'kiss and run' membrane retrieval.

6.5 Further experiments to investigate the model

First and foremost for investigation is whether or not 'kiss and run' recycling occurs in central nerve terminals (synaptosomes and CGNs) and the parameters that control the proportion of 'kiss and run' events compared to full fusion. Harata *et al* (2006) have published data that supports the existence of 'kiss and run' in hippocampal neurons and proposed that 'kiss and run' was responsible for the majority of fusion events at low frequency. It would be predicted therefore that kiss-and-run would also occur in CGNs since SV recycling shares the same molecular machinery

One of the assays designed by Harata *et al* (2006) uses the small hydrophilic molecule bromophenol blue which quenches the fluorescence of the styryl dye FM1-43. If all fusion events occurred by full fusion then all of the FM1-43 in loaded vesicles would be exposed to the aqueous environment resulting in a fluorescence decrease, since FM1-43 is only highly fluorescent when membrane-bound. Therefore, there should be no additional fluorescence drop in the presence of bromophenol blue. If vesicle fusion were to be followed by rapid vesicle retrieval, 'kiss and run', then some of the FM1-43 would remain in the vesicle lumen and thus when exposed to bromophenol blue during stimulation there would be an additional

fluorescence drop, due to quenching by bromophenol blue which had entered the vesicle while the fusion pore was open. This technique can thus be used to assay 'kiss and run' and investigate the factors involved in the mechanism and regulation.

This assay could be employed to look at the role of synaptophysin and to discover whether it is involved in 'kiss and run' recycling. It could be used in combination with the competitive peptide shown to inhibit SV endocytosis (Chapter 4) as well as with overexpression of the C-terminus of synaptophysin. The latter would have to be cloned into a red vector such as red fluorescent protein in order to be used in combination with FM1-43. Both the peptide and overexpression of the C-terminus of synaptophysin would be predicted to inhibit 'kiss and run', if the model were true, and thus would decrease or abolish any additional fluorescent drop in the presence of bromophenol blue. These experiments would show whether or not the C-terminus of synaptophysin had a role in 'kiss and run' recycling.

The experiments in chapter 4 showed that dynamin I and amphiphysin I bound independently to synaptophysin through the use of a peptide which blocks the interaction between dynamin I and amphiphysin ($DynI_{832-840}$). The chapter does not address, however, if the proteins are part of the same complex or if there are two separate pools of synaptophysin; one bound to dynamin and the other bound to amphiphysin. This could be addressed by performing a pulldown experiment with full length amphiphysin I, or dynamin I, in the presence of the $DynI_{832-840}$ peptide. If two separate synaptophysin complexes existed only synaptophysin would be extracted by either amphiphysin or dynamin, since the peptide inhibits the dynamin I

and amphiphysin I interaction. If a tripartite complex exists however, both synaptophysin and dynamin I would be extracted by full length amphiphysin in the presence of the peptide, for example.

The functional significance of these interactions could be investigated by mapping the synaptophysin binding site for dynamin I and/or amphiphysin I. Non-binding mutants could then be generated and expressed in cultured cells from synaptophysin knock out mice. The synaptophysin null background is essential to enable the effect of the mutants to be investigated directly without the presence of the wild type synaptophysin. The effect on 'kiss and run' and SV endocytosis could then be addressed using the bromophenol blue assay (above) and FM dye SV turnover assays (Chapters 3, 4 and 5).

In addition to the synaptophysin interaction having a role in rapid SV retrieval during low stimulation conditions, the model also predicts that during intense stimulation the slower clathrin-mediated mode of SV retrieval is evoked. This part of the model hypothesises that the role of the stimulation dependent dynamin I-syndapin I interaction may be to localise the actin cytoskeleton to the sites of SV fission. The functional significance of the dynamin I-syndapin I interaction was demonstrated in Chapter 5. The $DynI_{769\text{-}784}AA$ phosphomimetic peptide inhibited SV endocytosis and was also shown to disrupt the dynamin I-syndapin I interaction. To further characterise the function of this interaction the syndapin I binding sites could be mapped and a competitive peptide synthesised. This peptide could then be tested in a similar manner to the dynamin phosphomimetic peptides with the SV turnover assays

(figs 5.5 – 5.8). These assays could be complemented by overexpression of a syndapin non-binding mutant in CGNs and looking at the effect on SV turnover. These experiments would be predicted to have a similar phenotype to the dynamin phosphomimetic mutations since the same interaction is being perturbed.

Rescue of the endocytosis block created by the dynamin phosphomimic peptide could be attempted by overexpression of wild type syndapin I. This would be predicted to restore functional endocytosis. Likeweise, overexpression of wild type dynamin I should be able to rescue an endocytosis block created by a syndapin I competitive peptide. These experiments would also serve to confirm the specificity of the peptides for the dynamin I - syndapin I interaction.

To determine at which stage of the endocytosis pathway syndapin I is required, electron microscopy could be performed on CGNs where syndapin I was silenced using siRNA. A construct containing both the siRNA and a marker protein, such as GFP, would need to be expressed in cells in order to distinguish between transfected cells and non-transfected cells. Immuno-electron microscopy against the marker could then identify the transfected cells and hence the cells for morphological analysis. The morphology of the plasma membrane profiles would suggest whether syndapin I is involved at an early or late stage in endocytosis. Dynamin I mutants show a block at the deeply invaginated pit stage (Kosaka and Ikeda 1983; Takei et al. 1995), thus syndapin I knock-down would be expected to have a similar morphology since syndapin I binds dynamin I.

The dynamin I-syndapin I interaction is important for SV endocytosis. One possible mechanism is that the interaction induces localised actin polymerisation required for the final stages of vesicle fission. Actin polymerisation could occur via a syndapin I interaction with N-WASP, which in turn, would activate the Arp2/3 complex and nucleate filament formation. In order to test whether the dynamin I-syndapin I interaction does act on the actin cytoskeleton, the interaction between syndapin I and N-WASP could be perturbed. The binding site for N-WASP on syndapin I could be mapped, and reintroduced into cells as a competitive peptide or mutant N-WASP with deleted syndapin binding sites. Following stimulation, the effect on actin organisation could be monitored by staining for F-actin (phalloidin) and G-actin (Dnase). If the dynamin I-syndapin I interaction does function in regulating localised actin polymerisation then disruption of the syndapin I-N-WASP interaction would be predicted to have an effect on the actin cytoskeleton and on SV endocytosis. Actin staining could also be used to look at the effect of silencing N-WASP with siRNA. However, this may have non-specific effects since actin polymerisation is required for several cell processes and not just endocytosis.

If these experiments showed that the dynamin I-syndapin I interaction does not act on the cytoskeleton or that the interaction was not as important as the phosphoregulation of the dynamin I-syndapin I interaction, the function of the BAR domain of syndapin could be investigated. BAR domains bind to and in some cases tubulate membranes (Peter et al. 2004) and thus the BAR domain of syndapin I may have a more direct role in vesicle scission. This could be investigated by either overexpressing the BAR domain alone of syndapin I or overexpressing a version of

syndapin I with a mutant BAR domain. The effect on endocytosis could be monitored using the FM dye SV turnover assays. If the BAR domain is important for syndapin I function then either of the mutants would produce an inhibition of SV turnover. Using a syndapin I BAR domain deletion mutant would also be informative but might produce spurious effects, since syndapin I may need to bind to the neck of the vesicle for function, although it need not necessarily have a direct effect in scission.

6.6 Future perspectives

The main focus of SV endocytosis research has been the identification of the proteins involved and characterisation of these. Now that the majority of SV endocytosis proteins are identified the real test will be to determine the temporal and spatial regulation of the interactions of these proteins. Many endocytosis proteins are reversibly modified by phosphorylation for example, and so the identification of the relevant kinases and phosphatases and their regulation will also be key.

The particular modes of SV endocytosis in different nerve terminals and what regulates their proportion will also probably be an area of intense research. For example, the molecules that control 'kiss and run' have still to be determined and it will be very interesting to see whether they are unique to this process or a specific subset of those required for clathrin-mediated endocytosis.

Advancements in real-time cell imaging, including detection methods and temporal resolution are allowing questions of a more complex nature to be answered. With

progressing technology, the secrets of SV endocytosis will be unravelled allowing determination of the molecular mechanisms and development of new drugs and treatment paradigms for diseases involving abnormal neurotransmission.

REFERENCES

Alder J., Kanki H., Valtorta F., Greengard P., and Poo M. (1995) Overexpression of synaptophysin enhances neurotransmitter secretion at *Xenopus* neuromuscular synapses. *J Neurosci* **15,** 511-519.

Alder J., Lu B., Valtorta F., Greengard P., and Poo M. (1992a) Calcium-dependent transmitter secretion reconstituted in *Xenopus* oocytes: Requirement for synaptophysin. *Science* **257,** 657-661.

Alder J., Xie Z.-P., Valtorta F., Greengard P., and Poo M. (1992b) Antibodies to synaptophysin interfere with transmitter secretion at neuromuscular synapses. *Neuron* **9,** 759-768.

Ales E., Tabares L., Poyato J. M., Valero V., Lindau M., and Alvarez d. T. (1999) High calcium concentrations shift the mode of exocytosis to the kiss-and-run mechanism. *Nat Cell Biol* **1,** 40-44.

Artalejo C. R., Elhamdani A., and Palfrey H. C. (1996) Calmodulin is the divalent cation receptor for rapid endocytosis, but not exocytosis, in adrenal chromaffin cells. *Neuron* **16,** 195-205.

Artalejo C. R., Elhamdani A., and Palfrey H. C. (2002) Sustained stimulation shifts the mechanism of endocytosis from dynamin-1-dependent rapid endocytosis to clathrin- and dynamin-2-mediated slow endocytosis in chromaffin cells. *Proc Natl Acad Sci U S A* **99,** 6358-6363.

Augustin I., Rosenmund C., Sudhof T. C., and Brose N. (1999) Munc13-1 is essential for fusion competence of glutamatergic synaptic vesicles. *Nature* **400,** 457-461.

Baldwin M. L., Rostas J. A., and Sim A. T. (2003) Two modes of exocytosis from synaptosomes are differentially regulated by protein phosphatase types 2A and 2B. *J Neurochem* **85,** 1190-1199.

Bandyopadhyay J., Lee J., and Bandyopadhyay A. (2004) Regulation of calcineurin, a calcium/calmodulin-dependent protein phosphatase, in C. elegans. *Mol Cells* **18,** 10-16.

Betz W. J. and Henkel A. W. (1994) Okadaic acid disrupts clusters of synaptic vesicles in frog motor nerve terminals. *J Cell Biol* **124,** 843-854.

Betz W. J., Mao F., and Smith C. B. (1996) Imaging exocytosis and endocytosis. *Curr Opin Neurobiol* **6,** 365-371.

Broadie K. (2004) Synapse scaffolding: intersection of endocytosis and growth. *Curr Biol* **14,** R853-R855.

Brose N., Petrenko A. G., Südhof T. C., and Jahn R. (1992) Synaptotagmin: a calcium sensor on the synaptic vesicle surface. *Science* **256,** 1021-1025.

Brymora A., Cousin M. A., Roufogalis B. D., and Robinson P. J. (2001) Enhanced protein recovery and reproducibility from pull-down assays and immunoprecipitations using spin columns. *Anal Biochem* **295,** 119-122.

Burgoyne R. D. and Morgan A. (2003) Secretory granule exocytosis. *Physiol Rev* **83,** 581-632.

Calakos N. and Scheller R. H. (1994) Vesicle-associated membrane protein and synaptophysin are associated on the synaptic vesicle. *J Biol Chem* **269,** 24534-24537.

Carey R. M., Balcz B. A., Lopez-Coviella I., and Slack B. E. (2005) Inhibition of dynamin-dependent endocytosis increases shedding of the amyloid precursor protein ectodomain and reduces generation of amyloid beta protein. *BMC Cell Biol* **6,** 30.

Cataldo A. M., Barnett J. L., Pieroni C., and Nixon R. A. (1997) Increased neuronal endocytosis and protease delivery to early endosomes in sporadic Alzheimer's disease: neuropathologic evidence for a mechanism of increased beta-amyloidogenesis. *J Neurosci* **17,** 6142-6151.

Ceccarelli B., Hurlbut W. P., and Mauro A. (1973) Turnover of transmitter and synaptic vesicles at the frog neuromuscular junction. *J Cell Biol* **57,** 499-524.

Cestra G., Castagnoli L., Dente L., Minenkova O., Petrelli A., Migone N., Hoffmuller U., Schneider-Mergener J., and Cesareni G. (1999) The SH3 domains of endophilin and amphiphysin bind to the proline-rich region of synaptojanin 1 at distinct sites that display an unconventional binding specificity. *J Biol Chem* **274,** 32001-32007.

Chan S. A. and Smith C. (2001) Physiological stimuli evoke two forms of endocytosis in bovine chromaffin cells. *J Physiol* **537,** 871-885.

Chen C. Y., Reese M. L., Hwang P. K., Ota N., Agard D., and Brodsky F. M. (2002) Clathrin light and heavy chain interface: alpha-helix binding superhelix loops via critical tryptophans. *EMBO J* **21,** 6072-6082.

Chen H., Slepnev V. I., Di Fiore P. P., and De Camilli P. (1999) The interaction of epsin and eps15 with the clathrin adaptor AP-2 is inhibited by mitotic phosphorylation and enhanced by stimulation-dependent dephosphorylation in nerve terminals. *J Biol Chem* **274,** 3257-3260.

Chen Y., Deng L., Maeno-Hikichi Y., Lai M., Chang S., Chen G., and Zhang J. F. (2003) Formation of an endophilin-Ca2+ channel complex is critical for clathrin-mediated synaptic vesicle endocytosis. *Cell* **115,** 37-48.

Chen Y. J., Zhang P., Egelman E. H., and Hinshaw J. E. (2004) The stalk region of dynamin drives the constriction of dynamin tubes. *Nat Struct Mol Biol* **11,** 574-575.

Chen-Hwang M.-C., Chen H.-R., Elzinga M., and Hwang Y.-W. (2002) Dynamin is a minibrain kinase/Dyrk1A substrate. *J Biol Chem* **277,** 17597-17604.

Chin D. and Means A. R. (2000) Calmodulin: a prototypical calcium sensor. *Trends Cell Biol* **10,** 322-328.

Christiaens B., Grooten J., Reusens M., Joliot A., Goethals M., Vandekerckhove J., Prochiantz A., and Rosseneu M. (2004) Membrane interaction and cellular internalization of penetratin peptides. *Eur J Biochem* **271,** 1187-1197.

Christiaens B., Symoens S., Verheyden S., Engelborghs Y., Joliot A., Prochiantz A., Vandekerckhove J., Rosseneu M., and Vanloo B. (2002) Tryptophan fluorescence study of the interaction of penetratin peptides with model membranes. *Eur J Biochem* **269,** 2918-2926.

Conner S. D. and Schmid S. L. (2002) Identification of an adaptor-associated kinase, AAK1, as a regulator of clathrin-mediated endocytosis. *J Cell Biol* **156,** 921-929.

Conner S. D. and Schmid S. L. (2003) Regulated portals of entry into the cell. *Nature* **422,** 37-44.

Cousin M. A. (2000) Synaptic vesicle endocytosis: calcium works overtime in the nerve terminal. *Mol Neurobiol* **22,** 115-128.

Cousin M. A., Malladi C. S., Tan T. C., Raymond C. R., Smillie K. J., and Robinson P. J. (2003) Synapsin I-associated phosphatidylinositol 3-kinase mediates synaptic vesicle delivery to the readily releasable pool. *J Biol Chem* **278,** 29065-29071.

Cousin M. A., Nicholls D. G., and Pocock J. M. (1995) Modulation of ion gradients and glutamate release in cultured cerebellar granule cells by ouabain. *J Neurochem* **64,** 2097-2104.

Cousin M. A. and Robinson P. J. (1998) Ba^{2+} does not support synaptic vesicle retrieval in rat isolated presynaptic nerve terminals. *Neurosci Lett* **253,** 1-4.

Cousin M. A. and Robinson P. J. (1999) Mechanisms of synaptic vesicle recycling illuminated by fluorescent dyes. *J Neurochem* **73,** 2227-2239.

Cousin M. A. and Robinson P. J. (2000a) Ca^{2+} inhibition of dynamin arrests synaptic vesicle recycling at the active zone. *J Neurosci* **20,** 949-957.

Cousin M. A. and Robinson P. J. (2000b) Two mechanisms of synaptic vesicle recycling in rat brain nerve terminals. *J Neurochem* **75,** 1645-1653.

Cousin M. A. and Robinson P. J. (2001) The dephosphins: Dephosphorylation by calcineurin triggers synaptic vesicle endocytosis. *Trends Neurosci* **24,** 659-665.

Cousin M. A., Tan T. C., and Robinson P. J. (2001) Protein phosphorylation is required for endocytosis in nerve terminals. Potential role for the dephosphins dynamin I and synaptojanin, but not AP180 or amphiphysin. *J Neurochem* **76,** 105-116.

Daly C., Sugimori M., Moreira J. E., Ziff E. B., and Llinas R. (2000) Synaptophysin regulates clathrin-independent endocytosis of synaptic vesicles. *Proc Natl Acad Sci U S A* **97,** 6120-6125.

Daly C. and Ziff E. B. (2002) Ca2+-dependent formation of a dynamin-synaptophysin complex: potential role in synaptic vesicle endocytosis. *J Biol Chem* **277,** 9010-9015.

Damke H., Baba T., Warnock D. E., and Schmid S. L. (1994) Induction of mutant dynamin specifically blocks endocytic coated vesicle formation. *J Cell Biol* **127,** 915-934.

Danino D., Moon K. H., and Hinshaw J. E. (2004) Rapid constriction of lipid bilayers by the mechanochemical enzyme dynamin. *J Struct Biol* **147,** 259-267.

de Lange R. P., de Roos A. D., and Borst J. G. (2003) Two modes of vesicle recycling in the rat calyx of Held. *J Neurosci* **23,** 10164-10173.

Derossi D., Calvet S., Trembleau A., Brunissen A., Chassaing G., and Prochiantz A. (1996) Cell internalization of the third helix of the Antennapedia homeodomain is receptor-independent. *J Biol Chem* **271,** 18188-18193.

Derossi D., Chassaing G., and Prochiantz A. (1998) Trojan peptides: the penetratin system for intracellular delivery. *Trends Cell Biol* **8,** 84-87.

Derossi D., Joliot A. H., Chassaing G., and Prochiantz A. (1994) The third helix of the Antennapedia homeodomain translocates through biological membranes. *J Biol Chem* **269,** 10444-10450.

Di Paolo G., Sankaranarayanan S., Wenk M. R., Daniell L., Perucco E., Caldarone B. J., Flavell R., Picciotto M. R., Ryan T. A., Cremona O., and De Camilli P. (2002) Decreased synaptic vesicle recycling efficiency and cognitive deficits in amphiphysin 1 knockout mice. *Neuron* **33,** 789-804.

Doe C. Q. and Scott M. P. (1988) Segmentation and homeotic gene function in the developing nervous system of Drosophila. *Trends Neurosci* **11,** 101-106.

Dunkley P. R., Jarvie P. E., Heath J. W., Kidd G. J., and Rostas J. A. (1986) A rapid method for isolation of synaptosomes on Percoll gradients. *Brain Res* **372,** 115-129.

Earnest S., Khokhlatchev A., Albanesi J. P., and Barylko B. (1996) Phosphorylation of dynamin by ERK2 inhibits the dynamin-microtubule interaction. *FEBS Lett* **396,** 62-66.

Ehrlich M., Boll W., Van Oijen A., Hariharan R., Chandran K., Nibert M. L., and Kirchhausen T. (2004) Endocytosis by random initiation and stabilization of clathrin-coated pits. *Cell* **118,** 591-605.

El Far O. and Betz H. (2002) Synaptophysins: vesicular cation channels? *J Physiol* **539,** 2.

Engisch K. L. and Nowycky M. C. (1996) Calcium dependence of large dense-cored vesicle exocytosis evoked by calcium influx in bovine adrenal chromaffin cells. *J Neurosci* **16,** 1359-1369.

Fabian-Fine R., Verstreken P., Hiesinger P. R., Horne J. A., Kostyleva R., Zhou Y., Bellen H. J., and Meinertzhagen I. A. (2003) Endophilin promotes a late step in endocytosis at glial invaginations in Drosophila photoreceptor terminals. *J Neurosci* **23,** 10732-10744.

Farsad K., Ringstad N., Takei K., Floyd S. R., Rose K., and De Camilli P. (2001) Generation of high curvature membranes mediated by direct endophilin bilayer interactions. *J Cell Biol* **155,** 193-200.

Farsad K., Slepnev V., Ochoa G., Daniell L., Hauke V., and De Camilli P. (2003) A putative role for intramolecular regulatory mechanisms in the adaptor function of amphiphysin in endocytosis. *Neuropharmacology* **45,** 787-796.

Fingerhut A., Von Figura K., and Honing S. (2000) Binding of AP2 to sorting signals is modulated by AP2 phosphorylation. *J Biol Chem* **276,** 5476-5492.

Fischer P. M., Zhelev N. Z., Wang S., Melville J. E., Fahraeus R., and Lane D. P. (2000) Structure-activity relationship of truncated and substituted analogues of the intracellular delivery vector Penetratin. *J Pept Res* **55,** 163-172.

Flett A., Semerdjieva S., Jackson A. P., and Smythe E. (2005) Regulation of the clathrin-coated vesicle cycle by reversible phosphorylation. *Biochem Soc Symp* 65-70.

Floyd S. R., Porro E. B., Slepnev V. I., Ochoa G. C., Tsai L. H., and De Camilli P. (2001) Amphiphysin binds the cdk5 regulatory subunit p35 and is phosphorylated by cdk5 and cdc2. *J Biol Chem* **276,** 8104-8110.

Ford M. G., Mills I. G., Peter B. J., Vallis Y., Praefcke G. J., Evans P. R., and McMahon H. T. (2002) Curvature of clathrin-coated pits driven by epsin. *Nature* **419,** 361-366.

Fotin A., Cheng Y., Grigorieff N., Walz T., Harrison S. C., and Kirchhausen T. (2004) Structure of an auxilin-bound clathrin coat and its implications for the mechanism of uncoating. *Nature* **432,** 649-653.

Futaki S., Suzuki T., Ohashi W., Yagami T., Tanaka S., Ueda K., and Sugiura Y. (2001) Arginine-rich peptides: An abundant source of membrane-permeable peptides having potential as carriers for intracellular protein delivery. *J Biol Chem* **276,** 5836-5840.

Gad H., Low P., Zotova E., Brodin L., and Shupliakov O. (1998) Dissociation between Ca^{2+}-triggered synaptic vesicle exocytosis and clathrin-mediated endocytosis at a central synapse. *Neuron* **21,** 607-616.

Gad H., Ringstad N., Low P., Kjaerulff O., Gustafsson J., Wenk M., Di Paolo G., Nemoto Y., Crun J., Ellisman M. H., De Camilli P., Shupliakov O., and Brodin L. (2000) Fission and uncoating of synaptic clathrin-coated vesicles are perturbed by disruption of interactions with the SH3 domain of endophilin. *Neuron* **27,** 301-312.

Gandhi S. P. and Stevens C. F. (2003) Three modes of synaptic vesicular recycling revealed by single-vesicle imaging. *Nature* **423,** 607-613.

Garcia C. C., Blair H. J., Seager M., Coulthard A., Tennant S., Buddles M., Curtis A., and Goodship J. A. (2004) Identification of a mutation in synapsin I, a synaptic vesicle protein, in a family with epilepsy. *J Med Genet* **41,** 183-186.

Grabs D., Slepnev V. I., Songyang Z., David C., Lynch M., Cantley L. C., and De Camilli P. (1997) The SH3 domain of amphiphysin binds the proline-rich domain of dynamin at a single site that defines a new SH3 binding consensus sequence. *J Biol Chem* **272,** 13419-13425.

Graham M. E., O'Callaghan D. W., McMahon H. T., and Burgoyne R. D. (2002) Dynamin-dependent and dynamin-independent processes contribute to the regulation of single vesicle release kinetics and quantal size. *Proc Natl Acad Sci U S A* **99,** 7124-7129.

Gray N. W., Fourgeaud L., Huang B., Chen J., Cao H., Oswald B. J., Hemar A., and McNiven M. A. (2003) Dynamin 3 is a component of the postsynapse, where it interacts with mGluR5 and homer. *Curr Biol* **13,** 510-515.

Guatimosim C., Romano-Silva M. A., Gomez M. V., and Prado M. A. (1998) Recycling of synaptic vesicles at the frog neuromuscular junction in the presence of strontium. *J Neurochem* **70,** 2477-2483.

Gundelfinger E. D., Kessels M. M., and Qualmann B. (2003) Temporal and spatial coordination of exocytosis and endocytosis. *Nat Rev Mol Cell Biol* **4,** 127-139.

Hallbrink M., Floren A., Elmquist A., Pooga M., Bartfai T., and Langel U. (2001) Cargo delivery kinetics of cell-penetrating peptides. *Biochim Biophys Acta* **1515,** 101-109.

Hanahan D. (1983) Studies on transformation of Escherichia coli with plasmids. *J Mol Biol* **166,** 557-580.

Hao W., Luo Z., Zheng L., Prasad K., and Lafer E. M. (1999) AP180 and AP-2 interact directly in a complex that cooperatively assembles clathrin. *J Biol Chem* **274,** 22785-22794.

Harata N. C., Choi S., Pyle J. L., Aravanis A. M., and Tsien R. W. (2006) Frequency-dependent kinetics and prevalence of kiss-and-run and reuse at hippocampal synapses studied with novel quenching methods. *Neuron* **49,** 243-256.

Harris T. W., Hartwieg E., Horvitz H. R., and Jorgensen E. M. (2000) Mutations in synaptojanin disrupt synaptic vesicle recycling. *J Cell Biol* **150,** 589-600.

Haucke V. and De Camilli P. (1999) AP-2 recruitment to synaptotagmin stimulated by tyrosine-based endocytic motifs. *Science* **285,** 1268-1271.

Haucke V., Wenk M. R., Chapman E. R., Farsad K., and De Camilli P. (2000) Dual interaction of synaptotagmin with mu2- and alpha-adaptin facilitates clathrin-coated pit nucleation. *EMBO J* **19,** 6011-6019.

Henkel A. W. and Betz W. J. (1995) Monitoring of black widow spider venom (BWSV) induced exo- and endocytosis in living frog motor nerve terminals with FM1-43. *Neuropharmacology* **34,** 1397-1406.

Henley J. R., Krueger E. A., Oswald B. J., and McNiven M. A. (1998) Dynamin-mediated internalization of caveolae. *J Cell Biol* **141,** 85-99.

Heuser J. E. and Reese T. S. (1973) Evidence for recycling of synaptic vesicle membrane during transmitter release at the frog neuromuscular junction. *J Cell Biol* **57,** 315-344.

Hilton J. M., Plomann M., Ritter B., Modregger J., Freeman H. N., Falck J. R., Krishna U. M., and Tobin A. B. (2001) Phosphorylation of a synaptic vesicle-associated protein by an inositol hexakisphosphate-regulated protein kinase. *J Biol Chem* **276,** 16341-16347.

Hinshaw J. E. and Schmid S. L. (1995) Dynamin self-assembles into rings suggesting a mechanism for coated vesicle budding. *Nature* **374,** 190-192.

Holroyd P., Lang T., Wenzel D., De Camilli P., and Jahn R. (2002) Imaging direct, dynamin-dependent recapture of fusing secretory granules on plasma membrane lawns from PC12 cells. *Proc Natl Acad Sci U S A* **99,** 16806-16811.

Holt M., Cooke A., Wu M. M., and Lagnado L. (2003) Bulk membrane retrieval in the synaptic terminal of retinal bipolar cells. *J Neurosci* **23,** 1329-1339.

Honing S., Ricotta D., Krauss M., Spate K., Spolaore B., Motley A., Robinson M., Robinson C., Haucke V., and Owen D. J. (2005) Phosphatidylinositol-(4,5)-bisphosphate regulates sorting signal recognition by the clathrin-associated adaptor complex AP2. *Mol Cell* **18,** 519-531.

Hopper N. A. and O'Connor V. (2005) Ephrin tempers two-faced synaptojanin 1. *Nat Cell Biol* **7,** 454-456.

Horikawa H. P., Kneussel M., El Far O., and Betz H. (2002) Interaction of synaptophysin with the AP-1 adaptor protein gamma-adaptin. *Mol Cell Neurosci* **21,** 454-462.

Hosoya H., Komatsu S., Shimizu T., Inagaki M., Ikegami M., and Yazaki K. (1994) Phosphorylation of dynamin by cdc2 kinase. *Biochem Biophys Res Commun* **202,** 1127-1133.

Hou Q., Yi X., Jiang G., and Wei Q. (2004) The salt bridge of calcineurin is important for transferring the effect of CNB binding to CNA. *FEBS Lett* **577,** 294-298.

Hurley J. H. and Wendland B. (2002) Endocytosis: driving membranes around the bend. *Cell* **111,** 143-146.

Huttner W. B. and Schmidt A. A. (2002) Membrane curvature: a case of endofeelin' em leader. *Trends Cell Biol* **12,** 155-158.

Irie F., Okuno M., Pasquale E. B., and Yamaguchi Y. (2005) EphrinB-EphB signalling regulates clathrin-mediated endocytosis through tyrosine phosphorylation of synaptojanin 1. *Nat Cell Biol* **7,** 501-509.

Jackson A. P., Flett A., Smythe C., Hufton L., Wettey F. R., and Smythe E. (2003) Clathrin promotes incorporation of cargo into coated pits by activation of the AP2 adaptor mu2 kinase. *J Cell Biol* **163,** 231-236.

Jahn R., Schiebler W., Ouimet C., and Greengard P. (1985) A 38,000-dalton membrane protein (p38) present in synaptic vesicles. *Proc Natl Acad Sci U S A* **82,** 4137-4141.

Janz R. and Südhof T. C. (1998) Cellugyrin, a novel ubiquitous form of synaptogyrin that is phosphorylated by $pp60^{c\text{-}src}$. *J Biol Chem* **273,** 2851-2857.

Janz R., Sudhof T. C., Hammer R. E., Unni V., Siegelbaum S. A., and Bolshakov V. Y. (1999) Essential roles in synaptic plasticity for synaptogyrin I and synaptophysin I. *Neuron* **24,** 687-700.

Jarousse N. and Kelly R. B. (2001a) Endocytotic mechanisms in synapses. *Curr Opin Cell Biol* **13,** 461-469.

Jarousse N. and Kelly R. B. (2001b) The AP2 binding site of synaptotagmin 1 is not an internalization signal but a regulator of endocytosis. *J Cell Biol* **154,** 857-866.

Job C. and Lagnado L. (1998) Calcium and protein kinase C regulate the actin cytoskeleton in the synaptic terminal of retinal bipolar cells. *J Cell Biol* **143,** 1661-1672.

Johnston P. A. and Sudhof T. C. (1990) The multisubunit structure of synaptophysin. Relationship between disulfide bonding and homo-oligomerization. *J Biol Chem* **265,** 8869-8873.

Joliot A., Pernelle C., Deagostini-Bazin H., and Prochiantz A. (1991) Antennapedia homeobox peptide regulates neural morphogenesis. *Proc Natl Acad Sci U S A* **88,** 1864-1868.

Jorgensen E. M., Hartwieg E., Schuske K., Nonet M. L., Jin Y., and Horvitz H. R. (1995) Defective recycling of synaptic vesicles in synaptotagmin mutants of Caenorhabditis elegans. *Nature* **378,** 196-199.

Kawasaki F., Hazen M., and Ordway R. W. (2000) Fast synaptic fatigue in shibire mutants reveals a rapid requirement for dynamin in synaptic vesicle membrane trafficking. *Nat Neurosci* **3,** 859-860.

Kelly B. L., Vassar R., and Ferreira A. (2005) Beta-amyloid-induced dynamin 1 depletion in hippocampal neurons. A potential mechanism for early cognitive decline in Alzheimer disease. *J Biol Chem* **280,** 31746-31753.

Kelly R. B. (1999) New twists for dynamin. *Nat Cell Biol* **1,** E8-E9.

Kessels M. M. and Qualmann B. (2004) The syndapin protein family: linking membrane trafficking with the cytoskeleton. *J Cell Sci* **117,** 15-86.

Khvotchev M. V. and Sudhof T. C. (2004) Stimulus-dependent dynamic homo- and heteromultimerization of synaptobrevin/VAMP and synaptophysin. *Biochemistry* **43,** 15037-15043.

Kim W. T., Chang S., Daniell L., Cremona O., Di Paolo G., and De Camilli P. (2002) Delayed reentry of recycling vesicles into the fusion-competent synaptic vesicle pool in synaptojanin 1 knockout mice. *Proc Natl Acad Sci U S A* **99,** 17143-17148.

Kjaerulff O., Verstreken P., and Bellen H. J. (2002) Synaptic vesicle retrieval: still time for a kiss. *Nat Cell Biol* **4,** E245-E248.

Klee C. B., Ren H., and Wang X. T. (1998) Regulation of the calmodulin-stimulated protein phosphatase, calcineurin. *J Biol Chem* **273,** 13367-13370.

Klingauf J., Kavalali E. T., and Tsien R. W. (1998) Kinetics and regulation of fast endocytosis at hippocampal synapses. *Nature* **394,** 581-585.

Klyachko V. A. and Jackson M. B. (2002) Capacitance steps and fusion pores of small and large-dense-core vesicles in nerve terminals. *Nature* **418,** 89-92.

Koenig J. H. and Ikeda K. (1996) Synaptic vesicles have two distinct recycling pathways. *J Cell Biol* **135,** 797-808.

Koh T. W., Verstreken P., and Bellen H. J. (2004) Dap160/intersectin acts as a stabilizing scaffold required for synaptic development and vesicle endocytosis. *Neuron* **43,** 193-205.

Kosaka T. and Ikeda K. (1983) Possible temperature-dependent blockage of synaptic vesicle recycling induced by a single gene mutation in *Drosophila*. *J Neurobiol* **14,** 207-225.

Kuromi H., Honda A., and Kidokoro Y. (2004) Ca(2+) influx through distinct routes controls exocytosis and endocytosis at Drosophila presynaptic terminals. *Neuron* **41,** 101-111.

Kuromi H. and Kidokoro Y. (1998) Two distinct pools of synaptic vesicles in single presynaptic boutons in a temperature-sensitive *Drosophila* mutant, *shibire*. *Neuron* **20,** 917-925.

Kuromi H. and Kidokoro Y. (1999) The optically determined size of exo/endo cycling vesicle pool correlates with the quantal content at the neuromuscular junction of Drosophila larvae. *J Neurosci* **19,** 1557-1565.

Kuromi H. and Kidokoro Y. (2005) Exocytosis and endocytosis of synaptic vesicles and functional roles of vesicle pools: lessons from the Drosophila neuromuscular junction. *Neuroscientist* **11,** 138-147.

Kuromi H., Yoshihara M., and Kidokoro Y. (1997) An inhibitory role of calcineurin in endocytosis of synaptic vesicles at nerve terminals of Drosophila larvae. *Neurosci Res* **27,** 101-113.

Lai M. M., Hong J. J., Ruggiero A. M., Burnett P. E., Slepnev V. I., De Camilli P., and Snyder S. H. (1999) The calcineurin-dynamin 1 complex as a calcium sensor for synaptic vesicle endocytosis. *J Biol Chem* **274,** 25963-25966.

Lai M. M., Luo H. R., Burnett P. E., Hong J. J., and Snyder S. H. (2000) The calcineurin binding protein Cain is a negative regulator of synaptic vesicle endocytosis. *J Biol Chem* **275,** 34017-34020.

Larsen M. R., Graham M. E., Robinson P. J., and Roepstorff P. (2004) Improved detection of hydrophilic phosphopeptides using graphite powder microcolumns and mass spectrometry: evidence for in vivo doubly phosphorylated dynamin I and dynamin III. *Mol Cell Proteomics* **3,** 456-465.

Lauritsen J. P., Menne C., Kastrup J., Dietrich J., Odum N., and Geisler C. (2000) beta2-Adaptin is constitutively de-phosphorylated by serine/threonine protein phosphatase PP2A and phosphorylated by a staurosporine-sensitive kinase. *Biochim Biophys Acta* **1497,** 297-307.

Le R., I, Joliot A. H., Bloch-Gallego E., Prochiantz A., and Volovitch M. (1993) Neurotrophic activity of the Antennapedia homeodomain depends on its specific DNA-binding properties. *Proc Natl Acad Sci U S A* **90,** 9120-9124.

Lee M. C. and Schekman R. (2004) Cell biology. BAR domains go on a bender. *Science* **303,** 479-480.

Lee S. Y., Voronov S., Letinic K., Nairn A. C., Di Paolo G., and De Camilli P. (2005) Regulation of the interaction between PIPKI gamma and talin by proline-directed protein kinases. *J Cell Biol* **168,** 789-799.

Lee S. Y., Wenk M. R., Kim Y., Nairn A. C., and De Camilli P. (2004) Regulation of synaptojanin 1 by cyclin-dependent kinase 5 at synapses. *Proc Natl Acad Sci U S A* **101,** 546-551.

Legendre-Guillemin V., Wasiak S., Hussain N. K., Angers A., and McPherson P. S. (2004) ENTH/ANTH proteins and clathrin-mediated membrane budding. *J Cell Sci* **117,** 9-18.

Leube R. E., Wiedenmann B., and Franke W. W. (1989) Topogenesis and sorting of synaptophysin: synthesis of a synaptic vesicle protein from a gene transfected into nonneuroendocrine cells. *Cell* **59,** 433-446.

Li C., Ullrich B., Zhang J. Z., Anderson R. G. W., Brose N., and Südhof T. C. (1995a) Ca^{2+}-dependent and -independent activities of neural and non-neural synaptotagmins. *Nature* **375,** 594-599.

Li L., Chin L. S., Shupliakov O., Brodin L., Sihra T. S., Hvalby O., Jensen V., Zheng D., McNamara J. O., Greengard P., and Andersen P. (1995b) Impairment of synaptic vesicle clustering and of synaptic transmission, and increased seizure propensity, in synapsin I-deficient mice. *Proc Natl Acad Sci U S A* **92,** 9235-9239.

Li Z. and Murthy V. N. (2001) Visualizing postendocytic traffic of synaptic vesicles at hippocampal synapses. *Neuron* **31,** 593-605.

Lindgren M., Hallbrink M., Prochiantz A., and Langel U. (2000) Cell-penetrating peptides. *Trends Pharmacol Sci* **21,** 99-103.

Lindgren M. E., Hallbrink M. M., Elmquist A. M., and Langel U. (2004) Passage of cell-penetrating peptides across a human epithelial cell layer in vitro. *Biochem J* **377,** 1-76.

Lindner R. and Ungewickell E. (1992) Clathrin-associated proteins of bovine brain coated vesicles. An analysis of their number and assembly-promoting activity. *J Biol Chem* **267,** 16567-16573.

Liu J., Farmer J. D. Jr., Lane W. S., Friedman J., Weissman I., and Schreiber S. L. (1991) Calcineurin is a common target of cyclophilin-cyclosporin A and FKBP-FK506 complexes. *Cell* **66,** 807-815.

Liu J. P. (1997) Protein phosphorylation events in exocytosis and endocytosis. *Clin Exp Pharmacol Physiol* **24,** 611-618.

Liu J. P., Powell K. A., Südhof T. C., and Robinson P. J. (1994a) Dynamin I is a Ca^{2+}-sensitive phospholipid-binding protein with very high affinity for protein kinase C. *J Biol Chem* **269,** 21043-21050.

Liu J. P. and Robinson P. J. (1995) Dynamin and endocytosis. *Endocr Rev* **16,** 590-607.

Liu J. P., Sim A. T. R., and Robinson P. J. (1994b) Calcineurin inhibition of dynamin I GTPase activity coupled to nerve terminal depolarization. *Science* **265,** 970-973.

Liu J. P., Zhang Q.-X., Baldwin G., and Robinson P. J. (1996) Calcium binds dynamin I and inhibits its GTPase activity. *J Neurochem* **66,** 2074-2081.

Magzoub M., Eriksson L. E., and Graslund A. (2002) Conformational states of the cell-penetrating peptide penetratin when interacting with phospholipid vesicles: effects of surface charge and peptide concentration. *Biochim Biophys Acta* **1563,** 53-63.

Mansvelder H. D. and Kits K. S. (1998) The relation of exocytosis and rapid endocytosis to calcium entry evoked by short repetitive depolarizing pulses in rat melanotropic cells. *J Neurosci* **18,** 81-92.

Marie B., Sweeney S. T., Poskanzer K. E., Roos J., Kelly R. B., and Davis G. W. (2004) Dap160/intersectin scaffolds the periactive zone to achieve high-fidelity endocytosis and normal synaptic growth. *Neuron* **43,** 207-219.

Marks B. and McMahon H. T. (1998) Calcium triggers calcineurin-dependent synaptic vesicle recycling in mammalian nerve terminals. *Curr Biol* **8,** 740-749.

Marks B., Stowell M. H., Vallis Y., Mills I. G., Gibson A., Hopkins C. R., and McMahon H. T. (2001) GTPase activity of dynamin and resulting conformation change are essential for endocytosis. *Nature* **410,** 231-235.

Martin T. F. (2000) Racing lipid rafts for synaptic-vesicle formation. *Nat Cell Biol* **2,** E9-11.

Maruyama K., Mikawa T., and Ebashi S. (1984) Detection of calcium binding proteins by 45Ca autoradiography on nitrocellulose membrane after sodium dodecyl sulfate gel electrophoresis. *J Biochem* **95,** 511-519.

Matthews G. (2004) Cycling the synapse: scenic versus direct routes for vesicles. *Neuron* **44,** 223-226.

McMahon H. T. (1999) Endocytosis: an assembly protein for clathrin cages. *Curr Biol* **9,** R332-R335.

McMahon H. T., Bolshakov V. Y., Janz R., Hammer R. E., Siegelbaum S. A., and Südhof T. C. (1996) Synaptophysin, a major synaptic vesicle protein, is not essential for neurotransmitter release. *Proc Natl Acad Sci U S A* **93,** 4760-4764.

McMahon H. T., Wigge P., and Smith C. (1997) Clathrin interacts specifically with amphiphysin and is displaced by dynamin. *FEBS Lett* **413,** 319-322.

McNiven M. A. (2005) Dynamin in disease. *Nat Genet* **37,** 215-216.

Merrifield C. J. (2004) Seeing is believing: imaging actin dynamics at single sites of endocytosis. *Trends Cell Biol* **14,** 352-358.

Merrifield C. J., Feldman M. E., Wan L., and Almers W. (2002) Imaging actin and dynamin recruitment during invagination of single clathrin-coated pits. *Nat Cell Biol* **4,** 691-698.

Miele A. E., Watson P. J., Evans P. R., Traub L. M., and Owen D. J. (2004) Two distinct interaction motifs in amphiphysin bind two independent sites on the clathrin terminal domain beta-propeller. *Nat Struct Mol Biol* **11,** 242-248.

Morgan J. R., Prasad K., Hao W., Augustine G. J., and Lafer E. M. (2000) A conserved clathrin assembly motif essential for synaptic vesicle endocytosis. *J Neurosci* **20,** 8667-8676.

Morgan J. R., Prasad K., Jin S., Augustine G. J., and Lafer E. M. (2001) Uncoating of clathrin-coated vesicles in presynaptic terminals. Roles for hsc70 and auxilin. *Neuron* **32,** 289-300.

Morgan J. R., Prasad K., Jin S., Augustine G. J., and Lafer E. M. (2003) Eps15 homology domain - NPF motif interactions regulate clathrin coat assembly during synaptic vesicle recycling. *J Biol Chem* **278,** 33583-33592.

Morgan J. R., Zhao X., Womack M., Prasad K., Augustine G. J., and Lafer E. M. (1999) A role for the clathrin assembly domain of AP180 in synaptic vesicle endocytosis. *J Neurosci* **19,** 10201-10212.

Mozhayeva M. G., Sara Y., Liu X., and Kavalali E. T. (2002) Development of vesicle pools during maturation of hippocampal synapses. *J Neurosci* **22,** 654-665.

Muhlberg A. B., Warnock D. E., and Schmid S. L. (1997) Domain structure and intramolecular regulation of dynamin GTPase. *EMBO J* **16,** 6676-6683.

Mullany P. M. and Lynch M. A. (1998) Evidence for a role for synaptophysin in expression of long-term potentiation in rat dentate gyrus. *Neuroreport* **9,** 2489-2494.

Murthy V. N. and De Camilli P. (2003) Cell biology of the presynaptic terminal. *Annu Rev Neurosci* **26,** 701-728.

Nakase I., Niwa M., Takeuchi T., Sonomura K., Kawabata N., Koike Y., Takehashi M., Tanaka S., Ueda K., Simpson J. C., Jones A. T., Sugiura Y., and Futaki S. (2004) Cellular uptake of arginine-rich peptides: roles for macropinocytosis and actin rearrangement. *Mol Ther* **10,** 1011-1022.

Narayanan R., Leonard M., Song B. D., Schmid S. L., and Ramaswami M. (2005) An internal GAP domain negatively regulates presynaptic dynamin in vivo: a two-step model for dynamin function. *J Cell Biol* **169,** 117-126.

Neve R. L., Coopersmith R., McPhie D. L., Santeufemio C., Pratt K. G., Murphy C. J., and Lynn S. D. (1998) The neuronal growth-associated protein GAP-43 interacts with rabaptin-5 and participates in endocytosis. *J Neurosci* **18,** 7757-7767.

Nicholls D. G. (1993) The glutamatergic nerve terminal. *Eur J Biochem* **212,** 613-631.

Nicholls D. G. and Sihra T. S. (1986) Synaptosomes possess an exocytotic pool of glutamate. *Nature* **321,** 772-773.

Nicholls D. G., Sihra T. S., and Sanchez-Prieto J. (1987) Calcium-dependent and -independent release of glutamate from synaptosomes monitored by continuous fluorometry. *J Neurochem* **49,** 50-57.

Nichols B. J. and Lippincott-Schwartz J. (2001) Endocytosis without clathrin coats. *Trends Cell Biol* **11,** 406-412.

Nichols R. A., Suplick G. R., and Brown J. M. (1994) Calcineurin-mediated protein dephosphorylation in brain nerve terminals regulates the release of glutamate. *J Biol Chem* **269,** 23817-23823.

Nonet M. L., Holgado A. M., Brewer F., Serpe C. J., Norbeck B. A., Holleran J., Wei L., Hartwieg E., Jorgensen E. M., and Alfonso A. (1999) UNC-11, a Caenorhabditis elegans AP180 homologue, regulates the size and protein composition of synaptic vesicles. *Mol Biol Cell* **10,** 2343-2360.

Okamoto P. M., Herskovits J. S., and Vallee R. B. (1997) Role of the basic, proline-rich region of dynamin in Src homology 3 domain binding and endocytosis. *J Biol Chem* **272,** 11629-11635.

Olusanya O., Andrews P. D., Swedlow J. R., and Smythe E. (2001) Phosphorylation of threonine 156 of the mu2 subunit of the AP2 complex is essential for endocytosis in vitro and in vivo. *Curr Biol* **11,** 896-900.

Owen D. J., Wigge P., Vallis Y., Moore J. D., Evans P. R., and McMahon H. T. (1998) Crystal structure of the amphiphysin-2 SH3 domain and its role in the prevention of dynamin ring formation. *EMBO J* **17,** 5273-5285.

Paillart C., Li J., Matthews G., and Sterling P. (2003) Endocytosis and vesicle recycling at a ribbon synapse. *J Neurosci* **23,** 4092-4099.

Pang D. T., Wang J. K., Valtorta F., Benfenati F., and Greengard P. (1988) Protein tyrosine phosphorylation in synaptic vesicles. *Proc Natl Acad Sci U S A* **85,** 762-766.

Pearse B. M. (1976) Clathrin: a unique protein associated with intracellular transfer of membrane by coated vesicles. *Proc Natl Acad Sci U S A* **73,** 1255-1259.

Pennuto M., Bonanomi D., Benfenati F., and Valtorta F. (2003) Synaptophysin I controls the targeting of VAMP2/synaptobrevin II to synaptic vesicles. *Mol Biol Cell* **14,** 4909-4919.

Pennuto M., Dunlap D., Contestabile A., Benfenati F., and Valtorta F. (2002) Fluorescence resonance energy transfer detection of synaptophysin I and vesicle-associated membrane protein 2 interactions during exocytosis from single live synapses. *Mol Biol Cell* **13,** 2706-2717.

Peter B. J., Kent H. M., Mills I. G., Vallis Y., Butler P. J., Evans P. R., and McMahon H. T. (2004) BAR domains as sensors of membrane curvature: The amphiphysin BAR structure. *Science* **303,** 495-499.

Pieribone V. A., Shupliakov O., Brodin L., Hilfiker-Rothenfluh S., Czernik A. J., and Greengard P. (1995) Distinct pools of synaptic vesicles in neurotransmitter release. *Nature* **375,** 493-497.

Plomann M., Lange R., Vopper G., Cremer H., Heinlein U. A., Scheff S., Baldwin S. A., Leitges M., Cramer M., Paulsson M., and Barthels D. (1998) PACSIN, a brain protein that is upregulated upon differentiation into neuronal cells. *Eur J Biochem* **256,** 201-211.

Powell K. A., Valova V. A., Malladi C. S., Jensen O. N., Larsen M. R., and Robinson P. J. (2000) Phosphorylation of dynamin I on Ser-795 by protein kinase C blocks its association with phospholipids. *J Biol Chem* **275,** 11610-11617.

Praefcke G. J., Ford M. G., Schmid E. M., Olesen L. E., Gallop J. L., Peak-Chew S. Y., Vallis Y., Babu M. M., Mills I. G., and McMahon H. T. (2004) Evolving nature of the AP2 alpha-appendage hub during clathrin-coated vesicle endocytosis. *EMBO J* **23,** 4371-4383.

Prochiantz A. (1996) Getting hydrophilic compounds into cells: lessons from homeopeptides. *Curr Opin Neurobiol* **6,** 629-634.

Promega (1996) *Protocols and applications guide, 3rd Edition*, Promega corporation, USA.

Qiagen (2000) *Qiagen plasmid purification handbook*, Qiagen Ltd.

Qiagen (2003) *The QIAexpressionist, 5th Edition*, Qiagen Ltd.

Qualmann B. and Kelly R. B. (2000) Syndapin isoforms participate in receptor-mediated endocytosis and actin organization. *J Cell Biol* **148,** 1047-1062.

Qualmann B., Kessels M. M., and Kelly R. B. (2000) Molecular links between endocytosis and the actin cytoskeleton. *J Cell Biol* **150,** F111-F116.

Qualmann B., Roos J., DiGregorio P. J., and Kelly R. B. (1999) Syndapin I, a synaptic dynamin-binding protein that associates with the neural Wiskott-Aldrich syndrome protein. *Mol Biol Cell* **10,** 501-513.

Ralser M., Nonhoff U., Albrecht M., Lengauer T., Wanker E. E., Lehrach H., and Krobitsch S. (2005) Ataxin-2 and huntingtin interact with endophilin-A complexes to function in plastin-associated pathways. *Hum Mol Genet* **14,** 2893-2909.

Ramaswami M., Krishnan K. S., and Kelly R. B. (1994) Intermediates in synaptic vesicle recycling revealed by optical imaging of Drosophila neuromuscular junctions. *Neuron* **13,** 363-375.

Rehm H., Wiedenmann B., and Betz H. (1986) Molecular characterization of synaptophysin, a major calcium- binding protein of the synaptic vesicle membrane. *EMBO J* **5,** 535-541.

Reisinger C., Yelamanchili S. V., Hinz B., Mitter D., Becher A., Bigalke H., and Ahnert-Hilger G. (2004) The synaptophysin/synaptobrevin complex dissociates independently of neuroexocytosis. *J Neurochem* **90,** 1-8.

Rhee J. S., Betz A., Pyott S., Reim K., Varoqueaux F., Augustin I., Hesse D., Sudhof T. C., Takahashi M., Rosenmund C., and Brose N. (2002) beta Phorbol ester- and diacylglycerol-induced augmentation of transmitter release is mediated by munc13s and not by PKCs. *Cell* **108,** 121-133.

Richard J. P., Melikov K., Vives E., Ramos C., Verbeure B., Gait M. J., Chernomordik L. V., and Lebleu B. (2002) Cell-penetrating peptides: A re-evaluation of the mechanism of cellular uptake. *J Biol Chem* **278,** 585-590.

Richards D. A., Guatimosim C., and Betz W. J. (2000) Two endocytic recycling routes selectively fill two vesicle pools in frog motor nerve terminals. *Neuron* **27,** 551-559.

Richards D. A., Rizzoli S. O., and Betz W. J. (2004) Effects of wortmannin and latrunculin A on slow endocytosis at the frog neuromuscular junction. *J Physiol.*

Ricotta D., Conner S. D., Schmid S. L., Von Figura K., and Honing S. (2002) Phosphorylation of the AP2 mu subunit by AAK1 mediates high affinity binding to membrane protein sorting signals. *J Cell Biol* **156,** 791-795.

Ringstad N., Gad H., Low P., Di Paolo G., Brodin L., Shupliakov O., and De Camilli P. (1999) Endophilin/SH3p4 is required for the transition from early to late stages in clathrin-mediated synaptic vesicle endocytosis. *Neuron* **24,** 143-154.

Ringstad N., Nemoto Y., and DeCamilli P. (2001) Differential expression of endophilin 1 and 2 dimers at central nervous system synapases. *J Biol Chem* **276,** 40424-40430.

Rizo J. and Sudhof T. C. (2002) Snares and munc18 in synaptic vesicle fusion. *Nat Rev Neurosci* **3,** 641-653.

Rizzoli S. O. and Betz W. J. (2003) Neurobiology: All change at the synapse. *Nature* **423,** 591-592.

Rizzoli S. O. and Betz W. J. (2004) The structural organization of the readily releasable pool of synaptic vesicles. *Science* **303,** 2037-2039.

Rizzoli S. O., Richards D. A., and Betz W. J. (2003) Monitoring synaptic vesicle recycling in frog motor nerve terminals with FM dyes. *J Neurocytol* **32,** 539-549.

Robinson P. J. (1991) Dephosphin, a 96,000 dalton substrate of protein kinase C in synaptosomal cytosol is phosphorylated in intact synaptosomes. *FEBS Lett* **282,** 388-392.

Robinson P. J. and Dunkley P. R. (1983) Depolarisation-dependent protein phosphorylation in rat cortical synaptosomes: the effects of calcium, strontium, and barium. *Neurosci Lett* **43,** 85-90.

Robinson P. J., Liu J. P., Powell K. A., Fykse E. M., and Südhof T. C. (1994) Phosphorylation of dynamin I and synaptic vesicle recycling. *Trends Neurosci* **17,** 348-353.

Robinson P. J., Sontag J.-M., Liu J. P., Fykse E. M., Slaughter C., McMahon H. T., and Südhof T. C. (1993) Dynamin GTPase regulated by protein kinase C phosphorylation in nerve terminals. *Nature* **365,** 163-166.

Rohde G., Wenzel D., and Haucke V. (2002) A phosphatidylinositol (4,5)-bisphosphate binding site within mu2-adaptin regulates clathrin-mediated endocytosis. *J Cell Biol* **158,** 209-214.

Royle S. J. and Lagnado L. (2003) Endocytosis at the synaptic terminal. *J Physiol* **553,** 345-355.

Rusk N., Le P. U., Mariggio S., Guay G., Lurisci C., Nabi I. R., Corda D., and Symons M. (2003) Synaptojanin 2 functions at an early step of clathrin-mediated endocytosis. *Curr Biol* **13,** 659-663.

Rusnak F. and Mertz P. (2000) Calcineurin: form and function. *Physiol Rev* **80,** 1483-1521.

Ryan T. A., Smith S. J., and Reuter H. (1996) The timing of synaptic vesicle endocytosis. *Proc Natl Acad Sci U S A* **93,** 5567-5571.

Saito T., Guan F., Papolos D. F., Lau S., Klein M., Fann C. S., and Lachman H. M. (2001) Mutation analysis of SYNJ1: a possible candidate gene for chromosome 21q22-linked bipolar disorder. *Mol Psychiatry* **6,** 387-395.

Sankaranarayanan S., Atluri P. P., and Ryan T. A. (2003) Actin has a molecular scaffolding, not propulsive, role in presynaptic function. *Nat Neurosci* **6,** 127-135.

Sankaranarayanan S. and Ryan T. A. (2000) Real-time measurements of vesicle-SNARE recycling in synapses of the central nervous system. *Nat Cell Biol* **2,** 197-204.

Sankaranarayanan S. and Ryan T. A. (2001) Calcium accelerates endocytosis of vSNAREs at hippocampal synapses. *Nat Neurosci* **4,** 129-136.

Scales S. J. and Scheller R. H. (1999) Lipid membranes shape up [news; comment]. *Nature* **401,** 123-124.

Schikorski T. and Stevens C. F. (2001) Morphological correlates of functionally defined synaptic vesicle populations. *Nat Neurosci* **4,** 391-395.

Schmidt A. A. (2002) Membrane transport: the making of a vesicle. *Nature* **419,** 347-349.

Schuske K. R., Richmond J. E., Matthies D. S., Davis W. S., Runz S., Rube D. A., van der Bliek A. M., and Jorgensen E. M. (2003) Endophilin is required for synaptic vesicle endocytosis by localizing synaptojanin. *Neuron* **40,** 749-762.

Sever S., Damke H., and Schmid S. L. (2000) Dynamin:GTP controls the formation of constricted coated pits, the rate limiting step in clathrin-mediated endocytosis. *J Cell Biol* **150,** 1137-1148.

Sever S., Muhlberg A. B., and Schmid S. L. (1999) Impairment of dynamin's GAP domain stimulates receptor-mediated endocytosis. *Nature* **398,** 481-486.

Shpetner H. S. and Vallee R. B. (1989) Identification of dynamin, a novel mechanochemical enzyme that mediates interactions between microtubules. *Cell* **59,** 421-432.

Shupliakov O., Bloom O., Gustafsson J. S., Kjaerulff O., Low P., Tomilin N., Pieribone V. A., Greengard P., and Brodin L. (2002) Impaired recycling of synaptic vesicles after acute perturbation of the presynaptic actin cytoskeleton. *Proc Natl Acad Sci U S A* **99,** 14476-14481.

Shupliakov O., Low P., Grabs D., Gad H., Chen H., David C., Takei K., De Camilli P., and Brodin L. (1997) Synaptic vesicle endocytosis impaired by disruption of dynamin-SH3 domain interactions. *Science* **276,** 259-263.

Sigismund S., Woelk T., Puri C., Maspero E., Tacchetti C., Transidico P., Di Fiore P. P., and Polo S. (2005) Clathrin-independent endocytosis of ubiquitinated cargos. *Proc Natl Acad Sci U S A* **102,** 2760-2765.

Sihra T. S., Nairn A. C., Kloppenburg P., Lin Z., and Pouzat C. (1995) A role for calcineurin (protein phosphatase-2B) in the regulation of glutamate release. *Biochem Biophys Res Commun* **212,** 609-616.

Simpson F., Hussain N. K., Qualmann B., Kelly R. B., Kay B. K., McPherson P. S., and Schmid S. L. (1999) SH3-domain-containing proteins function at distinct steps in clathrin-coated vesicle formation. *Nat Cell Biol* **1,** 119-124.

Slepnev V. I. and De Camilli P. (2000) Accessory factors in clathrin-dependent synaptic vesicle endocytosis. *Nat Rev Neurosci* **1,** 161-172.

Slepnev V. I., Ochoa G. C., Butler M. H., Grabs D., and DeCamilli P. (1998) Role of phosphorylation in regulation of the assembly of endocytic coat complexes. *Science* **281,** 821-824.

Smillie K. J. and Cousin M. A. (2005) Dynamin I phosphorylation and the control of synaptic vesicle endocytosis. *Biochem Soc Symp* 87-97.

Smillie K. J., Evans G. J., and Cousin M. A. (2005) Developmental change in the calcium sensor for synaptic vesicle endocytosis in central nerve terminals. *J Neurochem* **94,** 452-458.

Smith C. J., Dafforn T. R., Kent H., Sims C. A., Khubchandani-Aswani K., Zhang L., Saibil H. R., and Pearse B. M. (2004) Location of auxilin within a clathrin cage. *J Mol Biol* **336,** 461-471.

Smythe E. (2002) Regulating the clathrin-coated vesicle cycle by AP2 subunit phosphorylation. *Trends Cell Biol* **12,** 352-354.

Smythe E. (2004) Cell biology: light on pits. *Nature* **431,** 641-642.

Solomaha E., Szeto F. L., Yousef M. A., and Palfrey H. C. (2005) Kinetics of Src homology 3 domain association with the proline-rich domain of dynamins: specificity, occlusion, and the effects of phosphorylation. *J Biol Chem* **280,** 23147-23156.

Song B. D. and Schmid S. L. (2003) A molecular motor or a regulator? Dynamin's in a class of its own. *Biochemistry* **42,** 1369-1376.

Song W. and Zinsmaier K. E. (2003) Endophilin and synaptojanin hook up to promote synaptic vesicle endocytosis. *Neuron* **40,** 665-667.

Spiwoks-Becker I., Vollrath L., Seeliger M. W., Jaissle G., Eshkind L. G., and Leube R. E. (2001) Synaptic vesicle alterations in rod photoreceptors of synaptophysin-deficient mice. *Neurosci* **107,** 127-142.

Stopkova P., Vevera J., Paclt I., Zukov I., and Lachman H. M. (2004) Analysis of SYNJ1, a candidate gene for 21q22 linked bipolar disorder: a replication study. *Psychiatry Res* **127,** 157-161.

Stowell M. H., Marks B., Wigge P., and McMahon H. T. (1999) Nucleotide-dependent conformational changes in dynamin: evidence for a mechanochemical molecular spring. *Nat Cell Biol* **1,** 27-32.

Sudhof T. C. (2000) The synaptic vesicle cycle revisited. *Neuron* **28,** 317-320.

Sudhof T. C. (2004) The synaptic vesicle cycle. *Annu Rev Neurosci* **27,** 509-547.

Sudhof T. C., Lottspeich F., Greengard P., Mehl E., and Jahn R. (1987) A synaptic vesicle protein with a novel cytoplasmic domain and four transmembrane regions. *Science* **238,** 1142-1144.

Sugita S., Janz R., and Sudhof T. C. (1999) Synaptogyrins regulate Ca2+-dependent exocytosis in PC12 cells. *J Biol Chem* **274,** 18893-18901.

Sun J. Y., Wu X. S., and Wu L. G. (2002) Single and multiple vesicle fusion induce different rates of endocytosis at a central synapse. *Nature* **417,** 555-559.

Sweitzer S. M. and Hinshaw J. E. (1998) Dynamin undergoes a GTP-dependent conformational change causing vesiculation. *Cell* **93,** 1021-1029.

Takei K., McPherson P. S., Schmid S. L., and De Camilli P. (1995) Tubular membrane invaginations coated by dynamin rings are induced by GTP-γS in nerve terminals. *Nature* **374,** 186-190.

Takei K., Mundigl O., Daniell L., and De Camilli P. (1996) The synaptic vesicle cycle: A single vesicle budding step involving clathrin and dynamin. *J Cell Biol* **133,** 1237-1250.

Takei K., Slepnev V. I., Haucke V., and De Camilli P. (1999) Functional partnership between amphiphysin and dynamin in clathrin-mediated endocytosis. *Nat Cell Biol* **1,** 33-39.

Tan T. C., Valova V. A., Malladi C. S., Graham M. E., Berven L. A., Jupp O. J., Hansra G., McClure S. J., Sarcevic B., Boadle R. A., Larsen M. R., Cousin M. A., and Robinson P. J. (2003) Cdk5 is essential for synaptic vesicle endocytosis. *Nat Cell Biol* **5,** 701-710.

Teng H., Cole J. C., Roberts R. L., and Wilkinson R. S. (1999) Endocytic active zones: hot spots for endocytosis in vertebrate neuromuscular terminals. *J Neurosci* **19,** 4855-4866.

Teng H. and Wilkinson R. S. (2000) Clathrin-mediated endocytosis near active zones in snake motor boutons. *J Neurosci* **20,** 7986-7993.

ter Haar E., Harrison S. C., and Kirchhausen T. (2000) Peptide-in-groove interactions link target proteins to the beta-propeller of clathrin. *Proc Natl Acad Sci U S A* **97,** 1096-1100.

Thiele C., Hannah M. J., Fahrenholz F., and Huttner W. B. (2000) Cholesterol binds to synaptophysin and is required for biogenesis of synaptic vesicles. *Nat Cell Biol* **2,** 42-49.

Thomas L., Hartung K., Langosch D., Rehm H., Bamberg E., Franke W. W., and Betz H. (1988) Identification of synaptophysin as a hexameric channel protein of the synaptic vesicle membrane. *Science* **242,** 1050-1053.

Thoren P. E., Persson D., Karlsson M., and Norden B. (2000) The Antennapedia peptide penetratin translocates across lipid bilayers - the first direct observation. *FEBS Lett* **482,** 265-268.

Thoren P. E., Persson D., Lincoln P., and Norden B. (2005) Membrane destabilizing properties of cell-penetrating peptides. *Biophys Chem* **114,** 169-179.

Tibbs G. R., Dolly J. O., and Nicholls D. G. (1996) Evidence for the induction of repetitive action potentials in synaptosomes by K^+-channel inhibitors: An analysis of plasma membrane ion fluxes. *J Neurochem* **67,** 389-397.

Tomizawa K., Sunada S., Lu Y. F., Oda Y., Kinuta M., Ohshima T., Saito T., Wei F. Y., Matsushita M., Li S. T., Tsutsui K., Hisanaga S. I., Mikoshiba K., Takei K., and Matsui H. (2003) Cophosphorylation of amphiphysin I and dynamin I by Cdk5 regulates clathrin-mediated endocytosis of synaptic vesicles. *J Cell Biol* **163,** 813-824.

Urrutia R., Henley J. R., Cook T., and McNiven M. A. (1997) The dynamins: redundant or distinct functions for an expanding family of related GTPases? *Proc Natl Acad Sci U S A* **94,** 377-384.

Vallis Y., Wigge P., Marks B., Evans P. R., and McMahon H. T. (1999) Importance of the pleckstrin homology domain of dynamin in clathrin-mediated endocytosis. *Curr Biol* **9,** 257-260.

Valtorta F., Pennuto M., Bonanomi D., and Benfenati F. (2004) Synaptophysin: leading actor or walk-on role in synaptic vesicle exocytosis? *BioEssays* **26,** 445-453.

van der Bliek A. M. and Meyerowitz E. M. (1991) Dynamin-like protein encoded by the Drosophila *shibire* gene associated with vesicular traffic. *Nature* **351,** 411-414.

Varoqueaux F., Sigler A., Rhee J. S., Brose N., Enk C., Reim K., and Rosenmund C. (2002) Total arrest of spontaneous and evoked synaptic transmission but normal synaptogenesis in the absence of Munc13-mediated vesicle priming. *Proc Natl Acad Sci U S A* **99,** 9037-9042.

Verderio C., Pozzi D., Pravettoni E., Inverardi F., Schenk U., Coco S., Proux-Gillardeaux V., Galli T., Rossetto O., Frassoni C., and Matteoli M. (2004) SNAP-25 modulation of calcium dynamics underlies differences in GABAergic and glutamatergic responsiveness to depolarization. *Neuron* **41,** 599-610.

Verstreken P., Kjaerulff O., Lloyd T. E., Atkinson R., Zhou Y., Meinertzhagen I. A., and Bellen H. J. (2002) Endophilin mutations block clathrin-mediated endocytosis but not neurotransmitter release. *Cell* **109,** 101-112.

Verstreken P., Koh T. W., Schulze K. L., Zhai R. G., Hiesinger P. R., Zhou Y., Mehta S. Q., Cao Y., Roos J., and Bellen H. J. (2003) Synaptojanin is recruited by endophilin to promote synaptic vesicle uncoating. *Neuron* **40,** 733-748.

Voet D. and Voet J. G. (1995) *Biochemistry 2nd Edition*, John Wiley and Sons, Inc., USA.

Vogel H. J. (2002) *Calcium binding protein protocols Volume 2: Methods and techniques*, Humana Press Inc., Totowa, New Jersey.

Wang L.-H., Südhof T. C., and Anderson R. G. (1995) The appendage domain of α-adaptin is a high affinity binding site for dynamin. *J Biol Chem* **270,** 10079-10083.

Warnock D. E., Hinshaw J. E., and Schmid S. L. (1996) Dynamin self-assembly stimulates its GTPase activity. *J Biol Chem* **271,** 22310-22314.

Weber T., Zemelman B. V., McNew J. A., Westermann B., Gmachl M., Parlati F., Sollner T. H., and Rothman J. E. (1998) SNAREpins: Minimal machinery for membrane fusion. *Cell* **92,** 759-772.

Wenk M. R., Pellegrini L., Klenchin V. A., Di Paolo G., Chang S., Daniell L., Arioka M., Martin T. F., and De Camilli P. (2001) PIP Kinase Iγ is the major $PI(4,5)P_2$ synthesizing enzyme at the synapse. *Neuron* **32,** 79-88.

Wiedenmann B. and Franke W. W. (1985) Identification and localization of synaptophysin, an integral membrane glycoprotein of Mr 38,000 characteristic of presynaptic vesicles. *Cell* **41,** 1017-1028.

Wigge P., Köhler K., Vallis Y., Doyle C. A., Owen D., Hunt S. P., and McMahon H. T. (1997a) Amphiphysin heterodimers: Potential role in clathrin-mediated endocytosis. *Mol Biol Cell* **8,** 2003-2015.

Wigge P., Vallis Y., and McMahon H. T. (1997b) Inhibition of receptor-mediated endocytosis by the amphiphysin SH3 domain. *Curr Biol* **7,** 554-560.

Wilde A. and Brodsky F. M. (1996) In vivo phosphorylation of adaptors regulates their interaction with clathrin. *J Cell Biol* **135,** 635-645.

Wilkinson R. S. and Cole J. C. (2001) Resolving the Heuser-Ceccarelli debate. *Trends Neurosci* **24,** 195-197.

Wray W., Boulikas T., Wray V. P., and Hancock R. (1981) Silver staining of proteins in polyacrylamide gels. *Anal Biochem* **118,** 197-203.

Xia Z. and Storm D. R. (2005) The role of calmodulin as a signal integrator for synaptic plasticity. *Nat Rev Neurosci* **6,** 267-276.

Yang Z., Li H., Chai Z., Fullerton M. J., Cao Y., Toh B. H., Funder J. W., and Liu J. P. (2000) Dynamin II regulates hormone secretion in neuroendocrine cells. *J Biol Chem* **276,** 4251-4260.

Yao P. J. (2004) Synaptic frailty and clathrin-mediated synaptic vesicle trafficking in Alzheimer's disease. *Trends Neurosci* **27,** 24-29.

Yao Q., Chen J., Cao H., Orth J. D., McCaffery J. M., Stan R. V., and McNiven M. A. (2005) Caveolin-1 interacts directly with dynamin-2. *J Mol Biol* **348,** 491-501.

Yelamanchili S. V., Reisinger C., Becher A., Sikorra S., Bigalke H., Binz T., and Ahnert-Hilger G. (2005) The C-terminal transmembrane region of synaptobrevin binds synaptophysin from adult synaptic vesicles. *Eur J Cell Biol* **84,** 467-475.

Yin Y., Dayanithi G., and Lemos J. R. (2002) Ca(2+)-regulated, neurosecretory granule channel involved in release from neurohypophysial terminals. *J Physiol* **539,** 2-18.

Yoshida Y., Kinuta M., Abe T., Liang S., Araki K., Cremona O., Di Paolo G., Moriyama Y., Yasuda T., De Camilli P., and Takei K. (2004) The stimulatory action of amphiphysin on dynamin function is dependent on lipid bilayer curvature. *EMBO J* **23,** 3483-3491.

Zhang B., Koh Y. H., Beckstead R. B., Budnik V., Ganetzky B., and Bellen H. J. (1998) Synaptic vesicle size and number are regulated by a clathrin adaptor protein required for endocytosis. *Neuron* **21,** 1465-1475.

Zhang B. and Zelhof A. C. (2002) Amphiphysins: Raising the BAR for synaptic vesicle recycling and membrane dynamics. *Traffic* **3,** 452-460.

Zhang J. Z., Davletov B. A., Südhof T. C., and Anderson R. G. (1994) Synaptotagmin I is a high affinity receptor for clathrin AP-2: Implications for membrane recycling. *Cell* **78,** 751-760.

Zhang P. and Hinshaw J. E. (2001) Three-dimensional reconstruction of dynamin in the constricted state. *Nat Cell Biol* **3,** 922-926.

Zhang Y., Baumgrass R., Schutkowski M., and Fischer G. (2004) Branches on the alpha-C atom of cyclosporin A residue 3 result in direct calcineurin inhibition and rapid cyclophilin 18 binding. *Chembiochem* **5,** 1006-1009.

Zuchner S., Noureddine M., Kennerson M., Verhoeven K., Claeys K., De Jonghe P., Merory J., Oliveira S. A., Speer M. C., Stenger J. E., Walizada G., Zhu D., Pericak-Vance M. A., Nicholson G., Timmerman V., and Vance J. M. (2005) Mutations in the pleckstrin homology domain of dynamin 2 cause dominant intermediate Charcot-Marie-Tooth disease. *Nat Genet* **37,** 289-294.